AD_____

Award Number: W81XWH-05-1-0546

TITLE: Alkylating derivatives of vitamin D hormone for prostate cancer

PRINCIPAL INVESTIGATOR: Rahul Ray, Ph.D.

CONTRACTING ORGANIZATION: Boston University, Boston, MA 02215-1301

REPORT DATE: October, 2010

TYPE OF REPORT: Final

PREPARED FOR: U.S. Army Medical Research and Materiel Command
Fort Detrick, Maryland 21702-5012

REPORT DOCUMENTATION PAGE

Form Approved
OMB No. 0704-0188

1. REPORT DATE *(DD-MM-YYYY)*	2. REPORT TYPE	3. DATES COVERED *(From - To)*
01-10-2010	Final	30 SEP 2005 - 29 SEP 2010

4. TITLE AND SUBTITLE
Alkylating derivatives of vitamin D hormone for prostate cancer

5a. CONTRACT NUMBER

5b. GRANT NUMBER
W81XWH-06-1-0766

5c. PROGRAM ELEMENT NUMBER

6. AUTHOR(S)
Dr. Rahul Ray

E-Mail: bapi@bu.edu

5d. PROJECT NUMBER

5e. TASK NUMBER

5f. WORK UNIT NUMBER

7. PERFORMING ORGANIZATION NAME(S) AND ADDRESS(ES)
Boston University
Boston, MA 02215

8. PERFORMING ORGANIZATION REPORT NUMBER

9. SPONSORING / MONITORING AGENCY NAME(S) AND ADDRESS(ES)
U.S. Army Medical Research and Materiel Command
Fort Detrick, Maryland 21702-5012

10. SPONSOR/MONITOR'S ACRONYM(S)

11. SPONSOR/MONITOR'S REPORT NUMBER(S)

12. DISTRIBUTION / AVAILABILITY STATEMENT
Approved for public release; distribution unlimited

13. SUPPLEMENTARY NOTE

14. ABSTRACT
Pro No abstract provided.

15. SUBJECT TERMS
Prostate cancer, vitamin D derivatives, animal models

16. SECURITY CLASSIFICATION OF:			17. LIMITATION OF ABSTRACT	18. NUMBER OF PAGES	19a. NAME OF RESPONSIBLE PERSON
a. REPORT	b. ABSTRACT	c. THIS PAGE			USAMRMC
U	U	U	UU	123	19b. TELEPHONE NUMBER *(include area code)*

14. ABSTRACT
Prostate cancer (PCa) is the most prevalent cancer among men, and second leading cause of cancer death among men in the US. Current clinical interventions for PCa include surgery and radiation therapy, and anti-hormone and androgen-deprivation therapy for early stage and hormone-sensitive PCa. But, practically no therapy is currently available for non-resectable and hormone-refractory PCa. We have developed 1α,25-Dihydroxyvitamin D_3-3-bromoacetate (**$1,25(OH)_2D_3$-3-BE**), a novel alkylating derivative of 1α,25-dihydroxyvitamin D_3 ($1,25(OH)_2D_3$), and in preliminary studies, demonstrated potent growth-inhibitory activity in several PCa cells. These results suggest a strong therapeutic potential of this compound in PCa.
The principal goal of this project is to evaluate the potential of $1,25(OH)_2D_3$-3-BE as a therapeutic agent for prostate cancer in animal models of human prostate cancer, and explore the molecular mechanism/s of this compound in prostate cancer cells. The ultimate goal of this project is to develop 1,25(OH)2D3-3-BE as a therapeutic agent for prostate cancer.

Specific Aim 1: In vivo studies of 1,25(OH)2D3-3-BE in mouse models
1A. Determine MTD of 1,25(OH)2D3-3-BE in non-tumor bearing SCID mice,
1B. Evaluate bio-availability of 1,25(OH)2D3-3-BE in a mouse model
1B. Determine efficacy of 1,25(OH)2D3-3-BE in mouse xenograft models for human prostate tumor

Specific Aim 2: Mechanistic studies of 1,25(OH)2D3-3-BE in prostate cancer cells
2A. Evaluate the regulation of cell-cycle and apoptotic markers by 1,25(OH)2D3-3-BE

Table of Contents

Page

Introduction

Therapeutic potential of 1,25-dihydroxyvitamin D_3 ($1,25(OH)_2D_3$) in prostate cancer is well-recognized. However, its clinical use has been restricted by its inherent calcemic toxicity. In recent studies we demonstrated that 1α,25-dihydroxyvitamin D_3-3-bromoacetate [$1,25(OH)_2D_3$-3-BE], a derivative of $1,25(OH)_2D_3$ that covalently links $1,25(OH)_2D_3$ inside the ligand-binding pocket of nuclear vitamin D receptor (VDR) is a strong antiproliferative and pro-apoptotic agent in several androgen-sensitive and androgen-refractory human prostate cancer cells. Furthermore, in a preliminary study $1,25(OH)_2D_3$-3-BE showed strong anti- tumor effect in a mouse model of prostate cancer without significant toxicity. The goal of this project is to evaluate translational potential of $1,25(OH)_2D_3$-3-BE as a therapeutic agent for prostate cancer. This will be achieved by determining the efficacy of $1,25(OH)_2D_3$-3-BE in mouse models of human androgen-sensitive and androgen-insensitive prostate cancer, as well as evaluating its molecular mechanisms of action in *in vitro* studies.

Synthesis of $1,25(OH)_2D_3$-3-BE

Success of all the studies included in this project are critically dependent on the availability of $1,25(OH)_2D_3$-3-BE in substantial quantities. In the past we synthesized this compound in a multi-step scheme using 1,25-dihydroxy-7-dehydrocholesterol as the starting material (R. Ray, S.A. Holick, and M.F. Holick. Synthesis of a photoaffinity-labelled analog of 1,25-dihydroxyvitamin D_3. *Journal of the Chemical Society*, **Chemical Communications** 11: 702-703, 1985). However, this starting material is no longer available. Therefore, we had to devise a synthetic scheme for obtaining substantial quantity of $1,25(OH)_2D_3$-3-BE required for our studies by a scheme shown below.

Synthetic procedures:

a. 3-TBDMS ether of 25-hydroxyvitamin D_3-SO_2 adduct (B): Approximately 10 ml of SO_2 was condensed (-78^0C) in a flask containing 200 mg of 25-hydroxyvitamin D_3 in a flask fitted with a trap that was cooled with dry ice-acetone (-78^0C). The yellow solution was refluxed with stirring for 4 hours followed by removal of SO_2 with a stream of nitrogen to produce a foamy solid. The foam was dissolved in 5 ml of anhydrous DMF (distilled fresh from CaO) and TBDMSCl (1.5 X), imidazole (2 X) were added and the solution was stirred at 25^0C for 20 hours followed by removal of DMF under vacuo, re-dissolving the residue in EtOAc. The organic solution was washed with water, organic layer was dried over anhydrous $MgSO_4$, and the solution was concentrated under vacuo. The residue was moved on to the next step without further purification.

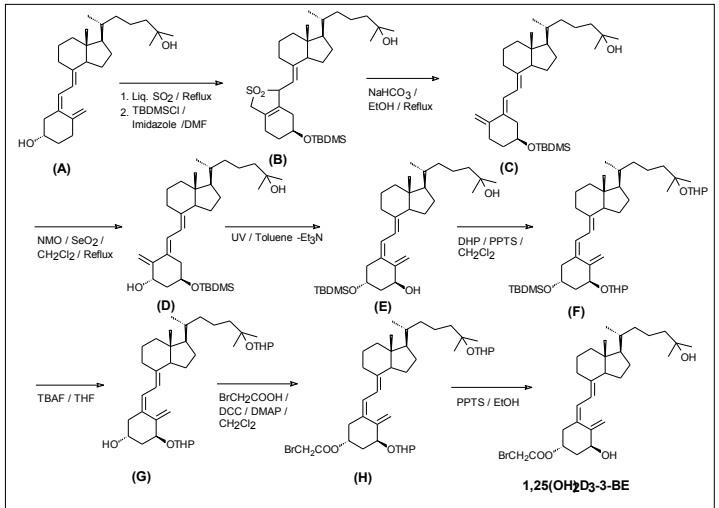

The scheme for the synthesis of $1,25(OH)_2D_3$-3-BE

b. Trans-25-hydroxyvitamin D_3-3-TBDMS ether (C): The crude from the previous step was dissolved in 95% EtOH (10 ml) and $NaHCO_3$ (244 mg) was added. The mixture was refluxed under argon for 90 min followed by addition of brine and extraction of the aqueous solution with EtOAc. The crude reaction product was purified by preparative TLC (silica plates, 1000μ, Analtech) to produce 56.7% of the desired product (C).

c. Trans-1α,25-dihydroxyvitamin D_3-3-TBDMS ether (D): A mixture of (C) (760 mg) and SeO_2 (192 mg) in 15 ml of anhydrous CH_2Cl_2 was refluxed under argon for 30 min followed by cooling to room temperature and addition of a solution of N-methylmorpholine-N-oxide (850 mg) in 15 ml of anhydrous CH_2Cl_2. The

mixture was refluxed for an additional 60 min when TLC indicated almost complete reaction, and refluxing was stopped. The mixture was filtered and concentrated under vacuo. The crude reaction product was purified by preparative TLC to produce almost a quantitative amount of the desired product (D).

d. 1α,25-Dihydroxyvitamin D_3-3-TBDMS ether (E): 80 mg of (D), anthracene (10 mg), Et_3N (40 µl) in 10 ml of toluene (in a quartz test tube) was irradiated from a Hanovia medium pressure mercury arc lamp for 75 min. The irradiated solution was concentrated and the crude mixture was purified by preparative TLC (1000 µ plate, 4:1 EtOAc-hexanes, multiple elutions, the desired product (most polar of all the photo-products) was isolated as a gummy liquid in 67% yield.

e. 1α,25-Di-tetrahydropyranyl, 3-TBDMS ether of 1α,25-dihydroxyvitamin D_3 (F): A solution of (E) (35 mg), DHP (60 µl) and a few crystal of PPTS in 1.0 ml of anhydrous CH_2Cl_2 was stirred for two days followed by preparative TLC procedure to produce 34 mg (74%) of the desired product (F).

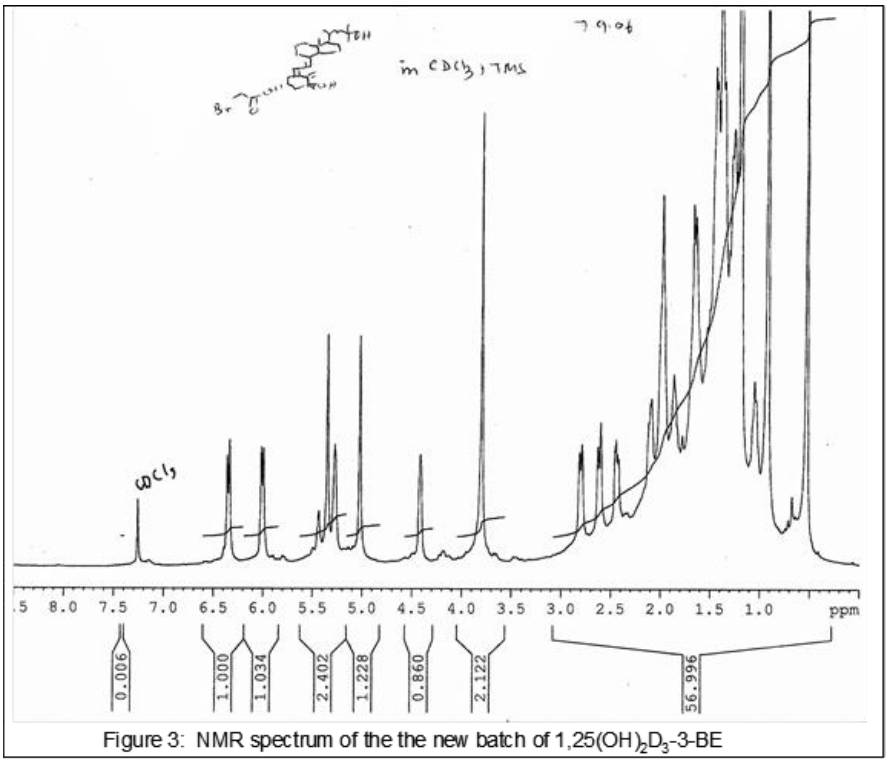

Figure 3: NMR spectrum of the the new batch of $1,25(OH)_2D_3$-3-BE

f. 1α,25-Di-tetrahydropyranyl,1α,25-dihydroxyvitamin D_3 (G): A solution of (F) (17 mg) and 20 µl of TBAF (1M in THF) was dissolved in anhydrous THF (1 ml) and stirred for 20 hours. The reaction mixture was diluted with EtOAc, washed with brine, dried over anhydrous $MgSO_4$, concentrated and purified by preparative TLC to produce quantitative amount of (G).

g. 1α,25-Di-tetrahydropyranyl,1α,25-dihydroxyvitamin D_3-3-bromoacetate (H): A solution of (G) (8 mg), DCC (2.5 X, 8.12 mg), DMAP (catalytic), bromoacetic acid (1.5 X, 3.3 mg) in one ml of anhydrous CH_2Cl_2 was stirred for 20 hours followed by filtration of the mixture, concentration of the filtrate by a stream of nitrogen and preparative TLC purification of the reaction mixture produced quantitative amount of the desired product (H).

h. 1α,25-Dihydroxyvitamin D_3-3-bromoacetate: A solution of (H) (7 mg) was dissolved in 3 ml of AcOH-THF-H_2O (4:2:1) and heated at 50^0C for 20 hours. Volatile matters were removed under a stream of nitrogen and the product was isolated by preparative TLC. Yield of the desired product 1α,25-dihydroxyvitamin D_3-3-bromoacetate was quantitative. NMR spectrum of the product ($1,25(OH)_2D_3$-3-BE), shown above corroborated well with its assigned structure.

Cellular Studies:

A. $1,25(OH)_2D_3$-3-BE is superior to $1,25(OH)_2D_3$ in inhibiting the growth of LNCaP (androgen-sensitive), DU-145 and PC-3 (androgen-insensitive) prostate cancer cells:

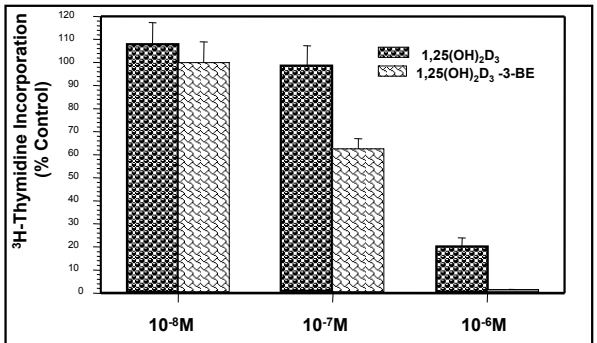

Figure 1: Dose-response study of $1,25(OH)_2D_3$-3-BE or $1,25(OH)_2D_3$ on the growth of LNCaP cells. Cells were treated with $10^{-7\text{-}6}$M of $1,25(OH)_2D_3$-3-BE or $1,25(OH)_2D_3$ or EtOH for 16 hours, and subjected to ^{3}H-thymidine incorporation assay in the usual fashion.

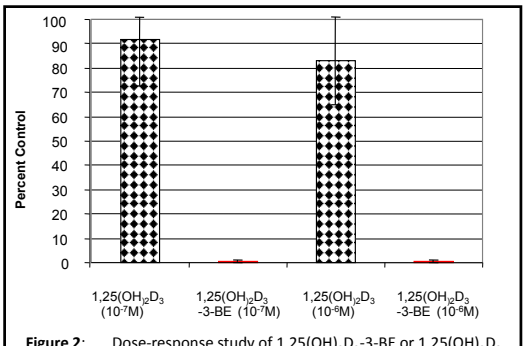

Figure 2: Dose-response study of $1,25(OH)_2D_3$-3-BE or $1,25(OH)_2D_3$ on the growth of DU-145 cells. Cells were treated with $10^{-7\text{-}6}$M of $1,25(OH)_2D_3$-3-BE or $1,25(OH)_2D_3$ or EtOH in serum-containing media for 48 hours (dosings at 0 and 24 hours), and subjected to ^{3}H-thymidine incorporation assay in the usual fashion

LNCaP and DU-145 cells were grown to approximately 60% confluence in RPMI medium with 5% FBS and then treated with

Table 1: Trypan blue assay to determine the effect of 10-7M of $1,25(OH)_2D_3$-3-BE or $1,25(OH)_2D_3$ on the growth of PC-3 cells

Sample	% Inhibition	% Live
Ethanol Control	0	100
$1,25(OH)_2D_3$ (10^{-7}M)	0	106.7
$1,25(OH)_2D_3$-3-BE (10^{-7}M)	66.7	33.3

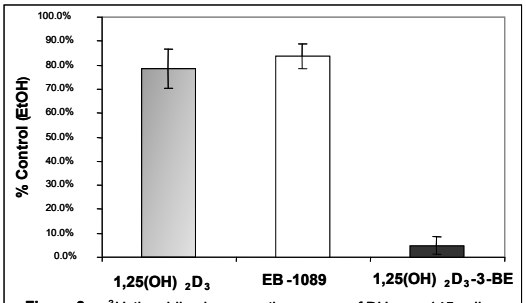

Figure 3 : ^{3}H-thymidine incorporation assays of DU -145 cells. Cells were treated with 10 $^{-8}$M of 1,25(OH) $_2D_3$-3-BE, EB -108, 1,25(OH) $_2D_3$ or ethanol (control) in serum -containing medium for 48 hours (two dosing at 0 and 48 hours) followed by ^{3}H-thymidine incorporation assays in the usual fashion.

various doses $1,25(OH)_2D_3$-3-BE and $1,25(OH)_2D_3$ in serum-containing medium for 16-48 hours followed by ^{3}H-thymidine incorporation assay (LNCaP and DU-145) or Trypan Blue assay for PC-3 cells. Results of this assay demonstrate that $1,25(OH)_2D_3$-3-BE is strongly antiproliferative in all the cell-lines. However, equivalent amounts of $1,25(OH)_2D_3$ showed significantly lower or no effects in these cells (**Figures 1 & 2, and Table 1**).

B. Comparison of the effects of $1,25(OH)_2D_3$-3-BE, $1,25(OH)_2D_3$ and EB-1089 in DU-145 cells:

At present EB-1089 is the most promising non-calcemic analog of $1,25(OH)_2D_3$ that has shown strong promise in inoperable hepatocellular carcinoma (Dalhoff K, Dancey J, Astrup L, Skovsgaard T, Hamberg KJ, Lofts FJ, Rosmorduc O, Erlinger S, BachHansen J, Steward WP, Skov T, Burcharth F, Evans TR. A phase II study of the vitamin D analogue Seocalcitol in patients with inoperable hepatocellular carcinoma. Brit. J. cancer 89: 252-257, 2003). We compared the antiproliferative effect of EB-1089, $1,25(OH)_2D_3$ and $1,25(OH)_2D_3$-3-BE in DU-145 cells by ^{3}H-thymidine incorporation assay. As shown in **Figure 3**, only $1,25(OH)_2D_3$-3-BE showed a strong antiproliferative effect in DU-145 cells.

C. Microscopic appearance of LNCaP cells dosed with $1,25(OH)_2D_3$-3-BE or $1,25(OH)_2D_3$:

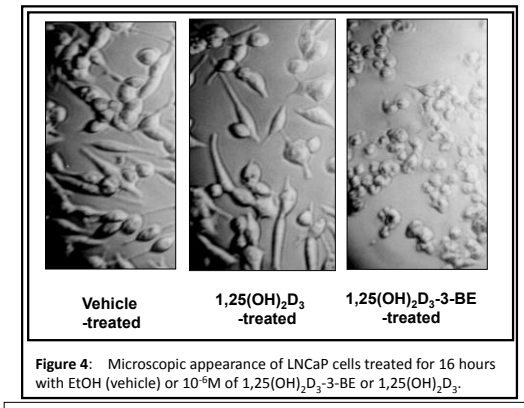

Figure 4: Microscopic appearance of LNCaP cells treated for 16 hours with EtOH (vehicle) or 10^{-6}M of $1,25(OH)_2D_3$-3-BE or $1,25(OH)_2D_3$.

LNCaP cells were dosed with 10^{-6}M of $1,25(OH)_2D_3$-3-BE or $1,25(OH)_2D_3$ for 6 hours and cells were visualized with a phase-contrast microscope. As shown in **Figure 4**, $1,25(OH)_2D_3$-3-BE-dosed cells appeared to round up and lift off the plate, denoting cell-death, while $1,25(OH)_2D_3$ or EtOH (control)-treated cells appeared normal.

D. Tumorigenic PC-3 cells are sensitive to $1,25(OH)_2D_3$-3-BE-treatment, but normal RWPE-1 prostate cells are not:

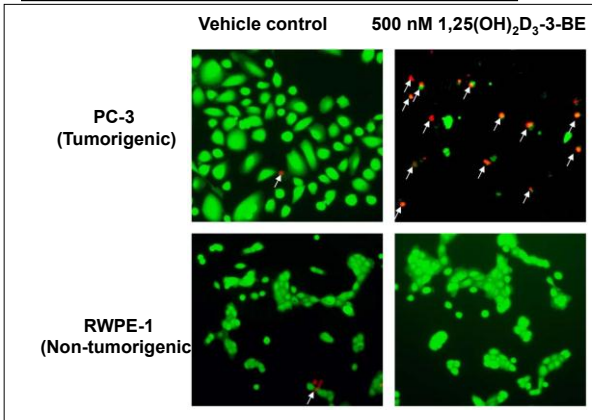

Figure 5: Confocal image of PC-3 (tumorigenic) and RWPE-1 (non-tumorigenic prostate cells): treated with 500 nM of $1,25(OH)_2D_3$-3-BE or EtOH for 24 hr in full serum medium; green: live cells, red: dead cells

PC-3 and RWPE-1 cells were dosed with 500 nM of $1,25(OH)_2D_3$-3-BE or EtOH (control) for 24 hr, and treated with dyes and visualized by confocal microscopy. As shown in **Figure 5**, tumorigenic PC-3 cells showed extensive cell-death, but not RWPE-1 normal cells. These results suggested that normal prostate cells may not be sensitive to $1,25(OH)_2D_3$-3-BE-treatment, but cancer cells are. This is a very interesting finding if we are to develop $1,25(OH)_2D_3$-3-BE as a therapeutic agent for prostate cancer.

Mechanistic Studies

A. <u>$1,25(OH)_2D_3$-3-BE causes apoptosis in prostate cancer cells</u>:

Results of **Figure 4** suggests that 1,25(OH)$_2$D$_3$-3-BE causes programmed cell death (apoptosis) in LNCaP cells. This phenomenon was confirmed in DU-145 cells, where treatment with 1,25(OH)$_2$D$_3$-3-BE increased caspase 3/7 activity, a marker for apoptosis, while caspase 3/7 activity was not induced in 1,25(OH)$_2$D$_3$ and EtOH-treated cells (**Figure 6**). This phenomenon was further confirmed in PC-3 cells in which 1,25(OH)$_2$D$_3$-3-BE-treatment caused 81% cells to undergo apoptosis, while only approximately 5-6% cells underwent apoptosis by 1,25(OH)$_2$D$_3$ or EtOH-treatment (**Figure 7**).

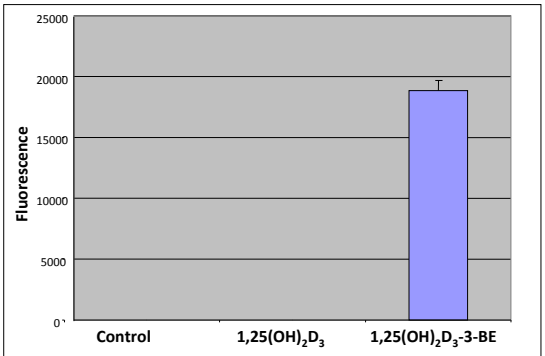

Figure 6: Caspase 3,7 activity assay in DU-145 cells following treatment with 10^{-6}M of 1,25(OH)$_2$D$_3$ and 1,25(OH)$_2$D$_3$-3-BE

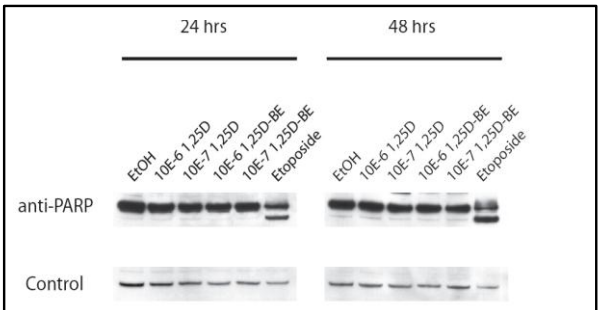

Figure 8: PARP-cleavage analysis of DU-145 cells treated with $10^{-6\text{-}7}$M of 1,25(OH)$_2$D$_3$ or 1,25(OH)$_2$D$_3$-3-BE

B. Apoptosis by 1,25(OH)$_2$D$_3$-3-BE doesn't involve PARP-cleavage:

In many cells apoptosis is accompanied by PARP-cleavage, but in DU-145 cells 1,25(OH)$_2$D$_3$-3-BE-induced apoptosis did not appear to involve PARP-cleavage (**Figure 8**).

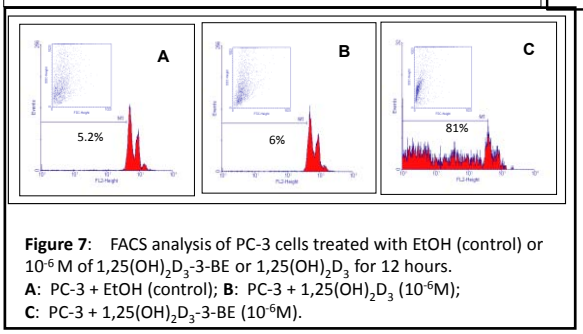

Figure 7: FACS analysis of PC-3 cells treated with EtOH (control) or 10^{-6} M of 1,25(OH)$_2$D$_3$-3-BE or 1,25(OH)$_2$D$_3$ for 12 hours.
A: PC-3 + EtOH (control); **B**: PC-3 + 1,25(OH)$_2$D$_3$ (10^{-6}M);
C: PC-3 + 1,25(OH)$_2$D$_3$-3-BE (10^{-6}M).

C. 25-Hydroxyvitamin D$_3$-3-BE (25-OH-D$_3$-3-BE) inhibits Akt-phosphorylation in DU-145 cells:

Akt is a pro-survival protein in the P13K/PTEN pathway. Many antiproliferative agents inhibit phosphorylation of Akt as a part of their mechanism to inhibit growth of cancer cells. We observed that 25-OH-D$_3$-3-BE, a counterpart of 1,25(OH)$_2$D$_3$-3-BE without the 1-hydroxyl group, inhibits Akt-phosphorylation in DU-145 cells (**Figure 9**).

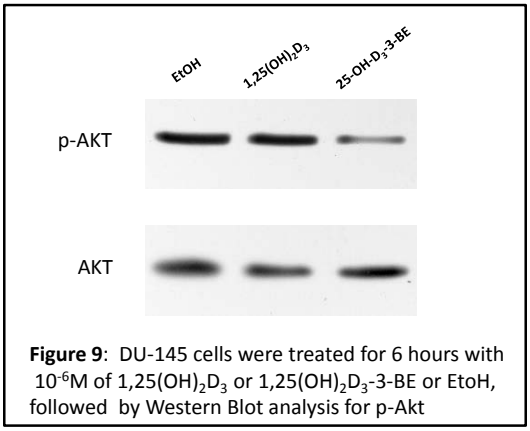

Figure 9: DU-145 cells were treated for 6 hours with 10^{-6}M of 1,25(OH)$_2$D$_3$ or 1,25(OH)$_2$D$_3$-3-BE or EtoH, followed by Western Blot analysis for p-Akt

D. Modulation of 1,25-dihydroxyvitamin D$_3$-24-hydroxylase (CYP24-OHase) gene by 1,25(OH)$_2$D$_3$ and 1,25(OH)$_2$D$_3$-3-BE in LNCaP cells:

The CYP24 gene product CYP24-OHase catalyzes the introduction of a hydroxyl group at the 24-position in 1,25(OH)$_2$D$_3$, followed by multiple oxidations of the side chain leading to calcitroic acid, the final catabolite that is excreted. Therefore, CYP24 is the initiator of the catabolic degradation of 1,25(OH)$_2$D$_3$ *in vivo*. Furthermore, CYP24 gene is a VDR-inducible gene. We hypothesized that covalent attachment of 1,25(OH)$_2$D$_3$-3-BE deep inside the ligand binding pocket of VDR will prevent it from reacting with CYP24-OHase and decrease its catabolism. In essence it would require more 1,25(OH)$_2$D$_3$-3-BE to induce the same level of CYP24 message as 1,25(OH)$_2$D$_3$.

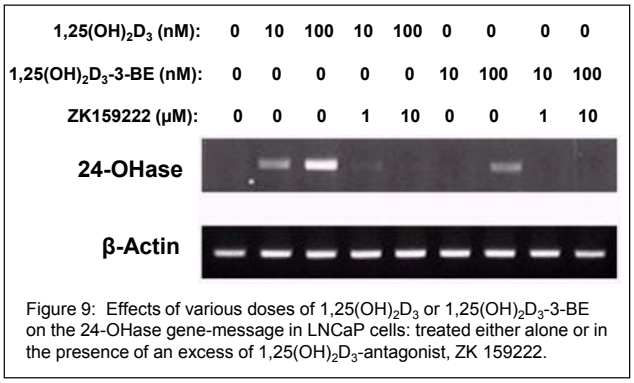

Figure 9: Effects of various doses of 1,25(OH)$_2$D$_3$ or 1,25(OH)$_2$D$_3$-3-BE on the 24-OHase gene-message in LNCaP cells: treated either alone or in the presence of an excess of 1,25(OH)$_2$D$_3$-antagonist, ZK 159222.

Results of this experiment, shown in **Figure 9**, demonstrate that treatment of LNCaP cells with 10^{-7}M of 1,25(OH)$_2$D$_3$ strongly induces CYP24-message, and moderately with 10^{-8}M. In the case of 1,25(OH)$_2$D$_3$-3-BE,

induction of CYP24 mRNA is observed only at 10^{-7}M, and intensity of message is similar to 10^{-8}M of $1,25(OH)_2D_3$. These results demonstrate a log scale difference in inducing the message for CYP24 between $1,25(OH)_2D_3$ and $1,25(OH)_2D_3$-3-BE.

To further investigate the requirement for VDR in $1,25(OH)_2D_3$-3-BE action, we used a VDR- specific antagonist, ZK159222 which has been shown to be effective in blocking VDR- mediated gene regulation. Therefore, LNCaP cells were treated with either $1,25(OH)_2D_3$-3-BE or ZK 15922 alone or in combination, and the levels of CYP24 mRNA analyzed by RT-PCR.

In our experiment we observed that CYP24-message (by $1,25(OH)_2D_3$ and $1,25(OH)_2D_3$-3-BE) was reduced by ZK15922 in a dose-dependent fashion, and completely obliterated with 10^{-4}M (of ZK15922). Collectively these results strongly suggest that cellular effects of $1,25(OH)_2D_3$-3-BE in LNCaP prostate cancer cells are VDR-dependent.

Bio-availability study: $1,25(OH)_2D_3$-3-BE remains in circulation for at least up to six hrs in mice:

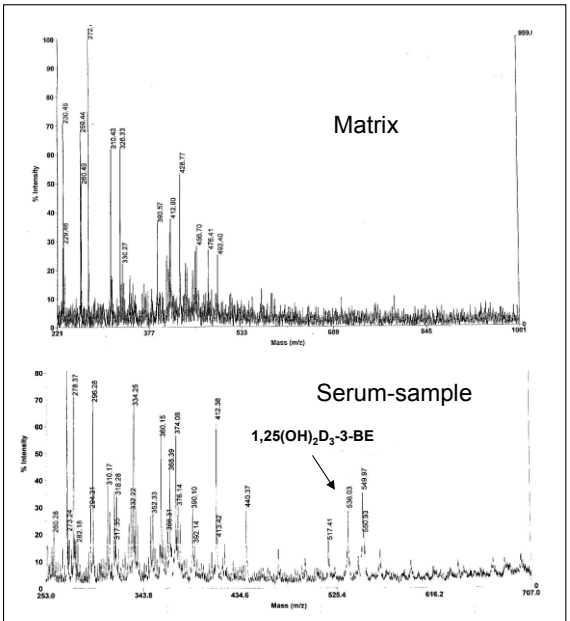

Figure 10: MS/MS analysis of organic-extract of serum sample of a mouse injected with $1,25(OH)_2D_3$-3-BE for 4 hr. $1,25(OH)_2D_3$-3-BE is indicated by an arrow (bottom). Note: **Matrix spectrum does not contain the 536.07 mass peak present in serum sample**.

Normal Balb C mice were dosed (*i.p.*) with 2 µg/kg of $1,25(OH)_2D_3$-3-BE or vehicle (5% DMA in sesame oil). The animals were sacrificed at 0.5, 1.0, 2.0, 4.0 and 6.0 hours, blood was withdrawn by cardiac puncture and sera made. Serum samples were extracted with ethyl acetate and analyzed in a HPLC/MS (Voyager). As shown in the **Fig. 10**, a serum sample (4 hr-treatment, a representative sample) contains a peak for $1,25(OH)_2D_3$-3-BE. Matrix sample and control sera samples do not contain this peak. This peak was visible at least up to 6 hr, indicating that $1,25(OH)_2D_3$-3-BE remains in circulation for at least 6 hr.

Determination of maximum tolerable dose (MTD) of $1,25(OH)_2D_3$-3-BE:

Twenty (20) male nu/nu mice, 6 weeks old (Charles River Laboratories, Wilmington, MA) were grouped in five (5) animals each and injected (i.p.) with either vehicle (sesame oil) or 0.75 µg/kg, 1.0 µg/kg and 1.25 µg/kg of $1,25(OH)_2D_3$-3-BE (in sesame oil) on every third day. Mice were observed for sign of toxicity including lack of apetite, weight loss, lethargy etc. After seven (7) injections three (3) mice (out of a total of 5) receiving 1.25 µg/kg of $1,25(OH)_2D_3$-3-BE died, and the experiment was stopped.

Dose	Number Dead
Sesame oil	0
0.75 µg/Kg	0
1.0 µg/Kg	0
1.25 µg/Kg	3

Based on the results shown in the above table MTD of $1,25(OH)_2D_3$-3-BE was ascertained to be between 1.0 – 1.25 µg/kg.

$1,25(OH)_2D_3$-3-BE inhibits the growth of established hormone-refractory tumor in a mouse xeonograft model (*p.o.* and *i.p.* administrations):

Male, athymic mice (average weight 20 gm), fed normal rat chow and water *ad lib* were inoculated with culture-grown DU 145 cells in the flank. When the tumor size grew to approximately 100 mm^3 the animals were randomized into groups of ten (10), and they were given 1,25(OH)$_2$D$_3$-3-BE, 1,25(OH)$_2$D$_3$, EB-1089, and vehicle (5% dimethyl-acetamide, DMA in sesame oil) by oral gavage (*p.o.*) or intraperitoneal injection (*i.p.*) on every third day (when body weights were determined); and one group was left untreated (<u>doses are noted in **Figures 11 & 12**</u>). Treatment started on day 11 and stopped on day 30; and animals were left untreated for two (2) additional days when they were sacrificed and blood was collected for serum-calcium determination.

<u>Summary of results</u>:

***<u>P.O.</u>* <u>mode</u>**:

(i) 1,25(OH)$_2$D$_3$-3-BE and 1,25(OH)$_2$D$_3$ (each 0.5 μg/kg) showed a strong and similar anti-tumor effect (**Figure 11A**), far greater than 0.5 μg/kg and 1.0 μg/kg of EB-1089. Molecular weights of 1,25(OH)$_2$D$_3$ and 1,25(OH)$_2$D$_3$-3-BE are 416.65 and 537.8 respectively. Therefore according to this graph 1,25(OH)$_2$D$_3$-3-BE is approximately 1.3-times more efficacious than an equimolar amount of 1,25(OH)$_2$D$_3$.

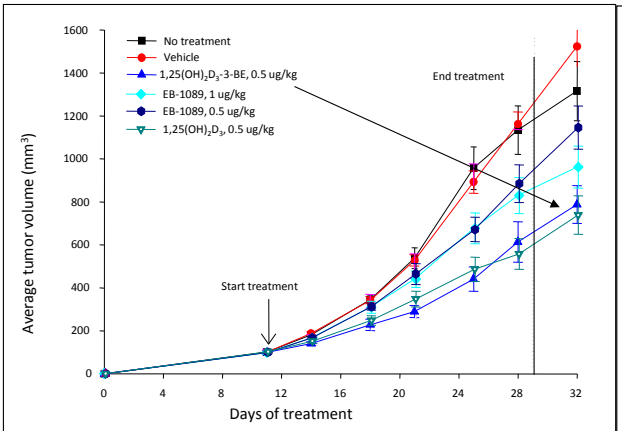

Figure 11A: Effect of 1,25(OH)$_2$D$_3$, 1,25(OH)$_2$D$_3$-3-BE and EB-1089 (q.o.d. X 10, **p.o**.) on **tumor volume** in DU-145 mouse xengraft model.

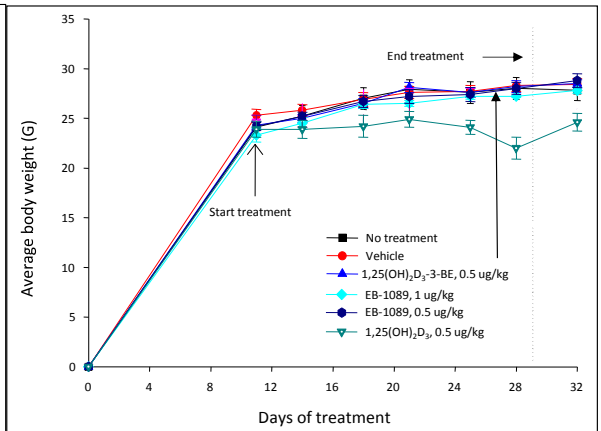

Figure 11B: Effect of 1,25(OH)$_2$D$_3$, 1,25(OH)$_2$D$_3$-3-BE and EB-1089 (q.o.d. X 10, **p.o**.) on **body weight** in DU-145 mouse xengraft model.

(ii) <u>1,25(OH)$_2$D$_3$-3-BE did not cause any gross toxicity</u>, as reflected in body weight in contrast with 1,25(OH)$_2$D$_3$ which caused significant toxicity (**Figure 11B**). EB-1089 was not toxic.

<u>I.P. mode</u>:

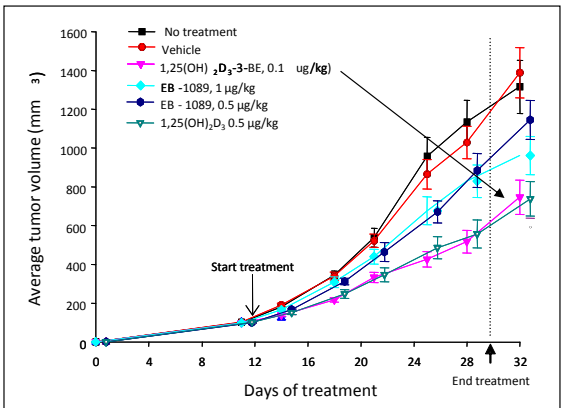

Figure 12A: Effect of 1,25(OH)$_2$D$_3$, 1,25(OH)$_2$D$_3$-3-BE and EB-1089 (q.o.d. X 10, **i.p**.) on **tumor volume** in DU-145 mouse xengraft model.

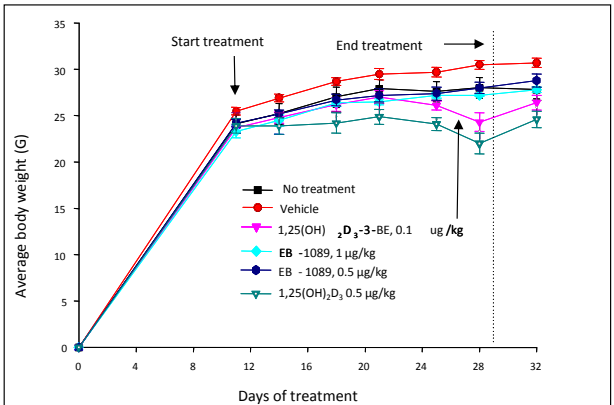

Figure 12B: Effect of 1,25(OH)$_2$D$_3$, 1,25(OH)$_2$D$_3$-3-BE and EB-1089 (q.o.d. X 10, **i.p**.) on **body weight** in DU-145 mouse xengraft model.

(i) Tumor inhibitory effect of 1,25(OH)$_2$D$_3$-3-BE (0.1 μg/kg) was similar to 1,25(OH)$_2$D$_3$ (0.5 μg/kg), and far greater than 0.5 μg/kg and 1.0 μg/kg of EB-1089 (**Figure 12A**). Considering the MWs of the compounds, 1,25(OH)$_2$D$_3$-3-BE is approximately 7-times more efficacious than an equimolar amount of 1,25(OH)$_2$D$_3$.

(ii) 1,25(OH)$_2$D$_3$-3-BE caused some gross toxicity, as reflected in body weight, however it was less than 1,25(OH)$_2$D$_3$ (**Figure 12B**). EB-1089 was not toxic.

Serum calcium: We waited for two additional days after stopping the dosing and sacrificing the animals**.** Serum-calcium values of treated animals were not significantly different from controls (un-treated and vehicle-treated, results not shown), demonstrating that $1,25(OH)_2D_3$-3-BE and $1,25(OH)_2D_3$ have no residual toxicity at this dose (results not shown).

In general, oral administration of any drug is far more desirable than any injectable form. Therefore, the *p.o.*-data is highly significant. Since $1,25(OH)_2D_3$-3-BE is non-toxic at 0.5 μg/kg, presumably considerably higher dose can be used with a stronger anti-tumor effect and less/no toxicity. *I.p.* data support our hypothesis that covalent attachment of $1,25(OH)_2D_3$ (to VDR ligand-binding domain, via $1,25(OH)_2D_3$-3-BE) will increase its half-life, engage and keep VDR transcriptionally active for a longer period which may result in better efficacy (7-times better in this case) but it may cause some toxicity. Dose-level can certainly be lowered to obtain better efficacy/toxicity index.

Attempts to develop of a mouse xenograft model of androgen-sensitive human prostate tumor:

Our overall goal for this project is to determine the efficacy of $1,25(OH)_2D_3$-3-BE in both androgen-sensitive, as well as androgen –insensitive human prostate tumor. As described above we have developed an athymic mouse xenograft model for androgen-insensitive (DU-145) prostate tumor. However, all our attempts to develop an androgen-sensitive prostate tumor model with androgen-sensitive prostate cancer cells failed. Upon investigating this matter with researchers who have published on this model we obtained an unequivocal response: it is 'unpredictable' at its best, and 'extremely difficult' at its worst.

There are several treatment-options for androgen-sensitive prostate cancer, but there is no therapy to date of androgen-insensitive and metastatic prostate cancer. Therefore, demonstration of the efficacy of $1,25(OH)_2D_3$-3-BE in reducing tumor-size in an androgen-insensitive tumor model is highly significant.

Summary of the abovementioned studies:

(i) Developed a synthetic scheme of $1,25(OH)_2D_3$-3-BE to obtain large quantities of this compound that will be required for future studies.

(ii) Carried out growth assays in androgen-sensitive and androgen-insensitive prostate cancer cells to demonstrate that $1,25(OH)_2D_3$-3-BE is far superior than $1,25(OH)_2D_3$ in inhibiting the growth of several prostate cancer cells.

(iii) Demonstrated that $1,25(OH)_2D_3$-3-BE does not inhibit the growth of normal prostate cells.

(iii) Carried out several mechanistic studies to determine **a.** role of VDR in its cellular activities of $1,25(OH)_2D_3$-3-BE, and **b.** various pathways for its apoptotic and growth-inhibitory activities.

(iv) Determined bio-availability $1,25(OH)_2D_3$-3-BE in mice.

(v) Determined maximum tolerated dose (MTD) of $1,25(OH)_2D_3$-3-BE in mice.

(vi) Developed a mouse model of androgen-insensitive prostate cancer, and demonstrated that $1,25(OH)_2D_3$-3-BE strongly reduces tumor size, and it is largely non-toxic, demonstrating a strong therapeutic potential of $1,25(OH)_2D_3$-3-BE in prostate cancer.

Completed projects/studies beyond the Specific Aims of this PCRP grant

During the tenure of this grant we completed the tasks specified in the Specific Aims. In addition, we initiated projects/carried out studies to **(i)** further investigate the potential of $1,25(OH)_2D_3$-3-BE in prostate cancer in terms of formulation and delivery, and **(ii)** evaluate therapeutic potential of $1,25(OH)_2D_3$-3-BE in other malignancies.

Liposomal preparation of $1,25(OH)_2D_3$-3-BE and demonstration that liposomal $1,25(OH)_2D_3$-3-BE [$(1,25(OH)_2D_3\text{-3-BE})_{LIP}$] is a significantly stronger antiproliferative agent than liposomal $1,25(OH)_2D_3$ in prostate cancer cells:

Phospholipid liposomes are small, uniform particles that are made up of biocompatible phospholipids and cholesterol; and they are designed to encapsulate drugs in the lipid-bilayer of the liposomes. Liposomal formulation of $1,25(OH)_2D_3$-3-BE is designed increase circulatory half-life and efficacy resulting in an improved therapeutic index for this vitamin D–based drug in prostate cancer.

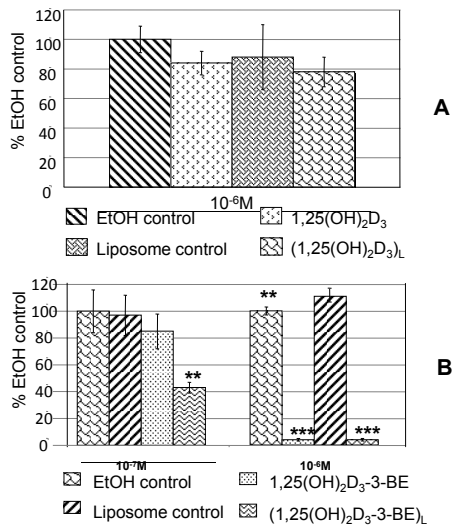

Figure 13: ^{3}H-Thymidine assays of DU-145 cells treated with naked or liposomal $1,25(OH)_2D_3$ or $1,25(OH)_2D_3$-3-BE and controls (EtOH or blank liposome)

We made a simple liposomal preparation of $1,25(OH)_2D_3$ and $1,25(OH)_2D_3$-3-BE from cholesterol (1 μg), dimethylphosphotidyl choline (DMPC) (20 μg) and $1,25(OH)_2D_3$ (1 μg) or $1,25(OH)_2D_3$-3-BE (1 μg) by drying a chloroform solution in a stream of argon, rehydration with PBS (2.5 ml) followed by mixing by brief vortexing and sonication for 15 min. The milky solution was incubated at 50^0C for 50 min and frozen at -77^0C for 20 min. This heating and freezing cycle was repeated once, and the preparation was stored at 4^0C for use in assays. These liposomal preparations were used in growth assays in DU-145 cells.

Results (**Figure 13**) show that growth inhibitory effect of liposomal $1,25(OH)_2D_3$-3-BE (10^{-7}M) is significantly stronger than naked $1,25(OH)_2D_3$-3-BE (**Figure 13B**). 10^{-6} M of liposomal and naked $1,25(OH)_2D_3$-3-BE almost killed all the cells, while an equivalent amount (10^{-6}M) of liposomal and naked $1,25(OH)_2D_3$ had no effect on cell-growth (**Figure 13A**). These results make a strong case developing tumor-targeted, pH-sensitive stealth liposomes of $1,25(OH)_2D_3$-3-BE for further development. Results of this study are delineated a recent publication [Liposomal 1,25-dihydroxyvitamin D3-3β-bromoacetate is a stronger growth-inhibiting agent than its un-encapsulated counterpart in prostate cancer cells. K. S. Persons, S. Hareesh, V. J. Eddy, R. Ray, Journal of Steroid and Hormonal Science (In Press, attached)].

Extending our studies with $1,25(OH)_2D_3$-3-BE beyond prostate cancer into other malignancies:

$1,25(OH)_2D_3$ has shown promise in many cancers and other diseases. Therefore, we explored therapeutic potential of $1,25(OH)_2D_3$-3-BE in other cancers, particularly pancreatic and kidney cancers, where therapeutic options are extremely limited.

Screening of cancer cells, other than prostate cancer for anti-proliferative activity of $1,25(OH)_2D_3$-3-BE

A summary of these studies are given below.

(i) $1,25(OH)_2D_3$-3-BE strongly inhibited the growth of several cell-lines of pancreatic, renal, colon cancers, but not breast cancer. $1,25(OH)_2D_3$-3-BE was also found to be highly effective in leukemia cells.

(ii) We have carried out extensive studies on the effect of $1,25(OH)_2D_3$-3-BE on renal cancer, including *in vivo* studies in a mouse model of renal cancer. These results are included in a recent publication from our group [A vitamin D receptor-alkylating derivative of 1α, 25-dihydroxyvitamin D_3 inhibits growth of human kidney cancer cells and suppresses tumor growth. J. R. Lambert, V. J. Eddy, C.D. Young, K.S. Persons, S. Sarkar, J.A. Kelly, E. Genova, M.S. Lucia, D.V. Faller, R. Ray. Cancer Prevention Research (In Press, attached)].

(iii) $1,25(OH)_2D_3$-3-BE displayed strong activity in several pancreatic cancer cells. In addition $1,25(OH)_2D_3$-3-BE showed strong synergistic activity with AICAR (a metformin group of compound). These results are described in our recent publication [Anti-growth Effect of 1,25-Dihydroxyvitamin D_3-3-bromoacetate Alone or in Combination with 5-Amino-imidazole-4-carboxamide-1-β-4-ribofuranoside in Pancreatic Cancer Cells**.** K.S. Persons, V.J. Eddy, S. Chadid, R. Deoliveira, A.K. Saha, R. Ray. Anticancer Research 30:1875-80, 2010] (attached).

KEY RESEARCH ACCOMPLISHMENTS

- Demonstrated strong growth-inhibitory activity of $1,25(OH)_2D_3$-3-BE in cells from prostate, kidney, and pancreatic cancers.

- Launched several mechanistic studies to evaluate the molecular pathway of action of $1,25(OH)_2D_3$-3-BE.

- Developed mouse models for androgen-sensitive prostate cancer and kidney cancer, and demonstrated strong anti-tumor activity of $1,25(OH)_2D_3$-3-BE.

- Showed strong synergistic activity of $1,25(OH)_2D_3$-3-BE with AICAR (in pancreatic cancer cells), and sorefenib in kidney cancer cells (results not shown).

- Demonstrated that $1,25(OH)_2D_3$-3-BE can potentially be developed as a therapeutic agent for several cancers.

REPORTABLE OUTCOME

During the tenure of this grant our efforts with $1,25(OH)_2D_3$-3-BE has generated ten (10) peer-reviewed publications (copies attached in the appendix), several abstracts (three attached in the appendix), one book chapter (copy attached in the appendix) and three invited lectures (included in the appendix).

CONCLUSION

Our effort for the past five years has established the groundwork for developing $1,25(OH)_2D_3$-3-BE, either alone or in combination with other chemotherapeutic agents for several cancers.

APPENDIX

Meeting Abstract 1:

IMPACT meeting, Atlanta, GA, September 5-8, 2007

A NOVEL VITAMIN D COMPOUND FOR PROSTATE CANCER

Rahul Ray; James Lambert (University of Colorado Health Science Center, Aurora, CO), Sibaji Sarkar, Kelly S. Persons.

Numerous epidemiological studies have demonstrated the importance of dietary vitamin D in preventing various cancers, including prostate cancer. In addition, therapeutic potential of 1,25-dihydroxyvitamin D_3 ($1,25(OH)_2D_3$), the biologically active metabolite of vitamin D, and its analogs in cancer is well-documented. However, inherent calcemic toxicity of this hormone, particularly at therapeutic doses, has prevented its general use as an anticancer agent, and opening the door for the development of vitamin D analogs with potent antiproliferative activity and reduced systemic toxicity.

Prostate cancer cells respond to $1,25(OH)_2D_3$ by decreasing proliferation and enhancing differentiation. These cell-regulatory processes result from a strong and specific interaction between $1,25(OH)_2D_3$ and vitamin D receptor (VDR) present in the nucleus of the tumor cells. With financial support from the Department of Defense Prostate Cancer Research Program, Fiscal Year 2005 Idea Development Award we have developed a novel derivative of $1,25(OH)_2D_3$ [1,25-dihydroxyvitamin D_3-3-bromoacetate, $1,25(OH)_2D_3$-3-BE] that covalently attaches $1,25(OH)_2D_3$ inside the ligand-binding pocket of VDR. We hyothesized that covalent attachment of $1,25(OH)_2D_3$ (via $1,25(OH)_2D_3$-3-BE) inside the VDR-binding pocket will not allow the catabolic enzymes to degrade $1,25(OH)_2D_3$, and effectively increase the potency of $1,25(OH)_2D_3$. As a result lesser amount of $1,25(OH)_2D_3$ –3-BE will be required for tumor-reduction with diminished toxicity.

In vitro assays of $1,25(OH)_2D_3$-3-BE demonstrated that this compound has strong growth-inhibitory property in several hormone-sensitive and hormone-insensitive prostate cancer cells (LNCaP, PC-3, DU-145, LAPC-4). This growth-inhibitory effect is considerably stronger than an equimolar amount of $1,25(OH)_2D_3$. Furthermore, we observed that $1,25(OH)_2D_3$-3-BE induces programmed cell death or apoptosis in these cells (contrary to $1,25(OH)_2D_3$) as demonstrated by fragmentation of nuclear DNA and activation of pro-apoptotic caspases. Most importantly preliminary *in vivo* studies showed that $1,25(OH)_2D_3$-3-BE strongly reduces androgen-refractory prostate tumor (DU-145) in a mouse xenograft model without causing significant toxicity. These results demonstrate strong therapeutic potential of $1,25(OH)_2D_3$-3-BE in prostate cancer.

Aphios Corporation, Woburn, MA has procured the exclusive right to use this compound in prostate cancer. They are in the process of making liposomal preparations of $1,25(OH)_2D_3$-3-BE in anticipation of clinical trial. Furthermore, $1,25(OH)_2D_3$-3-BE
has shown very strong promise in pancreatic, renal and bladder cancers.

In summary, we have used funds from DOD, PCRP to develop a vitamin D compound with strong therapeutic and commercial potential for prostate and other cancers.

IMPACT: No therapy is currently available for prostate cancer, localized or metastasized that fail to respond to androgen therapy. Our results demsonstrtate that $1,25(OH)_2D_3$-3-BE, a derivative of $1,25(OH)_2D_3$, has a strong therapeutic potential in such malignancies.

Meeting Abstract 2:

Nano Science and Technology Institute, Annual meeting, Santa Clara, CA, May 20-24, 2007.

Nanosomal formulation of a vitamin D receptor alkylating compound for prostate cancer. Rahul Ray[1], and Trevor Castor[2]. [1]Boston University School of Medicine, Boston, MA 02118, 617-638-8199, FAX 617-638-8194, bapi@bu.edu, and [2]Aphios Corporation, Woburn, MA 01801, 781-932-6933, FAX 781-932-6865, tcastor@aphios.com (**Cancer Ligands)**

Prostate cancer is the second leading cause of cancer death in men in the US. The mainstay of chemotherapy includes androgen-deprivation. However, no therapy is currently available for prostate cancer, localized or metastasized that fail to respond to androgen therapy. In addition to androgens, prostate cancer cells respond to 1,25-dihydroxyvitamin D_3 ($1,25(OH)_2D_3$) by decreasing proliferation and enhancing differentiation. Furthermore, most cancer cells contain nuclear vitamin D receptor (VDR) that is responsible for the biological actions of $1,25(OH)_2D_3$. However, use of $1,25(OH)_2D_3$ has been seriously limited by risk of hypercalcemia and hypercalciuria at pharmacological doses.

Interaction between $1,25(OH)_2D_3$ and VDR is an equilibrium process. Therefore, in the steady state a finite amount of free $1,25(OH)_2D_3$ (not bound to VDR) is always present in the equilibrium mixture, which undergoes rapid catabolic degradation. From a therapeutic standpoint such catabolic degradation is met clinically with high doses that cause toxicity. Therefore, if catabolic degradation of $1,25(OH)_2D_3$ is reduced or eliminated its therapeutic potency can be enhanced significantly.

1α,25-Dihydroxy vitamin D_3-3-bromoacetate ($1,25(OH)_2D_3$–3-BE) is a derivative of $1,25(OH)_2D_3$ which reacts specifically with a single Cysteine residue in the ligand binding pocket of VDR. We argued that, $1,25(OH)_2D_3$-3-BE, once covalently linked to VDR, cannot exit the binding pocket; making it an irreversible process. Furthermore, $1,25(OH)_2D_3$–3-BE, covalently linked inside VDR binding pocket is prevented from interacting with catabolic enzymes. We hypothesized that such a process will increase the effective concentration of $1,25(OH)_2D_3$; and lesser amount of $1,25(OH)_2D_3$–3-BE will be required for tumor-reduction with diminished toxicity.

In vitro tests of $1,25(OH)_2D_3$-3-BE demonstrated that this compound has strong growth-inhibitory and apoptosis-inducing properties in several hormone-sensitive and hormone-insensitive prostate cancer cells (LNCaP, PC-3, DU-145). This growth-inhibitory effect was significantly stronger than an equimolar amount of $1,25(OH)_2D_3$. Furthermore, $1,25(OH)_2D_3$-3-BE induces apoptosis in these cells contrary to $1,25(OH)_2D_3$. Additionally, preliminary *in vivo* studies showed that $1,25(OH)_2D_3$-3-BE is of low-toxicity, and it strongly reduces androgen-refractory prostate tumor (DU-145) in a mouse xenograft model. On a molar basis $1,25(OH)_2D_3$-3-BE is approximately six (6) times stronger than $1,25(OH)_2D_3$ in reducing tumor-size. It is also significantly less toxic than an equimolar amount of $1,25(OH)_2D_3$. Therefore, $1,25(OH)_2D_3$-3-BE has a strong therapeutic potential in prostate cancer.

Phospholipid nanosomes are small, uniform liposomes that are made up of biocompatible phospholipids and cholesterol; and they are designed to encapsulate vitamin D drugs in the lipid-bilayer of the nansomes. Nanosomal formulation of $1,25(OH)_2D_3$-3-BE is designed to further reduce systemic toxicity, increase circulatory half-life and efficacy resulting in an improved therapeutic index for this vitamin D–based drug in prostate cancer.

In summary, novelty of our approach is development of a derivative of $1,25(OH)_2D_3$ ($1,25(OH)_2D_3$-3-BE) to kinetically engage VDR to increase the half-life of $1,25(OH)_2D_3$, and increase its potency, Nansomal formulation will further increase its circulatory half-life and efficacy, and decrease toxicity.

Meeting Abstract 3:

Fourteenth Brown University Symposium on vitamin D, Providence, RI, June 22-23, 2007

Abstract:

Harnessing the pharmacodynamic properties of vitamin D analogs: an old wine in a new bottle. Rahul Ray, Ph.D., Boston University School of Medicine, Boston, MA

Therapeutic potential of $1,25(OH)_2D_3$-analogs depends on their pharmacodynamic/ pharmacokinetic properties including bioavailability and catabolic potential. Affinity labeling analogs of $1,25(OH)_2D_3$, that alkylate the ligand binding pocket of vitamin D receptor (VDR) can potentially avoid catabolism with the resultant effect of higher pharmacological efficacy at lower doses. 1,25-Dihydroxyvitamin D_3-3-bromoacetate [$1,25(OH)_2D_3$-3-BE], a VDR-affinity alkylating analog of $1,25(OH)_2D_3$ displays significantly stronger growth-inhibitory effect than the parent hormone in prostate (androgen-sensitive and androgen-insensitive), kidney, pancreas and bladder cancer cells, but not in breast, colon and lung cancer cells. $1,25(OH)_2D_3$-3-BE also shows strong tumor inhibition in a mouse xenograft model of androgen-insensitive prostate cancer. Probable mechanism of action of this VDR-alkylating analog will be discussed.

Meeting Abstract 4:

13th World Congress on Advances in Oncology, and 11th International Symposium on Molecular Medicine.October 9-11, 2008, Crete, Greece.

NUCLEAR TRANSCRIPTIONAL FACTORS AS MOLECULAR TARGETS FOR DRUG-DISCOVERY AND DELIVERY

Rahul Ray, Ph. D., Department of Medicine, Boston University School of Medicine, Boston, Massachusetts, USA

Nuclear vitamin D receptor (VDR) and estrogen receptor (ER) are ligand-activated transcriptional factors for 1,25-dihydroxyvitamin D_3 ($1,25(OH)_2D_3$) and estrogen (E2) respectively; and are key players in manifesting antiproliferative (for $1,25(OH)_2D_3$) and proliferative (for E2) properties of these ligands in cancer cells. VDR is our target for developing potential therapeutic agents for cancer. We have developed 1,25-dihydroxyvitamin D_3-3-bromoacetate ($1,25(OH)_2D_3$-3-BE), a derivative of $1,25(OH)_2D_3$ that affinity alkylates the ligand-binding pocket of VDR in target cells, thereby activating the transcriptional machinery, but eliminating/reducing its own catabolic degradation. Thus, we hypothesize that enhanced pharmacokinetic property of $1,25(OH)_2D_3$-3-BE might increase its antiproliferative property in cancer cells. We observed that $1,25(OH)_2D_3$-3-BE strongly inhibits the growth of prostate (androgen-sensitive and androgen-insensitive), kidney, pancreas and bladder cancer cells. Mechanism of growth-inhibition (by $1,25(OH)_2D_3$-3-BE) includes cell cycle arrest, apoptosis and autophagy. In addition, $1,25(OH)_2D_3$-3-BE down-regulates the message for 1α,25-dihydroxyvitamin D_3-24-hydroxylase (CYP24) gene attesting to its decreased catabolism as predicted by our hypothesis. Furthermore, $1,25(OH)_2D_3$-3-BE strongly reduced androgen-insensitive prostate tumor growth in a mouse xenograft model. Therefore, $1,25(OH)_2D_3$-3-BE has a strong therapeutic potential in several malignancies. On the other hand, we have targeted ER in ER-positive breast cancer cells for the selective delivery of a phototoxin (porphyrin) which can be activated (for cytotoxicity) by treatment with visible light. We have demonstrated that synthetic conjugates of estrogen and tamoxifen with a porphyrin are selectively taken up by ER-positive, but not by ER-negative breast cancer cells. Furthermore, highly selective and efficient cell-kill can be achieved only in ER-positive breast cancer cells with these conjugates upon exposure to red light. Therefore, this combination approach, including phototoxin conjugates of estrogen or anti-estrogen and a treatment-modality can potentially be applied clinically for hormone-sensitive cancers in organs where ER is significantly expressed. In summary, our studies have demonstrated that molecular targeting of transcriptional factors has significant benefits in drug development, delivery and therapy.

Invited Lectures:

Indian Institute of Chemical Biology, Kolkata, India, May 24, 2007

Title: Group specific component: a protein that wears multiple hats

University of Calcutta, Kolkata, India, Department of Biotechnology, April 28, 2008

Title: Signal transduction via nuclear receptors: biochemistry, structural biology and therapeutic targets.

Chittaranjan National Cancer Institute, Kolkata, India, July 8, 2009

Title: Vitamin D and cancer: vitamin D-based therapeutic agents for cancer.

Peer-reviewed publications (2004-2010)

• Swamy, N., Chen, T.C., Peleg, S., Dhawan, P., Christakos, S., Stewart, L.V., Weigel, N.L., Mehta, R.G., Holick, M.F., Ray, R. Inhibition of proliferation and induction of apoptosis by 25-hydroxyvitamin D_3-3 bromoacetate in prostate cancer cells. **Clinical Cancer Research** 10:8018-8027 (2004).
• Swamy, N., Purohit, A., Fernandez-Gacio, A., Jones, G.B., Ray, R**.** Nuclear Estrogen Receptor Targeted photodynamic therapy: Selective uptake and killing of MCF-7 breast cancer cells by a $C_{17\alpha}$-alkynylestradiol-porphyrin conjugate. **Journal of Cellular Biochemistry** 99:966-977 (2006).
• Fernandez-Gacio, A,., Fernandez-Marcos, C, Swamy, N, Dunne, D, Ray, R. Photodynamic cell-kill analysis of breast tumor cells with a tamoxifen-pyropheophorbide conjugate. **Journal of Cellular Biochemistry** 99:665-670 (2006).
• Lambert, J.L., Young, C.D., Persons, K.S., Ray, R**.** Mechanistic and pharmacodynamic studies of a 25-hydroxyvitamin D_3 derivative in prostate cancer cells. **Biochemical & Biophysical Research Communications** 361:189-195 (2007).
• Ray, A., Swamy, N., Ray, R**.** Cross-talk among structural domains of human DBP upon binding 25-hydroxyviatmin D_3. **Biochemical & Biophysical Research Communications** 365:746-750 (2008).

• Swamy, N., Ray, R. Fatty acid binding site environments of serum vitamin D-binding protein and albumin are different. **Bioorganic Chemistry** 36:165-168 (2008).

• Kaya, T., Swamy, N., Persons, K.S., Ray, S., Mohr, S.C., Ray, R. Covalent labeling of nuclear vitamin D receptor with affinity labeling reagents containing a cross-linking probe at three different positions of the parent ligand: structural and biochemical implications. **Bioorganic Chemistry** 37:57-63 (2009).

• Persons, K.S., Eddy, V.J., Chadid, S., Deoliveira, R., Saha, A.K., Ray, R**.** Anti-growth effect of 1,25-dihydroxyvitamin D3-3-bromoacetate alone or in combination with 5-amino-imidazole-4-caroxamide-1-β-4-ribofuranoside in pancreatic cancer cells**. Anticancer Research** 30: 1875-1880 (2010).

• Lambert, J.R., Eddy, V.J., Young, C.D., Persons, K.S., Sarkar, S., Kelly, J.A., Genova, E., Lucia, M.S., Faller, D.V., Ray, R. A vitamin D receptor-alkylating derivative of 1α,25-dihydroxyvitamin D_3 inhibits growth of human kidney cancer cells and suppresses tumor-growth. **Cancer Prevention Research** (*In Press*)

• Persons K.S., Hareesh, S., Eddy, V.J., Ray, R. Liposomal 1,25-dihydroxyvitamin D_3-3β-bromoacetate is a stronger growth-inhibiting agent than its un-encapsulated counterpart in prostate cancer cells. **Journal of Steroids and Hormonal Science** (*In Press*).

Inhibition of Proliferation and Induction of Apoptosis by 25-Hydroxyvitamin D_3-3β-(2)-Bromoacetate, a Nontoxic and Vitamin D Receptor-Alkylating Analog of 25-Hydroxyvitamin D_3 in Prostate Cancer Cells

Narasimha Swamy,[1] Tai C. Chen,[1] Sara Peleg,[2] Puneet Dhawan,[4] Sylvia Christakos,[4] LaMonica V. Stewart,[3] Nancy L. Weigel,[3] Rajendra G. Mehta,[5] Michael F. Holick,[1] and Rahul Ray[1]

[1]Endocrinology, Diabetes and Nutrition, Department of Medicine, Boston University School of Medicine, Boston, Massachusetts; [2]Department of Endocrine, Neoplasia and Hormonal Disorder, M. D. Anderson Cancer Center, and [3]Department of Molecular and Cellular Biology, Baylor College of Medicine, Houston, Texas; [4]Department of Biochemistry and Molecular Biology, New Jersey Medical School, Newark, New Jersey; and [5]Department of Surgical Oncology, University of Illinois Medical School, Chicago, Illinois

ABSTRACT

The 25-hydroxyvitamin D_3 (25-OH-D_3) is a nontoxic and low-affinity vitamin D receptor (VDR)-binding metabolic precursor of 1,25-dihydroxyvitamin D_3 [1,25$(OH)_2D_3$]. We hypothesized that covalent attachment of a 25-OH-D_3 analog to the hormone-binding pocket of VDR might convert the latter into transcriptionally active holo-form, making 25-OH-D_3 biologically active. Furthermore, it might be possible to translate the nontoxic nature of 25-OH-D_3 into its analog. We showed earlier that 25-hydroxyvitamin D_3-3-bromoacetate (25-OH-D_3-3-BE) alkylated the hormone-binding pocket of VDR. In this communication we describe that 10^{-8} mol/L of 25-OH-D_3-3-BE inhibited the growth of keratinocytes, LNCaP, and LAPC-4 androgen-sensitive and PC-3 and DU145 androgen-refractory prostate cancer cells, and PZ-HPV-7 immortalized normal prostate cells with similar or stronger efficacy as 1,25$(OH)_2D_3$. But its effect was strongest in LNCaP, PC-3, LAPC-4, and DU145 cells. Furthermore, 25-OH-D_3-3-BE was toxic to these prostate cancer cells and caused these cells to undergo apoptosis as shown by DNA-fragmentation and caspase-activation assays. In a reporter assay with COS-7 cells, transfected with a 1α,25-dihydroxyvitamin D_3-24-hydroxylase (24-OHase)-construct and VDR-expression vector, 25-OH-D_3-3-BE induced 24-OHase promoter activity. In a "pull down assay" with PC-3 cells, 25-OH-D_3-3-BE induced strong interaction between VDR and general transcription factors, retinoid X receptor, and GRIP-1. Collectively, these results strongly suggested that the cellular effects of 25-OH-D_3-3-BE were manifested via 1,25$(OH)_2D_3$/VDR signaling pathway. A toxicity study in CD-1 mice showed that 166 μg/kg of 25-OH-D_3-3-BE did not raise serum-calcium beyond vehicle control. Collectively, these results strongly suggested that 25-OH-D_3-3-BE has a strong potential as a therapeutic agent for androgen-sensitive and androgen-refractory prostate cancer.

INTRODUCTION

Alkylating agents, such as estramustine, lomustine, procarazine, busulfan, cyclophosphamide, and chlorambucil, platinum coordination complexes are important components in the standard cancer chemotherapeutic regimen. However, majority of these drugs are nonspecific and produce significant to severe side effects, particularly at doses required for the reduction/elimination of tumor (1). Affinity alkylating compounds, on the other hand, cross-link to the substrate/ligand-binding sites of target enzymes/receptors; thus, they can potentially modulate the biological property associated only with the target molecule/molecules (2). We postulated that such target specificity might lower the therapeutic dose of the compounds and can potentially avoid harmful side effects.

Vitamin D receptor (VDR), the nuclear receptor for the vitamin D hormone, 1α,25-dihydroxyvitamin D_3 [1,25$(OH)_2D_3$] is a known target for the potential development of anticancer drugs (3–5). The main obstacle in such efforts has been toxicity of 1,25$(OH)_2D_3$, and many of its synthetic analogs related to hypercalcemia, particularly at doses to have a beneficial effect. The cell-regulatory properties of 1,25$(OH)_2D_3$ and its synthetic analogs are associated with the activation of VDR, but a similar link with calcemic activity is yet to be established firmly. A robust effort has been underway to develop vitamin D derivatives with strong antiproliferative property and reduced toxicity. This effort has produced many vitamin D analogs; and it has been possible to dissociate, at least in part, hypercalcemia from antiproliferative properties in certain analogs, classified as "noncalcemic vitamin D analogs" (6). EB-1089, one such analog, is currently in clinical trials for breast, colorectal, pancreatic, and hepatocellular carcinomas (7–11). Such success has provided a strong impetus to addi-

Received 5/4/04; revised 8/25/04; accepted 9/3/04.
Grant support: A grant from the Community Technology Fund, Boston University (R. Ray) and NIH Grant DK 50583 (S. Peleg).
The costs of publication of this article were defrayed in part by the payment of page charges. This article must therefore be hereby marked "advertisement" in accordance with 18 U.S.C. Section 1734 solely to indicate this fact.
Note: N. Swamy is currently in Department of Pediatrics, Women's and Infants Hospital, Brown University School of Medicine, Providence, Rhode Island. This work was presented in part at the 25th Annual Meeting of the American Society for Bone and Mineral Research, September 19–23, 2003, Minneapolis, MN.
Requests for reprints: Rahul Ray, Boston University School of Medicine, 85 East Newton Street, Boston, MA 02118. E-mail: hapi@bu.edu.

tionally develop therapeutically important vitamin D analogs for a broad range of diseases, including cancer.

The 25-hydroxyvitamin D_3 (25-OH-D_3), the metabolic precursor of 1,25$(OH)_2D_3$, has a significantly reduced VDR-binding affinity. As a result, 25-OH-D_3 is not considered to be biologically active. Additionally, it is nontoxic [serum concentration of 25-OH-D_3 is 40 to 100 ng/mL *versus* 8 to 10 pg/mL for 1,25$(OH)_2D_3$]. We hypothesized that if 25-OH-D_3 could be covalently attached to the hormone-binding pocket of *apo*-VDR, it might be possible to convert the latter into transcriptionally active *holo*-form. This would make 25-OH-D_3 biologically active. Furthermore, it might be possible to translate the nontoxic nature of 25-OH-D_3 into its VDR-alkylating analog. Recently, we showed that 25-hydroxyvitamin D_3-3β-(2)-bromoacetate (25-OH-D_3-3-BE), a derivative of 25-OH-D_3, specifically alkylated the hormone-binding pocket of VDR (12). Therefore, 25-OH-D_3-3-BE became an ideal candidate to validate our hypothesis.

In the present study, we investigated the effect of 25-OH-D_3-3-BE in a set of normal and malignant cell lines and observed that antiproliferative property of 25-OH-D_3-3-BE was most pronounced in prostate cancer cells. In addition, we observed that 25-OH-D_3-3-BE caused apoptosis in prostate cancer cells; an observation supported by DNA fragmentation and caspase-activation studies. Mechanistic studies showed that the effects of 25-OH-D_3-3-BE were mediated by VDR. Moreover in a CD-1 mouse model, it was observed that 25-OH-D_3-3-BE did not raise serum calcium beyond control at doses considered to be highly toxic for 1,25$(OH)_2D_3$ and many of its synthetic analogs. Results of these studies and their implications are discussed in this communication.

MATERIALS AND METHODS

The 25-OH-D_3-3-BE was synthesized according to our published procedure (13). The majority of the chemicals were purchased from Sigma-Aldrich (St. Louis, MO) unless mentioned otherwise. The hVDR expression vector pAVhVDR was a generous gift from Dr. Wesley Pike (University of Wisconsin, Madison, WI). All of the cell lines were obtained from American Type Culture Collection (Manassas, VA), except LAPC4 cells that were obtained from the laboratory of Charles Sawyers (Department of Medicine, University of California at Los Angeles, Los Angeles, CA).

Male CD-1 mice 6 to 8 weeks old, average weight 30 g were purchased from The Jackson Laboratory (Bar Harbor, ME). They were housed in cages of five (5) in a group and were fed rat chow and water ad lib. Animal experiment was carried out in the animal facility of Boston University School of Medicine with strict adherence to the guidelines of Laboratory Animal Safety Committee. Serum calcium values in blood samples were determined at the Core Chemistry Laboratory of Boston University Medical Center.

Cell Culture. PZ-HPV-7 cells were grown in MCDB media containing pituitary extract, epidermal growth factor, and 1% penicillin/streptomycin. Keratinocytes were also grown in the same media with additional PG1 and insulin. PC-3, LNCaP, and DU-145 cells were grown in RPMI containing 10% fetal bovine serum (FBS) and antibiotics. MCF-7 cells were grown in DMEM containing 10% FBS and antibiotics. LAPC-4 cells were maintained in IMEM containing antibiotics including 1% L-glutamine and 10 nmol/L of R1881, a synthetic progestin. MC3T3 cells were grown in αMEM containing 10% FBS and antibiotics. In general, cells were grown in 35-mm dishes to 70 to 80% confluence and then plated into 24-well plates in respective media. After the cells grew to ~70% confluence, they were serum-starved for 20 hours (PC-3, LNCaP, and DU-145 cells) followed by incubation with steroid samples. Keratinocytes and PZ-HPV-7 cells, after reaching 70% confluence, were kept in MCDB media without additives for 20 hours before treatment with steroids. In general, reagents were dissolved in EtOH, and dilution with the media was adjusted in such a way that concentration of EtOH was 0.1% v/v.

In a separate experiment (cell counting), LAPC-4, LNCaP, MCF-7, and MC3T3 cells were grown to desired confluence and treated with the reagents (without serum starvation) for 24 hours (LNCaP, MC3T3, and LAPC-4) or 48 hours (MCF-7) with EtOH vehicle or 25-OH-D_3-3-BE (10^{-6} mol/L) or 1,25$(OH)_2D_3$ (10^{-7} mol/L). At the end of the experiment, cells were detached with trypsin-EDTA and counted in a Coulter counter.

Keratinocytes, procured from neonatal foreskin after overnight trypsinization at 4°C and treatment with 0.2% EDTA, were grown in culture with a modification of the published method (14). The 3T3 cells were plated at 10^4 cells/35-mm tissue-culture dish and were irradiated lethally after 2 days with a ^{60}Co source (5,000 rads). Keratinocytes, in 1 mL serum-free medium, were plated on lethally irradiated 3T3 cells. When these cells reached ~70% confluence, they were plated onto 24-well plates. Each experiment was done on primary or secondary keratinocyte cultures obtained from different skin samples.

The [^{3}H]Thymidine Incorporation Assay. In a typical assay, cells were grown to 60 to 70% confluence in 24-well plates in respective media containing 10% FBS, and serum starved for 20 hours, followed by treatment with various agents (in 0.1% ethanolic solution) or EtOH (vehicle) in serum-containing medium for 16 to 18 hours. After the treatment, media was removed from the wells and replaced with media containing [^{3}H]thymidine (0.1μCi) per well, and the cells were incubated for 3 hours at 37°C. After this period, media was removed by aspiration, and the cells were washed thoroughly (3 × 0.5 mL) with PBS. Then ice-cold 5% perchloric acid solution (0.5 mL) was added to each well, and the cells were incubated on ice for 20 minutes. After this incubation, perchloric acid was removed by aspiration, replaced with 0.5 mL of fresh perchloric acid solution, and the cells were incubated at 70°C for 20 minutes. Solution from each well was mixed with scintillation fluid and counted in a scintillation counter.

Majority of these assays were carried out in six (6) replicates with 10^{-6} mol/L of reagents. In the dose-response study, PC-3 cells were incubated with EtOH or 10^{-7} to 10^{-6} mol/L of 25-OH-D_3-3-BE or 1,25$(OH)_2D_3$ for 18 hours followed by [^{3}H]thymidine incorporation assay described above.

The 3-(4,5-Dimethylthiazol-2-yl)-5-(3-carboxymethoxyphenyl)-2-(4-sulfophenyl)-2*H*-tetrazolium (MTS) Cell Viability Assay. LNCaP, PC-3, and DU145 cells were plated in 96-well plates (7,500 cells per well), grown overnight in DMEM (with 10% FBS and antibiotics), and serum deprived for 24

hours. The cells were then treated with either EtOH or $1,25(OH)_2D_3$ (10^{-6} mol/L) or 25-OH-D_3-3-BE (10^{-6} mol/L) for 18 hours in complete media. Cell viability was measured with the CellTiter 96 AQueous Assay (Promega, Madison, WI). This assay used the tetrazolium compound (MTS, inner salt) and the electron-coupling reagent, phenazine methosulfate (15). This assay measured dehydrogenase enzyme activity found in metabolically active cells, which reduced MTS into soluble and colored formazan product, absorbance of which was measured at 490 nm. Because the production of formazan was proportional to the number of living cells, absorbance was a measure of cell-viability.

DNA-Fragmentation Analysis. PC-3 cells (2×10^6) were treated with 0.25×10^{-6} mol/L of $1,25(OH)_2D_3$, 25-OH-D_3, or 25-OH-D_3-3-BE for 10 hours. Then the cells were harvested and lysed in 0.5 mL of lysis buffer [20 mmol/L Tris-HCl, 10 mmol/L EDTA, 0.5% Triton X-100 (pH 8.0)], and DNA was extracted with phenol-chloroform procedure. The extracted DNA was resuspended in 0.1 mL of 20 mmol/L Tris-HCl (pH 8), and treated with RNase, followed by electrophoresis on a 1.2% agarose gel in TAE buffer. DNA bands were visualized under UV light after ethidinium bromide staining.

Caspase Activity. Caspase-3, -8, and -9 assays were done with Caspase colorimetric assay kit from R&D Systems (Minneapolis, MN) according to the manufacturer's instructions. Briefly, PC3 cells (1×10^6) were treated with 0.01×10^{-6} mol/L of $1,25(OH)_2D_3$, 25-OH-D_3, or 25-OH-D_3-3-BE for 14 hours in culture medium (DMEM, 10% FBS, and antibiotics). The cells were collected by centrifugation at 1,000 rpm for 5 minutes. The cell pellet was lysed with lysis buffer, and the lysate was incubated on ice for 10 minutes and centrifuged at 10,000 rpm for 5 minutes. Protein was estimated with Bradford protein estimation kit (Bio-Rad Laboratories, Hercules, CA). The enzymatic reactions were carried out in a 96-well plate. For each reaction, 100 μg lysate protein in 50 μL total volume was incubated with 50 μL of 2 × reaction buffer and 5 μL of caspase 3, caspase 8, or caspase 9 colorimetric substrates for 2 hours at 37°C. The absorbance was determined at 405 nm.

Induction of 1α,25-Dihydroxyvitamin D_3-24-Hydroxylase (24-OHase) Promoter Activity by 25-OH-D_3-3-BE and $1,25(OH)_2D_3$ in COS-7 Cells

Cell Transfections. Promoter constructs containing the rat 24-OHase promoter (−1,367/+74) linked to the chloramphenicol acetyltransferase (CAT) reporter gene were used for the experiment. COS-7 cells that were transfected with the hVDR expression vector pAVhVDR. All of the transfections were done with the calcium phosphate DNA precipitation method. The COS-7 cells were seeded with 1×10^6 cells/100 mm^2 tissue culture plate in DMEM supplemented with 10% FBS and 1% penicillin/streptomycin and allowed to grow for 18 to 20 hours or to 70 to 80% confluency. The DNA to be transfected was EtOH-precipitated. For each plate to be transfected, 450 μL of sterile ddH_2O and 50 μL of 2.5 mol/L $CaCl_2$ were added to the DNA pellet. This mixture was then added to 500 μL of 2 × HEPES buffer per sample dropwise while mixing. After the two solutions were combined, the resulting mixture was vortexed and allowed to sit at room temperature for 20 minutes to allow the DNA to precipitate. Finally, the DNA precipitate was mixed thoroughly, and 1 mL aliquots were added to each plate. Sixteen hours post transfection, cells were "shocked" for 1 minutes with PBS containing 10% dimethylsulfoxide, washed with PBS, and the DMEM supplemented with 2% of charcoal dextran-treated FBS was added to each plate. The cells were then treated with various doses of $1,25(OH)_2D_3$ or 25 OH-D_3-3-BE for 24 hours.

CAT Assay. Treated cells were harvested by trypsinization for about 2 minutes at 37°C, pelleted, washed with PBS, resuspended in 0.25 mol/L Tris-HCl (pH 8.0), and lysed by freezing and thawing five (5) times. Cellular extracts were collected and used for CAT assays.

CAT analysis was done by standard protocols on the cell extracts normalized to total protein content. Fifty microliters aliquots of cellular extracts containing equal amounts of protein were combined with 25 μL of 1 mol/L Tris-HCl (pH 8.0), 53 μL of ddH_2O, 20 μL of 4 mmol/L acetyl CoA, 2 μL of ^{14}C chloramphenicol (50 mCi/mmol; Sigma, St. Louis, MO), and 0.25 mmol/L Tris-HCl (pH 8.0) to a final volume of 150 μL. The reactions were carried out at 37°C for about 2 hours and stopped by adding 1 mL of ethyl acetate and vortexing. The samples were centrifuged at 14,000 rpm at 4°C for 10 minutes, and the upper ethyl acetate layer was removed to a microcentrifuge tube and dried under vacuum for 45 minutes. The samples were resuspended in 25 μL of ethyl acetate and spotted on a TLC plate. Chromatography was done in a chromatography chamber containing 100 mL of chloroform-methanol (95:5) for 40 minutes. The plate was dried and exposed to Kodak autoradiographic film. The resulting autoradiogram was analyzed by densitometric scanning with the Shimadzu CS9000U Dual-wavelength Flying Spot Scanner (Shimadzu Scientific Instruments, Princeton, NJ).

Pull Down Assays to Determine the Interaction of VDR with Retinoid X Receptor (RXR) and GRIP-1 in the Presence of $1,25(OH)_2D_3$ or 25-OH-D_3-3-BE in PC-3 Cells. In this assay, PC-3 cells were incubated for either 1 or 24 hours with the indicated concentrations of $1,25(OH)_2D_3$ or 25-OH-D_3-3-BE, and then the cells were scraped, homogenized, and whole-cell extracts were prepared in NETND buffer [100 mmol/L NaCl, 1 mmol/L EDTA, 20 mmol/L Tris-HCl (pH 7.8), 0.2% NP40, and 1 mmol/L dithiothreitol] containing 0.3 mol/L KCl. Then, 5 μg of purified glutathione *S*-transferase (GST) fusion protein (GST-GRIP or GST-RXR), and 20 μL of glutathione-Sepharose beads were added, and the volume was brought up to 100 μL with the same buffer. These mixtures were incubated for 1 or 24 hours at 4°C, and the beads were washed 3 times with 0.2 mL of NETND buffer. The bound proteins were eluted from the packed beads by boiling in Laemmli buffer for 3 minutes and were analyzed by SDS-PAGE. Detection of "bound-VDR" was done after SDS-PAGE by Western blots with VDR antibodies (Affinity BioReagents, Golden CO).

Determination of Systemic Toxicity (Calcemia) of 25-OH-D_3-3-BE in CD-1 Mice. Three doses of 25-OH-D_3-3-BE (3.3, 33, or 166.7 μg/kg) and two doses (3.3 or 33 μg/kg) of 25-OH-D_3 were prepared in 0.2 mL of saline-EtOH (0.1%) by diluting ethanolic solutions of the steroids with saline in such a way that the concentration of EtOH was 0.1% in the solution. These samples or saline-EtOH (0.1%) vehicle control (0.2 mL) were administered to the animals (in groups of five) intraperi-

hours. The cells were then treated with either EtOH or $1,25(OH)_2D_3$ (10^{-6} mol/L) or 25-OH-D_3-3-BE (10^{-6} mol/L) for 18 hours in complete media. Cell viability was measured with the CellTiter 96 AQueous Assay (Promega, Madison, WI). This assay used the tetrazolium compound (MTS, inner salt) and the electron-coupling reagent, phenazine methosulfate (15). This assay measured dehydrogenase enzyme activity found in metabolically active cells, which reduced MTS into soluble and colored formazan product, absorbance of which was measured at 490 nm. Because the production of formazan was proportional to the number of living cells, absorbance was a measure of cell-viability.

DNA-Fragmentation Analysis. PC-3 cells (2×10^6) were treated with 0.25×10^{-6} mol/L of $1,25(OH)_2D_3$, 25-OH-D_3, or 25-OH-D_3-3-BE for 10 hours. Then the cells were harvested and lysed in 0.5 mL of lysis buffer [20 mmol/L Tris-HCl, 10 mmol/L EDTA, 0.5% Triton X-100 (pH 8.0)], and DNA was extracted with phenol-chloroform procedure. The extracted DNA was resuspended in 0.1 mL of 20 mmol/L Tris-HCl (pH 8), and treated with RNase, followed by electrophoresis on a 1.2% agarose gel in TAE buffer. DNA bands were visualized under UV light after ethidinium bromide staining.

Caspase Activity. Caspase-3, -8, and -9 assays were done with Caspase colorimetric assay kit from R&D Systems (Minneapolis, MN) according to the manufacturer's instructions. Briefly, PC3 cells (1×10^6) were treated with 0.01×10^{-6} mol/L of $1,25(OH)_2D_3$, 25-OH-D_3, or 25-OH-D_3-3-BE for 14 hours in culture medium (DMEM, 10% FBS, and antibiotics). The cells were collected by centrifugation at 1,000 rpm for 5 minutes. The cell pellet was lysed with lysis buffer, and the lysate was incubated on ice for 10 minutes and centrifuged at 10,000 rpm for 5 minutes. Protein was estimated with Bradford protein estimation kit (Bio-Rad Laboratories, Hercules, CA). The enzymatic reactions were carried out in a 96-well plate. For each reaction, 100 μg lysate protein in 50 μL total volume was incubated with 50 μL of 2 × reaction buffer and 5 μL of caspase 3, caspase 8, or caspase 9 colorimetric substrates for 2 hours at 37°C. The absorbance was determined at 405 nm.

Induction of 1α,25-Dihydroxyvitamin D_3-24-Hydroxylase (24-OHase) Promoter Activity by 25-OH-D_3-3-BE and $1,25(OH)_2D_3$ in COS-7 Cells

Cell Transfections. Promoter constructs containing the rat 24-OHase promoter (−1,367/+74) linked to the chloramphenicol acetyltransferase (CAT) reporter gene were used for the experiment. COS-7 cells that were transfected with the hVDR expression vector pAVhVDR. All of the transfections were done with the calcium phosphate DNA precipitation method. The COS-7 cells were seeded with 1×10^6 cells/100 mm^2 tissue culture plate in DMEM supplemented with 10% FBS and 1% penicillin/streptomycin and allowed to grow for 18 to 20 hours or to 70 to 80% confluency. The DNA to be transfected was EtOH-precipitated. For each plate to be transfected, 450 μL of sterile ddH_2O and 50 μL of 2.5 mol/L $CaCl_2$ were added to the DNA pellet. This mixture was then added to 500 μL of 2 × HEPES buffer per sample dropwise while mixing. After the two solutions were combined, the resulting mixture was vortexed and allowed to sit at room temperature for 20 minutes to allow the DNA to precipitate. Finally, the DNA precipitate was mixed thoroughly, and 1 mL aliquots were added to each plate. Sixteen hours post transfection, cells were "shocked" for 1 minutes with PBS containing 10% dimethylsulfoxide, washed with PBS, and the DMEM supplemented with 2% of charcoal dextran-treated FBS was added to each plate. The cells were then treated with various doses of $1,25(OH)_2D_3$ or 25 OH-D_3-3-BE for 24 hours.

CAT Assay. Treated cells were harvested by trypsinization for about 2 minutes at 37°C, pelleted, washed with PBS, resuspended in 0.25 mol/L Tris-HCl (pH 8.0), and lysed by freezing and thawing five (5) times. Cellular extracts were collected and used for CAT assays.

CAT analysis was done by standard protocols on the cell extracts normalized to total protein content. Fifty microliters aliquots of cellular extracts containing equal amounts of protein were combined with 25 μL of 1 mol/L Tris-HCl (pH 8.0), 53 μL of ddH_2O, 20 μL of 4 mmol/L acetyl CoA, 2 μL of ^{14}C chloramphenicol (50 mCi/mmol; Sigma, St. Louis, MO), and 0.25 mmol/L Tris-HCl (pH 8.0) to a final volume of 150 μL. The reactions were carried out at 37°C for about 2 hours and stopped by adding 1 mL of ethyl acetate and vortexing. The samples were centrifuged at 14,000 rpm at 4°C for 10 minutes, and the upper ethyl acetate layer was removed to a microcentrifuge tube and dried under vacuum for 45 minutes. The samples were resuspended in 25 μL of ethyl acetate and spotted on a TLC plate. Chromatography was done in a chromatography chamber containing 100 mL of chloroform-methanol (95:5) for 40 minutes. The plate was dried and exposed to Kodak autoradiographic film. The resulting autoradiogram was analyzed by densitometric scanning with the Shimadzu CS9000U Dual-wavelength Flying Spot Scanner (Shimadzu Scientific Instruments, Princeton, NJ).

Pull Down Assays to Determine the Interaction of VDR with Retinoid X Receptor (RXR) and GRIP-1 in the Presence of $1,25(OH)_2D_3$ or 25-OH-D_3-3-BE in PC-3 Cells. In this assay, PC-3 cells were incubated for either 1 or 24 hours with the indicated concentrations of $1,25(OH)_2D_3$ or 25-OH-D_3-3-BE, and then the cells were scraped, homogenized, and whole-cell extracts were prepared in NETND buffer [100 mmol/L NaCl, 1 mmol/L EDTA, 20 mmol/L Tris-HCl (pH 7.8), 0.2% NP40, and 1 mmol/L dithiothreitol] containing 0.3 mol/L KCl. Then, 5 μg of purified glutathione *S*-transferase (GST) fusion protein (GST-GRIP or GST-RXR), and 20 μL of glutathione-Sepharose beads were added, and the volume was brought up to 100 μL with the same buffer. These mixtures were incubated for 1 or 24 hours at 4°C, and the beads were washed 3 times with 0.2 mL of NETND buffer. The bound proteins were eluted from the packed beads by boiling in Laemmli buffer for 3 minutes and were analyzed by SDS-PAGE. Detection of "bound-VDR" was done after SDS-PAGE by Western blots with VDR antibodies (Affinity BioReagents, Golden CO).

Determination of Systemic Toxicity (Calcemia) of 25-OH-D_3-3-BE in CD-1 Mice. Three doses of 25-OH-D_3-3-BE (3.3, 33, or 166.7 μg/kg) and two doses (3.3 or 33 μg/kg) of 25-OH-D_3 were prepared in 0.2 mL of saline-EtOH (0.1%) by diluting ethanolic solutions of the steroids with saline in such a way that the concentration of EtOH was 0.1% in the solution. These samples or saline-EtOH (0.1%) vehicle control (0.2 mL) were administered to the animals (in groups of five) intraperi-

toneally over a period of 12 days (injection on alternate days). At the end of the experiment the animals were lightly anesthetized, and blood was collected after decapitation for serum calcium-analysis. Body weights at the beginning and at the end of the experiment were recorded.

Data Analysis. Majority of the assays was carried out in three to six replicates. Statistical analyses of the data were done with linear regression analysis and one-way ANOVA followed by Fisher's protected least significant difference tests. $Ps \leq 0.05$ were considered statistically significant.

RESULTS AND DISCUSSION

The $1,25(OH)_2D_3$ and many of its synthetic analogs inhibit the growth of malignant cells (16). However, translation of the cellular results into *in vivo* studies has been problematic because of acute toxicity of the hormone and some of its analogs. Therefore, a major effort has been underway in designing analogs that would either inhibit cellular growth at physiologic concentrations to avoid systemic toxicity or be nontoxic at supraphysiologic doses.

VDR-binding affinity is crucial in developing $1,25(OH)_2D_3$ analogs because of the recognition that interaction between VDR and the analogs is pivotal in the genomic process (3, 4). Therefore, analogs with relatively low VDR-binding affinity have not been considered to be of therapeutic importance. For example, 25-OH-D_3, the metabolic precursor of $1,25(OH)_2D_3$, has a poor VDR-binding affinity [$K_d = 10^{-6}$ to 10^{-7} mol/L *versus* $K_d = 10^{-9}$ to 10^{-10} mol/L for $1,25(OH)_2D_3$]. Therefore, 25-OH-D_3 and its derivatives have not been studied significantly as candidates for drug-development.

We hypothesized that covalent linking of 25-OH-D_3 (via its derivative/analog) to the hormone-binding pocket of VDR might permanently lock VDR into its biologically active *holo*-form. This way, biologically inactive 25-OH-D_3 might acquire significant cell regulatory property. Furthermore, because of the recognition that calcemic property could be separated from cell regulatory properties, the nontoxic property of 25-OH-D_3 might be translated into its derivative. As a result, even supraphysiologic doses of this 25-OH-D_3 analog might be used to achieve inhibition of cell growth without systemic toxicity in an *in vivo* system.

In a recent, study we showed that 1α,25-dihydroxyvitamin D_3-3β-(2)-bromoacetate [$1,25(OH)_2D_3$-3-BE], an affinity labeling derivative of $1,25(OH)_2D_3$, displayed strong antiproliferative effect in several normal and malignant cell lines with strongest activity toward prostate cancer cells (17–21). In the current study, we focused on a structural 25-OH-D_3-prototype of $1,25(OH)_2D_3$-3-BE (*i.e.*, 25-OH-D_3-3-BE).

Growth-inhibitory effect of $1,25(OH)_2D_3$ and its analogs is known to vary among cell lines and even among lines from the same tissue. But, in general, strongest and predictable effect is observed at a 10^{-6} mol/L concentration of the hormone or its analogs (22). Although this concentration is considered to be physiologically irrelevant, it produces optimal effect. We treated primary culture of normal human skin cells, and several cell lines including LNCaP human androgen-sensitive and PC-3 human androgen-refractory prostate cancer cells, and PZ-HPV-7 immortalized normal human prostate cells with 10^{-6} mol/L of $1,25(OH)_2D_3$ or 25-OH-D_3-3-BE to compare the antiproliferative property of the analog (25-OH-D_3-3-BE) with the hormone.

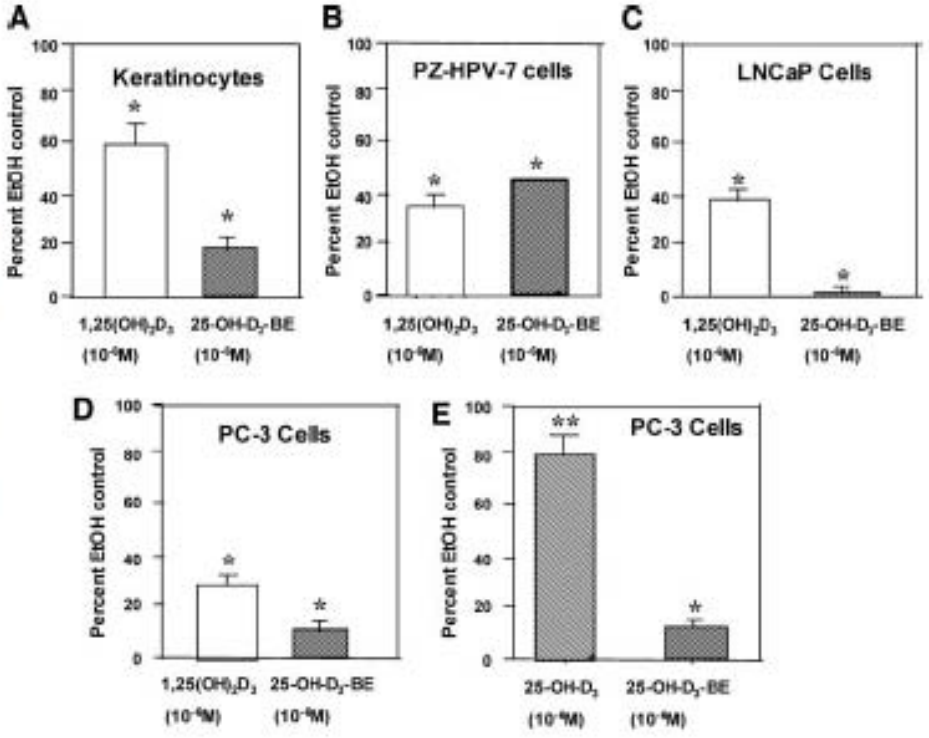

Fig. 1 [^{3}H]Thymidine incorporation assays of keratinocytes, PC-3, LNCaP, and PZ-HPV-7 cells. Cells, grown to 60 to 70% confluence were serum starved for 20 hours followed by treatment with 10^{-6} mol/L of 25-OH-D_3-3-BE, $1,25(OH)_2D_3$, 25-OH-D_3, or EtOH (control) for 16 hours followed by incubation with [^{3}H]thymidine and assaying for the incorporation of radioactivity in the cells. Results are expressed relative to EtOH control (100%). *, $P < 0.00032$; **, $P < 0.0075$. Bars, ±SD.

Effect of various agents on the growth of normal and malignant cells is often determined by [^{3}H]thymidine incorporation assay. In this assay, increase or decrease in the incorporation of [^{3}H]thymidine in the DNA of the growing cells by a reagent is used as an index of its proliferative/antiproliferative effect. As shown in Fig. 1, *A–E*, 10^{-6} mol/L of 25-OH-D_3-3-BE and 1,25$(OH)_2D_3$ inhibited the growth of all the cells with various efficiency. However, the effect of 25-OH-D_3-3-BE was strongest in LNCaP and PC-3 prostate cancer cells. For example, growth of LNCaP cells were inhibited by ~60% and 98% with 1,25$(OH)_2D_3$ and 25-OH-D_3-3-BE, respectively (Fig. 1*C*), whereas growth of PC-3 cells were retarded by 70% and 90% by 1,25$(OH)_2D_3$ and 25-OH-D_3-3-BE, respectively (Fig. 1*D*). In contrast, growth of normal immortalized prostate cells (PZ-HPV-7 cells) were inhibited by ~50% and 65% by 10^{-6} mol/L of 25-OH-D_3-3-BE and 10^{-6} mol/L of 1,25$(OH)_2D_3$, respectively (Fig. 1*B*). Growth inhibition by 25-OH-D_3-3-BE was stronger than an equivalent amount of 1,25$(OH)_2D_3$ in keratinocytes (Fig. 1*A*). Furthermore, 10^{-6} mol/L of 25-OH-D_3 showed marginal antiproliferative effect in PC-3 cells (Fig. 1*E*). We also observed that 10^{-6} mol/L of 25-OH-D_3-3-BE was cytotoxic only to LNCaP and PC-3 cells, causing the cells to lift, float, and die under phase contrast microscope.

In a cell counting assay, we observed that LNCaP and LAPC-4 cells had sharply reduced number with 10^{-6} mol/L of 25-OH-D_3-3-BE after 24 hours incubation (Fig. 2*A*), whereas MC3T3 cells were affected to a much lesser extent, and MCF-7 cells (incubated for 48 hours) were not significantly affected. It should be noted that in this assay cells were not serum starved before addition of the reagents, and 10^{-7} mol/L of 1,25$(OH)_2D_3$ had little effect in all of the cells. The 10^{-7} mol/L of 1,25$(OH)_2D_3$ was shown to produce significant effect in LNCaP cells after a longer period (3 to 6 days) of incubation (23). However, we observed that the effect of 10^{-6} mol/L of 25-OH-D_3-3-BE was relatively rapid (optimal antiproliferation and cytotoxicity in prostate cancer cells was observed within 16 to 24 hours of incubation). Therefore, within the short timeframe of our studies, 10^{-6} mol/L of 25-OH-D_3-3-BE produced a strong effect in LNCaP and LAPC-4 cells, whereas 10^{-7} mol/L of 1,25$(OH)_2D_3$ showed very little effect, if any, in all of the cells tested.

We conducted a dose-response study in which PC-3 cells were treated with 10^{-7} mol/L and 10^{-6} mol/L of either 25-OH-D_3-BE or 1,25$(OH)_2D_3$ for 18 hours followed by [^{3}H]thymidine incorporation assay. Results of this assay showed that 10^{-6} mol/L of 25-OH-D_3-BE decreased the proliferation of the cells

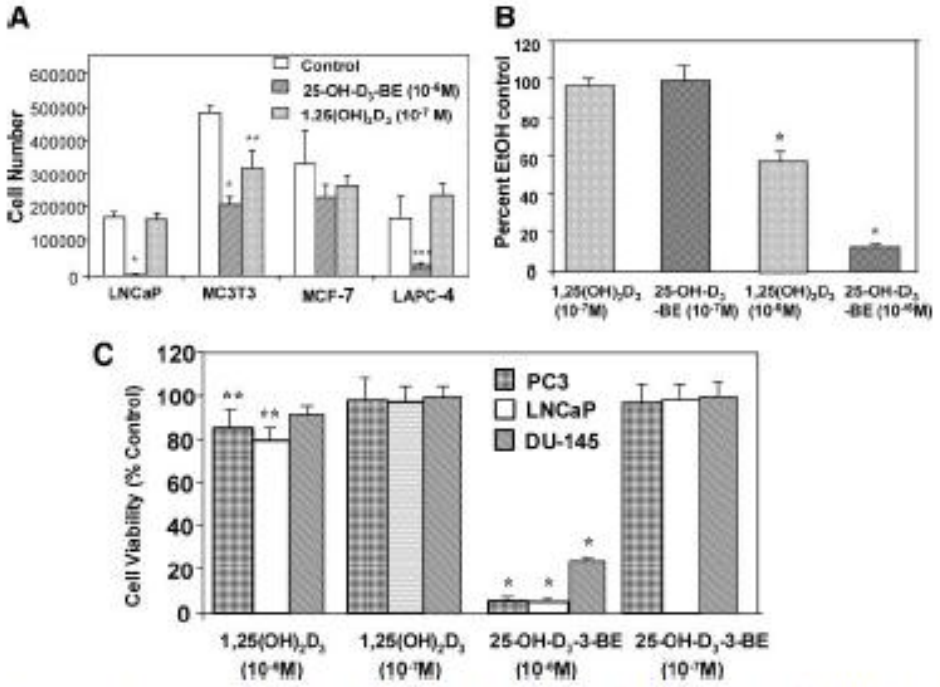

Fig. 2 *A*, cell counting assay of LAPC-4, LNCaP, MCF-7, and MC3T3 cells treated with 25-OH-D_3-3-BE or 1,25$(OH)_2D_3$. Each cell line was plated in 6-well plates at a density of either 80,000 cells per well (LNCaP, MCF-7, and MC3T3) or 160,000 cells per well (LAPC-4) and allowed to attach overnight. The cells were then treated for 24 hours (LNCaP, MC3T3, and LAPC-4) or 48 hours (MCF-7) with EtOH vehicle or 25-OH-D_3-3-BE (10^{-6} mol/L) or 1,25$(OH)_2D_3$ (10^{-7} mol/L). At the end of the experiment, cells were detached with trypsin-EDTA and counted in a Coulter counter. *, $P < 0.001$; **, $P = 0.003$; ***, $P = 0.014$. *B*, dose-response assays of 25-OH-D_3-3-BE or 1,25$(OH)_2D_3$ in PC-3 cells. Cells were incubated with either EtOH or 10^{-7} or 10^{-6} mol/L of 25-OH-D_3-3-BE or 1,25$(OH)_2D_3$ for 18 hours followed by [^{3}H]thymidine incorporation assay as described in Materials and Methods. *, $P < 0.005$. *C*, MTS cell viability assays of PC-3, LNCaP, and DU-145 cells. Cells were grown as described above and then treated with EtOH or 10^{-7} or 10^{-6} mol/L of either 25-OH-D_3-3-BE or 1,25$(OH)_2D_3$ for 20 hours followed by MTS assay as described in Materials and Methods, which included measurement of absorbance at 409 nm. Results are expressed in terms of percent of cell viability relative to EtOH-control (100%). *, $P < 0.0001$; **, $P < 0.05$. *Bars*, ±SD.

by ~90%, whereas there was ~45% reduction with 10^{-6} mol/L of $1,25(OH)_2D_3$. However, there was virtually no effect with 10^{-7} mol/L of either reagent (Fig. 2*B*). Furthermore, we observed that 25-OH-D_3-BE was toxic to these cells (as well as to LNCaP cells; Fig. 1*C*), as they were found detached and floating.

To elaborate on the cytotoxic nature of 25-OH-D_3-BE, we carried out MTS cell viability assay with LNCaP, PC-3, and DU-145 cells treated with 10^{-7} mol/L and 10^{-6} mol/L of 25-OH-D_3-BE or $1,25(OH)_2D_3$. Results of this assay (Fig. 2*C*) showed that 10^{-6} mol/L of 25-OH-D_3-BE reduced the number of viable cells to ~8% in LNCaP and PC-3 cells and 20% in DU-145 cells, whereas majority of the cells were viable when treated with 10^{-6} mol/L of $1,25(OH)_2D_3$. With 10^{-7} mol/L of 25-OH-D_3-BE and 10^{-7} mol/L and 10^{-6} mol/L of $1,25(OH)_2D_3$ majority of the cells were viable. These results suggested that 25-OH-D_3-BE induced toxicity in these cells at 10^{-6} mol/L. As mentioned earlier, repeated dosing of LNCaP cells with 10^{-7} mol/L of $1,25(OH)_2D_3$ for a prolonged period (48 hours) produced significant antiproliferative effect, whereas a single dose and shorter incubation period failed to produce such an effect (23). Therefore, it is probable that repeated dosing with 10^{-7} mol/L of 25-OH-D_3-BE for longer periods (we typically dosed the cells for 16 to 20 hours) might have produced significant antiproliferative and possibly cytotoxic effects.

Induction of toxicity in DU-145 cells deserves special attention, because it has been shown that DU-145 cells respond poorly to $1,25(OH)_2D_3$-treatment because of enhanced activity of the catabolic enzyme, 24-OHase (24, 25). We postulated that covalent attachment of 25-OH-D_3-BE into the ligand-binding pocket of VDR might prevent the catabolism of the analog and produce sufficient quantity of transcriptionally active VDR. Therefore, our results with DU-145 cells lend strong support for this hypothesis.

The growth inhibitory effect of $1,25(OH)_2D_3$ and its analogs is generally manifested via the arresting of cellular growth in G_0/G_1 phase; and such activity correlates well with the expression of cyclin-dependent kinase inhibitors, such as p21 and p27 (26). However, in some cases, apoptosis, or programmed cell death, has been reported. For example, it was reported that $1,25(OH)_2D_3$ induced apoptosis in MCF-7 cells (22, 27), although in prostate cancer cells reports are conflicting. For example, Blutt *et al.* (23) reported that $1,25(OH)_2D_3$ induced apoptosis in LNCaP cells, but another group failed to observe such an effect (28).

Fragmentation of nuclear DNA is a hallmark of the downstream process manifested by cells undergoing apoptosis. When PC-3 cells were treated with 0.25×10^{-6} mol/L of 25-OH-D_3-3-BE, 25-OH-D_3, or $1,25(OH)_2D_3$, DNA-fragmentation was observed only with cells treated with 25-OH-D_3-3-BE (Fig. 3*A*, *Lane 4*), whereas no such effect was visible with an equivalent amount of $1,25(OH)_2D_3$ (Fig. 3*A*, *Lane 2*) or 25-OH-D_3 (Fig. 3*A*, *Lane 3*). These results suggested that 25-OH-D_3-3-BE induced apoptosis in PC-3 cells, whereas an equivalent amount of 25-OH-D_3 and $1,25(OH)_2D_3$ failed to do so.

Caspases are key indicators of apoptosis in cells (29). For example, caspase 3 is activated during the cascade of events during apoptosis. It cleaves a variety of molecules containing DEVD amino acid motif. Such molecules include poly-ADP-ribose polymerase (PARP), U1-ribonucleoprotein, and so forth. Caspase 8 is an upstream caspase, and its activation leads to the activation of additional caspases and subsequent cleavage of PARP and other molecules. Caspase 9 is a key regulator of apoptosis *in vivo*. Activation of caspase 9 activates procaspase 3, which in turn is manifested through classical features of apoptosis such as cleavages of PARP, U1-ribonucleoprotein, and so forth.

Recently, Guzey *et al.* (30) reported that $1,25(OH)_2D_3$ activated caspase 3 and caspase 9, but not caspase 8, in ALVA-31 cells. Polek *et al.* (31) also showed that $1,25(OH)_2D_3$ did not induce apoptosis in PC-3 cells. When PC-3 cells were treated with 0.01×10^{-6} mol/L of 25-OH-D_3-3-BE or 25-OH-D_3 or $1,25(OH)_2D_3$, only 25-OH-D_3-3-BE showed strong induction of caspases 3, 8, and 9 (Fig. 3*B*). Therefore, DNA-fragmentation analysis and caspase-activation assay collectively suggested that 25-OH-D_3-3-BE induced apoptosis in PC-3 cells.

The 25-OH-D_3-3-BE contains an ester bond. Therefore, esterases in growing cells might hydrolyze this molecule to

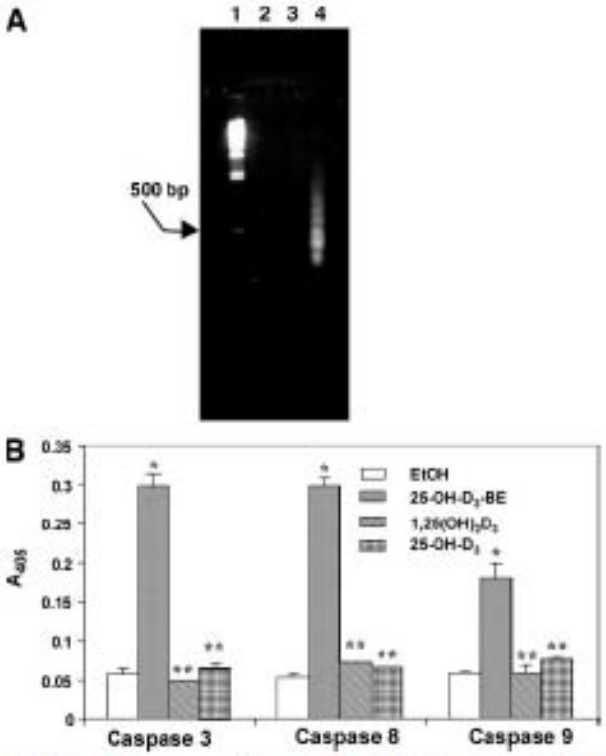

Fig. 3 *A*, DNA fragmentation analysis of PC-3 cells treated with 25-OH-D_3-3-BE or $1,25(OH)_2D_3$ or 25-OH-D_3. Cells were treated with 0.25×10^{-6} mol/L of reagents for 20 hours followed by extraction of the DNA of the cells undergoing apoptosis, and analysis on a DNA gel. The gel was visualized by ethidinium bromide staining. *Lane 1*, DNA markers; *Lane 2*, $1,25(OH)_2D_3$; *Lane 3*, 25-OH-D_3; *Lane 4*, 25-OH-D_3-3-BE. It should be noted that under the condition of our experiment, only the apoptotic DNA fragments leaking into the cytosol were extracted. *B*, caspase activation analysis of PC-3 cells treated with 25-OH-D_3-3-BE or $1,25(OH)_2D_3$ or 25-OH-D_3. Cells were incubated with 0.01×10^{-6} mol/L of 25-OH-D_3-3-BE, $1,25(OH)_2D_3$ or 25-OH-D_3 followed by colorimetric assays for caspase 3, 8, and 9 according to manufacturer's procedures. The X-axis represents absorbance of the solutions at 405 nm. *, $P < 0.0035$. *Bars*, ±SD.

produce equimolar amounts of 25-OH-D_3 and bromoacetic acid (Fig. 4, *top panel*). It could be argued that the observed effects of 25-OH-D_3-3-BE might be because of bromoacetic acid, 25-OH-D_3, or a combination of the two. To determine any role of *in situ*-produced bromoacetic acid (by the hydrolysis of 25-OH-D_3-3-BE), we carried out [^{3}H]thymidine incorporation assay in PC-3 cells treated with 10^{-6} mol/L of either bromoacetic acid or 25-OH-D_3-3-BE or a mixture containing 10^{-6} mol/L each of bromoacetic acid or 25-OH-D_3-3-BE. As shown in Fig. 4 (*bottom left panel*), 10^{-6} mol/L of 25-OH-D_3-3-BE was strongly antiproliferative to the cells, whereas 10^{-6} mol/L of bromoacetic acid did not have any significant effect on the proliferation of these cells. Furthermore, a mixture containing 10^{-6} mol/L each of bromoacetic acid and 25-OH-D_3-3-BE produced the same effects as 10^{-6} mol/L of 25-OH-D_3-3-BE alone (Fig. 4, *bottom right panel*). Therefore, these results strongly suggested that the observed properties of 25-OH-D_3-3-BE were related to its unhydrolyzed (intact) form.

However, the above results did not rule out the possibility that a part of 25-OH-D_3-3-BE might undergo hydrolysis, and 25-OH-D_3, produced *in situ* by this hydrolytic process, might be metabolically activated by 25-hydroxyvitamin D_3-1α-hydroxylase (1-OHase) to 1,25$(OH)_2D_3$, which could in turn produce the observed effects, at least partially. LNCaP cells are known to be deficient in the 1-OHase enzyme (32), yet 25-OH-D_3-3-BE showed strong antiproliferative effect in these cells (Fig. 1*C*). Furthermore, 10^{-6} mol/L of 25-OH-D_3 showed a very weak effect in PC-3 cells (Fig. 1*E*). These considerations essentially ruled out any role of *in situ*-produced 25-OH-D_3 in the observed antiproliferative and cytotoxic properties of 25-OH-D_3-3-BE.

The 25-OH-D_3-3-BE contains a chemically reactive α-halocarbonyl group; therefore, it could potentially alkylate any protein in a cellular system, and such random interaction could possibly be responsible for its observed effects. FBS contains many proteins, including a relatively large amount of vitamin D-binding protein, which could potentially react with 25-OH-D_3-3-BE, and eliminate it completely before it reacts with VDR. Typically, the assays described here were carried out in a media containing 5 to 10% FBS, suggesting that scavenging of 25-OH-D_3-3-BE by serum vitamin D-binding protein (and other cellular proteins in a random fashion) might not play a significant role in the observed properties of this compound.

Because VDR was our desired target to elicit the biological activity of 25-OH-D_3-3-BE, it became obligatory for us to show the involvement of processes related to 1,25$(OH)_2D_3$/VDR-signaling pathways. The 24-OHase gene is known to be strongly and predictably modulated by 1,25$(OH)_2D_3$ and its analogs. We carried out a study to evaluate the effect of 1,25$(OH)_2D_3$ and 25-OH-D_3-3-BE at various doses on the 24-OHase promoter activity in COS-7 cells that was transfected with a VDR construct, tagged with a CAT reporter gene. Results of this assay, shown in Fig. 5, showed that 24-OHase promoter activity was strongly up-regulated by 10^{-8}, 10^{-7}, and 10^{-6} mol/L of 1,25$(OH)_2D_3$. In contrast, strong promoter activity was displayed only with 10^{-6} mol/L of 25-OH-D_3-3-BE, and such activity declined almost to the basal level with 10^{-7} mol/L of 25-OH-D_3-3-BE. These results strongly suggested that the molecular action of 25-OH-D_3-3-BE might follow a path similar to 1,25$(OH)_2D_3$, however, with less efficiency.

An important aspect of ligand-receptor interaction is the ability of the hormone and the analogs to induce transcriptionally active conformation in VDR that can interact with RXR and other coactivators required for transcription, such as GRIP-1 (33). Therefore, to determine the potency of 1,25$(OH)_2D_3$ and 25-OH-D_3-3-BE to induce interaction of VDR with RXR and/or with the steroid receptor coactivator, GRIP-1, we used a pull

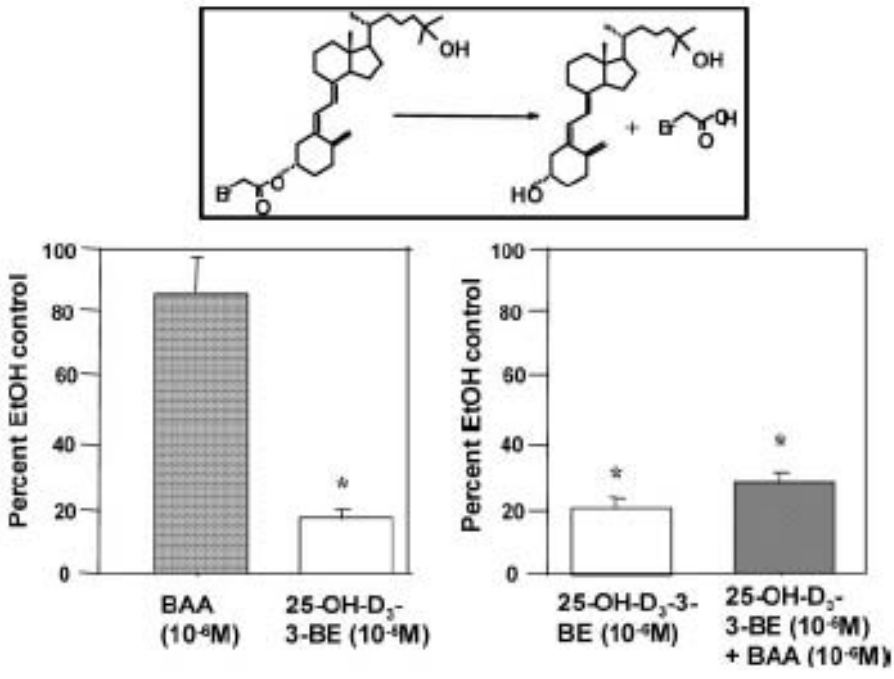

Fig. 4 top panel, scheme to show probable hydrolysis of the ester bond in 25-OH-D_3-3-BE to produce equimolar quantities of 25-OH-D_3 and bromoacetic acid. *bottom panel*, effects of 10^{-6} mol/L of 25-OH-D_3-3-BE or 1,25$(OH)_2D_3$ or bromoacetic acid or a combination of 25-OH-D_3-3-BE and bromoacetic acid (10^{-6} mol/L each) on the proliferation of PC-3 cells. Cells were treated with EtOH or 10^{-6} mol/L of the reagents and subjected to [^{3}H]thymidine incorporation assay in the usual fashion. *, $P < 0.005$. *Bars*, ±SD. (*BAA*, bromoacetic acid)

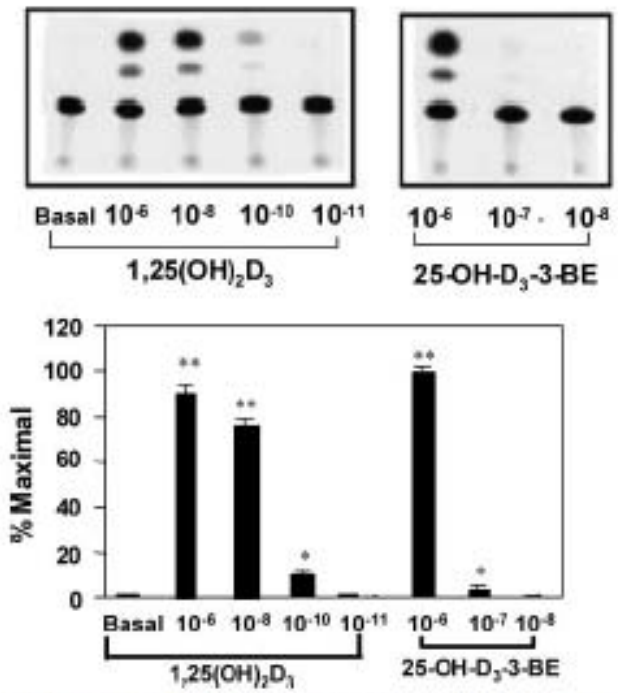

Fig. 5 Analysis of 24-OHase promoter activity in COS-7 cells, transiently transfected with a 24-OHase-construct, tagged with a chloramphenicon (CAT) reporter gene, and hVDR expression vector. Cells were treated with various doses (as indicated) of 25-OH-D_3-3-BE or $1,25(OH)_2D_3$, and CAT activity was determined as described in Materials and Methods. % *Maximal* in the X-axis denotes percentage of maximum activity (in this case with 10^{-6} mol/L of 25-OH-D_3-3-BE). *, $P < 0.005$; **, $P < 0.0001$. *Bars*, ±SD.

down assay in which PC-3 cells were incubated with various doses of $1,25(OH)_2D_3$ or 25-OH-D_3-3-BE, and VDR-interacting proteins were pulled down with GST-fused GRIP or RXR. Results of these assays showed strong interaction between VDR and GRIP-1 when the cells were incubated for 1 hour with 25-OH-D_3-3-BE (10^{-6} mol/L) or $1,25(OH)_2D_3$ (10^{-7} mol/L; Fig. 6, *left panel*). However, after 24 hours of incubation, strong interaction between VDR and GRIP-1 was observed with 10^{-7} mol/L of 25-OH-D_3-3-BE. With RXR, there was significant interaction even with 10^{-8} mol/L of 25-OH-D_3-3-BE (Fig. 6, *right panel*).

The above results provided the evidence that 25-OH-D_3-3-BE was able to activate VDR at substantially lower concentrations in PC-3 cells; which is consistent with the results of DNA-fragmentation and caspase-activation analysis. However, a significantly higher dose (10^{-6} mol/L) of 25-OH-D_3-3-BE was required to show 24-OHase–promoter activity in COS cells as well as antiproliferative activity in various cells. These discrepancies underscore the hypothesis that gene regulatory events leading to inhibition of cell growth might be different from those leading to apoptosis. Whether or not all of these cellular events are mediated through transcriptional activity of the VDR remains to be established. Furthermore, differences in the potency of analogs to induce different gene regulatory events through VDR in the same cell type have been reported by several studies, including Shevde *et al.* (34). This study with 2MD, an analog of $1,25(OH)_2D_3$, showed a range of sensitivity for regulating gene expression, from $ED_{50} = 10^{-11}$ mol/L for the up-regulation of RANKL to $ED_{50} > 10^{-10}$ mol/L for induction of the VDR responsive genes, osteopontin and 24-hydroxylase in mouse osteoblasts. Likewise, Ismail *et al.* (35) showed that the analog Ro-26-9228 had an ED_{50} of 2.1×10^{-8} mol/L for the induction of 24-OHase and an ED_{50} of 2.65×10^{-7} mol/L for induction of Calbindin D9k in Caco-2 cells.

A major concern involving $1,25(OH)_2D_3$ and its analogs is systemic toxicity (hypercalcemia, hypercalciuria) that is often found to be associated with these molecules. Therefore, if 25-OH-D_3-3-BE and related compounds were to be developed as therapeutic agents, they should be devoid of systemic toxicity. Although it is difficult to draw a direct correlation between *in vitro* and *in vivo* dosages, it was clear that doses (of 25-OH-D_3-BE) that might be required to reach a potential therapeutic level would be significantly higher than what has been customary

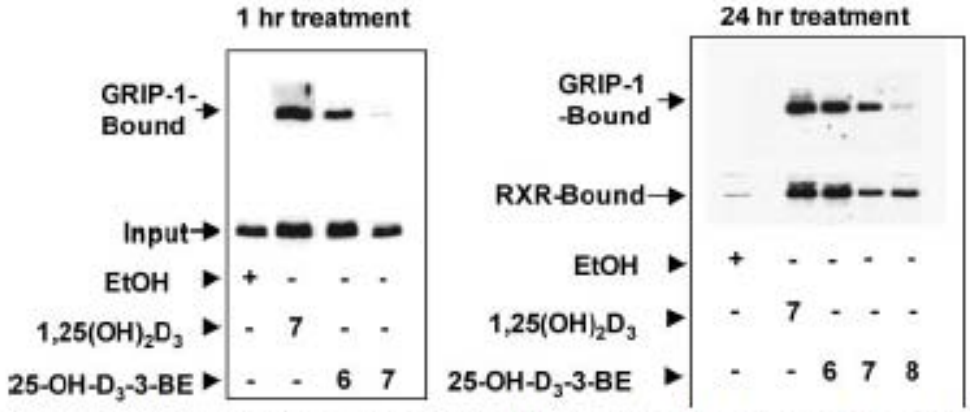

Fig. 6 Pull down assays in PC-3 cells to determine the interaction between VDR and RXR and GRIP-1, as the cells were treated with various doses of 25-OH-D_3-3-BE or $1,25(OH)_2D_3$ followed by incubation with GST-RXR or GST-GRIP-1 fusion proteins. The RXR and GRIP-1 bound proteins were adsorbed on glutathione-Sepharose beads. The bound proteins were eluted from the beads by boiling in Laemmli buffer and were analyzed by polyacrylamide gel electrophoresis. The protein bands were transferred onto a polyvinylidene difluoride membrane, and blots were visualized by Western blotting with an anti-VDR antibody.

Table 1 Body weight and serum calcium value of CD-1 mice treated with various doses of 25-OH-D_3 or 25-OH-D_3-3-BE

	Body weight on day 1 (grams)	Body weight on day 12 (grams)	Serum calcium on day 12 (mg/mL)
Saline-EtOH control	29.6 ± 2.4	29.6 ± 2.4	9.23 ± 0.15
25-OH-D_3-3-BE (3.3 μg/kg)	29.0 ± 0.6	29.0 ± 0.6	9.10 ± 0.20
25-OH-D_3-3-BE (33 μg/kg)	31.0 ± 0.83	32.9 ± 1.4	9.4 ± 0.20
25-OH-D_3-3-BE (166.7 μg/kg)	30.55 ± 0.7	30.7 ± 1.0	9.7 ± 0.10
25-OH-D_3 (3.3 μg/kg)	31.5 ± 1.56	33.5 ± 1	9.6 ± 0.2
25-OH-D_3 (33 μg/kg)	28.9 ± 2	30.66 ± 2	9.7 ± 0.8

with 1,25$(OH)_2D_3$ and its analogs. However, we surmised that an analog of 25-OH-D_3/1,25$(OH)_2D_3$ could be useful in higher concentrations as long as it did not show systemic toxicity. For example, higher than customary doses of 1α-hydroxyvitamin D_5 were used *in vivo* to elicit desired effects (36).

We carried out a toxicity study of 25-OH-D_3-BE in CD-1 mice where we used 25-OH-D_3 as a control. Our purpose was to determine whether we could extrapolate the nontoxic property of 25-OH-D_3 to its analog (*i.e.*, 25-OH-D_3-BE) and to obtain a preliminary idea about the safe dose levels of 25-OH-D_3-BE. As shown by the results (Table 1), there was no significant difference in serum calcium values and weights of the animals from the vehicle control with 3.3 or 33.0 μg/kg of 25-OH-D_3 or 25-OH-D_3-BE. Although there was a slight increase in serum calcium value only with the highest dose (166.7 μg/kg) of 25-OH-D_3-BE, body weights of the animals were not significantly different from the vehicle control. It should be emphasized that the above results simply denoted that 25-OH-D_3-BE had a significantly lower toxicity than 1,25$(OH)_2D_3$ or majority of its analogs without providing any information on its effective serum concentration and bioavailability. We have shown that 25-OH-D_3-BE is the active molecule that is responsible for the observed antiproliferative activity in prostate cancer cells (Fig. 4). But, we appreciate that 25-OH-D_3-BE can undergo hydrolytic cleavage *in vivo* to reduce its bioavailability. In the future, we will carry out pharmacokinetic and pharmacodynamic studies to shed light on this issue.

In toxicity studies, it is customary to use 1,25$(OH)_2D_3$ as a control. But 1,25$(OH)_2D_3$ and many of its synthetic analogs are known to be toxic at doses used in our study. For example, in a recent publication it was reported that 1.0 μg/kg of 1,25$(OH)_2D_3$ and EB-1089 [a noncalcemic analog of 1,25$(OH)_2D_3$] raised serum calcium beyond vehicle control, although significantly less with EB-1089 than 1,25$(OH)_2D_3$ (37). For obvious reasons, we could not use 1,25$(OH)_2D_3$ or EB-1089 as controls at high dose levels that were used in our toxicity study with 25-OH-D_3-BE.

The 1,25$(OH)_2D_3$ and its analogs are generally not known to have tissue/tumor specific effects because of the ubiquitous nature of VDR, the chief modulator of their actions. In this communication, we report that 25-OH-D_3-3-BE, a VDR-affinity alkylating derivative of the prehormone, displayed strong antiproliferative activity in androgen-sensitive LNCaP and LAPC-4 and androgen refractory PC-3 and DU-145 cells. In addition, 25-OH-D_3-3-BE induced apoptosis in these prostate cancer cells but not in normal immortalized prostate cells (PZ-HPV-7) at the same dose level. The reason behind the prostate cancer cell-specific effects of 25-OH-D_3-3-BE can only be speculated at this point. It is noteworthy that 1,25$(OH)_2D_3$-3-BE, the 1,25$(OH)_2D_3$ prototype of 25-OH-D_3-3-BE, showed very similar antiproliferative and apoptotic behavior (as 25-OH-D_3-3-BE) in prostate cancer cells (17). Therefore, we surmise that covalent labeling of the hormone binding pocket [by 25-OH-D_3-3-BE and 1,25$(OH)_2D_3$-3-BE] is crucial for their prostate cancer-specific effects. However, antiproliferative index of C-1 and C-11 bromoacetates of 1,25$(OH)_2D_3$ [which affinity alkylated VDR similar to 1,25$(OH)_2D_3$-3-BE] in keratinocytes was much lower than 1,25$(OH)_2D_3$-3-BE.[6] This suggested that covalent modification of a specific area of VDR [by 3-boromoactetates: 25-OH-D_3-3-BE and 1,25$(OH)_2D_3$-3-BE] has a profound effect on transcriptional activities. We postulate that 25-OH-D_3-3-BE changes the conformation of VDR (on alkylation) so that the liganded receptor specifically and uniquely modulate certain factor/factors directly or indirectly in the prostate cancer cells. We are currently in the process of identifying such factor/factors by gene-profiling experiments.

Several clinical trials involving 1,25$(OH)_2D_3$ and its analogs in prostate and other cancers are currently underway. Results of the studies described in this report strongly suggest that 25-OH-D_3-3-BE and related VDR-cross linking analogs of 25-OH-D_3 might be useful as potential therapeutic agents for androgen-sensitive and androgen-refractory prostate cancer.

ACKNOWLEDGMENTS

The authors would like to thank Kelly Persons for his assistance with cell culture experiments.

REFERENCES

1. Eckhardt S. Recent progress in the development of anticancer agents. Curr Med Chem Anti-Canc Agents 2002;2:419–39.

2. Sweet FW, Murdock GL. Affinity labeling of hormone-specific proteins. Endocr Rev 1987;8:154–84.

3. Haussler MR, Whitfield GK, Haussler CA, et al. The nuclear vitamin D receptor: biological and molecular regulatory properties revealed. J Bone Miner Res 1998;13:325–49.

4. Jones G, Strugnell SA, DeLuca HF. Current understanding of the molecular actions of vitamin D. Physiol Rev 1998;78:1193–231.

5. Johnson CS, Herrhberger PA, Bernardi RJ, Meguire TF, Trump DL, Vitamin D receptor: a potential target for intervention. Urology 2002; 60:123–30.

[6] Ray R., Swamy N., unpublished results.

6. Bouillon R, Okamura WH, Norman AW. Structure-function relationships in the vitamin D endocrine system. Endocr Rev 1995;16:200–57.

7. Dalhoff K, Dancey J, Astrup L, et al. A phase II study of the vitamin D analogue Seocalcitol in patients with inoperable hepatocellular carcinoma. Br J Cancer 2003;89:252–7.

8. Evans TR, Colston KW, Lofts FJ, et al. A phase II trial of the vitamin D analogue Seocalcitol (EB1089) in patients with inoperable pancreatic cancer. Br J Cancer 2002;86:680–5.

9. El Abdaimi K, Dion N, Papavasiliou V, et al. The vitamin D analogue EB 1089 prevents skeletal metastasis and prolongs survival time in nude mice transplanted with human breast cancer cells. Cancer Res 2000;60:4412–48.

10. Colston KW, Pirianov G, Bramm E, Hamberg KJ, Binderup L. Effects of Seocalcitol (EB1089) on nitrosomethyl urea-induced rat mammary tumors. Breast Cancer Res Treat 2003;80:303–11.

11. James SY, Mercer E, Brady M, Binderup L, Colston KW. EB1089, a synthetic analogue of vitamin D, induces apoptosis in breast cancer cells in vivo and in vitro. Br J Pharmacol 1998;125:953–62.

12. Swamy N, Addo J, Ray R. Development of an affinity-driven double cross-linker: isolation of a ligand-activated factor, associated with vitamin D receptor-mediated transcriptional machinery. Bioorg Med Chem Lett 2000;10:361–4.

13. Swamy N, Ray R. Affinity labeling of rat serum vitamin D binding protein. Arch Biochem Biophys 1996;333:139–44.

14. Rheinwald JG, Green H. Serial cultivation of strains of human epidermal keratinocytes: the formation of keratinizing colonies from single cells. Cell 1975;6:331–15.

15. Malich G, Markovic B, Winder C. The sensitivity and specificity of the MTS tetrazolium assay for detecting the in vitro cytotoxicity of 20 chemicals using human cell lines. Toxicology 1997;124:179–92.

16. Campbell MJ, Koeffler HP. Toward therapeutic intervention of cancer by vitamin D compounds. J Natl Cancer Inst (Bethesda) 1997; 89:82–5.

17. Swamy N, Persons K, Chen TC, Ray R. 1α,25-Dihydroxyvitamin D_3-3β-(2)-bromoacetate, an affinity labeling derivative of 1alpha,25-dihydroxyvitamin D_3 displays strong antiproliferative and cytotoxic behavior in prostate cancer cells. J Cell Biochem 2003;89:909–16.

18. Swamy N, Xu W, Paz N, et al. Molecular modeling, affinity labeling, and site-directed mutagenesis define the key points of interaction between the ligand-binding domain of the vitamin D nuclear receptor and 1 alpha,25-dihydroxyvitamin D_3. Biochemistry 2000;39: 12162–71.

19. Chen ML, Ray S, Swamy N, Holick MF, Ray R. Mechanistic studies to evaluate the enhanced antiproliferation of human keratinocytes by 1α,25-dihydroxyvitamin D_3-3-bromoacetate, a covalent modifier of vitamin D receptor, compared with 1-alpha,25-dihydroxyvitamin D_3. Arch Biochem Biophys 1999;370:34–44.

20. Swamy N, Kounine M, Ray R. Identification of the subdomain in the nuclear receptor for the hormonal form of vitamin D_3, 1α,25-dihydroxyvitamin D_3, vitamin D receptor, that is covalently modified by an affinity labeling reagent. Arch Biochem Biophys 1997;34:91–5.

21. Ray R, Swamy N, MacDonald PN, et al. Affinity labeling of the 1α,25-dihydroxyvitamin D_3 receptor. J Biol Chem 1996;271:2012–7.

22. Simbolli-Campbell M, Narvaez CJ, Tenniswood J, Welsh J. 1,25-Dihydroxyvitamin D_3 induces morphological and biochemical markers of apoptosis in MCF-7 breast cancer cells. J Steroid Biochem 1996;58: 367–76.

23. Blutt SE, McDonnell TJ, Polek TC, Weigel NL. Calcitriol-induced apoptosis in LNCaP cells is blocked by overexpression of Bcl-2. Endocrinology 2000;141:10–7.

24. Skowronski RJ, Peehl DM, Feldman D. Actions of vitamin D_3 analogs on human prostate cancer cell lines: comparison with 1,25-dihydroxyvitamin D_3. Endocrinology 1995;136:20–6.

25. Ly LH, Zhao XY, Holloway L, Feldman D. Liarozole acts synergistically with1-alpha,25-dihydroxyvitamin D_3 to inhibit growth of DU 145 human prostate cancer cells by blocking 24-hydroxylase activity. Endocrinology 1999;140:2071–6.

26. Liu M, Lee MH, Cohen M, Bommakanti M, Freedman L. Transcriptional activation of the CDK inhibitor p21 by vitamin D_3 leads to the induced differentiation of the myelomonocytic cell line. Genes Dev 1996;10:142–53.

27. Narvaez CJ, Welsh J. Role of mitochondria and caspases in vitamin D-mediated apoptosis of MCF-7 breast cancer cells. J Biol Chem 2001;276:9101–7.

28. Zhuang SH, Burnstein KL. Antiproliferative effect of 1α,25-dihydroxyvitamin D_3 in human prostate cancer cell line LNCaP involves reduction of cyclin-dependent kinase 2 activity and persistent G1 accumulation. Endocrinology 1998;139:1197–207.

29. Shi Y. Caspase activation: revisiting the induced proximity model. Cell 2004;117:855–8.

30. Guzey M, Kitada S, Reed C. Apoptosis induction by 1-alpha,25-dihydroxyvitamin D_3 in prostate cancer. Mol Cancer Ther 2002;1: 667–77.

31. Polek TC, Stewart LV, Ryu EJ, et al. p53 Is required for 1,25-dihydroxyvitamin D3-induced G0 arrest but is not required for G1 accumulation or apoptosis of LNCaP prostate cancer cells. Endocrinology 2003;144:50–32.

32. Whitlatch LW, Young MV, Schwartz GG, et al. 25-Hydroxyvitamin D-1-alpha-hydroxylase activity is diminished in human prostate cancer cells and is enhanced by gene transfer. J Steroid Biochem Mol Biol 2002;2002;81:135–40.

33. Liu YY, Nguyen C, Peleg S. Regulation of ligand-induced heterodimerization and coactivator interaction by the activation function-2 domain of the vitamin D receptor. Mol Endocrinol 2000;14:1776–8.

34. Shevde NK, Plum LA, Clagett-Dame M, Yamamoto H, Pike JW. A potent analog of 1–1alpha, 25-dihydroxyvitamin D_3 selectively induces bone formation. Proc Natl Acad Sci USA 2002;99:13487–91.

35. Ismail A, Nguyen CV, Ahene A, et al. Effect of cellular environment on the selective activation of the vitamin D receptor by 1-alpha, 25-dihydroxyvitamin D_3 and its analog 1-alpha-fluoro-16-ene-20-epi-23-ene-26,27-bishomo-25-hydroxyvitamin D_3 (Ro-26-9228). Mol Endocrinol 2004;18:874–87.

36. Hussain EA, Mehta RR, Ray R, Das Gupta TK, Mehta RG. Efficacy and mechanism of action of 1α-hydroxy2-ethyl-cholecalciferol (1α[OH]D5) in breast cancer prevention and therapy. Recent Results Cancer Res 2003;164:393–411.

37. Lokeshwar BL, Schwartz GG, Selzer MG, et al. Inhibition of prostate metastasis in vivo: a comparison of 1,25-dihydroxyvitamin D_3 (Calcitriol) and EB 1089. Cancer Epidemol Biomark Prev 1999;8: 241–8.

Journal of Cellular Biochemistry 99:966–977 (2006)

Nuclear Estrogen Receptor Targeted Photodynamic Therapy: Selective Uptake and Killing of MCF-7 Breast Cancer Cells by a $C_{17\alpha}$-Alkynylestradiol-Porphyrin Conjugate

Narasimha Swamy,[1] Ajay Purohit,[2] Ana Fernandez-Gacio,[1] Graham B. Jones,[2] and Rahul Ray[1]*

[1]Bioorganic Chemistry and Structural Biology, Section in Endocrinology, Diabetes and Nutrition, Department of Medicine, Boston University School of Medicine, Boston, Massachusetts
[2]Department of Chemistry, Northeastern University, Boston, Massachusetts

Abstract We hypothesized that over-expression of estrogen receptor (ER) in hormone-sensitive breast cancer could be harnessed synergistically with the tumor-migrating effect of porphyrins to selectively deliver estrogen-porphyrin conjugates into breast tumor cells, and preferentially kill the tumor cells upon exposure to red light. In the present work we synthesized four (4) conjugates of C_{17}-α-alkynylestradiol and chlorin e6-dimethyl ester with varying tether lengths, and showed that all these conjugates specifically bound to recombinant ERα. In a cellular uptake assay with ER-positive MCF-7 and ER-negative MDA-MB 231 human breast cancer cell-lines, we observed that one such conjugate (E_{17}-POR, XIV) was selectively taken up in a dose-dependent and saturable manner by MCF-7 cells, but not by MDA-MB 231 cells. Furthermore, MCF-7 cells, but not MDA-MB 231 cells, were selectively and efficiently killed by exposure to red light after incubation with E_{17}-POR. Therefore, the combination approach, including drug- and process modalities has the potential to be applied clinically for hormone-sensitive cancers in organs where ER is significantly expressed. This could potentially be carried out either as monotherapy involving a photo-induced selective destruction of tumor cells and/or adjuvant therapy in post-surgical treatment for the destruction of residual cancer cells in tissues surrounding the tumor. J. Cell. Biochem. 99: 966–977, 2006.

Key words: estrogen receptor targeted delivery of phototoxins; targeted photodynamic therapy; estrogen-porphyrin conjugates; cellular assays for uptake and cell-kill; breast cancer

Porphyrins are photosensitizers; and they have a useful property of being retained somewhat preferentially by malignant tissues, possibly due to their unique chemical structure. Porphyrins absorb in the visible region of electromagnetic radiation. Therefore, upon activation with visible light (often red light), porphyrins produce singlet oxygen that kills tumor cells (Photodynamic therapy, PDT). In general, PDT is a localized therapy for the treatment of early stage malignancy, palliative therapy for late-stage disease and for tumor bed sterilization by destroying any residual tumor cells after surgery or any metastasized cells in the area of light-illumination [Dougherty et al., 1998; Dalla Via and Marciani, 2001; Sibata et al., 2001; Dougherty, 2002; Moan and Peng, 2003; Axer-Siegel et al., 2004; Marmur et al., 2004]. Recently two PDT dyes, namely Visudyne and Foscan have been approved by the Food and Drug Administration for the treatment of age-related macular degeneration, and palliative treatment of head and neck cancer respectively. In the case of breast cancer, PDT was investigated as a palliative treatment for the cutaneous recurrence [Khan et al., 1993; Mang et al., 1998; Allison et al., 2001], and was suggested as a probable treatment. Recently

Narasimha Swamy is deceased.

Ana Fernandez-Gacio is Fulbright Fellow from Departamento Química Orgánica, Facultad de Química, Universidad de Santiago de Compostela, Spain.

Grant sponsor: Community Technology Development Fund, Boston University.

*Correspondence to: Rahul Ray, Boston University School of Medicine, 85 east Newton Street, Boston, MA 02118. E-mail: bapi@bu.edu

Received 28 October 2005; Accepted 21 March 2006
DOI 10.1002/jcb.20955

Dolmans et al. [2002] reported that PDT delayed tumor-growth in a murine orthotopic breast tumor model.

Accumulation of most PDT dyes in malignant cells is, however, modest, and several methods for the enhanced delivery of PDT dyes to tumors by chemical conjugation or association with LDL, liposomes and microspheres have been attempted with limited success [Hasan, 1992; Kramer et al., 1996; Derycke and Witte, 2004; Sharman et al., 2004]. Recently unique immune-signals on the surface of certain cancer cells have been harnessed by chemically conjugating PDT dyes to antibodies to these signals [Goff et al., 1994, 1996; Vrouenraets et al., 2000, 2001, 2002]. However, paucity of active mechanism for the internalization of these immunotoxins has limited their applicability.

Nuclear receptors, by virtue of their high-affinity binding to their cognate ligands, have been employed as molecular targets to deliver ligand-mimics as drugs. For example, estrogen receptor (ER), the primary modulator of the biological effects of estrogens and anti-estrogens, has been targeted with estrogens as carriers of cytotoxins [nitrogen mustards, genotoxins, geldanamycin, enediynes [Rink et al., 1996; Kuduk et al., 1999, 2000; Essigman et al., 2001; Purohit et al., 2001; Sharma et al., 2004], and radioisotopes (for radioimaging [Skaddan et al., 1999, 2000]), taking advantage of the over-expression of ER in cancerous cells relative to healthy tissues [Gotteland et al., 1994; Traish et al., 1995; Soubeyran et al., 1996; Struse et al., 2000]. However, these "double-headed" conjugates in general have low ER-binding affinities due in parts to modification of the parent estradiol molecule, and addition of appendages of varying chemical nature and steric bulk. As a result desired degree of accumulation of the conjugate selectively into tumor often remains unachieved.

We hypothesized that tumor-accumulation (of the conjugates) could be enhanced significantly if we couple estrogen with a toxin that has propensity for accumulation into tumor cells. This way it might be possible to diminish the sole dependency of these conjugates on ER-binding. Such a strategy will have the benefit of providing significantly higher efficiency over traditional PDT, and might constitute a potential tumor-specific therapeutic modality for hormone-sensitive cancer of organs where ER is expressed in significant degree.

Based on the above hypothesis we synthesized a conjugate of $C_{11\beta}$-estradiol and tetraphenylporphyrin, and showed that this compound selectively accumulated in MCF-7 breast tumor cells [James et al., 1999; Swamy et al., 2002]. However, we noted that the photosensitizing capability of neither the un-conjugated porphyrin nor the conjugate was sufficiently high to kill the cells under the conditions of our experiment [Swamy et al., 2002].

In the present study we anchored chlorin e6-dimethyl ester, a known photo-toxin to C_{17}-α-alkynylestradiol via tethers of various lengths and determined their ER-binding capabilities. In addition, we carried out cellular uptake and light-induced cell-killing studies of one of these conjugates (E_{17}-POR, n = 3, XIV, Fig. 1) with ER positive MCF-7 and ER-negative MDA-MB 231 human breast cancer cells. These experiments demonstrated that this conjugate selectively accumulated into MCF-7 cells; and viable cells were significantly reduced by exposure to red light. Results of these studies and their implications are discussed in this communication.

MATERIALS AND EXPERIMENTAL METHODS

MCF-7 and MDA-MB 231 human breast cancer cells were purchased from ATCC (Manasas, VA). Baculovirus expressed recombinant ERα was obtained from PanVera, Madison, WI. All the chemicals, except chlorin e6-dimethyl ester (Frontier Science, Logan, UT), were purchased from Sigma-Aldrich Chemical Co., Milwaukee, WI. Solvents were obtained from American Bioanalytical, Natick, MA. [^{3}H]17-β-estradiol (sp. activity 3 Ci/mmol) was synthesized in-house by reducing 3-*t*-butyldimethylsilyl estrone with NaB^3H_4 (Amersham Corpn., Springfield, IL, sp. activity 12 mCi/mmol) followed by removal of the tert-butyldimethylsilyl protecting group. Synthesis of the compounds (Fig. 1), included in this communication, was reported earlier in a scientific meeting abstract [Swamy et al., 2001]. Detailed description of the synthesis will be published elsewhere.

Competitive Binding Assays of C_{17}-α-alkynylestradiol-chlorin e6 Conjugates (XII–XV) with ERα

Baculovirus-expressed recombinant ERα (2 nM) was incubated with 0.13 nmol of [^{3}H]17-β-estradiol in the presence of increasing concentrations of estradiol or the conjugates (as

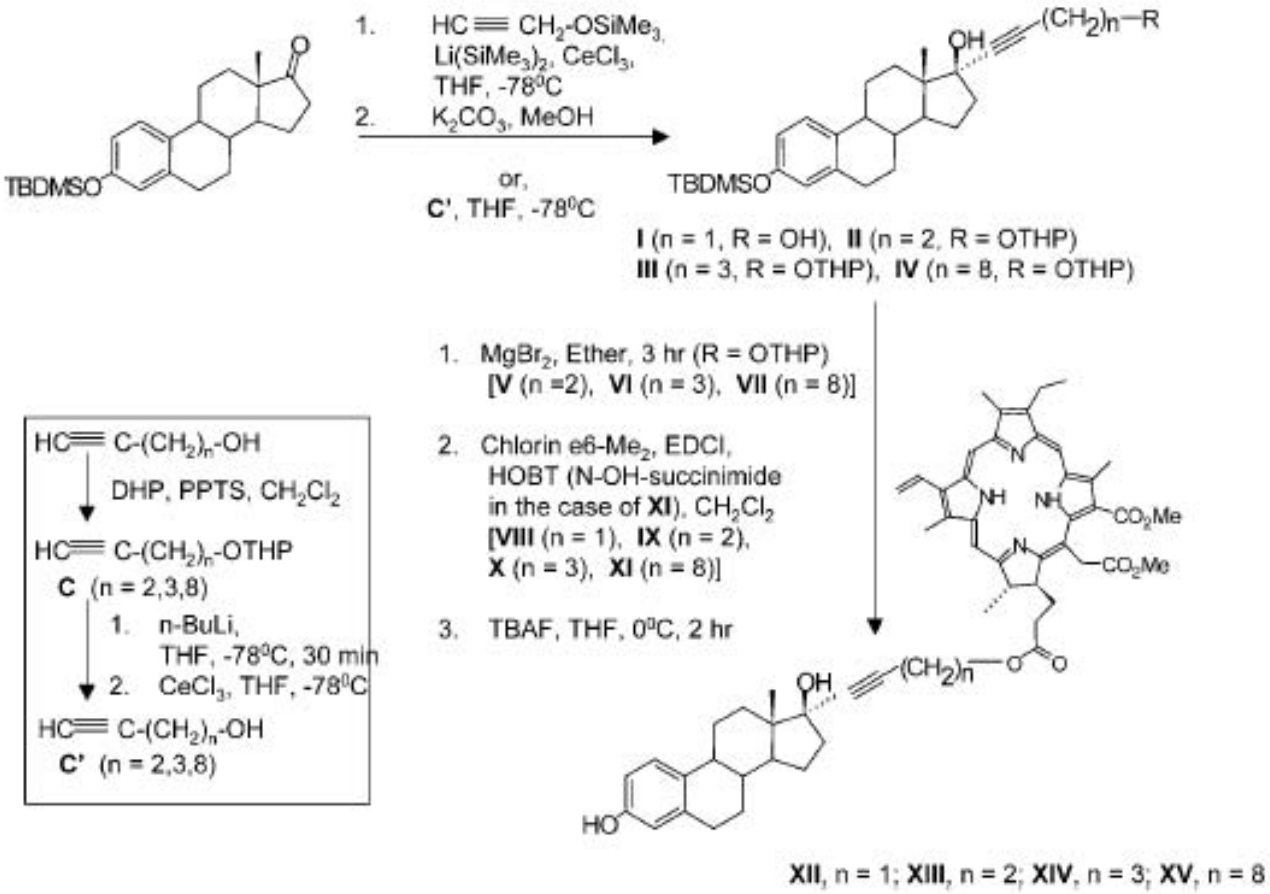

Fig. 1. Scheme for the synthesis of C_{17}-α-alkynylestradiol-chlorin e6 conjugates.

denoted in (Fig. 2), dissolved in 10 µl of ethanol, in an assay buffer (10 mM Tris, pH 7.5, 10% glycerol, 2 mM of monothioglycerol, and 1 mg/ml BSA, total volume 0.5 ml) for 15 h at 4 °C. A 50% hydroxylapatite (HAP) slurry was added to remove [^{3}H]-17β-estradiol, bound to the protein from unbound [^{3}H]17β-estradiol. After centrifugation and three washes in the ER wash buffer (40 mM Tris, pH 7.4, 100 mM KCl, 1 mM EDTA, 1 mM EGTA) the HAP pellet was transferred to a scintillation vial and resuspended in 200 µl of ethanol. Radioactivity, bound to the HAP-pellet, was determined in a liquid scintillation counter after the addition of scintillation cocktail. Total binding was determined by treating ER samples with [^{3}H]-17β-estradiol only, while non-specific binding was determined by incubating ER samples with [^{3}H]17β-estradiol and 1 µg of estradiol. Maximum specific binding (B_0) was calculated by subtracting non-specific binding from total binding, while specific binding (B) at each concentration was calculated by subtracting non-specific binding from binding at each concentration. Each concentration was run in triplicate.

Cell-Culture

MCF-7 and MDA MB 231 cells (approximately 10^6 cells/well) were seeded into 24-well plates and grown in DMEM media containing 1% Penn/Strep and 5% fetal bovine serum (FBS) till approximately 70% confluence, followed by treatment with various reagents. E_{17}-POR (estradiol porphyrin conjugate, XIV) or chlorin e6 dimethyl ester (Ce6-Me_2, the un-conjugated porphyrin) were dissolved in ethanol to desired concentration, and the cells were dosed with these solutions.

MCF-7 and MDA MB 231 Cell-Uptake Assay

MCF-7 or MDA MB 231 cells were treated with various concentrations of either E_{17}-POR, XIV or Ce6-Me_2 in cell culture media without FBS for 30 min. After the incubation media was withdrawn and the cells were washed 3 times with PBS, and 1 ml of methanol was added to each plate, and cells were allowed to lyse for

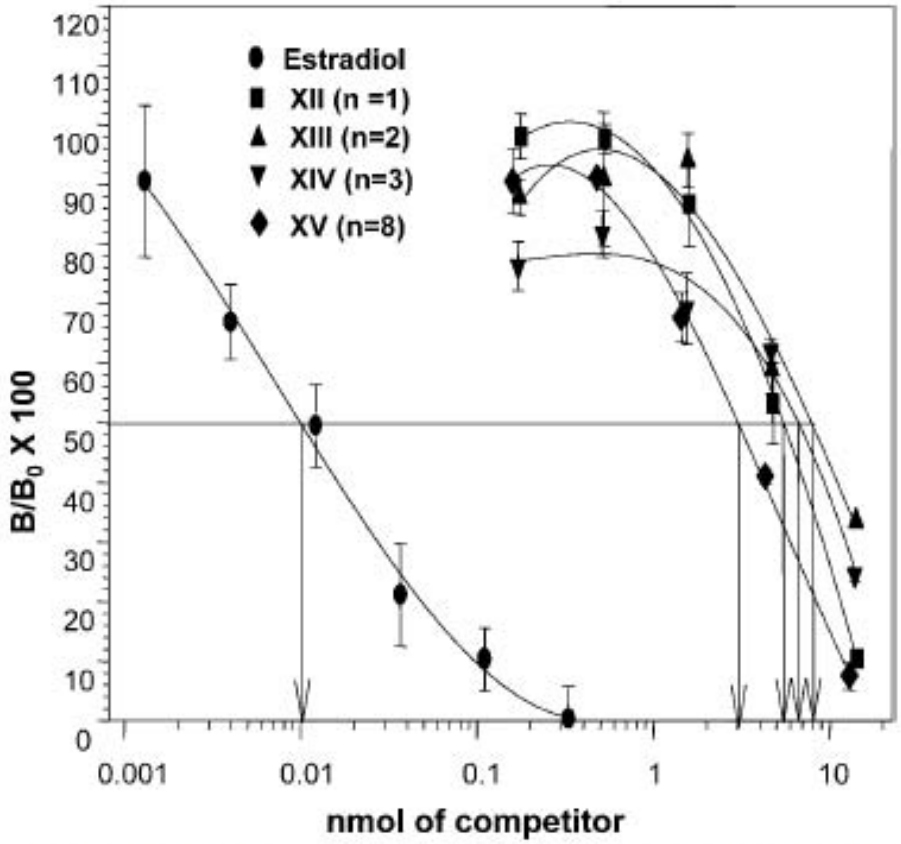

Fig. 2. Competitive binding assays of estardiol and C_{17}-α-alkynylestradiol-chlorin e6 conjugates with baculovirus expressed recombinant ER. Briefly ERα (2 nM) was incubated with 0.125 nmol of [^{3}H]17-β-estradiol in the presence of increasing concentrations of estradiol or the conjugates for 15 h at 4°C, followed by treatment with a 50% hydroxylapatite (HAP) slurry to remove [^{3}H]17β-estradiol, bound to the protein from unbound [^{3}H]17β-estradiol. After centrifugation and three washes in the ER wash buffer the HAP pellet was transferred to a scintillation vial, re-suspended in 200 µl of ethanol, and radioactivity was measured in scintillation counter. At each concentration specific binding divided by maximum specific binding (B/B_0) in percent was plotted against concentration. 50% specific binding (EC_{50}) for each compound is denoted in the X-axis. Each concentration was run in triplicate.

15 min. The cells were scraped with a rubber policeman and the mixture was transferred to a test tube. This step was repeated twice. The combined mixture was centrifuged and supernatants were concentrated under nitrogen, dissolved in 1 ml of methanol, and fluorescence in the extracts was determined in a Hitachi U2000 spectrofluorimeter ($E_x = 405$ nm and $E_m = 670$ nm). To determine the extraction-efficiency, known amounts of the conjugate (XIV) and chlorin e6-dimethylester were added to MCF-7 cells and they were extracted with methanol in the same fashion as described before; and the methanol-extracts were assayed fluorimetrically. The extraction-efficiency was >95% (results not shown). In general each concentration was run in six (6) replicates. Statistics was done by student's *t*-test. Although cellular uptake assays are usually carried out by dispersing the cells in a detergent (e.g., 1% SDS) after the incubation with a porphyrin, and measuring the fluorescence of the mixture [Momma et al., 1998], we found that addition of methanol to the cells (after removing the media and washing the cells with PBS) lysed the cells completely and allowed a near complete extraction of the porphyrins inside the cells. A similar procedure for the extraction of tri(glucosyloxyphenyl)chlorin with an organic solvent was described recently [Laville et al., 2004].

Cell-Viability Assays of MCF-7 and MDA-MB 231 Cells Treated With Various Doses of E_{17}-POR (XIV) or Ce6-Me_2

MCF-7 and MDA-MB 231 cells were treated with E_{17}-POR (XIV, 0.02, 0.03, 0.07, 0.13, 0.27, 0.54, or 1.07 µM) or chlorin e6 dimethyl ester (Ce6-Me_2, 0.01, 0.02, 0.05, 0.09, 0.18, 0.36, or 0.73 µM) in DMEM in the absence of FBS for 1 h in the cell culture incubator. Then the plates

were exposed to red light for 10 min at 25°C (heat was dissipated with a cooling fan). Illumination of the cells was carried out by placing the cell-culture dishes on the top of a light box covered in the top with a red plastic sheet. The lamp was equilibrated for 15 min prior to placing the cell culture dishes. Transmittance of the red filter was determined in a UV-VIS spectrophotometer (Hewlet-Packard, Model 8453). Fluence was determined by a Coherent Lasermate detector with a 2.54 cm^2 detection-area (total fluence was 3.5 J/cm^2). A control plate was set up in parallel, but the plate was not exposed to light. At the end, the media was replaced with fresh media containing FBS and the cells were allowed to recover and grow for an additional 14 h. This was followed by Methylene Blue cell-viability assay (vide infra). We also carried out an assay where cells were exposed to light for 10, 20, 30, and 90 min; and observed that a 10-min exposure was sufficient for significant and consistent reduction in the number of viable cells (results not shown). Furthermore, a shorter exposure-time was deemed desirable to avoid "heating" related to longer exposures.

Methylene Blue Cell-Viability Assay

After the experiment the cells were washed with ice-cold PBS (0.5 ml), followed by the addition of methanol (chilled at −20°C) and the cells were allowed to incubate on ice for 10 min. Methanol was removed by suction and the cells were air-dried for 20 min followed by the addition of 0.25 ml of Methylene Blue solution to each well. The cells were allowed to incubate at 25°C for 30 min. Methylene Blue solution was aspirated off, and the cells were washed four (4) times with 10 mM borate buffer, pH 8.5 (1.0 ml at a time). Then the cell-bound dye was released by adding 1.0 ml of ethanol-0.1 M HCl (1:1 v/v) mixture. The absorbance of the solution from each well was determined at 650 nm against ethanol-HCl solvent. The cell viability was expressed as percent of the control (which did not receive any compound, but received only plain DMEM).

Imaging of MCF-7 or MDA-MB 231 Cells after Incubation With E_{17}-POR or Ce6-Me_2 and Either Exposed to Red Light or Kept in the Dark

MCF-7 or MDA-MB 231 cells (~200,000) were seeded in 30 mm dishes and grown overnight in DMEM containing Penn/Strep and 5% FBS. The cells were treated with 1.07 μM of E_{17}-POR or Ce6-Me_2 in DMEM in the absence of FBS for 1 h. Then the plates were exposed to red light (light box fitted with a red filter, as described before) for 10 min at 25°C. A control plate was set up in parallel but the plate was not exposed to light. At the end, the media was replaced with fresh media containing FBS and the cells were allowed to recover and grow for an additional 14 h. After this period the wells were washed twice with PBS (1.0 ml), and fixed by adding 1.0 ml of methanol (−20°C) to each well and incubating on ice for 20 min. Methanol was aspirated off and the plates were dried in air for 30 min. One ml of 1% Methylene Blue solution was added to each well and cells were incubated at 25°C for 30 min. The plates were washed three times with 10 mM borate buffer pH 8.5, and photographed using an inverted microscope fitted with digital imaging system (Twin-Cam Digital imaging system by Camdek Precision instruments, Boston, MA).

RESULTS AND DISCUSSION

Targeting ER in the nucleus of breast cancer cells with an estrogen-toxin conjugate has certain advantages. For example, it has been shown that the nucleus of cancer cells contains higher number of copies of ER than the non-cancerous tissues where ER is expressed [Gotteland et al., 1994; Traish et al., 1995; Soubeyran et al., 1996; Struse et al., 2000]. Therefore, it is expected that a larger quantity of an estrogen-conjugate would accumulate in the cancer cells than the non-cancerous ones. Furthermore, nucleus contains the genomic DNA; and its damage is most desired in cancer therapy. Additionally, cancer cells divide rapidly and the chromosomal DNA remains in a bare form instead of being surrounded by histones and thus protected from damage. Therefore maximum damage to cells could be expected if the toxins are targeted to the nucleus of the cancer cells.

Support for the benefit of nuclear targeting was provided in a recent article where Akhlynina et al. demonstrated that coupling chlorin e_6, a PDT dye, to a nuclear localization signal and targeting nuclear insulin receptor in PLC/PRF/5 and rat glioma C6 cells resulted in a more than 2,000-fold reduction of EC_{50} (opposed to chlorin e_6 alone) and significantly increased the photosensitizing activity of chlorin e6 [Akhlynina et al., 1997].

In a previous report we delineated the synthesis of a C_{11}-estradiol-tetraphenyl porphyrin conjugate and showed specific binding of this conjugate to ER [James et al., 1999]. Furthermore, we demonstrated that this compound selectively accumulated in ER-positive MCF-human breast cancer cells opposed to ER-negative HS578t cells [Swamy et al., 2002].

Although the above results provided the "proof-of-the principle" of our hypothesis about targeting ER in cancer cells with a "double-headed molecule" in which one half has ER-localizing property while the other has tumor-localizing property, this compound showed very low photosensiting capability under the conditions of our experiment [Swamy et al., 2002]. This prompted us to consider chlorin e6 as the photosensitizer, particularly in conjugation with estrogen-mimics. Hamblin et al. recently described that conjugation of polyethylene glycol to chlorin e6 significantly enhanced the phototoxicity of chlorin e6 in ovarian cancer cells [Hamblin et al., 2001]. Furthermore, as described earlier, coupling chlorin e_6 to a nuclear localization signal significantly increased the photosensitizing activity of chlorin e6 [Akhlynina et al., 1997]. These data provided potential support for our hypothesis involving estrogen-porphyrin conjugates for targeting ER in breast cancer cells and killing them in a selective fashion upon light-exposure.

An important consideration in the tumor-selective delivery of estrogen-conjugates is high binding affinity between these compounds and ER. This is necessary for the selective accumulation of these compounds in the desired ER-targeted tissues, and not in other healthy tissues where is ER is expressed, that is, brain, ovary etc. C_{17}-α-alkynylestradiol and its derivatives are known to bind ER with high affinity [Anstead et al., 1997]. Therefore, we postulated that C_{17}-α-alkynylestradiol-porphyrin conjugates might be endowed with high ER-binding and enhanced tumor-localizing properties.

In the present study, we synthesized four (4) conjugates of C_{17}-α-alkynylestradiol with various tether lengths and chlorin e6-dimethyl ester (Fig. 1; n = 1–3, 8). Introduction of the tethers at the C_{17}-α position of estradiol was carried out by nucleophilic addition of suitably derivatized alkynyl carbanions to protected estrone followed by standard synthetic manipulations.

It is known that alkyne group and its derivatives at C_{17}-α position of estradiol are tolerated well by ER [Anstead et al., 1997], but the effect of a large porphyrin group at the end of the alkyne on ER-binding is not known. Competitive binding assays of these conjugates (XII–XV) with recombinant ER demonstrated that all of them specifically bound to ERα in a dose-dependent manner, however, with significantly less affinity than estradiol (Fig. 2). Concentration at half-maximal binding of XII-XV (n = 1–3 and 8) were 5.6, 8.1, 6.8 and 3.0 nM respectively compared with 0.01 nM for estradiol. Although these compounds showed low ER-binding properties, we hypothesized that such deficiency might be mitigated, at least to some extent by the tendency of the porphyrin part of the conjugates to be retained by the tumor cells.

We continued our biochemical studies with one of the conjugates (E_{17}-POR, XIV, n = 3), because we had maximum amount of this compound available to us. Since ER-binding affinities of these compounds (XII–XV) were very similar, we argued that XIV would be a valid representative of the four conjugates. Purity of this compound (E_{17}-POR, XIV) was determined by HPLC analysis, which showed that XIV was not contaminated with chlorin e_6 dimethyl ester (results not shown).

We observed that when MCF-7 or MDA-MB 231 cells were incubated with various doses of either E_{17}-POR or Ce_6-Me_2, the conjugate was taken up by ER-positive MCF-7 cells in a dose-dependent and saturable manner, while Ce_6-Me_2 was not (Fig. 3). Both E_{17}-POR and Ce_6-Me_2 showed a low-level and dose-independent uptake by ER-negative MDA-MB 231 cells. These results strongly suggested that binding of E_{17}-POR by endogenous ER in MCF-7 cells might be responsible for dose-dependent and saturable uptake of this compound.

In the next study, MCF-7 cells were incubated with various doses of either E_{17}-POR or Ce_6-Me_2 followed by exposure to red light, under conditions described in the Materials and Methods section. Following the light-exposure the cells were allowed to grow back, and cell-viability was determined by Methylene Blue assay. We used this assay in our experiment because it has been used traditionally for cell survivability/viability. In this assay only the live cells are stained by Methylene Blue, providing an index for cell viability. Recently this assay was used to

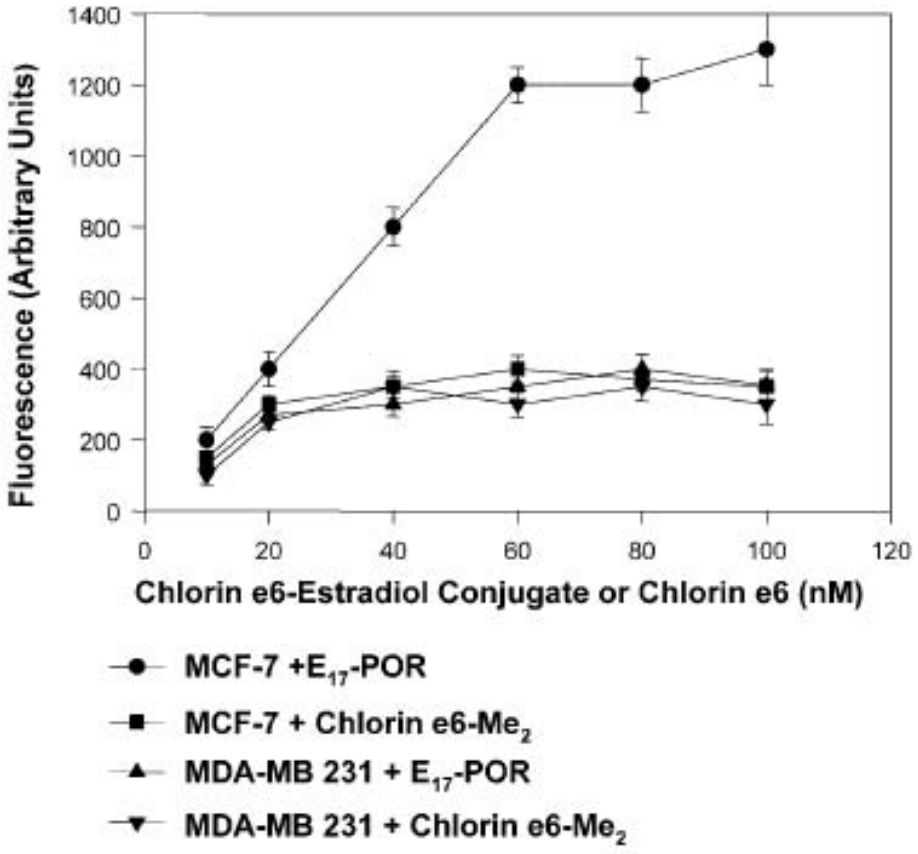

Fig. 3. Cellular uptake assay of E_{17}-POR and Ce6-Me_2 in MCF-7 and MDA-MB 231 cells. Cells were treated with increasing concentrations of either E_{17}-POR or Ce6-Me_2 in cell culture media without FBS for 30 min. Then the cells were washed three times with PBS, and were extracted with 1 ml of methanol. The fluorescence in methanol extracts was determined ($E_x = 405$ nm and $E_m = 670$ nm). Each point in the graph represents an average of six (6) replicates.

determine cell-survivability after PDT with a photoproduct of protoporphyrin IX induced by 5-aminolevulinic acid [Ma et al., 2000]. We observed that there was a dose-dependent decrease of viable cells in cells treated with E_{17}-POR and red light; and 0.18 μmol of the conjugate was required for 50% cell-viability/cell-kill (Fig. 4A). On the other hand, there was almost 100% cell-viability with E_{17}-POR (no light-exposure) and Ce_6-Me_2 (no light-exposure). The Ce_6-Me_2-control that was exposed to light showed some cell-killing properties at higher concentrations reflecting low-efficiency tumor cell-retaining tendency of porphyrins.

The above results strongly suggested that presence of ER in MCF-7 cells might be responsible for the enhanced accumulation of the conjugate into cells that led to significantly higher degree of cell-kill upon light-exposure compared to un-exposed sample. Another important observation was that conjugation of Ce_6-Me_2 to estrogen strongly reduced the amount of porphyrin required for cell-kill. For example, at a concentration of 0.18 μM there was 50% cell-viability with the conjugate (light-exposed), while there was almost 100% viability with Ce_6-Me_2 (light-exposed) at this concentration.

In the case of ER-negative MDA-MB 231 cells there was no significant cell-kill with Ce_6-Me_2 in the presence or absence of light (Fig. 4B). This is in contrast with MCF-7 cells where low but significant cell-kill was observed at high doses of Ce_6-Me_2 (Fig. 4A). This might be a reflection of the inherent difference between these cell lines towards photo-sensitivity. On the other hand, almost equal level of cell-kill was observed in the absence or in the presence of light when the cells were treated with high concentrations of E_{17}-POR. This phenomenon may be related to "dark toxicity" involving low-level toxicity of porphyrins that are not exposed to light, that has been shown in several systems, particularly when the core porphyrin moiety is modified [Stilts

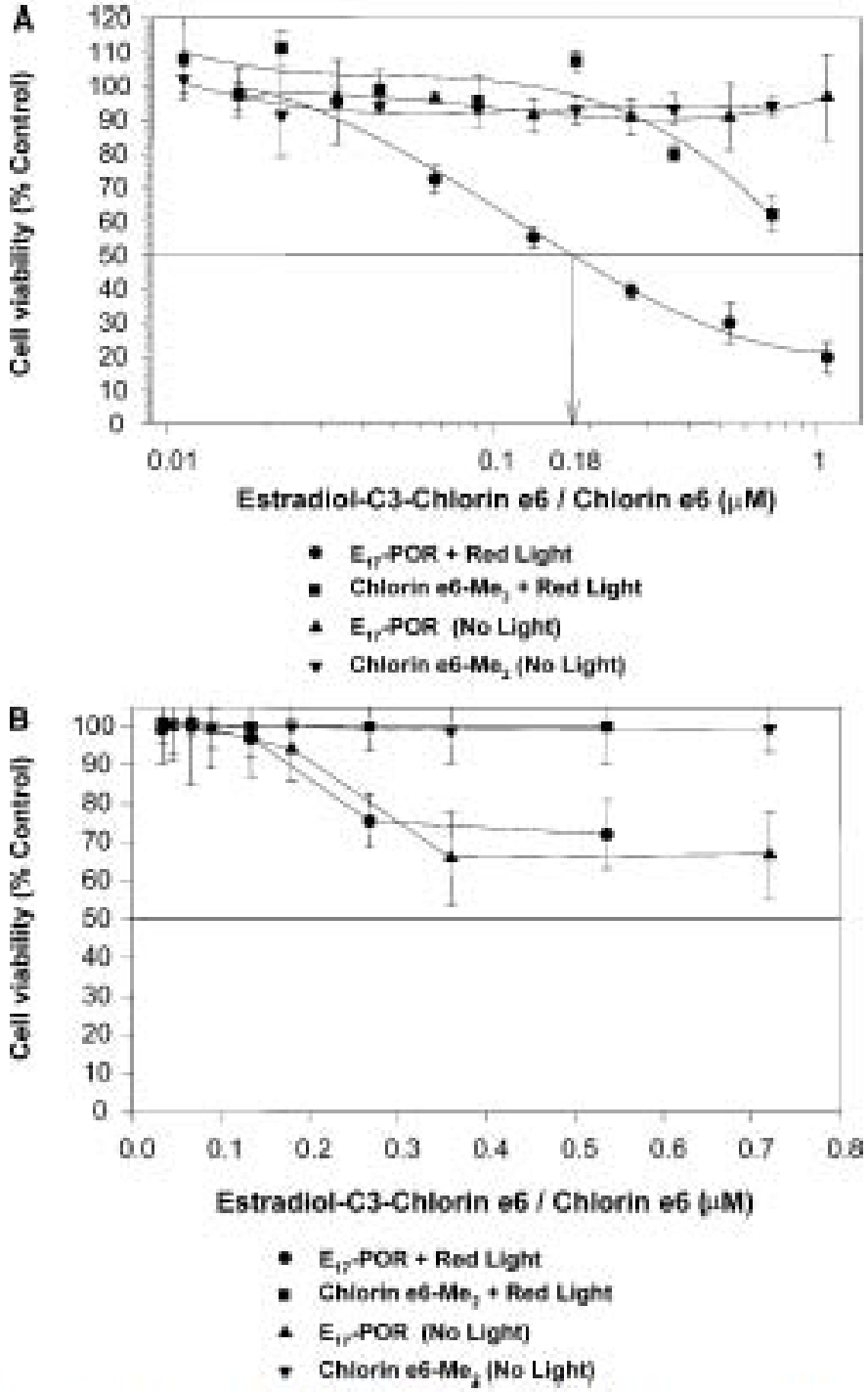

Fig. 4. A: Methylene Blue cell-viability assays of MCF-7 cells treated with various concentrations of E_{17}-POR and Ce6-Me_3 followed by exposure to red light. Briefly MCF-7 cells were treated with E_{17}-POR (0.02, 0.03, 0.07, 0.13, 0.27, 0.54, or 1.07 μM) or Ce6-Me_3 (0.01, 0.02, 0.05, 0.09, 0.18, 0.36, or 0.73 μM) in DMEM in the absence of FBS for 1 h, followed by exposure of the plates to red light for 10 min. A control plate was not exposed to light. At the end, the media was replaced with fresh media containing FBS and grown for 14 h followed by Methylene Blue cell-viability assay. Each position in the graph represents an average of six (6) replicates. B: Methylene Blue cell-viability assays of MDA-MB 231 cells treated with various concentrations of E_{17}-POR and Ce6-Me_3 followed by exposure to red light. Briefly MDA-MB 231 cells were treated with 0.02, 0.03, 0.07, 0.13, 0.27, and 0.54 μM of E_{17}-POR or Ce6-Me_3 in DMEM in the absence of FBS for 1 h, followed by exposure of the plates to red light for 10 min. At the end, the media was replaced with fresh media containing FBS and grown for 14 h followed by Methylene Blue cell-viability assay. Another set of cells, incubated with 0.01, 0.02, 0.05, 0.07, 0.18, 0.36, and 0.73 μM of E_{17}-POR or Ce6-Me_3 was treated exactly the same way, except they were not exposed to red light. Each point in the graph represents an average of six (6) replicates.

et al., 2000; Vicente et al., 2002]. This is exemplified by the "leveling off" of toxicity at 60%–70% cell viability (Fig. 4B). Furthermore, it should be appreciated that such an effect was observed at high concentrations. For example, with MCF-7 cells 50% cell-kill was observed at a concentration of 0.18 μmol of E_{17}-POR (Fig. 4A). But at this concentration cell-kill in MDA-MB-231 cells was only approximately 5% in "light-exposed" and "dark" samples (Fig. 4B) (please note that different scaling methods in the abscissa were used in Fig. 4A,B).

Collectively, the above results showed that the presence of ER significantly increased the accumulation of the conjugate and strongly reduced the concentration of the porphyrin required for effective cell-kill. Observations in Figure 4A,B were visualized by incubating MCF-7 and MDA-MB 231 cells with a fixed concentration of either XIV or Ce6-Me_2 and then exposing them to red light for 10 min, or keeping the cells in the dark. After the treatment the cells were allowed to grow back and Methylene Blue was added to stain viable cells followed by photographic imaging of the cells. Results of these assays are shown in Figures 5 and 6.

With MCF-7 cells there was no significant difference in viable cells between E_{17}-POR and Ce6-Me_2-treated samples when the cells were not exposed to light (Fig. 5, upper half, middle, and right panels respectively). Although number of viable cells in untreated dark control (Fig. 5, upper half, left panel) appeared to be less than the treated samples, this could be due to photographing of an area with less density in

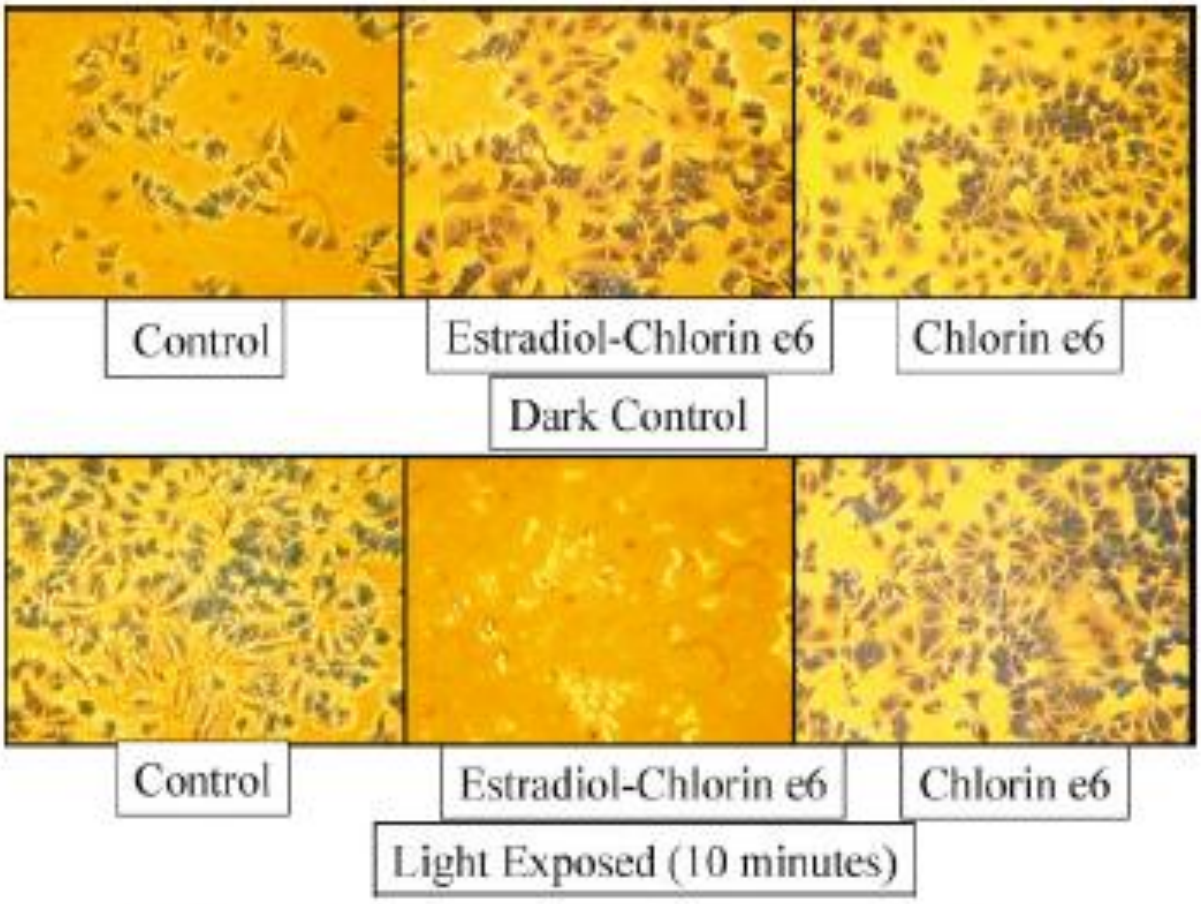

Fig. 5. Imaging of MCF-7 cells after incubation with E_{17}-POR or Ce6-Me_2 and either exposed to red light or kept in the dark. MCF-7 cells were treated with 1.07 μM of E_{17}-POR or Ce6-Me_2 in DMEM in the absence of FBS for 1 h. Then the plates were exposed to red light for 10 min at 25°C. A control plate was set up in parallel that was not exposed to light. At the end, the media was replaced with fresh media containing FBS and grown for 14 h. After this period the wells were washed twice with PBS (1.0 ml) followed by Methylene Blue cell-viability assay. The cells were photographed using an inverted microscope fitted with digital imaging system. [Color figure can be viewed in the online issue, which is available at www.interscience.wiley.com.]

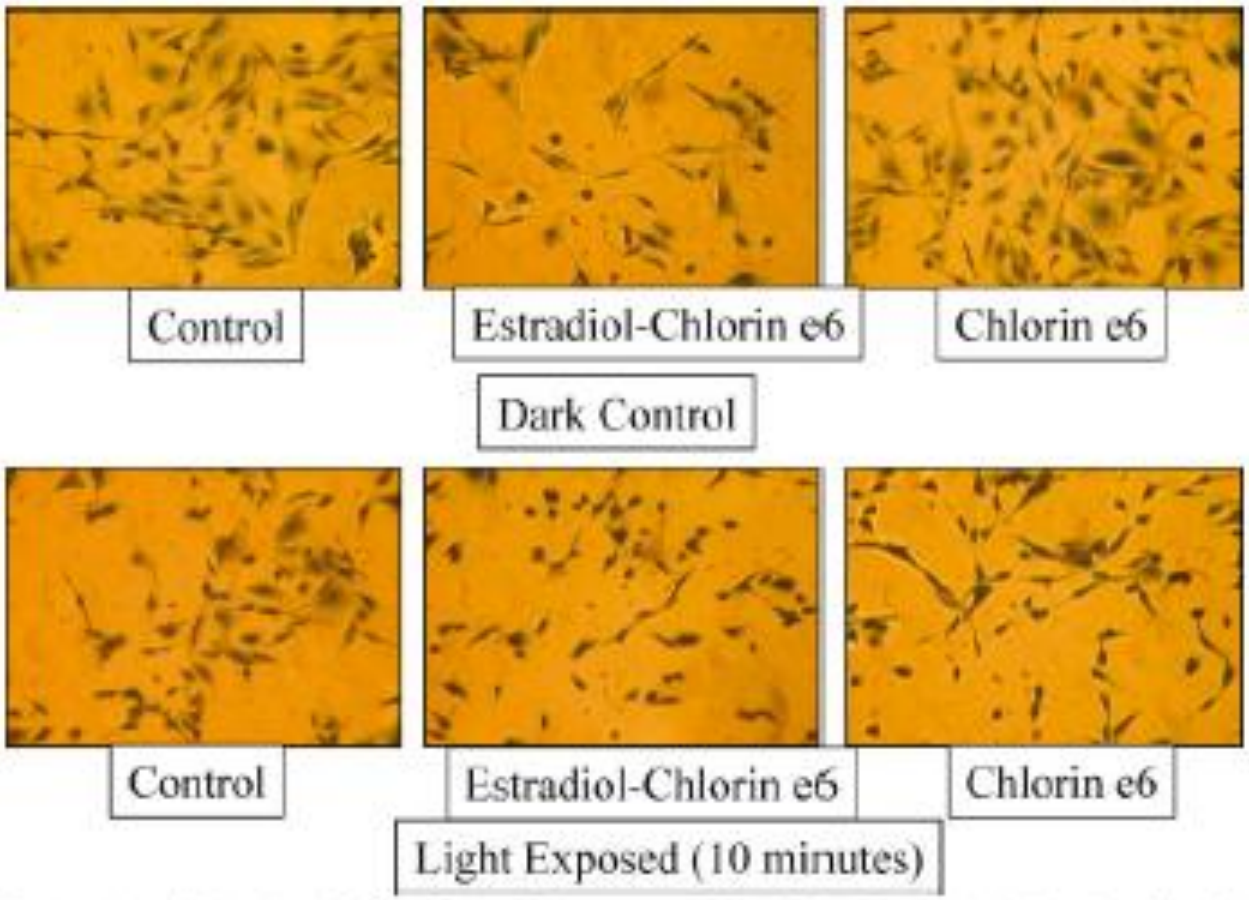

Fig. 6. Imaging of MDA-MB231 cells after incubation with E_{17}-POR or Ce6-Me_2 and either exposed to red light or kept in the dark. The cells were treated with 1.07 μM of E_{17}-POR or Ce6-Me_2 in DMEM in the absence of FBS for 1 h. Then the plates were exposed to red light for 10 min at 25°C. A control plate was set up in parallel that was not exposed to light. At the end, the media was replaced with fresh media containing FBS and grown for 14 h. After this period the wells were washed twice with PBS (1.0 ml) followed by Methylene Blue cell-viability assay. The cells were photographed using an inverted microscope fitted with digital imaging system. [Color figure can be viewed in the online issue, which is available at www.interscience.wiley.com.]

cell-population. In the light-exposed samples, there was strong cell-kill in the case of E_{17}-POR-treated sample (Fig. 5, lower half, middle panel). But there was no significant difference between untreated and Ce6-Me_2-treated cells (Fig. 5, lower half, left and right panels respectively).

In contrast, MDA-MB 231 cells appeared to be practically unchanged when exposed to light or kept in the dark in the presence of the conjugate (E_{17}-POR) or un-conjugated porphyrin (Ce6-Me_2) (Fig. 6, all the panels).

Collectively above results demonstrated that presence of ER in tumor cells significantly increased the uptake of the conjugate, despite relatively low ER-binding efficiency of the latter. This observation supported our hypothesis that poor ER-binding affinity (of the conjugates) might be mitigated by the tendency of the porphyrin part of the conjugate to be retained by tumor cells. Thus, higher accumulation of the conjugate in the ER-positive tumor cells lead to significantly higher cell-kill upon light-exposure. This phenomenon might also be further augmented by increased photosensitivity of the unconjugated porphyrin (chlorin e6-dimethyl ester) upon chemical conjugation with a hydrophobic molecule (a derivative of estradiol in this case) as noted by others [Hamblin et al., 2001].

Furthermore, these results strongly suggested that conjugation of chlorin e6 to estrogen sharply lowered the amount of the dye to obtain cell-kill in ER-positive breast cancer cells. Therefore, collectively these results underscored the strong potential of targeting ER in ER-expressing breast, ovarian and cervical tumors for selective and efficient delivery of phototoxins to allow selective tumor cell-kill sparing surrounding healthy tissues. Therefore, this

approach could potentially alleviate certain drawbacks in traditional photodynamic therapy of cancer involving less-than desirable accumulation of PDT dyes into cancer cells.

However, it should be noted that the results described in this communication were generated strictly in cellular assays. Therefore, translation of this data into an animal model or into a clinical situation requires further work. In all the assays, cells were dosed for an hour in a media that was free of serum. This was done to enhance the sensitivity of the assays, although it represents a non-physiological situation. Furthermore, tumors are often heterogeneous, and some ER positive tumors might express ER at significantly higher amounts than others, and vice versa. As a result there will be differential accumulation of the conjugate into ER-positive tumors depending on their ER-content. However, it should also be appreciated that low ER-content in some tumors would still allow a low dose of the conjugate to accumulate into tumor and preserve its phototoxic nature. In such cases the tumor-retaining property of the conjugate will probably be governed predominantly by the porphyrin part of the conjugate. Therefore, in a clinical set up, low ER-containing tumors could still be treated with these conjugates by intratumoral injection of the conjugate, opposed to systemic administration. Such a delivery route might be beneficial for the desired accumulation of the conjugate in the tumor.

It should also be noted that in an in vivo system an estrogen-porphyrin conjugate is bound to accumulate into organs, including breast, where ER is significantly expressed. However, for breast tumor, for example, light will strictly be focused on the breast. Thus other ER-containing organs will be spared from toxicity (due to the photoactivating nature of the conjugate). Therefore, by harnessing the higher expression of ER in hormone-sensitive breast tumor and focusing the light only on the tumor it might be possible to induce phototoxicity and resultant cell-death in the tumor selectively.

In conclusion, the combination approach, involving a "double-headed drug" with dual mechanism of action has the potential to be applied clinically for hormone-sensitive cancers in organs where ER is significantly expressed, either as monotherapy involving a photo-induced selective destruction of tumor cells and/or adjuvant therapy in post-surgical treatment for the destruction of residual cancer cells in tissues surrounding the tumor. However, much further studies will be required to bring this method to the realm of treating breast tumor.

ACKNOWLEDGMENTS

Part of the work was conducted by a grant from the Community Technology Development Fund, Boston University. The authors acknowledge the assistance from Dr. Tayyaba Hasan, Professor of Medicine, Massachusetts General Hospital, Boston, MA in carrying out light-dosimetry measurements.

REFERENCES

Akhlynina TV, Jans DA, Rosenkranz AA, Statsyuk NV, Rakhmilova IY, Toth G, Pavo I, Rubin AB, Sobolev AS. 1997. Nuclear targeting of chlorin e_6 enhances its photosensitizing activity. J Biol Chem 272:20328–20331.

Allison R, Moghissi T, Hawson G, Snider W, Dougherty TJ. 2001. Photodynamic therapy for chest wall progression from breast carcinoma is an underutilized treatment modality. Cancer (Phila) 91:1–8.

Anstead GM, Carlson KM, Katzenellenbogen JA. 1997. The estradiol pharmacophore: Ligand structure-estrogen receptor binding affinity relationships and a model for the receptor binding site. Steroids 62:268–303.

Arnon-Sturgel R, Ehrlich R, Yassur Y, Rosenblatt I, Kramer M, Priel E, Benjamini Y, Weinberg D. 2004. Photodynamic therapy for age-related macular degeneration in a clinical setting: Visual results and angiographic patterns. Am J Ophthalmol 137:258–264.

Dalla Via L, Marcinni Magno S. 2001. Photochemotherapy in the treatment of cancer. Curr Med Chem 12:1403–1418.

Derycke AS, Witte PA. 2004. Liposomes for photodynamic therapy. Adv Drug Deliv Rev 56:17–30.

Dolmans DE, Kadambi A, Hill JS, Flores KR, Gerber JN, Walker JP, Rinkes IH, Jain RK, Fukumura D. 2002. Targeting tumor vasculature and cancer cells in orthotopic breast tumor by fractionated photosensitizer dosing photodynamic therapy. Cancer Res 62:4283–4284.

Dougherty TJ. 2002. An update on photodynamic therapy applications. J Clin Laser Med Surg 20:3–7.

Dougherty TJ, Gomer CJ, Henderson BW, Jori G, Kessel D, Korbelik M, Moan J, Peng Q. 1998. Photodynamic therapy. J Natl Cancer Inst 90:889–905.

Rewcastle JM, Rink SM, Park HJ, Gray RG. 2001. Design of DNA damaging agents that hijack transcription factors and block DNA repair. Adv Exp Med Biol 500:301–313.

Goff BA, Hasmato U, Bamburgh J, Blake J, Bamberg M, Hasan T. 1994. Photoimmunotherapy and biodistribution with an OC125-chlorin immunoconjugate in an in vivo murine ovarian cancer model. Br J Cancer 70:474–480.

Goff BA, Blake J, Bamberg MP, Hasan T. 1996. Treatment of ovarian cancer with photodynamic therapy and immunoconjugates in a murine ovarian cancer model. Br J Cancer 74:1194–1198.

Gotteland M, May E, May-Levin F, Contesso G, Delarue JC, Mouriesse H. 1994. Estrogen receptors (ER) in human breast cancer. Cancer 74:864–867.

Hamblin MR, Miller JL, Rizvi I, Ortel B, Maytin EV, Hasan T. 2001. Pegylation of a chlorin(e6) polymer conjugate increases tumor targeting of photosensitizer. Cancer Res 61:7155–7162.

Hasan T. 1992. Photosensitizing delivery by macromolecular carrier systems. In: Henderson BW, Dougherty TJ, editors. Photodynamic therapy: Basic principles and clinical applications. New York: Marcel Dekker. pp 187–200.

James DA, Swamy N, Hanson RN, Ray R. 1999. Synthesis and estrogen receptor binding affinity of a porphyrin-estradiol conjugate for photodynamic therapy of cancer. Bioorg Med Chem Lett 9:2379–2384.

Khan SA, Dougherty TJ, Mang TS. 1993. An evaluation of photodynamic therapy in the management of cutaneous metastases of breast cancer. Eur J Cancer 29A:1686–1690.

Kramer M, Miller JW, Michaud N, Moulton RS, Hasan T, Flotte TJ, Gragoudas ES. 1996. Liposomal benzoporphyrin derivative verteporfin photodynamic therapy. Selective treatment of choroidal neovascularization in monkeys. Ophthalmology 103:427–438.

Kuduk SD, Zheng FF, Sepp-Lorenzino L, Rosen N, Danishefsky SJ. 1999. Synthesis and evaluation of geldanamycin-estradiol hybrids. Bioorg Med Chem Lett 9:1233–1238.

Kuduk SD, Harris TC, Zheng FF, Sepp-Lorenzino L, Ouerfelli O, Rosen N, Danishefsky SJ. 2000. Synthesis and evaluation of geldanamycin-testosterone hybrids. Bioorg Med Chem Lett 10:1303–1306.

Laville I, Pigaglio S, Blais J-C, Loock B, Maillard Ph, Grierson DS, Blais J. 2004. A study of the stability of tri(glucosyloxyphenyl)chlorin, a sensitizer for photodynamic therapy, in human colon tumoural cells: a liquid chromatography and MALDI-TOF mass spectrometry analysis. Bioorg Med Chem 12:3673–3682.

Ma LW, Bagdonas S, Moan J. 2001. The photosensitizing effect of the photoproduct of protoporphyrin IX. J Photochem Photobiol 60:108–113.

Mang TS, Allison R, Hewson G, Snider W, Moskowitz RA. 1998. Phase II/III clinical study of tin ethyl etiopurpurin (purlytin)-induced photodynamic therapy for the treatment of recurrent cutaneous metastatic breast cancer. Cancer J Sci Am 4:378–384.

Marmur ES, Schmults CD, Goldberg DJ. 2004. A review of laser and photodynamic therapy for the treatment of nonmelanoma skin cancer. Dermatol Surg 30:264–271.

Moan J, Peng Q. 2003. An outline of the hundred-year history of PDT. Anticancer Res 23:3591–3600.

Momma T, Hamblin MR, Wu HC, Hasan T. 1998. Photodynamic therapy of orthotopic prostate cancer with benzoporphyrin derivative: Local control and distant metastasis. Cancer Res 58:5425–5431.

Purohit A, Wyatt J, Hynd G, Wright J, El-Shafey A, Swamy N, Ray R, Jones GB. 2001. Chemical synthesis of hormone receptor probes: High affinity photoactivated enediyne-estrogens. Tet Lett 42:8579–8582.

Rink SM, Yarema KJ, Solomon MS, Paige LA, Tadayoni-Rebek BM, Essigmann JM, Croy RG. 1996. Synthesis and biological activity of DNA damaging agents that form decoy binding sites for the estrogen receptor. Proc Natl Acad Sci USA 93:15063–15068.

Sharma U, Marquis JC, Nicole Dinaut A, Hillier SM, Fedeles B, Rye PT, Essigmann JM, Croy RG. 2004. Design, synthesis, and evaluation of estradiol-linked genotoxicants as anti-cancer agents. Bioorg Med Chem Lett 14:3829–3833.

Sharman WM, van Lier JE, Allen CM. 2004. Targeted photodynamic therapy via receptor mediated delivery systems. Adv Drug Deliv Rev 56:53–76.

Sibata CH, Colussi VC, Oleinick NL, Kinsella TJ. 2001. Photodynamic therapy in oncology. Expert Opin Pharmacother 2:917–927.

Skaddan MB, Wust FR, Katzenellenbogen JA. 1999. Synthesis and binding of novel Re-containing 7-alpha-substituted estradiol complexes: Models for breast cancer imaging agents. J Org Chem 64:8108–8121.

Skaddan MB, Wust FR, Johnson S, Syhre R, Welch MJ, Katzenellenbogen JA. 2000. Radiochemical synthesis and tissue distribution of Tc-99m-labeled 7-alpha-substituted estradiol complexes. Nucl Med Biol 27:269–278.

Soubeyran I, Quenel N, Mauriac L, Durand M, Bonichon F, Coindre J-M. 1996. Variation of hormonal receptor, pS2, c-erbB-2 and GSTpi contents in breast carcinomas under tamoxifen: A study of 74 cases. Br J Cancer 73:735–743.

Stilts CE, Nelen MI, Hilmey DG, Davies SR, Gollnick SO, Oseroff AR, Gibson SL, Hilf R, Detty MR. 2000. Water-soluble, core-modified porphyrins as novel, longer-wavelength-absorbing sensitizers for photodynamic therapy. J Med Chem 43:2403–2410.

Strase K, Audretsch W, Rezai M, Pott G, Bojar H. 2000. The estrogen receptor paradox in breast cancer: Association of high receptor concentrations with reduced overall survival. Breast J 6:118–126.

Swamy N, Purohit A, Garcia-Fernandez A, Jones GB, Ray R. 2001. Estrogen receptor-mediated targeted photodynamic therapy. Twenty Third Annual Meeting of the American Society for Bone and Mineral Research, Phoenix, AZ.

Swamy N, James DA, Mohr SC, Hanson RN, Ray R. 2002. An estradiol-porphyrin conjugate selectively localizes into estrogen receptor-positive breast cancer cells. Bioorg Med Chem 10:3237–3243.

Traish AM, Newton AW, Styperek K, Beazley R, Kavanah M. 1995. Estrogen receptor functional status in human breast cancer. Diagn Mol Pathol 4:220–228.

Vicente MG, Nurco DJ, Shetty SJ, Osterloh J, Ventre E, Hegde V, Deutsch WA. 2002. Synthesis, dark toxicity and induction of in vitro DNA photodamage by a tetra(4-nido-carboranylphenyl)porphyrin. J Photochem Photobiol B 68:123–132.

Vrouenraets MB, Visser GW, Loup C, Meunier B, Stigter M, Oppelaar H, Stewart FA, Snow GB, van Dongen GA. 2000. Targeting of a hydrophilic sensitizer by use of internalizing monoclonal antibodies: A new possibility for use in photodynamic therapy. Int J Cancer 88:108–114.

Vrouenraets MB, Visser GW, Stigter M, Oppelaar H, Snow GB, van Dongen GA. 2001. Targeting of aluminum (III) phthalocyanine tetrasulfonate by use of internalizing monoclonal antibodies: Improved efficacy in photodynamic therapy. Cancer Res 61:1970–1975.

Vrouenraets MB, Visser GW, Stigter M, Oppelaar H, Snow GB, van Dongen GA. 2002. Comparison of aluminium (III) phthalocyanine tetrasulfonate- and meta-tetrahydroxyphenylchlorin-monoclonal antibody conjugates for their efficacy in photodynamic therapy in vitro. Int J Cancer 98:793–798.

Journal of Cellular Biochemistry 99:665–670 (2006)

FAST TRACK

Photodynamic Cell-Kill Analysis of Breast Tumor Cells With a Tamoxifen-Pyropheophorbide Conjugate

Ana Fernandez Cacio[†], Carlos Fernandez-Marcos,[‡] Narasimha Swamy,[§] Darra Dunn, and Rahul Ray*

Bioorganic Chemistry and Structural Biology, Section in Endocrinology, Diabetes and Metabolism, Department of Medicine, Boston University School of Medicine, Boston, Massachusetts

Abstract We hypothesized that estrogen receptor (ER) in hormone-sensitive breast cancer cells could be targeted for selective photodynamic killing of tumor cell with antiestrogen-porphyrin conjugates by combining the over-expression of ER in hormone-sensitive breast cancer cells and tumor-retention property of porphyrin photosensitizers. In this study we describe that a tamoxifen (TAM)-pyropheophorbide conjugate that specifically binds to ERα, caused selective cell-kill in MCF-7 breast cancer cells upon light exposure. Therefore, it is a potential candidate for ER-targeted photodynamic therapy of cancers (PDT) of tissues and organs that respond to estrogen/antiestrogens. J. Cell. Biochem. 99: 665–670, 2006. © 2006 Wiley-Liss, Inc.

Key words: estrogen receptor targeted delivery of photocotoxins; tamoxifen-porphyrin conjugate; photodynamic cell-kill; breast cancer

Breast cancer continues to be a major threat towards women's health, and a leading cause of fatality. Extensive research has emphasized the critical role of endogenous estrogen in the development and progression of breast cancer, and stressed the interaction between estrogen and its cellular receptor, estrogen receptor (ER) in these processes. 'Double-headed' molecules containing estradiol and toxins (geldanamycin, chlorambucil, diynes) have been synthesized to target endogenous ER in hormone-sensitive breast tumor for tumor-selective delivery and toxicity as well as radioimaging of tumor, potentially taking advantage of the over-expression of ER in tumor cells relative to healthy tissues [Kuduk et al., 1999; Shaddan et al., 1999; Easigman et al., 2001; Purohit et al., 2001; Sharma et al., 2004]. These conjugates, however, contain toxins that do not have any particular tendency to be retained by tumor cells. As a result the toxin part of the linked drug do not contribute towards tumor-accumulation of the conjugate. Considering that the ER-content of estrogen-responsive cells is roughly 100,000 copies per cell [Webb et al., 1992], ER binding affinities of majority of these compounds are not high enough for their selective accumulation into the tumor.

Porphyrins are photosensitizers. Therefore, when they are exposed to visible light they catalyze the formation of singlet oxygen, that is, cytotoxic. In addition, porphyrins have a useful property of being retained somewhat preferentially by malignant tissues, possibly due to their unique chemical structures. This is the basis of photodynamic therapy of cancer (PDT) [Sibata et al., 2001].

We hypothesized that chemical coupling of estradiol with a porphyrin might diminish the sole dependency of the conjugate on ER binding. Recently we synthesized several estrogen-porphyrin conjugates to harness the tumor-retention property of porphyrins. We showed that

[†]Fulbright Fellow from Departamento de Química Orgánica, Facultad de Química, Universidad de Santiago de Compostela, Spain.

[‡]On leave from Departamento de Química Orgánica, Facultad de Veterinaria, Universidad de Extremadura, Caceres, Spain.

[§]Deceased.

Grant sponsor: Community Technology Fund, Boston University.

*Correspondence to: Rahul Ray, Boston University School of Medicine, M-1002, 85 East Newton Street, Boston, MA 02118. E-mail: hapi@bu.edu

Received 22 December 2005; Accepted 27 February 2006

DOI 10.1002/jcb.20982

these conjugates accumulated into ER-positive breast tumor cells, despite low ER binding affinities [James et al., 1999; Swamy et al., 2002; Swamy et al., in press] and selectively killed ER-positive breast tumor cells [Swamy et al., in press].

As noted earlier, estradiol is implicated in the development and progression of breast cancer. As a result antiestrogens that disrupt the interaction between ER and estrogen (specific estrogen receptor modulators, SERMs) have been developed. Tamoxifen (TAM), a SERM, has enjoyed considerable success in the hormone treatment of breast tumor [Dardes et al., 2002; Park and Jordan, 2002]. Several other SERMS are currently under various phases of clinical trials with strongly encouraging results. We hypothesize that an antiestrogen-porphyrin conjugate might produce selective phototoxicity in breast tumor without any untoward systemic effect. In this communication we describe results of our initial effort to demonstrate photodynamic cell-kill of MCF-7 breast cancer cells with a TAM-porphyrin conjugate.

EXPERIMENTAL METHODS

Synthesis of the TAM-pyropheophorbide conjugate (TAM-Pyro) (Scheme 1), included in this communication, was reported earlier in a scientific meeting [Swamy et al., 2001]. Detailed description of the synthesis will be published elsewhere.

Competitive Binding Assay of TAM-Pyro With ERα

Competitive ER binding analysis was carried out by incubating baculovirus-expressed recombinant ER-α (Panvera, Madison, WI) with 0.125 nM of [^{3}H]-17β-estradiol (sp. activity 3 Ci/mmol) in the presence of increasing concentrations of estradiol or TAM-Pyro (as denoted in Fig. 1), dissolved in 10 μl of ethanol, in an assay buffer (10 mM Tris, pH 7.5, 10% glycerol, 2 mM of monothioglycerol, and 1 mg/ml BSA, total volume 0.5 ml) for 15 h at 4°C. This was followed by the addition of hydroxylapatite (HAP) slurry to remove protein-bound to [^{3}H]-17β-estradiol from unbound [^{3}H]-17β-estradiol. After centrifugation and three washes with a wash buffer (40 mM Tris, pH 7.4, 100 mM KCl, 1 mM EDTA, 1 mM EGTA) the HAP pellet was transferred to a scintillation vial and re-suspended in 200 μl of ethanol. Radioactivity, bound to the HAP-pellet was determined in a liquid scintillation counter after the addition of scintillation cocktail. Total binding was determined by treating ER samples with [^{3}H]-17β-estradiol only, while non-specific binding was determined by incubating ER samples with [^{3}H]-17β-estradiol and 1 μg of estradiol. Maximum specific binding (B_0) was calculated by subtracting non-specific binding from total binding, while specific binding (B) at each concentration was calculated by subtracting non-specific binding from binding at each concentration. Each concentration was run in triplicate.

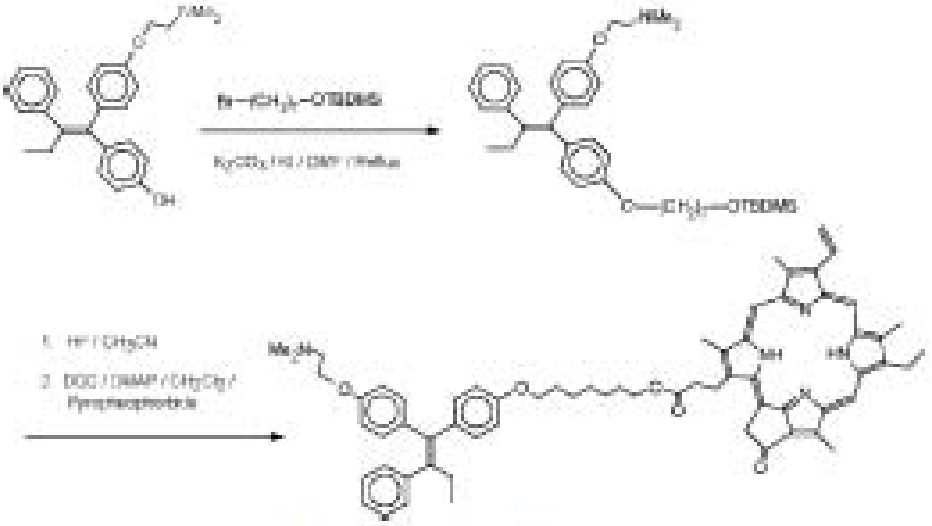

Scheme 1. Synthesis of TAM-PYRO.

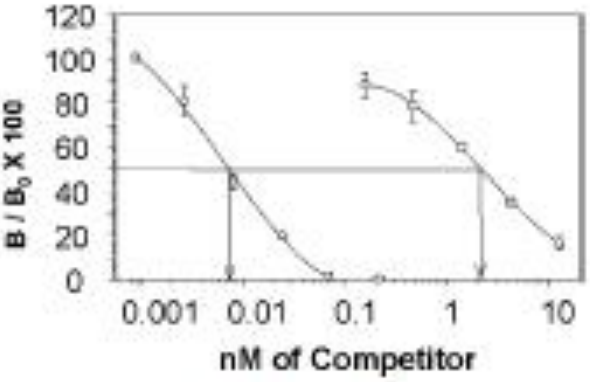

Fig. 1. Competitive ERα binding assays of TAM-Pyro (—□—) and estradiol (—○—).

Photodynaimc Cell-Kill Analysis of MCF-7 Cells Treated With TAM-Pyro or Pyropheophorbide

MCF-7 cells (ATCC, Manassas, VA) were grown in 0.5 ml of DMEM media containing 1% antibiotics and 5% fetal bovine serum to approximately 60% confluence in 24-well cell culture plates. Then the cells were dosed with ethanol, or 5.3 μM of pyropheophorbide or 5.3 μM of TAM-Pyro for 60 min (pyropheophorbide and TAM-Pyro were dissolved in ethanol, and required amounts were diluted with DMEM media so that amount of ethanol was 0.1%). At the end of the incubation one plate was exposed to red light for 10 min and the other was not. Light exposure was carried out by placing the cell culture plate on a slide-viewing box whose lighted surface was covered with a red plastic sheet. [The lamp was equilibrated for 15 min prior to placing the cell culture dishes. Heat was dissipated with a cooling fan. Transmittance of the red filter was determined in a UV-VIS spectrophotometer (Hewlet-Packard, Model 8453). Fluence was determined by a Coherent Lasermate detector with a 2.54 cm^2 detection area (total fluence was 3.5 J/(cm^2)].

After the irradiation step, media were removed from both the plates and replaced with DMEM containing 5% FBS and 1% antibiotics, and the cells were allowed to recover for 16 h. Then the wells were washed twice with PBS (1.0 ml), and fixed by adding 1.0 ml of methanol (−20°C), and incubating on ice for 20 min. Then methanol was aspirated off and the plates were dried in air for 30 min. One milliliter of methylene blue solution (1% in 10 mM borate buffer, pH 8.5) was added to each well and incubated at 25°C for 30 min. The plates were washed three times with 10 mM borate buffer, pH 8.5, and the cells were photographed with an inverted microscope fitted with digital imaging system (Twin-Cam Digital imaging system, Camdek Precision instruments, Boston, MA). The entire assay was carried out three times and the photograph shown in Figure 2 is a representative one.

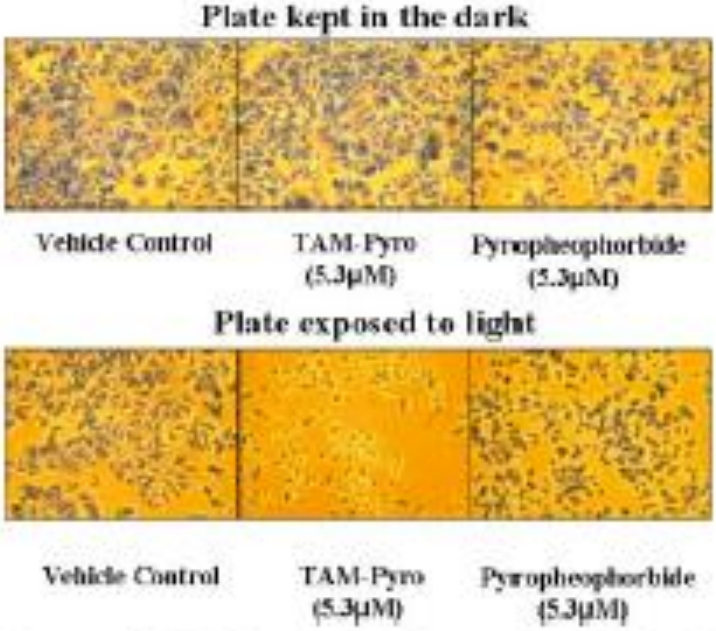

Fig. 2. Cell-killing assays of MCF-7 cells treated with TAM-Pyro or pyropheophorbide, and either exposed to red light or kept in the dark. [Color figure can be viewed in the online issue, which is available at www.interscience.wiley.com.]

RESULTS AND DISCUSSION

PDT is a localized therapy for the treatment of early stage malignancy, palliative therapy for late stage disease, and for tumor bed sterilization to destroy any residual tumor cells detached during resection or any metastasized cells in the area of light illumination. In the US, PDT has been approved for early or late stage lung cancer that are not amenable to surgery, obstructive esophageal cancer, actinic keratoses of the skin, as well as for age-related macular degeneration of the eye [Fisher et al., 1995; Azzer-Siegel et al., 2004; Marmur et al., 2004]. PDT was investigated for palliative treatment for the cutaneous recurrence of breast cancer [Mang et al., 1998; Allison et al., 2001]. Recently Dolmans et al. [2002] reported delay of tumor growth in the PDT of a murine orthotopic breast tumor model.

A limiting factor in PDT involves insufficient localization of the PDT dyes into tumor leading to significant damage to surrounding normal tissue. Development of PDT dyes that localize into tumors with high degree of selectivity has been a major challenge. Several methods for the enhanced delivery of PDT dyes to tumors by chemical conjugation or association with LDL, liposomes, and microspheres have been attempted with limited success [Derycke and Witte, 2004; Sharman et al., 2004]. Recently unique immune signals on the surface of certain cancer cells have been harnessed by chemically conjugating PDT dyes to antibodies to these signals [Goff et al., 1996; Vrouenraets et al., 2001]. However, paucity of active mechanism for the internalization of these immunotoxins has limited their applicability.

On the other hand, TAM, clinically the most widely used antiestrogen, was shown to have cytostatic effects in ER-positive and ER-negative breast cancer cells in vitro [Goldenberg and Fross, 1982]. Paradoxically, TAM was found to stimulate cellular growth in the endometrium, putting the women taking TAM into small but significant risk of endometrial cancer [Dardes et al., 2002]. This puzzle was deciphered after the discovery of ERβ phenotype [Peach et al., 1997]. It was realized that TAM acts as an AP-1 site antagonist in ERα and AP-1 site agonist in ERβ. It was also discovered that endometrial tissues predominantly contains ERβ [Peach et al., 1997]. Therefore, duality of action of TAM is ascribed to its undesired migration into endometrium and the subsequent side effect.

We hypothesized that by chemically conjugating TAM with a porphyrin it might be possible to reduce the dependence on ER binding, and direct the conjugate selectively to the tumor cells. To provide a proof of this hypothesis we synthesized a TAM-porphyrin conjugate (Scheme 1). In this synthetic scheme (Z)-4-hydroxytamoxifen (Sigma Chemical Co., St. Louis, MO), a naturally occurring metabolite of TAM and a strong ER binder, was used as the starting material. Pyropheophorbide (Frontier Science, Logan, UT), a porphyrin, was attached to TAM via a seven-carbon long tether.

Results of the ER binding assays showed that the half-maximal concentrations of TAM-Pyro and E_2 were 2.2 and 0.0075 nM, respectively, suggesting a significantly lower ER binding affinity of TAM-Pyro compared with E_2 (Fig. 1). In a recent study we observed that low ER binding affinity of an estradiol-porphyrin conjugate did not prevent the conjugate to be taken up at a significantly higher concentration by ER-positive MCF-7 human breast cancer cells compared with ER-negative Hs578t human breast cancer cells, as well as demonstrating selective phototoxicity in MCF-7 cells [Swamy et al., 2002; Swamy et al., in press]. These results suggested that low ER binding of the estradiol-porphyrin conjugate might be compensated for, at least in part, by the natural tumor-retaining property of the porphyrin part of the conjugate. In the same token we anticipated that TAM-Pyro, despite low ER binding affinity might be taken up by MCF-7 cells, and display enhanced phototoxicity relative to an equivalent amount of pyropheophorbide, the unconjugated porphyrin.

Targeting a nuclear component (i.e., ER, a nuclear receptor) of tumor cells for phototoxicity has certain advantage. For example, Akhlynina et al. [1997] recently demonstrated that targeting a nuclear signal in glioma cells with a chlorin e6 conjugate dramatically increased the photodynamic cell-kill relative to the un-conjugated porphyrin (chlorin e6).

We incubated MCF-7 cells with 5.3 μM of pyropheophorbide or 5.3 μM of TAM-Pyro for 60 min in the dark followed by exposure to red light. In this preliminary study we used this dose based on our experience with estrogen-porphyrin conjugates [Swamy et al., in press] as well as literature procedure. For example, Yamamoto et al. [2005] recently carried out an in vitro PDT study of glial cells with a dose of

3.5–20 μg/ml of the porphyrin. In our case, 5.3 μM of TAM-Pyro used for our study translates into approximately 5.4 μg/ml of TAM-Pyro. After the light exposure the cells were allowed to recover for 16 h and methylene blue assay was performed. This assay is routinely used for cell viability, because only the live cells are stained by methylene blue, providing an index for cell viability.

As shown in Figure 2, upper panel, when the cells were not exposed to red light, there was no significant cell-kill by pyropheophorbide or TAM-Pyro. In contrast, when the cells were exposed to red light, strong cell-kill (reduced number of viable cells after 16 h of recovery period) was observed with TAM-Pyro (Fig. 2, lower panel, middle figure), but there was very little cell death in pyropheophorbide and light-treated cells (Fig. 2, lower panel, right figure). We have carried out this assay three times and Figure 2 is a representation of a typical case. We counted the live cells after methylene blue treatment under a microscope. There were approximately 10–15% of live cells (average of three experiments) in TAM-Pyro and light-treated cells (Fig. 2, middle figure of the bottom panel) compared with 100% (live cells) with vehicle-treated cells. In all other cases there was no significant difference between vehicle-treated cells and cells treated with TAM-Pyro (no light) or pyropheophorbide

The above results strongly suggest that the interaction between the endogenous ER in the cells and the TAM part of the TAM-Pyro conjugate might have caused a selective accumulation of the conjugate into the cells, which resulted in a higher cell-kill upon exposure to red light. It is to be noted that we did not use a ER-negative cell as control, because TAM has been shown to be effective in killing ER-negative cells also by an ER-independent pathway [Goldenberg and Fromm, 1982]. Such a phenomenon might confound our photodynamic cell-kill data.

On the other hand, lack of cell-death in pyropheophorbide light-treated cells indicated that either an insignificant amount of the dye was taken up by the cells to cause any cell-death or pyropheophorbide light treatment caused minor damage to the cells that recovered quickly. In the former case, majority of pyropheophorbide probably stayed dissolved in a large volume of the media. Although exposure to light produced cytotoxic singlet oxygen in the media (as well as in the cells), these molecules (singlet oxygen) are very short-lived and travel very short distance to result any cell-kill. In the latter case considerably higher dose of pyropheophorbide would have been required to impart significant cell death. These results also suggest that in a clinical set up considerably less amount of the conjugate (TAM-Pyro) would be required to cause tumor cell death, thus avoiding side effects.

In summary, TAM-Pyro, a TAM-pyropheophorbide conjugate showed specific binding affinity for ERα and displayed stronger cell-killing property in MCF-7 breast cancer cells compared with un-conjugated pyropheophorbide upon exposure to red light. Therefore, this conjugate is potentially a reagent for ER-targeted PDT of hormone-sensitive cancers of breast and other estrogen-sensitive organs and tissues. In addition this compound might be devoid of systemic adverse effects of the corresponding estrogen compounds. However, it should be noted that this report includes data that are preliminary in nature to basically provide the proof of the concept.

ACKNOWLEDGMENTS

This work was partially funded by a grant from the Community Technology Fund, Boston University. The authors gratefully acknowledge the assistance from Dr. Tayyaba Hasan, Massachusetts General Hospital, Boston, MA in carrying out light dosimetry measurements.

REFERENCES

Akhlynina TV, Jans DA, Rosenkranz AA, Statsyuk NV, Rakhmilova IY, Toth G, Pavo I, Rubin AB, Sobolev AS. 1997. Nuclear targeting of chlorin e_6 enhances its photosensitizing activity. J Biol Chem 272:20328–20331.

Allison R, Moore T, Bowen C, Snider W, Dougherty TJ. 2001. Photodynamic therapy for chest wall progression from breast carcinoma is an underutilized treatment modality. Cancer (Phila) 91:1–8.

Asser-Siegal R, Ehrlich R, Yassur Y, Rosenblatt I, Kramer M, Priel E, Benjamini Y, Weinberg D. 2004. Photodynamic therapy for age-related macular degeneration in a clinical setting: Visual results and angiographic patterns. Am J Ophthalmol 137:258–264.

Davidse RC, O'Reagan RM, Gajdos C, Robinson SP, Bentrem D. 2002. Effects of a new clinically relevant antiestrogen (GW5638) related to tamoxifen on breast and endometrial cancer growth in vitro. Clin Cancer Res 8:1295–1301.

Derycke AS, Witte PA. 2004. Liposomes for photodynamic therapy. Adv Drug Deliv Rev 56:17–30.

Dolmans DEJGJ, Kadambi A, Hill JS, Flores KR, Gerber JN, Walker JP, Borel Rinkes IHM, Jain RK, Fukumura D. 2002. Targeting tumor vasculature and cancer cells in orthotopic breast tumor by fractionated photosensitizer dosing photodynamic therapy. Cancer Res 62:4289–4294.

Essigmann JM, Rink SM, Park HJ, Croy RG. 2001. Design of DNA damaging agents that hijack transcription factors and block DNA repair. Adv Exp Med Biol 500:301–313.

Fisher AM, Murphree AL, Gomer CJ. 1995. Clinical and pre-clinical photodynamic therapy. Laser Surg Med 17:2–31.

Goff BA, Blake J, Bamberg MP, Hasan T. 1996. Treatment of ovarian cancer with photodynamic therapy and immunoconjugates in a murine ovarian cancer model. Br J Cancer 74:1194–1198.

Goldenberg GJ, Froese EK. 1982. Drug and hormone sensitivity of estrogen receptor positive and negative human breast cancer cells in vitro. Cancer Res 42:5147–5151.

James DA, Swamy N, Hanson RN, Ray R. 1999. Synthesis and estrogen receptor binding affinity of a porphyrin-estradiol conjugate for photodynamic therapy of cancer. Bioorg Med Chem Lett 9:2379–2384.

Kuduk SD, Zheng FF, Sepp-Lorenzino L, Rosen N, Danishefsky SJ. 1999. Synthesis and evaluation of geldanamycin-estradiol hybrids. Bioorg Med Chem Lett 9:1233–1238.

Mang TS, Allison R, Hewson G, Snider W, Moskowitz RA. 1998. Phase II/III clinical study of tin ethyl etiopurpurin(Purlytin)-induced photodynamic therapy for the treatment of recurrent cutaneous metastatic breast cancer. Cancer J Sci Am 4:378–384.

Marmur ES, Schmults CD, Goldberg DJ. 2004. A review of laser and photodynamic therapy for the treatment of nonmelanoma skin cancer. Dermatol Surg 30:264–271.

Park W-C, Jordan VC. 2002. Selective estrogen receptor modulators (SERMs) and their roles in breast cancer prevention. Trends Mol Med 8:82–88.

Paech K, Webb P, Kuiper GG, Nilsson S, Gustafsson J, Kushner PJ, Scanlan TS. 1997. Differential ligand activation of estrogen receptors ER alpha and ER beta at AP-1 sites. Science 277:1508–1510.

Purohit A, Wyatt J, Hynd G, Wright J, El-Shafey A, Swamy N, Ray R, Jones GB. 2001. Chemical synthesis of hormone receptor probes: High affinity photoactivated enediyne-estrogens. Tetrahedron Lett 42:8579–8582.

Sharma U, Marquis JC, Nicole Dinaut A, Hillier SM, Fedeles B, Rye PT, Essigmann JM, Croy RG. 2004. Design, synthesis, and evaluation of estradiol-linked genotoxicants as anti-cancer agents. Bioorg Med Chem Lett 14:3829–3833.

Sharman WM, van Lier JE, Allen CM. 2004. Targeted photodynamic therapy via receptor mediated delivery systems. Adv Drug Deliv Rev 56:53–76.

Sibata CH, Colussi VC, Oleinick NL, Kinsella TJ. 2001. Photodynamic therapy in oncology. Expert Opin Pharmacother 2:917–927.

Skaddan MB, Wust FR, Katzenellenbogen JA. 1999. Synthesis and binding of novel Re-containing 7-alpha-substituted estradiol complexes: Models for breast cancer imaging agents. J Org Chem 64:8108–8121.

Swamy N, Purohit A, Gacio Fernandez A, Jones GB, Ray R. 2001. Estrogen receptor-mediated targeted photodynamic therapy. Twenty Third Annual Meeting of the American Society for Bone and Mineral Research, Phoenix, AZ, 2001.

Swamy N, James DA, Mohr SC, Hanson RN, Ray R. 2002. An estradiol-porphyrin conjugate selectively localizes into estrogen receptor-positive breast cancer cells. Bioorg Med Chem 10:3237–3243.

Swamy N, Purohit A, Fernandez-Gacio A, Jones GB, Ray R. Nuclear estrogen receptor targeted photodynamic therapy: Selective uptake and killing of MCF-7 breast cancer cells by αC_{11}-α-alkynylestradiol-porphyrin conjugate. J Cell Biochem (in press).

Vrouenraets MB, Visser GW, Stigter M, Oppelaar H, Snow GB, van Dongen GA. 2001. Targeting of aluminum (III) phthalocyanine tetrasulfonate by use of internalizing monoclonal antibodies: Improved efficacy in photodynamic therapy. Cancer Res 61:1970–1975.

Webb P, Lopez GN, Greene GL, Baxter JD, Kushner PJ. 1992. The limits of the cellular capacity to mediate an estrogen response. Mol Endocrinol 6:157–167.

Yamamoto J, Hirano T, Koide M, Kohno E, Inenaga C, Tokuyama T, Yokota N, Yamamoto S, Terakawa S, Namba H. 2005. Selective accumulation and strong photodynamic effects of a new photosensitizer, ATX-S10.Na (II), in experimental malignant glioma. Int J Oncol 27:1207–1213.

Available online at www.sciencedirect.com
ScienceDirect
Biochemical and Biophysical Research Communications 361 (2007) 189–195
BBRC
www.elsevier.com/locate/ybbrc

Mechanistic and pharmacodynamic studies of a 25-hydroxyvitamin D_3 derivative in prostate cancer cells

James R. Lambert [b], Christian D. Young [b], Kelly S. Persons [a], Rahul Ray [a,*]

[a] Department of Medicine, Boston University School of Medicine, 85 East Newton Street, Boston, MA 02118, USA
[b] Department of Pathology, University of Colorado Health Science Center, Aurora, CO, USA

Received 2 July 2007
Available online 16 July 2007

Abstract

1,25-Dihydroxyvitamin D_3 ($1,25(OH)_2D_3$), the biologically active form of vitamin D has strong antiproliferative effects in cancer cells. But it is highly toxic at therapeutic doses. We have observed that 25-hydroxyvitamin D_3-3-bromoacetate (25-OH-D_3-3-BE), a derivative of 25-hydroxyvitamin D_3, the pro-hormonal form of $1,25(OH)_2D_3$ has strong growth-inhibitory and proapoptotic properties in hormone-sensitive and hormone-refractory prostate cancer cells. In the present investigation we demonstrate that the antiproliferative effect of 25-OH-D_3-3-BE is predominantly mediated by VDR in ALVA-31 prostate cancer cells. In other mechanistic studies we show that the proapoptotic property of 25-OH-D_3-3-BE is related to the inhibition of phosphorylation of Akt, a pro-survival protein. Furthermore, we carried out cellular uptake and serum stability studies of 25-OH-D_3-3-BE to demonstrate potential therapeutic applicability of 25-OH-D_3-3-BE in hormone-sensitive and hormone-insensitive prostate cancer.

Keywords: 25-Hydroxyvitamin D_3-derivative; 1,25-Dihydroxyvitamin D_3; Prostate cancer; Vitamin D receptor; Akt pathway; Apoptosis; Serum stability; Bio-availability; Cellular uptake

Prostate cancer is the second leading cause of cancer death among men in the US. Although it mostly affects elderly men, the number of younger men with prostatic carcinoma is significant and increasing. Change in life style and increase in longevity has further emphasized the need for the effective treatment of prostate cancer, particularly those cancers that do not respond to androgen-ablation therapy [1]. The current clinical interventions for prostate cancer include surgical removal of prostate, radiation, cryotherapy and chemotherapy. However, these clinical strategies are associated with life-altering side effects including, but not limited to, incontinence and impotence. The mainstay of hormone therapy to reduce the level of testosterone and block its harmful effect in the development and growth of prostate tumor includes agents that are involved in androgen-deprivation and androgen receptor antagonism. However, for prostate cancers, localized and/or metastatic, which fail to respond to androgen-ablation therapy no therapy is currently available.

Numerous epidemiological studies have demonstrated the importance of dietary vitamin D in preventing various cancers [2–4]. In addition, the therapeutic potential of 1α,25-dihydroxyvitamin D_3 ($1,25(OH)_2D_3$), the biologically active metabolite of vitamin D, and its analogs either as monotherapy or in combination with chemotherapeutic agents in cancer is well-documented [5–13]. Although some analogs (e.g. EB-1089) have shown promise [14,15], and Calcipotriene (Dovonex) has been approved by FDA for psoriasis, availability of efficacious vitamin D-based cancer drugs with low toxicity has remained elusive.

The design, synthesis and development of non-toxic analogs of vitamin D has focused primarily on chemical modifications of various parts of $1,25(OH)_2D_3$ because this dihydroxy metabolite of vitamin D_3 is biologically the most active form of the hormone. Although 25-hydroxyvitamin

* Corresponding author. Fax: +1 617 638 8194.
E-mail address: bapi@bu.edu (R. Ray).

0006-291X/$ - see front matter © 2007 Elsevier Inc. All rights reserved.
doi:10.1016/j.bbrc.2007.07.012

D_3 (25-OH-D_3), the non-toxic pre-hormonal form of 1,25$(OH)_2D_3$ has long been considered to be biologically inactive, two recent publications demonstrate considerable antiproliferative activity of this molecule in prostate and pancreatic cancer cells underscoring the potential of 25-OH-D_3 as a potential antiproliferative agent for prostate cancer therapy [16,17]. We reported that 25-hydroxyvitamin D_3-3β-(2)-bromoacetate (25-OH-D_3-3-BE), a derivative of 25-OH-D_3, shows strong antiproliferative and pro-apoptotic properties in a host of androgen-sensitive and androgen-refractory prostate cancer cells suggesting a translational potential of this compound in prostate cancer [18]. In the present study, we investigated mechanistic aspects of the growth inhibitory and pro-apoptotic properties of 25-OH-D_3-3-BE in prostate cancer cells. We also carried out cellular uptake and serum-stability analyses of this compound in view of its translational potential. A thorough understanding of the molecular mechanisms of 25-OH-D_3-3-BE in human prostate cancer cells will aid in the development of this compound as a potential chemotherapeutic agent for prostate cancer.

Materials and methods

Compounds. 25-OH-D_3-3-BE and 25-hydroxyvitamin D_3-3β-[2-^{14}C]-bromoacetate [^{14}C-25-OH-D_3-3-BE] (sp. activity 14.3 mCi/mmol) was synthesized according to published procedures from our laboratory [19]. [25(26)-^{3}H]25-Hydroxyvitamin D_3-3β-bromoacetate [^{3}H-25-OH-D_3-3-BE] (sp. activity 0.02 μCi/μmol) was synthesized by spiking a sample of 25-OH-D_3 with [25(26)-^{3}H]25-hydroxyvitamin D_3 (50,000 cpm, specific activity 20.6 Ci/mmol and treating the mixture with bromoacetaic acid, dicyclohexylcarbodiimide and 4-*N*,*N*′-dimethylaminopyridine in anhydrous dichloromethane, and purifying the product by preparative thin layer chromatography on a silica plate with 25% ethyl acetate in hexanes as eluant [19].

Cell culture. ALVA-31, DU-145 and PC-3 cells were purchased from American Type Culture Collection, Manassas, VA; and were grown in RPMI 1640 or DMEM media (Gibco) containing 5% fetal bovine serum (FBS). ALVA-31 VDR-sense and VDR-antisense cells were grown in RPMI 1640 containing 5% FBS and 400 μg/mL G418 (Invitrogen).

Cellular proliferation assay. ALVA-31 human prostate cancer cells were stably transfected with an antisense VDR expression vector and an empty vector, and assayed for their response to 1,25$(OH)_2D_3$ or 25-OH-D_3-3-BE [20]. Antisense cells (3000 cells/well) and vector control cells (1000 cells/well) were seeded in 24 well dishes and allowed to attach for 16 h. The cells were treated with 1,25$(OH)_2D_3$, 25-OH-D_3-3-BE or ethanol control, and incubated for 6 days with treatment changes every 2 days. Monolayers were harvested after six days for DNA quantitation by the Hoechst 33258 fluorescence assay [21]. Triplicate determinations were used to calculate the mean DNA concentration +/− standard error.

Phosphorylated Akt analysis. PC-3 cells were grown to 70–80% confluency in RPMI media containing 10% FBS in 35 mm tissue culture dishes. The media was replaced with media containing 10^{-6} M each of either 1,25$(OH)_2D_3$ or 25-OH-D_3-3-BE or ethanol control and allowed to incubate 24 h in a humidified 37 °C, 5% CO_2 incubator. Following the treatment, the cell monolayers were washed with 1 ml cold PBS and then lysed in 100 μl RIPA (50 mM Tris pH 7.4, 1% Triton X-100, 0.5% deoxycholic acid, 0.1% SDS, 150 mM NaCl, 2 mM EDTA, 50 mM NaF and 1 mM Na_3VO_4) containing Roche Complete Protease Inhibitors. Cell lysates were subjected to centrifugation (13,000*g*, 15 min) and the clarified lysate was collected and the protein concentration determined by Bradford Assay (Bio-Rad). Electrophoresis was performed using 10% SDS–PAGE gels and 40 μg of lysate per lane followed by transfer to Immobilon membrane (Millipore). Membrane was blocked with PBS containing 5% non-fat dry milk and 0.05% Tween-20, probed with anti-phospho-Ser473-Akt antibody and anti-Akt antibody (Cell Signaling Technologies) and detected by enhanced chemiluminescence (Perkin Elmer).

Cellular uptake of ^{14}C-25-OH-D_3-3-BE in DU-145 cells. DU-145 cells were grown to approximately 50% confluence in 35 mm dishes in DMEM media containing 10% FBS and additives, and incubated with ^{14}C-25-OH-D_3-3-BE (10,000 cpm in 10 μl of ethanol) in 1 ml of the media at 37 °C for 60 min. Following the incubation media was withdrawn and the cells were washed thoroughly (5 × 5 ml) with phosphate buffered saline (PBS). Then 5 ml of methanol was added to the plate and the cells were scraped off with a rubber policeman. The plate was washed thoroughly with 3 × 1 ml of methanol and 3 × 1 ml of PBS. Combined media and cell extracts were lyophilized and re-dissolved/suspended in 3 ml of water. The aqueous mixtures from cells and media fraction were extracted with 5 × 2 ml of ethyl acetate. The organic extract of each fraction was dried under nitrogen and re-dissolved in the mobile phase (10% H_2O–MeOH) for HPLC analysis. These extracts were analyzed by reverse phase HPLC using an Agilent 5 μm C_{18} column, 10% H_2O in methanol mobile phase, 1.5 ml/min flow rate, 254 nm detection wave length (for the unlabeled standards) in an Agilent Series 1100 HPLC system with photo diode array detector. Effluent from the HPLC was directly introduced into a Radiomatic OnLine radioactivity detector (Radiomatic Instruments, Tampa, FL). Prior to the analysis of the organic extracts, a mixture containing a standard sample of 25-OH-D_3-3-BE was analyzed by the same system. This assay was run in duplicate.

Serum-stability of ^{3}H-25-OH-D_3-3-BE. A 0.5 ml aliquot of a pooled human serum sample was incubated with ^{3}H-25-OH-D_3-3-BE (10,000 cpm, dissolved in 10 μl of ethanol) at 37 °C for 60 min followed by extraction with 10 × 0.5 ml of ethyl acetate. The organic extracts were dried under a stream of argon, re-dissolved in mobile phase (10% H_2O in methanol) and analyzed by reverse phase HPLC as described before, except in this case fractions from HPLC were collected manually at one min intervals. The fractions were mixed with scintillation cocktail and counted for radioactivity in a scintillation counter. A solution containing standard samples of 25-OH-D_3 and 25-OH-D_3-3-BE was run in the HPLC as a standard.

Results and discussion

The antiproliferative effect of 25-OH-D_3-3-BE is mediated by VDR in ALVA-31 prostate cancer cells

In previous studies, we described that 25-OH-D_3-3-BE, a derivative of 25-OH-D_3 that affinity alkylates the hormone-binding pocket of VDR [22], strongly inhibits the growth of several androgen-sensitive and androgen insensitive prostate cancer cells via induction of apoptotic pathways [18]. We also demonstrated that 25-OH-D_3-3-BE induces 1α,25-dihydroxyvitamin D_3-24-hydroxylase (24-OHase) promoter activity, and promotes strong interaction between VDR and general transcriptional factors RXR and GRIP-1 [18]. These results suggested that the cellular activities of 25-OH-D_3-3-BE are similar to those of 1,25$(OH)_2D_3$, and mediated by a VDR-activation pathway.

To confirm that the growth inhibitory properties of 25-OH-D_3-3-BE are mediated by its interaction with VDR, we performed cellular proliferation assays in ALVA-31 "VDR-null" prostate cancer cells. We argued that since growth inhibitory effects of 1,25$(OH)_2D_3$ is manifested via its interaction with VDR in ALVA-31 cells [20], if the antiproliferative effects of 25-OH-D_3-3-BE is also modulated through VDR, we can expect that 25-OH-D_3-3-BE-mediated

growth inhibition of ALVA-31 cells would be either eliminated or diminished in cells transfected with a VDR-antisense vector.

As shown in Fig. 1 growth of VDR-sense cells (empty vector) is strongly inhibited by $10^{-7\text{-}6}$ M of $1,25(OH)_2D_3$ as reported earlier [20]. Conversely, the growth of antisense cells treated with $10^{-7\text{-}6}$ M of $1,25(OH)_2D_3$ is similar to that of ethanol-control, confirming the requirement of VDR in the antiproliferative activity of $1,25(OH)_2D_3$ in ALVA-31 cells. In the case of 25-OH-D_3-3-BE, 10^{-6} M of this compound strongly inhibited the growth of empty vector (sense cells), while growth of anti-sense cells is similar to that of ethanol control. However, with 10^{-7} M of 25-OH-D_3-3-BE, the growth of both sense and antisense cells are similar to that of the control. This result is in accordance with our previous studies where we observed the antiproliferative effect of 25-OH-D_3-3-BE is strongest at 10^{-6} M dose, and decreased significantly at lower doses [18]. Overall, the result of this assay strongly emphasizes the requirement for VDR in mediating the antiproliferative effect of 25-OH-D_3-3-BE in prostate cancer cells.

We observed that 25-OH-D_3-3-BE is approximately one log scale less efficient than $1,25(OH)_2D_3$ in inhibiting the growth of wild type ALVA-31. Earlier we reported similar dose-dependence (of 25-OH-D_3-3-BE) in modulating the message for 24-OHase and inducing interaction of VDR with RXR GRIP-1 transcription factors [18]. Differences in the potency of vitamin D analogs to induce various gene-regulatory events through VDR have been reported. For example, 2MD, an analog of $1,25(OH)_2D_3$ shows a range of sensitivity for regulating gene expression from $ED_{50} = 10^{-11}$ mol/L for the up-regulation of RANKL to $ED_{50} > 10^{-10}$ mol/L for induction of osteopontin and 24-OHase in mouse osteoblasts [23]. Similarly, it was shown that RO-26-9228, an analog of $1,25(OH)_2D_3$ has an ED_{50} of 2.1×10^{-8} mol/L for the induction of 24-OHase, and an ED_{50} of 2.7×10^{-7} mol/L for the induction of Calbindin D9K in Caco-2 cells [24]. Therefore, the lower efficacy of 25-OH-D_3-3-BE compared with $1,25(OH)_2D_3$ in modulating gene-regulatory events is not unexpected.

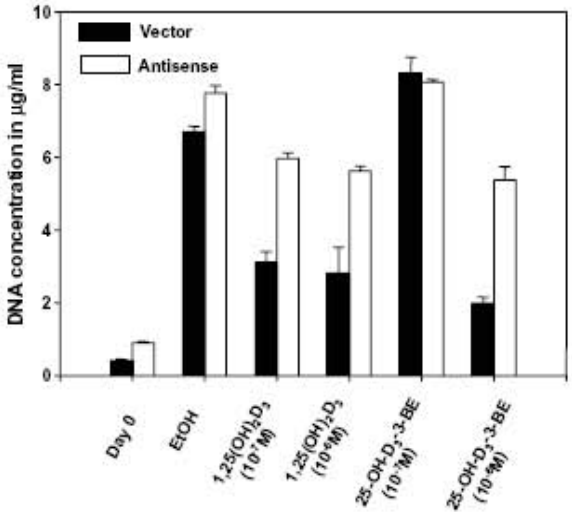

Fig. 1. 25-OH-D_3-3-BE inhibits the growth of ALVA-31 prostate cancer cells through a VDR-dependent mechanism. ALVA-31 control (vector) and ALVA-31 VDR "null" cells (antisense) were treated with the indicated doses of $1,25(OH)_2D_3$, 25-OH-D_3-3-BE and ethanol control for 6 days. Monolayers were harvested for DNA quantification. Each condition was conducted in triplicate. Values are presented as mean DNA concentration ± standard error.

25-OH-D_3-3-BE inhibits Akt phosphorylation in PC3 prostate cancer cells

Previously, we reported that 25-OH-D_3-3-BE induced nuclear DNA-fragmentation and activated caspases 3, 8 and 9, hallmarks of apoptosis, in PC3 cells while an equimolar concentration of $1,25(OH)_2D_3$ and 25-OH-D_3 failed to do so [18]. Induction of caspases and fragmentation of nuclear DNA represent downstream signaling markers of apoptosis and these markers are regulated by their upstream modulators such as Akt kinase. We postulated that induction of apoptosis by 25-OH-D_3-3-BE might be mediated by the down-regulation of Akt-activity resulting in the observed up-regulation of pro-apoptotic proteins.

Akt (*aka* protein kinase B, PKB) is a serine/threonine kinase that is involved in signal transduction by phosphoinositol-3′-kinase/Akt pathway. Akt is involved in a variety of normal cellular functions. In addition, Akt has profound effects in tumorigenesis, cell proliferation, growth and survival. Recently it has been shown that Akt regulates G(1) cell cycle progression and cyclin expression in prostate cancer cells [25]. Another study showed upregulation of Akt and other growth promoting signaling molecules in malignant prostate epithelial cells [26]. We postulated that induction of apoptosis by 25-OH-D_3-3-BE might be mediated by the down-regulation of Akt-activity resulting in the up-regulation of pro-apoptotic proteins. As shown in Fig. 2, we observed significant inhibition of phosphorylated Akt in prostate cancer cells treated with 25-OH-D_3-3-BE, while Akt phosphorylation was unaffected by $1,25(OH)_2D_3$.

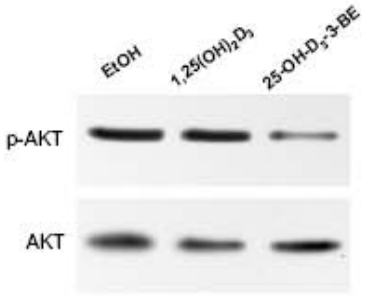

Fig. 2. 25-OH-D_3-3-BE inhibits Akt phosphorylation in PC-3 prostate cancer cells. PC-3 cells were treated with equimolar concentrations of $1,25(OH)_2D_3$, 25-OH-D_3-3-BE and ethanol control and Western analysis performed for phosphorylated Akt (p-Akt). The blot was stripped and re-probed for total Akt to ensure equal loading of protein in the lanes.

These results suggested that 25-OH-D_3-3-BE may exert its antiproliferative effects, at least in part, by inhibiting this pro-survival pathway.

25-OH-D_3-3-BE is taken up in its intact form by DU-145 cells

The antiproliferative and apoptotic activities of 25-OH-D_3-3-BE in prostate cancer cells strongly endorse its potential as a therapeutic agent for prostate cancer. However, evaluation of this potential requires examination of its pharmacodynamic properties, including its bio-availability and stability in serum.

25-OH-D_3-3-BE contains a hydrolytically unstable ester bond and its hydrolysis would produce equivalent amounts of 25-OH-D_3 and bromoacetic acid. In an earlier study we demonstrated that the growth inhibitory property of 25-OH-D_3-3-BE is related strictly to the intact molecule

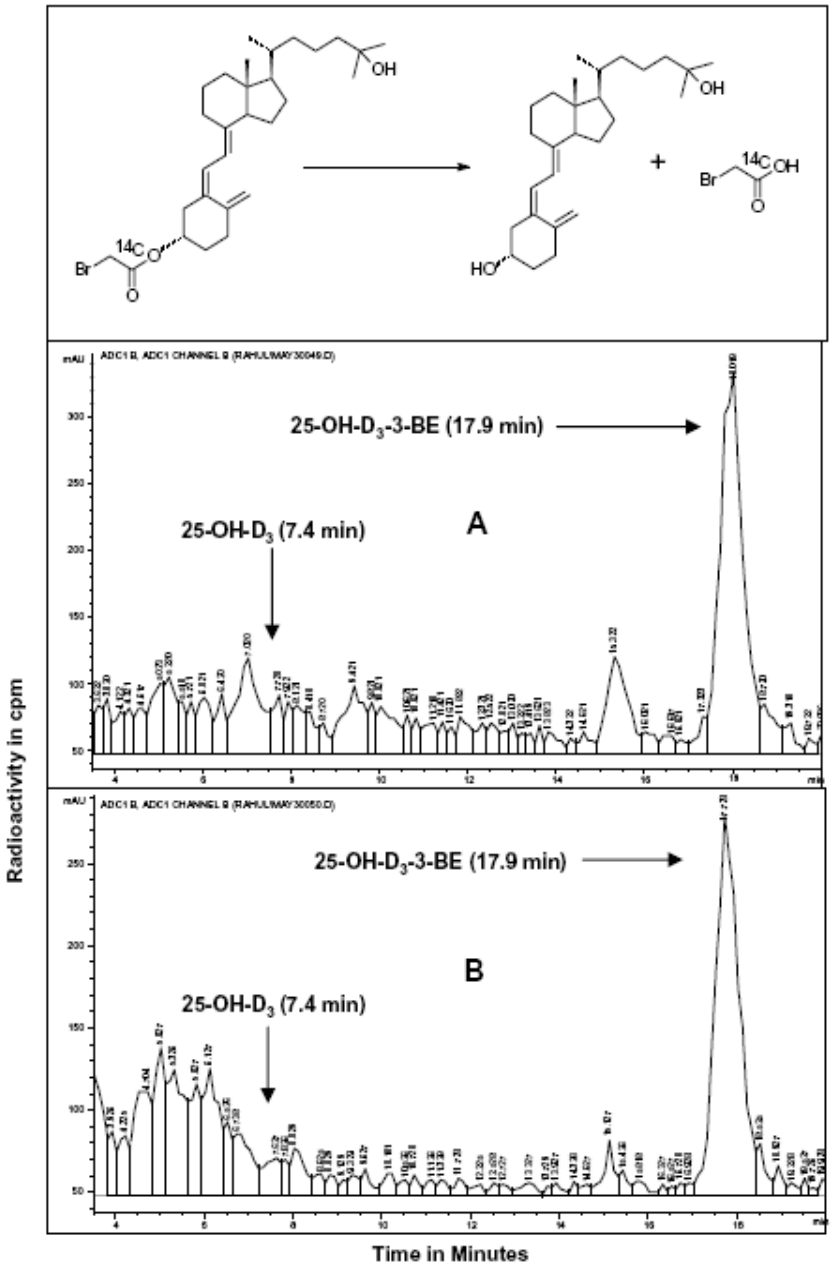

Fig. 3. 25-OH-D_3-3-BE is taken up by DU-145 prostate cancer cells in its intact form. DU-145 prostate cancer cells were treated with ^{14}C-25-OH-D_3-3-BE and HPLC analysis performed on the media (A) and whole cell extracts (B). Fractions were counted for radioactive content. Hydrolysis of ^{14}C-25-OH-D_3-3-BE producing unlabeled 25-OH-D_3 and ^{14}C-bromoacetic acid is shown in the top of the figure. (A) Media extract; (B) Cellular extract. Position of the 25-OH-D_3 peak (retention time 7.4 min) is shown with an arrow.

and its hydrolysis products [18]. Therefore, we carried out a cellular uptake study of 25-OH-D_3-3-BE in DU-145 cells. The goal of this study was to determine whether we can isolate 25-OH-D_3-3-BE in its intact form from cellular extracts. For this study we employed a radiolabeled version of 25-OH-D_3-3-BE, i.e. 25-hydroxyvitamin D_3-3β-[2^{14}C]-bromoacetate (^{14}C-25-OH-D_3-3-BE). We argued that hydrolysis of ^{14}C-25-OH-D_3-3-BE should produce unlabeled 25-OH-D_3 and radiolabeled bromoacetic acid (^{14}C-bromoacetic acid) (Top panel, Fig. 3). Bromoacetic acid is a polar molecule and therefore it will not be extracted from the media and cellular extracts by an organic solvent. Therefore, the presence of a radioactive peak corresponding to 25-OH-D_3-3-BE would represent intact 25-OH-D_3-3-BE.

HPLC analysis of the organic extracts of media and DU-145 cells incubated with ^{14}C-25-OH-D_3-3-BE demonstrate that chromatograms of both media (Fig. 3A) and cellular fractions (Fig. 3B) contain a single well-defined peak at 17.9 min representing ^{14}C-25-OH-D_3-3-BE (Fig. 3, middle and bottom Panels). There are low-level and unresolved polar peaks in media and cellular extracts, particularly in the cellular extract, possibly representing alkylated small molecules derived from the buffer (alkylated proteins are usually not extracted from aqueous phase by an organic solvent, like ethyl acetate used in this study). Collectively these results strongly suggest that 25-OH-D_3-3-BE is taken up by the cells in its intact form.

25-OH-D_3-3-BE is stable in human serum

Serum-stability is an important aspect of a potential therapeutic agent, because it determines the availability of the molecule in its intact and bioactive form. This study required that we incubate human serum with 25-OH-D_3-3-BE and then carry out an organic solvent extraction and HPLC-analysis of the extract. We argued that ^{14}C-25-OH-D_3-3-BE, used for the previous study, could not be used here, because hydrolysis of ^{14}C-25-OH-D_3-3-BE would result in a loss of radioactivity (as ^{14}C-bromoacetic

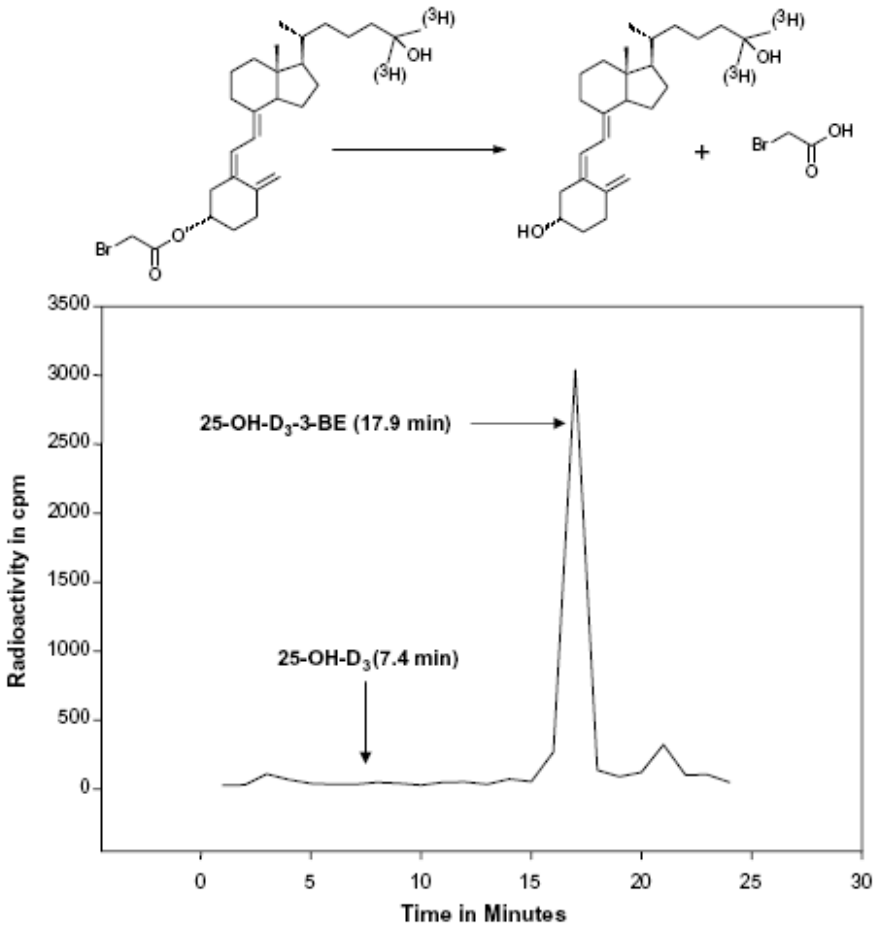

Fig. 4. 25-OH-D_3-3-BE is stable in human serum. ^{3}H-25-OH-D_3-3-BE was synthesized and incubated with human serum, followed by extraction with an organic solvent, and HPLC analysis of the organic extract. Fractions from HPLC were mixed with scintillation cocktail and counted for radioactivity. (Upper panel) Representation of the hydrolysis of ^{3}H-25-OH-D_3-3-BE leading to the production of ^{3}H-25-OH-D_3 and unlabeled bromoacetic acid. (Lower panel) Peak indicating intact ^{3}H-25-OH-D_3-3-BE. Position of the 25-OH-D_3 peak (retention time 7.4 min) is shown with an arrow.

acid) in the aqueous phase. Therefore, in order to determine the extent of hydrolysis of 25-OH-D_3-3-BE in serum we synthesized ^{3}H-25-OH-D_3-3-BE in which the radiolabel (^{3}H) is in the 25-OH-D_3 moiety. Hence, its hydrolysis would produce ^{3}H-25-OH-D_3 and unlabeled bromoacetic acid (as noted in Fig. 4, inset); and the organic extract will thus contain a combination of ^{3}H-25-OH-D_3 and ^{3}H-25-OH-D_3-3-BE if hydrolysis occurs.

The results of this assay (Fig. 4) show that the majority of radioactivity is concentrated in a single peak corresponding to ^{3}H-25-OH-D_3-3-BE. The absence of a radioactive peak corresponding to ^{3}H-25-OH-D_3 (hydrolysis product) indicates that ^{3}H-25-OH-D_3-3-BE is fully stable under these experimental conditions. Absence of hydrolysis also suggests that 25-OH-D_3-3-BE maintains considerable bio-availability in its intact form to attest its potential as a therapeutic agent for prostate cancer.

In summary, results of the studies described herein strongly suggest that the growth inhibitory properties of 25-OH-D_3-3-BE are mediated by a VDR-dependent pathway similar to the native hormone, 1,25$(OH)_2D_3$, while its apoptotic property is manifested via activation of Akt-phosphorylation pathway. Additionally, results included in this communication demonstrate favorable phramacodynamic properties, including cellular uptake in intact form and serum-stability leading to the belief that 25-OH-D_3-3-BE can potentially be developed as a therapeutic agent for prostate cancer.

Acknowledgments

Supported by Department of Defense Grant PC 051136 and Community Technology Fund, Boston University (to R.R.), and American Cancer Society Research Scholar Grant RSG-04-170-01-CNE (to J.R.L.).

References

[1] A. Jemal, R. Siegel, E. Ward, T. Murray, J. Xu, C. Smigal, M.J. Thun, Cancer Statistics 2006. CA, Cancer J. Clin. 56 (2) (2006) 106–130.

[2] E. Giovannucci, Y. Liu, E.B. Rimm, B.W. Hollis, C.S. Fuchs, M.J. Stampfer, W.C. Willett, Prospective study of predictors of vitamin D status and cancer incidence and mortality in men, J. Natl. Cancer Inst. 98 (2006) 451–459.

[3] E. Giovannucci, Y. Liu, M.J. Stampfer, W.C. Willett, A prospective study of calcium intake and incident and fatal prostate cancer, Cancer Epidemiol. Biomarkers Prev. 15 (2006) 203–210.

[4] E.K. Wei, E. Giovannucci, C.S. Fuchs, W.C. Willett, C.S. Mantzoros, Low plasma adiponectin levels and risk of colorectal cancer in men: a prospective study, J. Natl. Cancer Inst. 97 (2005) 1688–1694.

[5] S. Matsuda, G. Jones, Promise of vitamin D analogues in the treatment of hyperproliferative conditions, Mol. Cancer Ther. 5 (2006) 797–808.

[6] . D.L. Trump, J. Muindi, M. Fakih, W.D. Yu, C.J. Johnson, Vitamin D compounds: clinical development as cancer therapy and prevention agents, Anticancer Res. 26 (2006) 2551–2556.

[7] A.L. Sutton, P.N. MacDonald, Vitamin D: more than a "bone-a-fide" hormone, Mol. Endocrinol. 17 (2003) 777–791.

[8] M.G. Fakih, D.L. Trump, J.R. Muindi, J.D. Black, R.J. Bernardi, P.J. Creaven, J. Schwartz, M.G. Brattain, A. Hutson, R. French, C.S. Johnson, A phase I pharmacokinetic and pharmacodynamic study of intravenous calcitriol in combination with oral gefitinib in patients with advanced solid tumors, Clin Cancer Res. 13 (2007) 1216–1223.

[9] D.L. Trump, D.M. Potter, J. Muindi, A. Brufsky, C.S. Johnson, Phase II trial of high-dose, intermittent calcitriol (1,25 dihydroxyvitamin D3) and dexamethasone in androgen-independent prostate cancer, Cancer 106 (2006) 2136–2142.

[10] J.R. Muindi, Y. Peng, D.M. Potter, P.A. Hershberger, J.S. Tauch, M.J. Capozzoli, M.J. Egorin, C.S. Johnson, D.L. Trump, Pharmacokinetics of high-dose oral calcitriol phase I trial of calcitriol and paclitaxel, Clin. Pharmacol. Ther. 72 (2003) 648–659.

[11] P.A. Hershberger, W-D. Yu, R.A. Modzelewski, R.M. Rueger, C.S. Johnson, D.L. Trump, Calcitriol (1,25-dihydroxycholecalciferol) enhances paclitaxel antitumor activity *in vitro* and *in vivo* and accelerates paclitaxel-induced apoptosis, Clin. Cancer Res. 7 (2001) 1043–1051.

[12] W-D. Yu, M.C. McElwain, R.A. Modzelewski, D.M. Russell, D.C. Smith, D.L. Trump, C.S. Johnson, Enhancement of 1,25-dihydroxyvitamin D3-mediated antitumor activity with dexamethasone, J. Natl. Cancer Inst. 90 (1998) 34–141.

[13] D.C. Smith, C.S. Johnson, C.C. Freeman, J. Muindi, J.W. Wilson, D.L. Trump, A phase I trial of calcitriol (1,25-dihydroxycholecalciferol) in patients with advanced malignancy, Clin. Cancer Res. 5 (1999) 1339–1345.

[14] K. Dalhoff, J. Dancey, L. Astrup, T. Skovsgaard, K.J. Hamberg, F.J. Lofts, O. Rosmorduc, S. Erlinger, J. BachHansen, W.P. Steward, T. Skov, F. Burcharth, T.R. Evans, A phase II study of the vitamin D analogue Seocalcitol in patients with inoperable hepatocellular carcinoma, Br. J. Cancer 89 (2003) 252–257.

[15] T.R. Evans, K.W. Colston, F.J. Lofts, D. Cunningham, D.A. Anthoney, H. Gogas, J.S. de Bono, K.J. Hamberg, T. Skov, J.L. Mansi, A phase II trial of the vitamin D analogue Seocalcitol (EB1089) in patients with inoperable pancreatic cancer, Br. J. Cancer 86 (2002) 680–685.

[16] G.G. Schwartz, D. Eads, A. Rao, S.D. Cramer, M.C. Willingham, T.C. Chen, D.P. Jamieson, L. Wang, K.L. Burnstein, M.F. Holick, C. Koumenis, Pancreatic cancer cells express 25-hydroxyvitamin D-1 alpha-hydroxylase and their proliferation is inhibited by the prohormone 25-hydroxyvitamin D3, Carcinogenesis 25 (2004) 1015–1026.

[17] T.C. Chen, G.G. Schwartz, K.L. Burnstein, B.L. Lokeshwar, M.F. Holick, The in vitro evaluation of 25-hydroxyvitamin D3 and 19-nor-1alpha,25-dihydroxyvitamin D2 as therapeutic agents for prostate cancer, Clin. Cancer Res. 6 (2000) 901–908.

[18] N. Swamy, T.C. Chen, S. Peleg, P. Dhawan, S. Christakos, L.V. Stewart, N. Weigel, R.G. Mehta, M.F. Holick, R. Ray, Inhibition of proliferation and induction of apoptosis by 25-hydroxyvitamin D_3-3β-(2)-bromoacetate, a non-toxic and vitamin D receptor-alkylating analog of 25-hydroxyvitamin D_3 in prostate cancer cells, Clin. Cancer Res. 10 (2004) 8018–8027.

[19] N. Swamy, R. Ray, Affinity labeling of rat serum vitamin D-binding protein, Arch. Biochem. Biophys. 333 (1996) 139–144.

[20] T.E. Hedlund, K.A. Moffatt, G.J. Miller, Vitamin D receptor expression is required for growth modulation by 1 alpha,25-dihydroxyvitamin D3 in the human prostatic carcinoma cell line ALVA-31, J. Steroid Biochem. Mol. Biol. 58 (1996) 277–288.

[21] C. Labarca, K. Paigen, A simple, rapid, and sensitive DNA assay procedure, Anal. Biochem. 102 (1980) 344–352.

[22] N. Swamy, J. Addo, R. Ray, Development of an affinity-driven double cross-linker: isolation of a ligand-activated factor, associated with vitamin D receptor-mediated transcriptional machinery, Bioorg. Med. Chem. Lett. 10 (2000) 361–364.

[23] N.K. Shevde, L.A. Plum, M. Clagett-Dame, H. Yamamoto, J.W. Pike, A potent analog of 1-alpha,25-dihydroxyvitamin d_3 selectively induces bone formation, Proc. Natl. Acad. Sci. USA 99 (2002) 13487–13491.

[24] A. Ismail, C.V. Nguyen, A. Ahene, J.C. Fleet, M.R. Uskokovic, S. Peleg, Effect of cellular environment on the selective activation of the vitamin D receptor by 1-alpha,25-dihydroxyvitamin D_3 and its analog 1-alpha-fluoro-16-ene-20-epi-23-ene-26,27-bishomo-25-hydroxyvitamin D_3 (Ro-26-9228), Mol. Endocrinol. 18 (2004) 393–411.

[25] N. Gao, Z. Zhang, B.H. Jiang, X. Shi, Role of PI3K/Akt/mTOR signaling in the cell cycle progression of human prostate cancer, Biochem. Biophys. Res. Commun. 310 (2003) 1124–1132.

[26] A.R. Uzgare, J.T. Isaacs, Enhanced redundancy of in Akt and mitogen-activated protein kinase induced survival of malignant versus normal prostate epithelia, Cencer Res. 64 (2004) 6190–6199.

Available online at www.sciencedirect.com
ScienceDirect
Biochemical and Biophysical Research Communications 365 (2008) 746–750
BBRC
www.elsevier.com/locate/ybbrc

Cross-talk among structural domains of human DBP upon binding 25-hydroxyvitamin D

Arjun Ray, Narasimha Swamy [†], Rahul Ray [*]

Bioorganic Chemistry & Structural Biology, Department of Medicine, Boston University School of Medicine, 85 East Newton Street, Boston, MA 02118, USA

Received 1 November 2007
Available online 21 November 2007

Abstract

Serum vitamin D-binding protein (DBP) is structurally very similar to serum albumin (ALB); both have three distinct structural domains and high cysteine-content. Yet, functionally they are very different. DBP possesses high affinity for vitamin D metabolites and G-actin, but ALB does not. It has been suggested that there may be cross-talk among the domains so that binding of one ligand may influence the binding of others. In this study we have employed 2-*p*-toluidinyl-6-sulfonate (TNS), a reporter molecule that fluoresces upon binding to hydrophobic pockets of DBP. We observed that recombinant domain III possesses strong binding for TNS, which is not influenced by 25-hydroxyvitamin D_3 (25-OH-D_3), yet TNS fluorescence of the whole protein is quenched by 25-OH-D_3. These results provide a direct evidence of cross-talk among the structural domains of DBP.

Keywords: Structural domains of vitamin D-binding protein (DBP); 25-Hydroxyvitamin D_3 (25-OH-D_3); 2-*p*-Toluidinyl-6-sulfonate (TNS); Reporter molecule; Conformational change; Cross-talk among domains

Vitamin D-binding protein (DBP) or group specific component (Gc) is a relatively abundant, polymorphic, and sparsely glycosylated serum protein with multiple functions. DBP binds vitamin D and its metabolites with high affinity ($K_d = 10^{8-11}\ M^{-1}$); and this property (of DBP) is manifested in the organ-specific transportation of vitamin D and its metabolites to target tissues and stepwise oxidation of vitamin D_3 into its physiologically active metabolite, 1α,25-dihydroxyvitamin D_3 [1–3]. DBP also binds serum G-actin with high affinity ($K_d \approx 10^8\ M^{-1}$). Such an interaction is aided by plasma gelsolin and prevents G-actin from polymerizing into F-actin and blocking arteries under conditions of cellular injury or death. This property has serious implications in thrombosis and heart attack [4–8]. DBP also binds chemotactic agents such as C5a and C5a des Arg, thus enhancing complement activation on neutrophil chemotaxis [9,10]. In addition, DBP binds saturated and poly-unsaturated fatty acids with high affinities [11,12]. Moreover, a post-translationally modified version of DBP (DBP-macrophage activating factor) has been shown to have strong macrophage- and osteoclast-activating [13–17], as well as antiangiogenic and anti-tumor properties [18,19].

DBP belongs to the albumin gene family; and it is structurally highly homologous with albumin (ALB), alpha-feto protein, and afamin [20–22]. All these proteins are characterized by modular structures with three structural domains (domains I–III) and high cysteine (Cys)-content. In the case of DBP domain III is considerably truncated compared with other members of this gene family. In addition, all the Cys residues in DBP, in contrast with ALB, are oxidized to disulfide linkages.

During the past decade several structure–function studies were carried out to strongly suggest that different domains of DBP are responsible for its various ligand-binding activities. For example, domain I was shown to be exclusively reserved for vitamin D sterol-binding [23–27], while G-actin-binding takes place in domain III [23,26,27]. DBP-*maf* activities, which are manifested by

* Corresponding author. Fax: +1 617 638 8194.
E-mail address: rray@bu.edu (R. Ray).
† Deceased.

0006-291X/$ - see front matter © 2007 Elsevier Inc. All rights reserved.
doi:10.1016/j.bbrc.2007.11.033

the partial deglycosylation of carbohydrate-containing DBP, are also restricted to domain III of the protein [28]. In the light of these observations it has been suggested that there may be a cross-talk among the structural domains of DBP so that binding of one ligand may influence the binding of another.

In this investigation we probed 25-hydroxyvitamin D_3 (25-OH-D_3)-binding (the strongest binder among all naturally occurring vitamin D metabolites) by human DBP using 2-*p*-toluidinyl-6-sulfonate (TNS) as a fluorescent reporter molecule. Results of the above studies are discussed in this communication in the light of multiple ligand-binding by DBP and its probable physiological implications.

Materials and methods

Purified human DBP was obtained from commercially available pooled human serum (American Red Cross, Dedham, MA) by a ligand affinity chromatographic method developed in our laboratory [29]. The recombinant C-terminal domain of hDBP (domain III, hDBP 277–458) was expressed in bacteria by our published procedure [25,30]. All other chemicals and biochemicals were obtained from Sigma–Aldrich Chemical Co., Milwaukee, WI, except [26(27)-^{3}H]25-hydroxyvitamin D_3 (^{3}H-25-OH-D_3, specific activity 20 Ci/mmol), that was purchased from DuPont—NEN, Boston, MA.

hDBP + TNS + 25-OH-D_3 (various amounts). Samples (20 μg) of hDBP in Tris buffer, pH 8.4, were incubated with TNS (2 μg) at 25 °C for 20 min. After this period, different amounts of 25-OH-D_3 (0.001, 0.01, 0.1, and 1 μg) were added to the DBP–TNS solutions, and fluorescence intensities were recorded in a Hitachi F 2000 Fluorescence Spectrophotometer. In a separate experiment, fluorescence spectra of TNS alone (in Tris buffer), TNS + 25-OH-D_3, hDBP + TNS, and hDBP + TNS + 25-OH-D_3 (1 μg) were recorded.

hDBP + ^{3}H-25-OH-D_3 + TNS (various amounts). Samples of hDBP (20 μg each) in Tris buffer, pH 8.4, were incubated for 20 h at 4 °C with ^{3}H-25-OH-D_3 (4000 cpm) either without or with various amounts of TNS (0.25–8.5 μg, as shown in Fig. 2). After the incubation, the samples were incubated on ice with Dextran-coated charcoal for 15 min. The samples were centrifuged (3000 rpm, 4 °C). Supernatant from each sample was mixed with scintillation cocktail and counted for radioactivity.

Competitive binding assay of hDBP with ^{3}H-25-OH-D_3 and a fixed amount of TNS. Samples (20 μg) of hDBP were incubated at 4 °C for 20 h with ^{3}H-25-OH-D_3 (4000 cpm) either with or without TNS (1.5 μg) and an increasing concentration of 25-OH-D_3 (0.05–51.2 ng, as shown in Fig. 3). Another set of samples without any TNS was treated the same way (control). The rest of the procedure is same as described earlier.

hDBP 277–458 + TNS + 25-OH-D_3. Samples of hDBP 277–458 (20 μg each) in Tris buffer, pH 8.4, were incubated with TNS (2 μg) at 25 °C for 20 min. After this period, 25-OH-D_3 (1 μg) was added to the solutions, and fluorescence spectra were recorded.

Results and discussion

DBP, similar to other members of albumin (ALB) gene family, has a triple-domain modular structure and a large number of cysteine (Cys) residues. All twenty-eight (28) Cys residues in DBP are engaged in forming fourteen (14) disulfide bonds leading to the formation of these domains. Domain I spans about 200 amino acids and stabilized by five disulfide bonds, and contains the only Trp (145) residue which is involved in vitamin D sterol-binding [31]. Domain II is about one hundred and seventy-five (175) amino acids long and contains six (6) disulfide bonds. Domain III spans about eighty-five (85) amino acid residues (starting from amino acid residue 375) to the carboxy terminus and is stabilized by two (2) disulfide bonds.

ALB also has a triple-domain structure like DBP, but, in spite of high sequence and structural homology, DBP and ALB are functionally quite different. For example, DBP is a highly specific binder of vitamin D sterols and G-actin, while ALB is not. Moreover, DBP-*maf*-like activities of ALB are unknown to date. Accommodation of multiple high-specificity binders and multifunctional nature of DBP raises the possibility that binding of one ligand might influence the binding of other(s) via 'cross-talk' among interacting domains, and such a process might ultimately influence its functions. However, to date there has not been any direct evidence of such cross-talk among domains of DBP.

Changes in the intrinsic fluorescence of proteins (of aromatic amino acid residues) upon ligand/substrate-binding have been used quite extensively to study the micro-environment around these amino acids [32]. In addition, certain fluorescent hydrophobic molecules have been used as reporter molecules to probe micro-environment in proteins. 2-*p*-Toluinidylnaphthalene-6-sulfonate (TNS) is such a molecule. TNS does not fluoresce in an aqueous solvent, but fluoresces strongly in non-polar organic solvents and when bound to hydrophobic regions of a protein. In some cases this binding is strongly influenced by the binding of the natural ligand/ligands. For example, TNS produces high quantum-yield fluorescence with serum ALB, beta-lactalbumin, and chymotrypsin, while with other proteins, like lysozyme, IgG, and ovalbumin, quantum-yields are considerably lower [32].

Goldschmidt-Clermont et al. showed that DBP displays strong fluorescence upon binding TNS, and this fluorescence is reduced in a dose-dependent manner by G-actin, and fluorescence is completely quenched at a concentration ratio of 1:1 [33]. Dose-dependent decrease in TNS fluorescence was explained as a representation of a change in conformation of DBP upon binding G-actin, instead of a simple displacement of TNS by G-actin. Such alteration in physicochemical properties has been reported in the literature. For example, binding between hemoglobin and haptaglobin has been shown to be accompanied by altered hydrophobicity and anodal shift in isoelectric focusing [34]. We carried out the present study to investigate the effect of 25-OH-D_3 on TNS-binding by hDBP.

Effect of 25-OH-D_3 on DBP–TNS fluorescence

We observed that TNS fluorescence decreased steadily with increasing concentration of 25-OH-D_3, and fluorescence intensity was almost completely obliterated by 1 μg of 25-OH-D_3 (Fig. 1). In support of this observation the strong hDBP-TNS-fluorescence peak at 435 nm (Fig. 1, inset, curve A) was almost completely obliterated by 25-

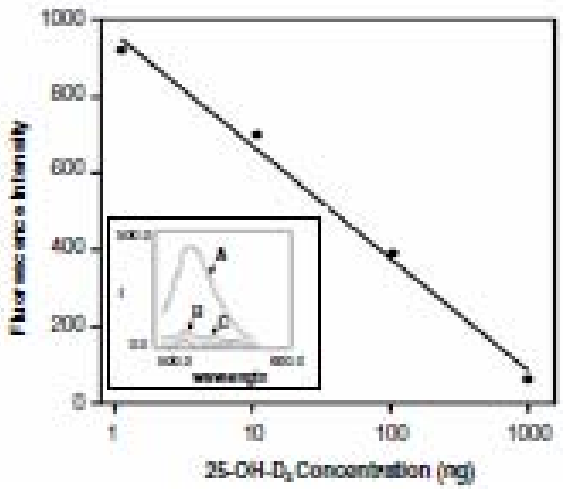

Fig. 1. TNS-fluorescence assays of human serum DBP (hDBP) in the presence of various amounts of 25-OH-D_3. (Inset) TNS-fluorescence spectra of hDBP + TNS (curve A), hDBP + TNS + 25-OH-D_3 (1 μg) (curve B), and TNS + 25-OH-D_3 (curve C).

OH-D_3 (1 μg) (Fig. 1, inset, curve B), while a combination of TNS and 25-OH-D_3 (1 μg) had very little fluorescence (Fig. 1, inset, curve C).

This dose-dependent decrease in TNS fluorescence by 25-OH-D_3 can be explained by either a direct competition between TNS and 25-OH-D_3 for binding site on DBP, or a change in physicochemical property (hydrophobicity, conformation) of DBP upon 25-OH-D_3-binding so that hydrophobic TNS-binding site/sites become progressively less available upon addition of 25-OH-D_3. To determine the mechanism of the above observation we carried out the following experiment.

Binding assay of hDBP with ^{3}H-25-OH-D_3 in the presence of various amounts of TNS

Results of this assay show that ^{3}H-25-OH-D_3-binding by DBP is not influenced at all by TNS (Fig. 2), strongly suggesting that there is no direct competition between 25-OH-D_3 and TNS for binding site/sites in hDBP. However, it could not be ascertained (from these results) whether nature of 25-OH-D_3-binding to DBP (binding affinity) is altered by the binding of TNS. This was determined by the following experiment.

Assay to determine whether binding affinity of hDBP for 25-OH-D_3 is altered by TNS-binding

The competitive binding assay curves of DBP and ^{3}H-25-OH-D_3 in the presence of 15 μg of TNS or in its absence are almost overlapping, indicating that TNS does not significantly alter interaction between 25-OH-D_3 and DBP qualitatively and quantitatively (Fig. 3).

Collectively the above results re-emphasize that there is no direct competition between 25-OH-D_3 and TNS for DBP-binding. In addition these studies indicate that TNS-binding does not alter the nature of binding between 25-OH-D_3 and DBP.

In the past our laboratory and others have shown that vitamin D sterol binding by DBP is largely restricted to domain I of the protein [23–25], while G-actin-binding takes place largely via domain III of DBP [23]. Furthermore, DBP–TNS fluorescence is reduced in a dose-dependent manner by G-actin, and is completely quenched at a concentration ratio of 1:1 [33], suggesting that TNS-binding might take place largely in domain III of DBP. In order to investigate that possibility we carried out TNS-binding by a recombinant domain III (mostly domain III and a small segment of domain II) of hDBP in the presence and in the absence of 25-OH-D_3.

Fluorescence spectra of recombinant hDBP 277–458 with TNS and 25-OH-D_3

We observed that hDBP 277–458 alone does not have any significant fluorescence activity (Fig. 4, curve B), but it displays strong fluorescence with a maximum at

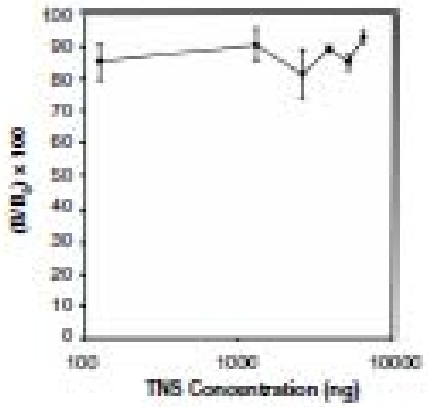

Fig. 2. ^{3}H-25-OH-D_3 binding assay of hDBP in presence of various amounts of TNS.

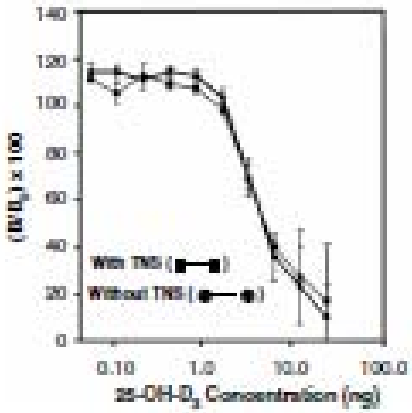

Fig. 3. Competitive binding assay of hDBP and ^{3}H-25-OH-D_3 in the presence or in the absence of 15 μg of TNS.

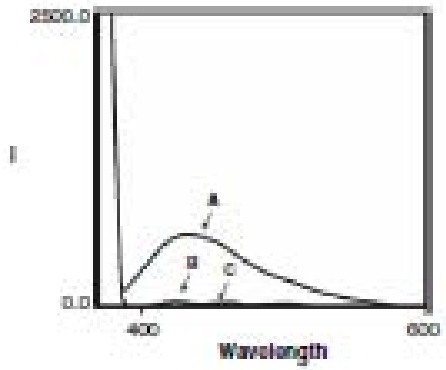

Fig. 4. TNS-fluorescence spectra of hDBP 277–458 peptide + TNS (curve A), hDBP 277–458 peptide alone (curve B), and hDBP 277–458 peptide + TNS + 25-OH-D_3 (curve C).

435 nm in the presence of TNS (Fig. 4, curve A, please note the change in the scale of the *Y*-axis from Fig. 1, inset). This peak was not at all influenced by the addition of an excess of 25-OH-D_3 (Fig. 4, curve C).

Collectively the above results suggest that major TNS-binding pocket in DBP may lie in domain III (C-terminal) of the protein. It could be argued that since domain III is not involved in 25-OH-D_3-binding [23–26], TNS fluorescence by this recombinant domain III is not influenced by 25-OH-D_3-treatment. However, this is in contrast with results displayed in Fig. 1 where we demonstrated that TNS fluorescence by full-length DBP is almost completely quenched by 25-OH-D_3. This apparent anomaly can be explained by significant conformational change in the whole protein upon 25-OH-D_3-binding (in domain I) to influence TNS-binding in domain III. As a result TNS fluorescence of full-length hDBP is quenched by 25-OH-D_3 in a dose-dependent manner (Fig. 1).

In summary, results of this study strongly imply that a considerable conformational change takes place in hDBP molecule upon binding 25-OH-D_3 in domain I of the protein; and this change is propagated into domain III to strongly influence TNS-binding in domain III of the protein, suggesting a cross-talk among the domains. DBP is a multi-functional protein. Therefore, this direct evidence of cross-talk has strong implications in the structure-functional aspects of this serum protein.

Acknowledgment

This work was supported in part by a grant from National Institute of Diabetes, Digestive and Kidney Diseases (ROI DK 44837).

References

[1] J.G. Haddad, Plasma vitamin D-binding protein (Gc-globulin): multiple tasks, J. Steroid Biochem. Mol. Biol. 53 (1995) 579–582.
[2] R. Ray, Molecular mechanisms in vitamin D-binding protein, Proc. Soc. Exp. Biol. Med. 212 (1996) 305–312.
[3] J.G. Haddad, N.E. Cooke, Vitamin D-binding protein (Gc-globulin), Endocr. Rev. 10 (1989) 294–307.
[4] H. Van Baelen, R. Bouillon, P. DeMoor, Vitamin D-binding protein (Gc globulin) binds actin, J. Biol. Chem. 255 (1980) 2270–2272.
[5] J.G. Haddad, Human serum binding protein for vitamin D and its metabolites (DBP): evidence that actin is the DBP binding component in human skeletal muscle, Arch. Biochem. Biophys. 213 (1982) 538–544.
[6] P.J. Goldschmidt-Clermont, H. van Baelen, R. Bouillon, T.E. Shook, M.H. Williams, A.E. Nel, R.M. Galbraith, Role of group-specific component (vitamin D binding protein) in clearance of actin from the circulation in rabbit, J. Clin. Invest. 81 (1988) 1519–1527.
[7] W.M. Lee, R.M. Galbraith, The extracellular actin-scavenger system and actin toxicity, N. Engl. J. Med. 326 (1992) 1335–1341.
[8] S.E. Lind, D.B. Smith, P.A. Janmey, T.P. Stossel, Role of plasma gelsolin and vitamin D binding protein in clearing actin from circulation, J. Clin. Invest. 78 (1986) 736–742.
[9] A.R. Shah, S.J. DeMartino, G. Trujillo, R.R. Kew, Selective inhibition of the C5a chemotactic cofactor function of the vitamin D binding protein by 1,25(OH)2vitamin D3, Mol. Immunol. 43 (2006) 1109–1115.
[10] J. Zhang, R.R. Kew, Identification of a region in the vitamin D binding protein that mediates its C5a chemotactic function, J. Biol. Chem. 279 (2004) 53202–53207.
[11] J.M. Ena, C. Sanchez, M.D. Perez, J. Uriel, M. Calvo, Fatty acids bound to vitamin D-binding protein (DBP) from human and bovine sera, Biochem. Int. 19 (1989) 1–7.
[12] R. Bouillon, D.Z. Xiang, R. Convents, H. Van Baelen, Polyunsaturated fatty acids decrease the apparent affinity of vitamin D metabolites for human vitamin D-binding protein, J. Steroid Biochem. Mol. Biol. 42 (1992) 855–861.
[13] N. Yamamoto, S. Homma, Vitamin D_3 binding protein (group-specific component) is a precursor for the macrophage-activating signal factor from lysophosphatidylcholine-treated lymphocytes, Proc. Natl. Acad. Sci. 88 (1991) 8539–8543.
[14] N. Yamamoto, R. Kumashiro, Conversion of vitamin D_3 binding protein (group-specific component) to a macrophage activating factor by the stepwise action of beta-galactosidase of B cells and sialidase of T cells, J. Immunol. 151 (1993) 2794–2802.
[15] N. Yamamoto, D.D. Lindsay, V.R. Narayanaju, R.A. Ireland, S.N. Popoff, A defect in the inflammation-primed macrophage-activation cascade in osteopetrotic rats, J. Immunol. 152 (1994) 5100–5107.
[16] G.B. Schneider, K.A. Bare, N.W. Hay, R.A. Ireland, S.N. Popoff, Effects of vitamin D binding protein-macrophage activating factor (DBP-MAF) infusion on bone resorption in two osteopenotic mutations, Bone 16 (1995) 657–662.
[17] N. Swamy, S. Ghosh, G.B. Schneider, R. Ray, Baculovirus-expressed vitamin D-binding protein-macrophage activating factor (DBP-maf) activates osteoclasts, and binding of 25-hydroxyvitamin D_3 does not influence this activity, J. Cell Biochem. 81 (2001) 535–546.
[18] Y. Koga, V.R. Narayanaju, N. Yamamoto, Antitumor effect of vitamin D-binding protein-derived macrophage activating factor on Ehrlich ascites tumor-bearing mice, Proc. Soc. Exp. Biol. Med. 220 (1999) 20–26.
[19] O. Kisker, S. Onisto, C.M. Becker, M. Fannon, E. Flynn, R. D'Amato, B. Zetter, J. Folkman, R. Ray, N. Swamy, S. Pirie-Shepherd, Vitamin D binding protein macrophage activating factor (DBP-maf) inhibits angiogenesis and tumor growth in mice, Neoplasia 5 (2003) 32–40.
[20] N.E. Cooke, E.V. David, Serum vitamin D-binding protein is a third member of the albumin and alpha-fetoprotein gene family, J. Clin. Invest. 76 (1985) 2420–2424.
[21] F. Yang, J.J. Brune, S.L. Naylor, R.L. Cupples, K.H. Naberhaus, B.H. Bowman, Human group specific component (Gc) is a member of the albumin family, Proc. Natl. Acad. Sci. USA 82 (1985) 7994–7998.
[22] H.S. Lichenstein, D.E. Lyons, M.M. Wurfel, D.A. Johnson, M.D. McGinley, J.C. Lodik, D.S. Trollinger, J.P. Mayer, S.D. Wright, M.M. Kaleowski, Albumin is a new member of the albumin, alpha

fetoprotein and vitamin d-binding protein gene family, J. Biol. Chem. 269 (1994) 18149–18154.
[23] J.G. Haddad, Y.Z. Hu, M.A. Kowalski, C. Laramore, K. Ray, P. Robzyk, N.E. Cooke, Identification of the sterol- and actin-binding domains of plasma vitamin D binding protein (Gc-globulin), Biochemistry 31 (1992) 7174–7181.
[24] R. Ray, R. Bouillon, H.G. Van Baelen, M.F. Holick, Photoaffinity labeling of human serum vitamin D binding protein, and chemical cleavages of the labeled protein: identification of a 11.5 KDa peptide, containing the putative 25-hydroxyvitamin D_3-binding site, Biochemistry 30 (1991) 7638–7642.
[25] N. Swamy, J.F. Head, D. Weitz, R. Ray, Biochemical and preliminary crystallographic characterization of the vitamin d sterol- and actin-binding by human vitamin d-binding protein, Arch. Biochem. Biophys. 402 (2002) 14–23.
[26] J.F. Head, N. Swamy, R. Ray, Crystal structure of the complex between actin and human vitamin D-binding protein at 2.5A resolution, Biochemistry 41 (2002) 9015–9020.
[27] C. Verboven, I. Bogaerts, E. Waelkens, A. Rabijns, H. Van Baelen, R. Bouillon, C. De Ranter, Actin-DBP: the perfect structural fit? Acta Crystallogr. D Biol. Crystallogr. 59 (2003) 263–273.
[28] F. Schoentgen, M. Metz-Boutigue, J. Jolles, J. Constans, P. Jolles, Complete amino acid sequence of human vitamin D-binding protein (group specific component): evidence of a three fold internal homology as in serum albumin and alpha-feto protein, Biochim. Biophys. Acta 871 (1986) 189–198.
[29] N. Swamy, A. Roy, R. Chang, M. Brisson, R. Ray, Affinity purification of human plasma vitamin D-binding protein, Protein Expr. Purif. 6 (1995) 185–188.
[30] N. Swamy, S. Ghosh, R. Ray, Bacterial expression of human vitamin D-binding protein (Gc2) in functional form, Protein Expr. Purif. 10 (1997) 115–122.
[31] N. Swamy, M. Brisson, R. Ray, Trp 145 is essential for the binding of 25-hydroxyvitamin D_3 to human serum vitamin D-binding protein, J. Biol. Chem. 270 (1995) 2636–2639.
[32] W.O. McClure, G.M. Edelman, Fluorescent probes for conformational states of proteins. I. Mechanism of fluorescence of 2-p-toluidinylnaphthalene-6-sulphonate, a hydrophobic probe, Biochemistry 5 (1966) 1908–1918.
[33] P.J. Goldschmidt-clermont, M.H. Williams, R.M. Galbraith, Altered conformation of Gc (vitamin D binding protein) upon complexing with cellular actin, Biochem. Biophys. Res. Commun. 146 (1987) 611–617.
[34] A.V. Ernes, A.L. Latner, J.A. Martin, F.A. Mulligan, Studies on the binding of haemoglobin by haptoglobin using electrofocusing and gradient electrophoresis, Biochim. Biophys. Acta 420 (1976) 57–68.

Available online at www.sciencedirect.com
ScienceDirect
Bioorganic Chemistry 36 (2008) 165–168
BIOORGANIC CHEMISTRY
www.elsevier.com/locate/bioorg

Preliminary Communication

Fatty acid-binding site environments of serum vitamin D-binding protein and albumin are different

Narasimha Swamy [†], Rahul Ray [*]

Bioorganic Chemistry & Structural Biology, Department of Medicine, Boston University School of Medicine, Boston, MA, USA

Received 23 January 2008
Available online 28 March 2008

Abstract

Vitamin D-binding protein (DBP) and albumin (ALB) are abundant serum proteins and both posses high-affinity binding for saturated and unsaturated fatty acids. However, certain differences exist. We surmised that in cases where serum albumin level is low, DBP presumably can act as a transporter of fatty acids. To explore this possibility we synthesized several alkylating derivatives of ^{14}C-palmitic acid to probe the fatty acid-binding pockets of DBP and ALB. We observed that *N*-ethyl-5-phenylisoxazolium-3′-sulfonate-ester (WRK-ester) of ^{14}C-palmitic acid specifically labeled DBP, but *p*-nitrophenyl- and *N*-hydroxysuccinimidyl-esters failed to do so. However, *p*-nitrophenyl ester of ^{14}C-palmitic acid specifically labeled bovine ALB, indicating that the micro-environment of the fatty acid-binding domains of DBP and ALB may be different, and DBP may not replace ALB as a transporter of fatty acids.

Keywords: Fatty acid-binding by vitamin D-binding protein (DBP) and albumin (ALB); Serum transport of fatty acids; Affinity labeling analogs of palmitic acid; Affinity labeling of fatty acid-binding sites of DBP and ALB

1. Introduction

Group specific component (Gc) or vitamin D-binding protein (DBP) is a sparsely glycosylated and polymorphic serum protein. The two major phenotypes are Gc1 and Gc2, differing from each other by four (4) amino acids in the primary structure as well as structure of attached polysaccharide. Gc1 is further divided into two subtypes differing in primary structure as well as structure of the attached carbohydrates [1–3].

DBP is a multi-functional protein [4]. Its binding of vitamin D and its metabolites has been studied extensively leading to the understanding that DBP is responsible for the stepwise activation of vitamin D_3 to 25-hydroxyvitamin D_3 (25-OH-D_3) and finally to its physiologically most active metabolite, 1α,25-dihydroxyvitamin D_3 ($1,25(OH)_2D_3$). It is also involved in the transportation of these small molecules to organs and cells wherever they are required. In addition DBP plays an integral role in the circulating actin-scavenging system in plasma. Plasma gelsolin severe filaments of F-actin, and DBP binds to actin monomer (G-actin) with high affinity, thus preventing G-actin to polymerize and clog arteries during cell-injury and lysis [5,6]. Presence of actin–DBP complex in the sera of human and animals sustaining injuries/inflammation, e.g. trophoblastic emboli, severe hepatitis, acute lung injury, etc. positively implicates DBP in thrombosis and heart attack [7]. DBP also binds chemotactic agents such as C5a and C5a des Arg, thus enhancing complement activation on neutrophil chemotaxis [8,9]. Furthermore, a post-translationally modified form of DBP (DBP-macrophage activating factor, DBP-*maf*) has been shown to have strong macrophage- and osteoclast-activating [10–14] and anti-angiogenic and anti-tumor properties [15,16].

In addition to above properties of DBP and its derivative (DBP-*maf*), DBP binds saturated and unsaturated fatty acids with high affinity ($K_d = 10^7$–10^8 M^{-1}), similar to plasma ALB [17,18]. However, certain differences do

* Corresponding author. Fax: +1 617 638 8194.
E-mail address: bsp@bu.edu (R. Ray).
† Deceased.

0045-2068/$ - see front matter © 2008 Elsevier Inc. All rights reserved.
doi:10.1016/j.bioorg.2008.02.002

exist. For example, Ena et al. demonstrated that molar ratio of fatty acids, bound to human DBP to DBP is 0.4 compared with 1.8 for human ALB [19]. Furthermore, majority of DBP-bound fatty acids are mono-unsaturated or saturated, and abundance of poly-unsaturated fatty acids is less than 5% (of the total bound fatty acids) [19]. Another interesting observation includes competition between vitamin D sterols and fatty acids in terms of binding to DBP. For example, it was reported that poly-unsaturated fatty acids, such as arachidonic or linoleic acid, strongly compete with 25-OH-D_3 and 1,25(OH)$_2D_3$ for binding to DBP, in sharp contrast with saturated fatty acids e.g. palmitic acid, which offer no significant competition [19,20]. Furthermore, Bouillon et al. observed that addition of human ALB in a physiological ALB:DBP ratio did not impair the inhibitory effect of linoleic acid towards DBP-25-OH-D_3-binding [20].

We hypothesized that this apparent anomaly between DBP and ALB in terms of fatty acid-binding might be related to the actual binding process between these proteins and fatty acids, which, in turn, might be related to the micro-environment of the fatty acid-binding pockets of these proteins. In order to evaluate this possibility we synthesized several reactive esters of ^{14}C-palmitic acid as potential affinity labeling reagents for DBP and ALB. Results of these studies and their probable physiological implications are discussed in this report.

2. Materials and methods

Purified human DBP was obtained from commercially available pooled human serum (American Red Cross, Dedham, MA) by a ligand affinity chromatographic method developed in our laboratory [21]. Defatted bovine serum ALB (BSA) and all chemicals were purchased from Sigma–Aldrich, Milwaukee, WI, except 1-^{14}C-palmitic acid (specific activity 56 mCi/mmol) which was a product of NEN-DuPont, Boston, MA.

2.1. Synthesis (Fig. 1)

The *N*-hydroxysuccinimido- and *p*-nitrophenyl-esters of palmitic acid were synthesized by dicyclohexylcarbodiimide (DCC)-coupling of palmitic acid with *N*-hydroxysuccinimide, or *p*-nitrophenol in the presence of a catalytic amount of *N*,*N*′-dimethylaminopyridine (DMAP) in anhydrous dichloromethane. Synthesis of WRK-palmitate was carried out by treating palmitic acid with *N*-ethyl-5-phenyl-isoxazolium-3′-sulfonate (Woodward's reagent K) and triethylamine in acetonitrile. Product from each reaction was purified by preparative chromatography on silica plates (Analtech, Vineland, NJ), and each product was characterized by NMR. Radioactive synthesis was carried out exactly the same way except palmitic acid was replaced with ^{14}C-palmitic acid. Products from the radioactive reaction were isolated by TLC matching with corresponding unlabeled compounds.

2.2. Affinity labeling studies of bovine serum ALB and DBP with *N*-hydroxy-succinimido-^{14}C-palmitate (A), *p*-nitrophenyl-^{14}C-palmitate (B), and WRK-^{14}C-palmitate (C)

Twenty-microgram samples each of BSA and DBP in 20 μl of TEST buffer (50 mM Tris–HCL, 150 mM NaCl, 1.5 mM EDTA, 0.1% Triton X-100, pH 8.8) were treated with *N*-hydroxysuccinimido-^{14}C-palmitate (A), *p*-nitrophenyl-^{14}C-palmitate (B), or WRK-^{14}C-palmitate (C) (each 20,000 cpm) at 25 °C for 20 h. Parallel samples of BSA and DBP containing additional sodium palmitate (1 μg in 10 μl of buffer) were also treated the same way. At the end of the experiment all the samples were analyzed on a 7.5% SDS–polycarylamide gel, followed by drying the gel and scanning of radioactivity in a Biosan phosphorimager.

3. Results and discussion

There is a remarkable structural homology among ALB, DBP, α-feto protein (AFP) and afamin, members of the albumin gene family. All these proteins have modular structures with three domains (domains I–III) and high cysteine-content [22]. In the case of DBP all the Cys residues (total 28) are oxidized to form 14 disulfide bonds. In contrast, ALB contains several free sulphydryl groups in its primary structure. Furthermore, DBP has a shorter domain III than ALB. These structural differences may explain gross functional differences between DBP and ALB. For instance, vitamin D sterols- and G-actin binding and related functions are unique to DBP. On the other hand, DBP possesses relatively weaker binding for fatty acids compared with ALB. Furthermore, DBP contains a single high-affinity fatty acid-binding site compared to ALB which contains several low- and high-affinity binding sites [18]. In ALB these binding sites are distributed among various domains of the protein, although high-affinity-binding sites are located in domain III [23]. Moreover, as described earlier, DBP, in contrast with ALB, discriminates between saturated and unsaturated fatty acids in terms of binding.

All the above observations point to difference in the nature of binding between ALB and DBP and fatty acids, which in turn may be related to the fatty acid-binding pocket structure of these proteins. Affinity and photo-affinity labeling techniques have been used widely to probe binding pockets and catalytic active sites of receptors and enzymes, respectively [24]. Our laboratory has used these techniques, and others to probe the vitamin D and actin-binding domain structures of DBP, leading to crystal structure of the DBP-actin complex [25–35].

In the current study we synthesized radiolabeled versions of three reactive esters of palmitic acid to probe the fatty acid-binding pockets of DBP and ALB. We chose palmitic acid, a saturated fatty acid as model because DBP has a propensity to bind saturated and mono-unsaturated fatty acids stronger that poly-unsaturated fatty acids [19,20].

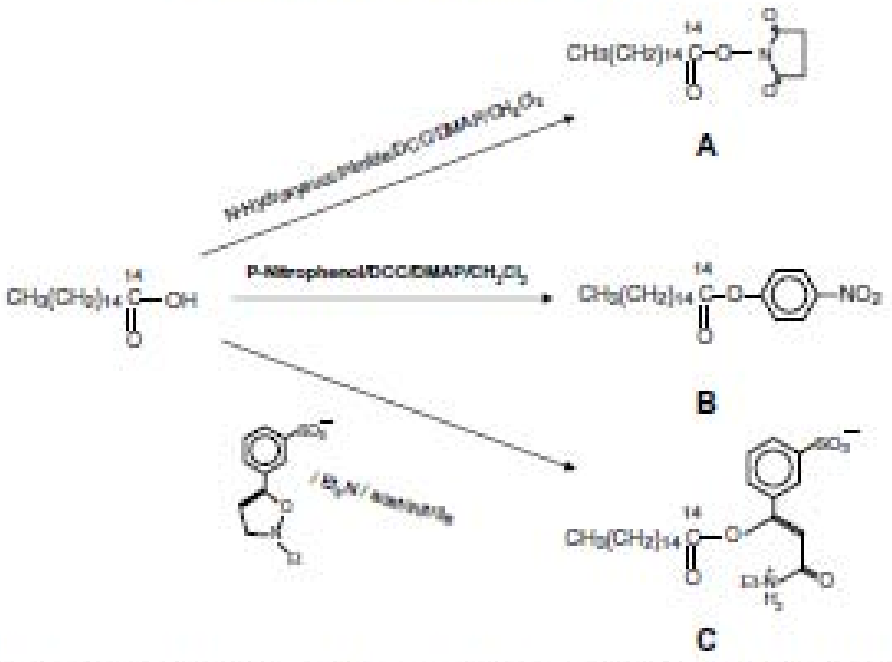

Fig. 1. Scheme for the synthesis of *N*-hydroxy-succinimido-^{14}C-palmitate (A), *p*-nitrophenyl-^{14}C-palmitate (B), and WRK-^{14}C-palmitate (C).

Reed employed WRK-^{14}C-palmitate (C) to affinity label the fatty acid-binding pocket/s of bovine serum ALB [36]. In our case, incubation of a sample of human serum DBP (hDBP) with WRK-^{14}C-palmitate (C) covalently labeled the protein as determined by autoradiography (Fig. 2, lane 1). When the incubation was carried out in the presence of an excess of sodium palmitate, labeling was completely obliterated (Fig. 2, lane 2). These results strongly indicated that WRK-^{14}C-palmitate (C) specifically labeled the palmitic acid-binding pocket in hDBP. These results also suggested that structure and chemical environment of the fatty acid-binding pockets of DBP and ALB are similar.

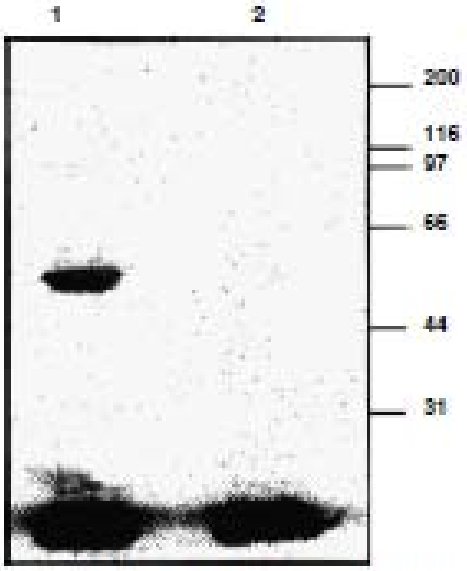

Fig. 2. Affinity labeling of hDBP with WRK-^{14}C-palmitate (C): samples of hDBP were incubated at 25 °C with WRK-^{14}C-palmitate (C) alone (lane 1), or in the presence of an excess of sodium palmitate (lane 2). The samples were electrophoresed on a SDS gel and exposed to a phosphor-imager. Positions of the standard molecular weight markers are denoted on the right.

Surprisingly other activated esters of palmitic acid i.e. *N*-hydroxysuccinimidyl-^{14}C-palmitate (A) and *p*-nitrophenyl-^{14}C-palmitate (B) failed to label DBP in the presence or in the absence of an excess of sodium palmitate. In the case of BSA, *N*-hydroxysuccinimidyl-^{14}C-palmitate (A) failed to label this protein. But, *p*-nitrophenyl-^{14}C-palmitate (B) labeled BSA, and labeling was significantly reduced in the presence of an excess of palmitic acid, denoting specific labeling of the fatty acid-binding pocket (results not shown).

Collectively the above results suggest that chemical/electronic environments of the fatty acid-binding pockets of DBP and ALB are different, so that ALB can tolerate a hydrophobic (*p*-nitrophenyl) as well as a hydrophilic (Woodward K reagent) head group at the carboxy terminal of palmitic acid. But, fatty acid-binding site of DBP can only accommodate a polar and Zwitterionic head group (Woodward K reagent).

Analbuminemia is a rare hereditary disease in which the afflicted individuals have very low or negligible amount of circulating serum ALB [37–39]. We surmised that since both ALB and DBP bind fatty acids with high affinity, DBP may replace ALB in carrying fatty acids, particularly saturated and mono-unsaturated fatty acids in the cases of low or negligible amount of circulating ALB. However,

results of the study delineated in this communication suggest that chemical and electronic environment of the fatty acid-binding pockets of DBP and ALB might be different. As a result binding and transportation of various fatty acids might be different. Thus, DBP may not replace ALB in terms of fatty acid scavenging and transportation.

Acknowledgment

This work was supported in part by a grant from National Institute of Diabetes, Digestive and Kidney Diseases (RO1 DK 44337).

References

[1] H.S. Lichenstein, D.E. Lyons, M.M. Wurfel, D.A. Johnson, M.D. McGinley, J.C. Leidy, D.B. Trollinger, J.P. Mayer, S.D. Wright, M.M. Zukowski, J. Biol. Chem. 269 (1994) 18149–18154.
[2] R. Ray, Proc. Soc. Exp. Biol. Med. 212 (1996) 305–312.
[3] N.E. Cooke, E.V. David, J. Clin. Invest. 76 (1985) 2420–2424.
[4] J.G. Haddad, J. Steroid Biochem. Mol. Biol. 53 (1995) 579–582.
[5] P.J. Goldschmidt-Clermont, H. van Baelen, R. Bouillon, T.E. Shook, M.H. Williams, A.E. Nel, R.M. Galbraith, J. Clin. Invest. 81 (1988) 1519–1527.
[6] W.M. Lee, R.M. Galbraith, N. Engl. J. Med. 326 (1992) 1335–1341.
[7] S.E. Lind, D.B. Smith, P.A. Janmey, T.P. Stossel, J. Clin. Invest. 78 (1986) 736–742.
[8] A.B. Shah, S.J. DiMartino, G. Trujillo, R.R. Kew, Mol. Immunol. 43 (2006) 1109–1115.
[9] J. Zhang, R.R. Kew, J. Biol. Chem. 279 (2004) 53282–53287.
[10] N. Yamamoto, S. Homma, Proc. Natl. Acad. Sci. USA 88 (1991) 8539–8543.
[11] N. Yamamoto, R. Kumashiro, J. Immunol. 151 (1993) 2794–2802.
[12] N. Yamamoto, D.D. Lindsay, V.R. Naraparaju, R.A. Ireland, S.N. Popoff, J. Immunol. 152 (1994) 5100–5107.
[13] G.B. Schneider, K.A. Benis, N.W. Flay, R.A. Ireland, S.N. Popoff, Bone 16 (1995) 657–662.
[14] N. Swamy, S. Ghosh, G.B. Schneider, R. Ray, J. Cell. Biochem. 81 (2001) 535–546.
[15] Y. Koga, V.R. Naraparaju, N. Yamamoto, Proc. Soc. Exp. Biol. Med. 220 (1999) 20–26.
[16] O. Kisker, S. Onizuka, C.M. Becker, M. Fannon, E. Flynn, R. D'Amato, B. Zetter, J. Folkman, R. Ray, N. Swamy, S. Pirie-Shepherd, Neoplasia 5 (2003) 32–40.
[17] M.H. Williams, E.L. Van Alstyne, R.M. Galbraith, Biochem. Biophys. Res. Commun. 153 (1988) 1019–1024.
[18] M. Calvo, J.M. Ena, Biophys. Res. Commun. 163 (1989) 14–17.
[19] J.M. Ena, C. Esteban, M.D. Perez, J. Uriel, M. Calvo, Biochem. Int. 19 (1989) 1–7.
[20] R. Bouillon, D.Z. Xiang, R. Convents, H. Van Baelen, J. Steroid Biochem. Mol. Biol. 42 (1992) 855–861.
[21] N. Swamy, A. Roy, R. Chang, M. Brisson, R. Ray, Protein Expr. Purif. 6 (1995) 185–188.
[22] J. Svasti, A. Kurosky, A. Bennett, B.H. Bowman, Biochemistry 18 (1979) 1611–1617.
[23] A.A. Spector, in: A.M. Scanu, A.A. Spector (Eds.), Biochemistry Ad Biology of Plasma Lipoproteins, Marcel Dekker Inc., NY, 1986, pp. 247–279.
[24] F.W. Sweet, G.L. Murdock, Endo. Rev. 8 (1987) 154–184.
[25] R. Ray, S.A. Holick, N. Hanafin, M.F. Holick, Biochemistry 25 (1986) 4729–4733.
[26] R. Ray, R. Bouillon, H.G. Van Baelen, M.F. Holick, Biochemistry 30 (1991) 4809–4813.
[27] R. Ray, R. Bouillon, H.G. Van Baelen, M.F. Holick, Biochemistry 30 (1991) 7638–7642.
[28] N. Swamy, R. Ray, Arch. Biochem. Biophys. 319 (1995) 504–507.
[29] N. Swamy, R. Ray, Arch. Biochem. Biophys. 333 (1996) 139–144.
[30] J.K. Addo, R. Ray, Steroids 63 (1998) 218–223.
[31] J.K. Addo, N. Swamy, R. Ray, Steroids 64 (1999) 273–282.
[32] N. Swamy, J. Addo, M.R. Uskokovic, R. Ray, Arch. Biochem. Biophys. 373 (2000) 471–478.
[33] A. Ray, N. Swamy, R. Ray, Biochem. Biophys. Res. Commun. 365 (2007) 746–750.
[34] N. Swamy, J.F. Head, D. Weitz, R. Ray, Arch. Biochem. Biophys. 402 (2002) 14–23.
[35] J.F. Head, N. Swamy, R. Ray, Biochemistry 41 (2002) 9015–9020.
[36] R.G. Reed, J. Biol. Chem. 261 (1986) 15619–15624.
[37] S. Watkins, J. Madison, M. Galliano, L. Minchiotti, F.W. Putnam, Proc. Natl. Acad. Sci. USA 91 (1994) 9417–9421.
[38] F. Campagna, F. Fioretti, M. Burattin, S. Romeo, F. Sentinelli, M. Bifulco, M.J. Sirtori, M. Del Ben, F. Angelico, M. Arca, Clin. Chem. 51 (2005) 1256–1258.
[39] L. Dottori, G. Caridi, M. Dagnino, A. Sala, G. Gokce, S. Sokucu, M. Campagnoli, M. Galliano, L. Minchiotti, Clin. Chem. 53 (2007) 1549–1552.

Bioorganic Chemistry 37 (2009) 57–63

Contents lists available at ScienceDirect

Bioorganic Chemistry

journal homepage: www.elsevier.com/locate/bioorg

Covalent labeling of nuclear vitamin D receptor with affinity labeling reagents containing a cross-linking probe at three different positions of the parent ligand: Structural and biochemical implications

Taner Kaya[b], Narasimha Swamy[a,1], Kelly S. Persons[a], Swapna Ray[a], Scott C. Mohr[b], Rahul Ray[a,*]

[a] Boston University School of Medicine, 85 East Newton Street, Boston, MA 02118, USA
[b] Boston University, Boston, MA 02215, USA

ARTICLE INFO

Article history:
Received 9 December 2008
Available online 14 February 2009

Keywords:
1α,25-Dihydroxyvitamin D_3
Vitamin D receptor
Vitamin D receptor-ligand-binding domain
Affinity labeling derivatives of 1α,25-dihydroxyvitamin D_3
Growth inhibitory property of 1α,25-dihydroxyvitamin D_3 and its affinity labeling derivatives in keratinocytes
Structural elements in vitamin D receptor-ligand-binding domain
Molecular modeling

ABSTRACT

Structure–functional characterization of vitamin D receptor (VDR) requires identification of structurally distinct areas of VDR-ligand-binding domain (VDR-LBD) important for biological properties of 1α,25-dihydroxyvitamin D_3 (1,25(OH)$_2$D$_3$). We hypothesized that covalent attachment of the ligand into VDR-LBD might alter 'surface structure' of that area influencing biological activity of the ligand. We compared anti-proliferative activity of three affinity alkylating derivatives of 1,25(OH)$_2$D$_3$ containing an alkylating probe at 1, 3 and 11 positions. These compounds possessed high-affinity binding for VDR; and affinity labeled VDR-LBD. But, only the analog with probe at 3-position significantly altered growth inhibitor activity, compared with 1,25(OH)$_2$D$_3$. Molecular models of these analogs, docked inside VDR-LBD tentatively identified Ser 237 (helix-3: 1,25(OH)$_2$D$_3$-1–88), Cys 288 (β-hairpin region: 1,25(OH)$_2$D$_3$-3–88) and Tyr 295 (helix-6: 1,25(OH)$_2$D$_3$-11–88) amino acids that are potentially modified by these reagents. Therefore, we conclude that the β-hairpin region (modified by 1,25(OH)$_2$D$_3$-3–88) is most important for growth inhibition by 1,25(OH)$_2$D$_3$, while helices 3 and 6 are less important for such activity.

1. Introduction

1α,25-Dihydroxyvitamin D_3 (1,25(OH)$_2$D$_3$), the dihydroxylated metabolite of vitamin D_3 serves multiple functions. Its biological properties include calcium and phosphorus-homeostasis, growth and maturation-control of a broad range of malignant cells, and immuno-regulation. As a result the therapeutic potential of 1,25(OH)$_2$D$_3$ in a broad range of diseases, including mineral homeostatic diseases such as renal osteodystrophy, proliferative diseases such as psoriasis and cancer, and immune-deficiency diseases, such as type I diabetes mellitus is well-recognized [1–7]. However, inherent toxicity of the parent hormone (hypercalcemia, hypercalciuria), particularly at pharmacological doses, has largely precluded its general use as a therapeutic agent. This limitation has spawned a strong interest in developing analogs of 1,25(OH)$_2$D$_3$ that retain intact beneficial effects but display reduced toxicity. Several such analogs have shown promise, but have displayed only a moderate effect clinically in non-toxic doses [8–12]. It is amply clear that rational development of such analogs will require proper understanding of their mechanism of action at the molecular level.

According to current dogma, 1,25(OH)$_2$D$_3$ binds to its nuclear receptor, vitamin D receptor (VDR) in target cells with high specificity; allosterically promoting heterodimerization with the retinoid X receptor (RXR); and binding of the VDR–1,25(OH)$_2$D$_3$–RXR complex to vitamin D response elements (VDREs) in the vitamin D-regulated genes [e.g., osteopontin, osteocalcin, 1α,25-dihydroxyvitamin D_3-24-hydroxylase (CYP-24)] and recruitment of co-activators to initiate transcription and translation [13,14]. In an alternative proposal apo-VDR, bound to co-repressors, remains transcriptionally inactive till 1,25(OH)$_2$D$_3$ binds to initiate the multi-step transcriptional process. The most important among all the steps in this transcriptional process is highly specific interaction between 1,25(OH)$_2$D$_3$ and VDR. Therefore, structure–functional knowledge, from the sides of both VDR and 1,25(OH)$_2$D$_3$ is

Abbreviations: 1,25(OH)$_2$D$_3$, 1α,25-dihydroxyvitamin D_3; VDR, nuclear vitamin D receptor; rVDR, recombinant vitamin D receptor; VDR-LBD, vitamin D receptor-ligand-binding domain; 1,25(OH)$_2$D$_3$-1–88, 1α,25-dihydroxyvitamin D_3-1α-(2)-bromoacetate; ^{3}H-1,25(OH)$_2$D$_3$-1–88, 1α,3β-dihydroxy(26,27-^{3}H)vitamin D_3-1α-(2)-bromoacetate; 1,25(OH)$_2$D$_3$-3–88, 1α,25-dihydroxyvitamin D_3-3β-(2)-bromoacetate; ^{14}C-1,25(OH)$_2$D$_3$-3–88, 1α,3β-dihydroxyvitamin D_3-3β-(1-^{14}C)-(2)-bromoacetate; 1,25(OH)$_2$D$_3$-6–88, 1α,25-dihydroxyvitamin D_3-6-propoxy-(2)-bromoacetate; 1,25(OH)$_2$D$_3$-11–88, 1α,25-dihydroxyvitamin D_3-11α-hydroxy-(2)-bromoacetate; ^{14}C-1,25(OH)$_2$D$_3$-11–88, 1α,25-dihydroxyvitamin D-11α-hydroxy-(1-^{14}C)-(2)-bromoacetate.

* Corresponding author.
E-mail address: bup@bu.edu (R. Ray).
[1] Deceased.

0045-2068/$ - see front matter © 2009 Elsevier Inc. All rights reserved.
doi:10.1016/j.bioorg.2009.01.001

crucial for a complete understanding of the molecular mechanism of this hormone, as well as development of new generations of $1,25(OH)_2D_3$-based drugs for various diseases with high efficacy and low toxicity.

Recently reports describing the X-ray crystal structures of VDR-LBD, bound to its natural ligand ($1,25(OH)_2D_3$) and several $1,25(OH)_2D_3$-analogs have been published [15–18]. These studies have provided structural evidence for the crucial role played by helix 12 (H-12) in the C-terminal region of VDR in co-activator recruitment and ligand-activated transcriptional process [19]. In addition, a recent study has indicated important role played by H-3 in the transcriptional process and ligand-related activities [20]. Beyond this, there is very little information available about possible role of other structurally distinct areas/features in VDR-LBD that may play an important role in the VDR–$1,25(OH)_2D_3$-mediated transcriptional process.

Mutation in a protein introduces structural/conformational perturbation that is sometimes translated into changes in biological properties related to this protein. We hypothesized that structural perturbation could also be brought about by covalently attaching appendages that mimic the actual ligand to specific areas of the VDR-LBD (chemical modification by "mutated" ligand). Such a change might influence the signal transduction process (as reflected in the biological activity of the ligand) by altering the 'surface structure', micro-environment and polarity of that area of the protein, and that may result in differential recruitment of co-activators for transcription. This way we might be able to identify yet unrecognized structural motifs inside VDR-LBD for the control of the transcriptional process.

Affinity labeling is a classical biochemical method to study interaction between a ligand and its receptor [21]. Such an interaction leads to covalent and specific labeling of the ligand-binding domain by a ligand-analog. In recent times this method has been extended to proteomic studies to investigate protein–protein interaction in complex cellular systems as well.

We have previously demonstrated that 1α,25-dihydroxyvitamin D_3-3-bromoacetate ($1,25(OH)_2D_3$-3-BE), an affinity labeling analog of $1,25(OH)_2D_3$ containing a reactive electrophilic group at the 3-position, covalently labels a single cysteine residue (Cys288) in VDR-LBD [22]. We argued that affinity labeling analogs of $1,25(OH)_2D_3$ with reactive affinity probe attached to various parts of the parent molecule could potentially attach $1,25(OH)_2D_3$ to different parts of the VDR-LBD, and cause perturbation maximally localized in that area; and such a process might be reflected in the biological activities of these analogs. Therefore, in the present study we compared the anti-proliferative activity of three affinity labeling analogs of $1,25(OH)_2D_3$ containing affinity probe at the 1, 3 and 11 positions of the parent molecule. Furthermore, we computationally docked these compounds inside the VDR-LBD crystal coordinates to identify areas of the protein that may be specifically labeled by these compounds, and compared cellular activity of each compound with the parent hormone, $1,25(OH)_2D_3$ in normal human keratinocytes. This communication reports results of these studies, and their implications.

2. Methods

2.1. Synthesis

1α,25-Dihydroxyvitamin D_3-1α-(2)-bromoacetate ($1,25(OH)_2D_3$-1-BE) and 1α,25-dihydroxy[26(27)-^{3}H]vitamin D_3-1α-(2)-bromoacetate (^{3}H-$1,25(OH)_2D_3$-1-BE, specific activity 175 Ci/mmol) and 1α,25-dihydroxyvitamin D_3-3β-(2)-bromoacetate ($1,25(OH)_2D_3$-3-BE) and 1α,25-dihydroxyvitamin D_3-3β-[1-^{14}C]-(2)-bromoacetate (^{14}C-$1,25(OH)_2D_3$-3-BE, specific activity 18.65 mCi/mmol) were synthesized by previously published procedures [23]. 1α,25-Dihydroxyvitamin D_3-6-propoxy-(2)-bromoacetate ($1,25(OH)_2D_3$-6-BE) was obtained by a method described earlier by us [24]. 1α,25-Dihydroxyvitamin D_3-11α-hydroxy-(2)-bromoacetate ($1,25(OH)_2D_3$-11-BE) and 1α,25-dihydroxyvitamin D_3-11α-hydroxy-[1-^{14}C]-(2)-bromoacetate (^{14}C-$1,25(OH)_2D_3$-11-BE, specific activity 18.65 mCi/mmol) were synthesized according to our published procedure [25].

2.2. Recombinant VDR

Full-length recombinant VDR was expressed in *E. coli* as a GST-fusion protein, and purified according to Swamy et al. [26].

2.3. Competitive binding assays of 1,25(OH)$_2$D$_3$-1-BE, 1,25(OH)$_2$D$_3$-3-BE, 1,25(OH)$_2$D$_3$-6-BE and 1,25(OH)$_2$D$_3$-11-BE with rVDR

These assays were carried out by a standard procedure. Typically 50 ng of rVDR was incubated with ^{3}H-$1,25(OH)_2D_3$ (4000 cpm, sp. activity 120 Ci/mmol, Amersham) in the presence of increasing concentrations of $1,25(OH)_2D_3$ or analogs (44.7 fmol–2.4 pmol) in VDR assay buffer (50 mM Tris HCl, 150 mM NaCl, 1.5 mM EDTA, 10 mM sodium molybdate, 5 mM DTT and 0.1% Triton X 100, pH 7.4) for 15 h at 4 °C. Rat liver nuclear extract was included in the binding assays to provide the nuclear accessory factor/s [27]. After the incubation Dextran-coated charcoal was added to remove unbound ^{3}H-$1,25(OH)_2D_3$ and the radioactivity in the supernatants, after centrifugation, was determined by liquid scintillation counting. Assays were carried out in triplicate.

2.4. Affinity labeling studies of rVDR with ^{3}H-1,25(OH)$_2$D$_3$-1-BE, ^{14}C-1,25(OH)$_2$D$_3$-3-BE and ^{14}C-1,25(OH)$_2$D$_3$-11-BE

Samples of rVDR (5 μg) were incubated with 2000 cpm (0.07 nmol) of ^{14}C-$1,25(OH)_2D_3$-3-BE or ^{14}C-$1,25(OH)_2D_3$-11-BE or 10,000 cpm of ^{3}H-$1,25(OH)_2D_3$-1-BE (0.06 fmol) in the presence or in the absence of $1,25(OH)_2D_3$ (1 μg, 2.4 nmol) in 50 mM Tris HCl buffer, pH 7.4 containing 5 mM DTT for 2 h at 4 °C, and reaction was terminated by boiling with SDS–PAGE sample buffer for 5 min. The samples were analyzed by SDS–PAGE, followed by radioactive scanning (^{3}H-containing samples) and phosphorimaging (^{14}C-containing samples).

2.5. Cell culture

Briefly, 3T3 cells were plated at 10^4 cells per 35 mm tissue-culture dish, and were irradiated lethally after 2 days with a ^{60}Co source (5000 rads). Keratinocytes were obtained from neonatal foreskin after overnight trypsinization at 4 °C and treatment with 0.2% EDTA. The cells, in serum-free medium, were placed on lethally-irradiated 3T3 cells. Each experiment was performed on primary or secondary keratinocyte cultures obtained from different skin samples. The serum-free medium consisted of MCDB 153 medium (Sigma Chemical Co.) with additives and calcium (0.15 mM). The cells were grown to 50–60% confluence, when medium was removed and replaced with 1 mL of fresh medium containing either ethanol (0.1% v/v) or various doses of $1,25(OH)_2D_3$ or analogs.

2.6. ^{3}H-Thymidine-incorporation assays

Cells, grown to approximately 50% confluence in MCDB medium were incubated at 37 °C with various concentrations (10^{-10} M and 10^{-8} M) of either $1,25(OH)_2D_3$ or an analog (in 1 μL of ethanol per mL of medium) for 24 h. Each experiment was carried out in triplicate. Control experiments were carried out by incubating cells

with ethanol for the same period of time. After the incubation, medium was removed from each plate and was replaced with ^{3}H-thymidine (one μCi, Sigma–Aldrich Chemical Co., St. Louis, MO) in 1 mL of fresh medium. The cells were incubated at 37 °C for 3 h followed by the removal of the medium and washing with salinated phosphate buffer. The cells were cooled on ice, and 1 mL of ice-cold perchloric acid solution (5%) was added to each dish followed by incubation on ice for 15 min. After the incubation, aqueous medium was removed, and the cells were washed with 1 mL of ice-cold perchloric acid solution, and finally replaced with 1 mL of fresh perchloric acid solution. The cells were incubated in a shaking water bath at 70 °C for 15 min. After this period, medium from each dish was removed, mixed with 10 mL of liquid scintillation cocktail, and counted for radioactivity. Results of this experiment are reported as percentage of cpm for ethanol control for each compound and at each dose level. These results (Fig. 4) are representative of same experiments carried out twice. Statistical analysis was done by student's *t* test.

2.7. Modeling studies

The VDR-LBD structure, taken directly from the co-crystallized protein–ligand complex (Protein Data Bank, PDB ID: 1DB1) was prepared by removing any water molecules, adding hydrogen atoms and assigning Kollman partial charges using Autodock tools before performing actual docking with AutoDock3 suite. Dockings were performed using the Lamarckian Genetic Algorithm (LGA) with default GA parameters using 60 × 60 × 60 grid map calculated by Autogrid. During the run the bromoacetate and hydroxyl groups on the ligand structure were flexible whereas rest of the steroid-derived skeleton was kept rigid in the original conformation. Runs (50 GA) were performed on each analog and results were cross-checked with multiple Simulated Annealing (SA) dockings each with 10(100) runs, varying number of cycles, step parameters and temperature factors, both for partially flexible and fully-flexible performed SA dockings were carried out. The cluster conformations with lowest docked energy (defined as intermolecular interaction energy plus torsional free energy) were manually inspected and superimposed. The amino acid residues in VDR-LBD in close proximity of the carbon atom bearing Br (atom) were identified.

3. Results and discussion

Affinity alkylating derivatives of naturally occurring bio-molecules constitute high-affinity substrate/ligand-analogs that can provide valuable information about the three-dimensional geometries of the substrate/ligand-binding pockets of their cognate proteins including identity of key amino acid residues (contact points) and orientation of the substrate/ligand inside the pocket. The affinity labeling process involves interaction between a nucleophilic amino acid residue in the substrate/ligand-binding pocket with an electrophile in the affinity reagent that lies in close enough proximity to form a covalent bond. In summary, the technique of affinity/photoaffinity labeling, coupled with mutational analysis and functional assay provide a dynamic picture of the binding event between a ligand/substrate with its cognate receptor/enzyme [21].

For the past several years our laboratory has focused on the development of affinity and photoaffinity labeling derivatives of $1,25(OH)_2D_3$ to probe VDR-LBD and obtain structure–functional information about VDR–$1,25(OH)_2D_3$ interaction [22,28–31]. In this effort we synthesized $1,25(OH)_2D_3$-3-BE, an affinity labeling derivative of $1,25(OH)_2D_3$, and demonstrated that this compound specifically labels a single Cysteine residue (Cys288) in VDR-LBD [22]. Functional importance of this residue was confirmed by mutation and $1,25(OH)_2D_3$-binding analysis. Additionally we identified several other contact points inside VDR-LBD using Cys288 as the 'docking point' for the 3-hydroxyl group in $1,25(OH)_2D_3$ (vide infra). One criticism that is usually leveled at the affinity labeling technique is that the alkylation process could be random, i.e. irrelevant amino acid residue/s in- and/or outside the actual ligand-binding/substrate-binding pocket could be alkylated by these analogs. Our experience, however, is quite different; and we observed that $1,25(OH)_2D_3$-3-BE specifically labeled a single cysteine residue (Cys288) out of three (3) inside the ligand-binding pocket of VDR strongly suggesting that VDR has a very tight binding pocket in the vicinity of the A-ring (of $1,25(OH)_2D_3$). Interestingly Cys288 is one of the conserved Cys residues in the VDR-LBD among other steroid hormone receptors; and prior to our report Nakajima et al. demonstrated a crucial role of Cys288 towards ligand binding [32].

In addition to the demonstration of specific labeling (of VDR-LBD) by $1,25(OH)_2D_3$-3-BE, we established that labeling by $1,25(OH)_2D_3$-3-BE is rapid and quantitative, and labeling process leads to relative stabilization of the holo-VDR-retinoic acid vitamin D responsive element (VDRE) complex. In addition, we observed that $1,25(OH)_2D_3$-3-BE has a considerably stronger anti-proliferative activity compared with $1,25(OH)_2D_3$ in human keratinocytes [31]. So, we asked the question of whether or not other affinity labeling derivatives of $1,25(OH)_2D_3$ containing affinity probes attached at different parts of $1,25(OH)_2D_3$ that can potentially cross-link different sites in the VDR-LBD can have differential cellular effects compared with $1,25(OH)_2D_3$.

As a part of an earlier study we synthesized $1,25(OH)_2D_3$-1-BE, $1,25(OH)_2D_3$-6-BE and $1,25(OH)_2D_3$-11-BE (Fig. 1). Competitive radio-ligand binding assays of four affinity analogs with affinity probe at 1, 3, 6 and 11 positions with recVDR demonstrated half-maximal binding concentrations of $1,25(OH)_2D_3$-1-BE, $1,25(OH)_2D_3$-3-BE, $1,25(OH)_2D_3$-11-BE and $1,25(OH)_2D_3$ (control) are 0.52, 0.18, 0.52 and 0.0015 nmol, respectively. By contrast, $1,25(OH)_2D_3$-6-BE showed no specific binding to VDR (Fig. 2). Therefore, we used $1,25(OH)_2D_3$-1-BE, $1,25(OH)_2D_3$-3-BE, $1,25(OH)_2D_3$-11-BE for subsequent experiments.

Incubation of VDR samples with ^{3}H-$1,25(OH)_2D_3$-1-BE, ^{14}C-$1,25(OH)_2D_3$-3-BE and ^{14}C-$1,25(OH)_2D_3$-11-BE shows that all these compounds covalently label the protein (Fig. 3). However, carrying out the incubation with an excess of $1,25(OH)_2D_3$ significantly reduced labeling in each case indicating specific labeling of VDR-LBD by these compounds (Fig. 3). It should be noted although excess of $1,25(OH)_2D_3$ reduced the intensity of labeling in each case, it did not obliterate cross-linking of the compounds to VDR-LBD. A possible explanation would be that if interaction between the affinity reagent and VDR-LBD is rapid and irreversible, as we have observed [31], covalently labeled VDR should accumulate with time, even when $1,25(OH)_2D_3$-X-BE (x = 1, 3, 11) has to compete with $1,25(OH)_2D_3$ to occupy the binding site in VDR-LBD. Furthermore, as seen in Fig. 3, decrease of labeling (decrease in the intensity of the labeled band) in the presence of a constant amount of $1,25(OH)_2D_3$ varies with different affinity reagents indicating various degrees of competition between $1,25(OH)_2D_3$ and its affinity derivatives. Overall, these results indicated that all these analogs specifically and covalently labeled the $1,25(OH)_2D_3$-binding site in the VDR-LBD.

In our next experiment anti-proliferative activities of $1,25(OH)_2D_3$-1-BE, $1,25(OH)_2D_3$-3-BE and $1,25(OH)_2D_3$-11-BE were compared with $1,25(OH)_2D_3$ at two dose levels. Results of these assays demonstrated that 10^{-8} M of $1,25(OH)_2D_3$ exhibits approximately 20% growth inhibition (Fig. 4). At the same dose $1,25(OH)_2D_3$-3-BE inhibits the growth by approximately 45%. At 10^{-10} M dose level $1,25(OH)_2D_3$ practically has no effect on the growth, while an equimolar amount of $1,25(OH)_2D_3$-3-BE inhibits the growth by approximately 25%. Interestingly, at both doses ef-

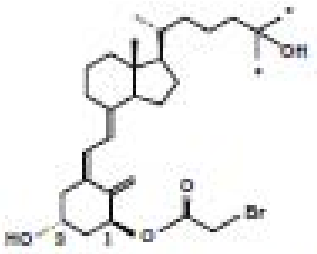

1α,25-Dihydroxyvitamin D_3-1α-(z)-bromoacetate [1,25(OH)$_2$D$_3$-1-BE], and 1α,25-dihydroxy[ze(zr)-^{3}H] vitamin D_3-1α-(z)-bromoacetate [^{3}H-1,25(OH)$_2$D$_3$-1-BE]

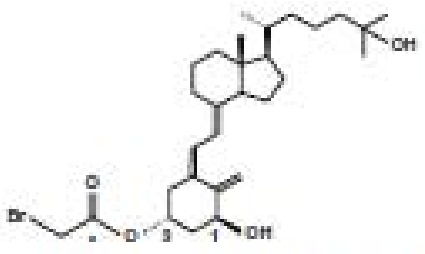

1α,25-Dihydroxyvitamin D_3-3β-(z)-bromoacetate [1,25(OH)$_2$D$_3$-3-BE], and 1α,25-dihydroxyvitamin D_3-3β-[1-^{14}C]-(z)-bromoacetate [^{14}C-1,25(OH)$_2$D$_3$-3-BE]

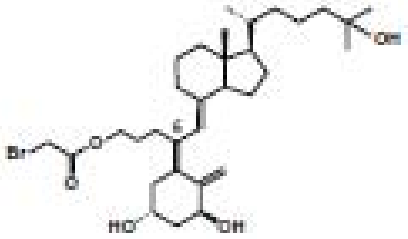

1α,25-Dihydroxyvitamin D_3-6-propoxy -(z)-bromoacetate [1,25(OH)$_2$D$_3$-6-BE]

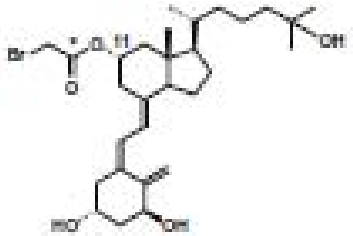

1α,25-Dihydroxyvitamin D_3-11α-hydroxy -(z)-bromoacetate [1,25(OH)$_2$D$_3$-11-BE], and 1α,25-dihydroxyvitamin D_3-11α-hydroxy-[1-^{14}C] -(z)-bromoacetate [^{14}C-1,25(OH)$_2$D$_3$-11-BE].

Fig. 1. Structures of various affinity labeling derivatives of 1,25(OH)$_2$D$_3$ and their radiolabeled counterparts. * Denotes positions of radiolabeling.

fects of 1,25(OH)$_2$D$_3$-1-BE and 1,25(OH)$_2$D$_3$-11-BE are not significantly different from that of 1,25(OH)$_2$D$_3$.

We have demonstrated that 1,25(OH)$_2$D$_3$-1-BE, 1,25(OH)$_2$D$_3$-3-BE and 1,25(OH)$_2$D$_3$-11-BE bind VDR with high and almost equal affinity (Fig. 2), and specifically label VDR-LBD (Fig. 3). Therefore, the growth assay data suggest that simple perturbation of specific areas of VDR-LBD by cross-linking of these analogs might not contribute significantly towards differential growth-inhibitory activity of these compounds in keratinocytes.

Construction of molecular models of these affinity labels, and docking them inside VDR-LBD, based on crystal coordinates identified Ser237, Cys288 and Tyr295 as amino acids that are potentially modified by 1,25(OH)$_2$D$_3$-1-BE, 1,25(OH)$_2$D$_3$-3-BE and 1,25(OH)$_2$D$_3$-11-BE, respectively (Figs. 5–7). Ser237, present in helix-3 has been implicated in ligand-binding by others and us [20,22]. However, according to our growth inhibition assays 1,25(OH)$_2$D$_3$-1-BE is similar to 1,25(OH)$_2$D$_3$ in inhibiting the growth of keratinocytes. A similar conclusion is drawn about helix-6 (containing Tyr295). However, the β-hairpin region, containing Cys288 (contact point

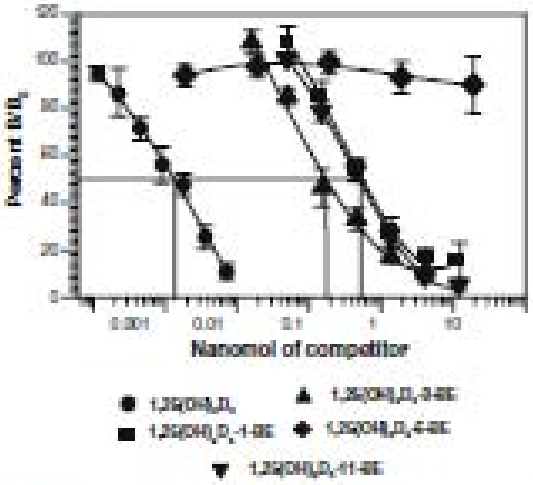

Fig. 2. Competitive radio-ligand binding assay of 1,25(OH)$_2$D$_3$-1-BE, 1,25(OH)$_2$D$_3$-3-BE, 1,25(OH)$_2$D$_3$-6-BE and 1,25(OH)$_2$D$_3$-11-BE with rVDR. Briefly, rVDR was incubated with ^{3}H-1,25(OH)$_2$D$_3$ in the presence of increasing concentrations of 1,25(OH)$_2$D$_3$ or analogs (44.7 fmol–2.4 pmol) for 15 h at 4 °C. After the incubation Dextran-coated charcoal was added to remove unbound ^{3}H-1,25(OH)$_2$D$_3$ and the radioactivity in the supernatants, after centrifugation, was determined by liquid scintillation counting.

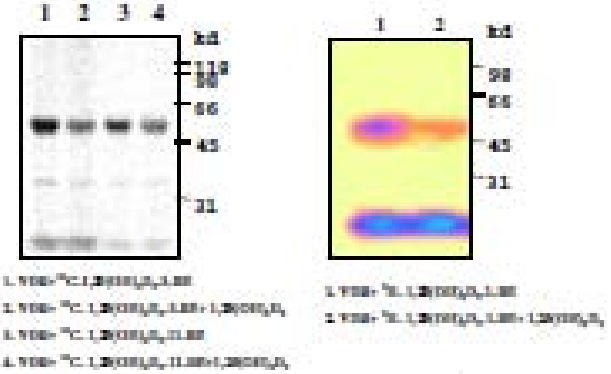

Fig. 3. Affinity labeling of rVDR with ^{3}H-1,25(OH)$_2$D$_3$-1-BE, ^{14}C-1,25(OH)$_2$D$_3$-3-BE and ^{14}C-1,25(OH)$_2$D$_3$-11-BE. Briefly, samples of rVDR were incubated with 2000 cpm (0.07 nmol) of ^{14}C-1,25(OH)$_2$D$_3$-3-BE or ^{14}C-1,25(OH)$_2$D$_3$-11-BE or 10,000 cpm of ^{3}H-1,25(OH)$_2$D$_3$-1-BE (0.05 fmol) in the presence or in the absence of 1,25(OH)$_2$D$_3$ (1 μg, 2.4 nmol) for 2 h at 4 °C, followed by SDS-PAGE analysis and radioactive scanning.

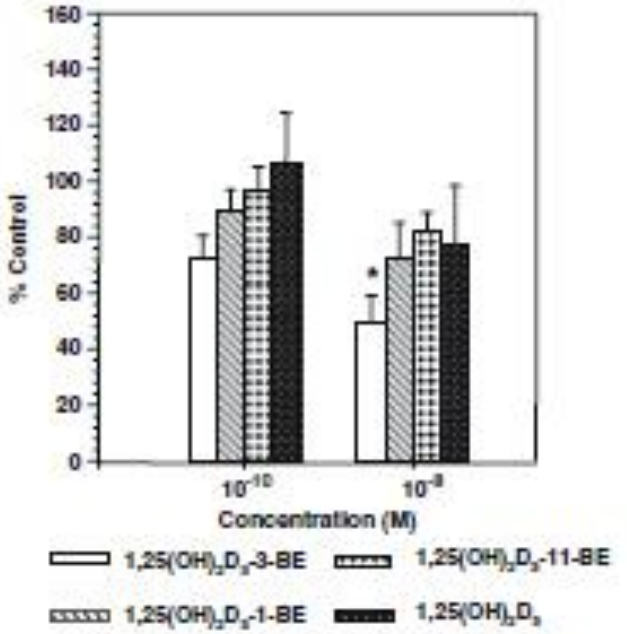

Fig. 4. ^{3}H-thymidine incorporation assay of normal human keratinocytes with 1,25(OH)$_2$D$_3$-1-BE, 1,25(OH)$_2$D$_3$-3-BE, and 1,25(OH)$_2$D$_3$-11-BE. Briefly, keratinocytes were grown to approximately 50% confluence and then incubated with 10^{-10} M or 10^{-8} M of either 1,25(OH)$_2$D$_3$ or an analog for 24 h followed by ^{3}H-thymidine incorporation assay by standard procedure. Each experiment was carried out in triplicate. Control experiments were carried out by incubating cells with ethanol for the same period of time. Results of this experiment are reported as percentage of cpm for ethanol control for each compound and at each dose level. * Represents $p < 0.05$.

for 1,25(OH)$_2$D$_3$-3-BE) is different, and its perturbation lead to modulation of cellular activity. It should be emphasized that Cys288 was implicated to be crucial for ligand-binding in an earlier study by a different group [32]. In addition, in our earlier study we mutated Trp286 and Met284, two neighboring amino acid residues

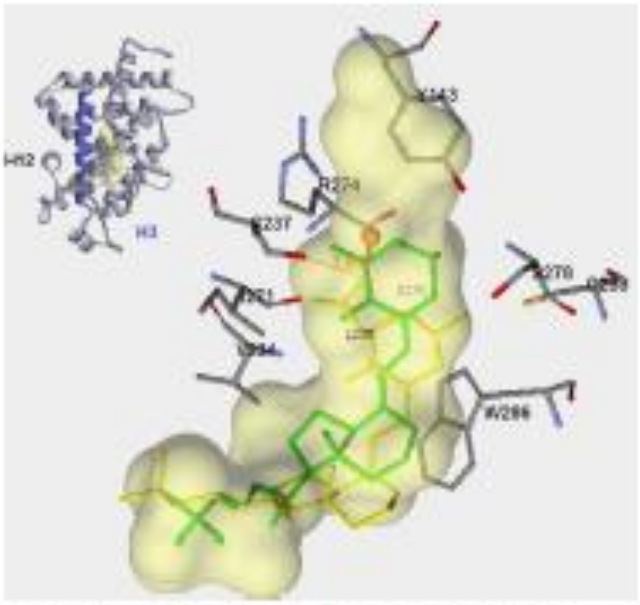

Fig. 5. Molecular modeling of human VDR-LBD with 1,25(OH)$_2$D$_3$-1-BE (green) and 1,25(OH)$_2$D$_3$ (yellow) inside VDR-LBD. Note that the CH2, bearing the 3r atom is closest to S237 in helix-3. (For interpretation of the references to color in this figure legend, the reader is referred to the web version of this article.)

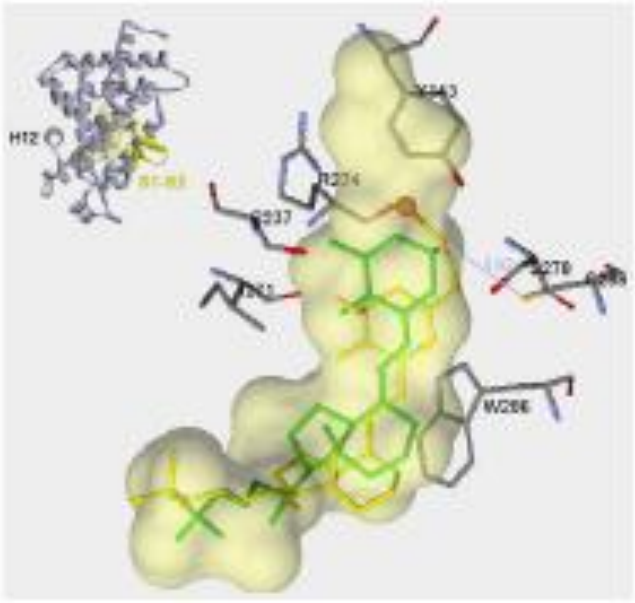

Fig. 6. Molecular modeling of human VDR-LBD with 1,25(OH)$_2$D$_3$-3-BE (green) and 1,25(OH)$_2$D$_3$ (yellow) inside VDR-LBD. Note that the CH2, bearing the 3r atom is closest to Cys288 in the base of the β-hairpin loop. (For interpretation of the references to color in this figure legend, the reader is referred to the web version of this article.)

of Cys288 (Fig. 8). Mutation of Trp286 to Ala or Phe almost completely removed 1,25(OH)$_2$D$_3$-binding, while conversion of Met284 to Ser or Ala reduced such binding by approximately 70% [22]. Met284, Trp286 and Cys288 are constituent amino acid residues in the unstructured β-hairpin region. Therefore, we concluded that the β-hairpin region is important for growth-inhibitory prop-

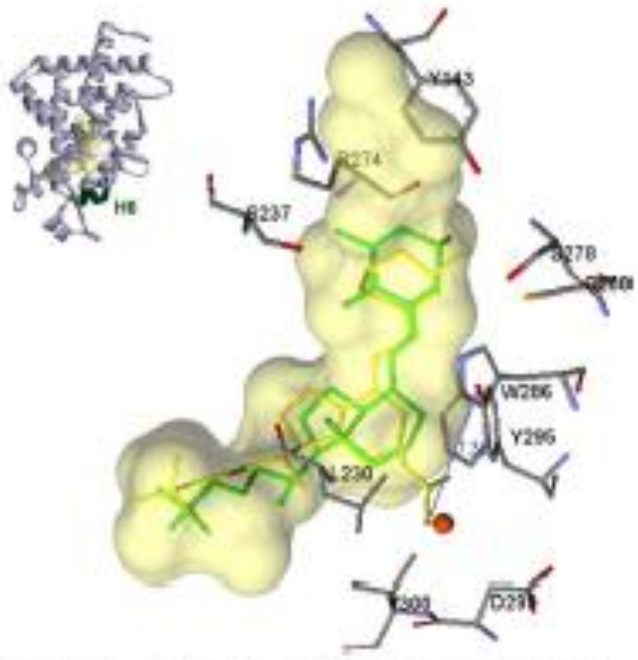

Fig. 7. Molecular modeling of human VDR-LBD with 1,25(OH)$_2$D$_3$-11-BE (green) and 1,25(OH)$_2$D$_3$ (yellow) inside VDR-LBD. Note that the CH2, bearing the 3r atom is closest to Tyr295 in helix-6. (For interpretation of the references to color in this figure legend, the reader is referred to the web version of this article.)

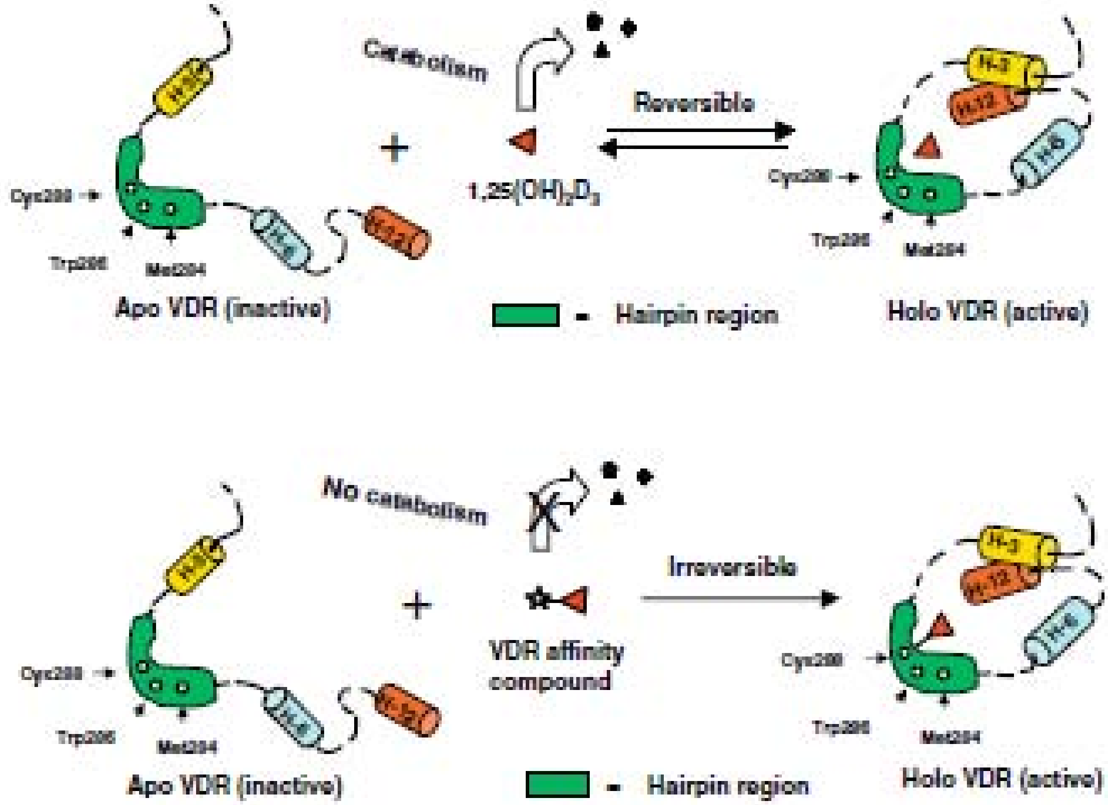

Fig. 8. Cartoon depicting interaction between various amino acid residues inside VDR-LBD with $1,25(OH)_2D_3$ and $1,25(OH)_2D_3$-affinity analogs. It should be noted that interaction between VDR and $1,25(OH)_2D_3$ is reversible with possibility of catabolism by the reverse reaction in the steady state. But interaction between VDR-LBD and $1,25(OH)_2D_3$-affinity labeling analogs is an irreversible process thereby potentially eliminating/reducing catalytic degradation.

ety of $1,25(OH)_2D_3$, while helices 3 and 6 are less important for such activity.

In recent years our laboratory and others have reported strong agonistic activity of the 3-bromoacetate derivative of $1,25(OH)_2D_3$ and 25-hydroxyvitamin D_3, the pro-hormonal precursor of $1,25(OH)_2D_3$ [33–35]. Previously such activities have been solely attributed to the enhanced catabolic stability of these compounds compared with $1,25(OH)_2D_3$, as illustrated by the cartoon in Fig. 8. However, our current studies demonstrate that mere catabolic stability of these compounds (by affinity labeling) may not contribute equally towards their cellular activity; and a combination of enhanced catabolic stability and specific area of perturbation (by covalent attachment of the ligand) might be responsible for the enhanced anti-proliferative activity.

In conclusion, majority of structure–function studies have identified helix 12 as the most important structural region of VDR-LBD for the biological activities of $1,25(OH)_2D_3$ and its analogs. Results of the current study strongly suggest that the β-hairpin region of VDR-LBD might also contribute significantly towards such activities. The 3-bromoacetate derivative of $1,25(OH)_2D_3$ and 25-hydroxyvitamin D_3 have been projected to have strong potential in several malignancies [33–35]. Therefore, information presented in this communication will be extremely important in providing molecular basis of their action, and develop next generation compounds with enhanced pharmacological properties.

Acknowledgments

This work was supported by grants (to RR) from Department of Defense, Prostate Cancer Research Program (PC051136), National Cancer Institute of the National Institutes of Health (1R41 CA126317-01A1 and 1R21 CA127629-01A2), and Community Technology Fund, Boston University. The authors would also like to thank Dr. Sandor Vajda, College of Engineering, Boston University.

References

[1] C. Eelen, C. Gysemans, L. Verlinden, E. Vanoirbeek, P. De Clercq, D. Van Haver, C. Mathieu, R. Bouillon, A. Verstuyf, Curr. Med. Chem. 14 (2007) 1893–1910.
[2] R. Bouillon, G. Eelen, L. Verlinden, C. Mathieu, G. Carmeliet, A. Verstuyf, J. Steroid Biochem. Mol. Biol. 102 (2006) 156–162.
[3] S. Masuda, G. Jones, Mol. Cancer Ther. 5 (2006) 797–808.
[4] X. Palomer, J.M. González-Clemente, F. Blanco-Vaca, D. Mauricio, Diabetes Obes. Metab. 10 (2008) 185–197.
[5] M.J. Campbell, L. Adorini, Expert Opin. Ther. Targets 10 (2006) 735–748.
[6] C. Penna, S. Amuchastegui, C. Laverny, L. Adorini, J. Bone Miner. Res. 22 (Suppl. 2) (2007) V69–V73.
[7] C. Gysemans, E. van Etten, L. Overbergh, A. Giulietti, G. Eelen, M. Waer, A. Verstuyf, R. Bouillon, C. Mathieu, Diabetes 57 (2008) 269–275.
[8] C.S. Johnson, J.R. Muindi, P.A. Hershberger, D.L. Trump, Anticancer Res. 26 (2006) 2543–2549.
[9] D.L. Trump, P.A. Hershberger, R.J. Bernardi, S. Ahmed, J. Muindi, M. Fakih, W.D. Yu, C.S. Johnson, J. Steroid Biochem. Mol. Biol. 89–90 (2004) 519–526.
[10] J.R. Wu-Wong, J. Tian, D. Goltzman, Curr. Opin. Invest. Drugs 5 (2004) 320–326.
[11] K. Dalhoff, J. Dancey, L. Astrup, T. Skovsgaard, K.J. Hamberg, F.J. Lofts, O. Rosmorduc, S. Erlinger, J. Bach Hansen, W.P. Steward, T. Skov, F. Burcharth, T.R. Evans, Brit. J. Cancer 89 (2003) 252–257.
[12] T.R. Evans, K.W. Colston, F.J. Lofts, D. Cunningham, D.A. Anthoney, H. Gogas, J.S. de Bono, K.J. Hamberg, T. Skov, J.L. Mansi, Brit. J. Cancer 86 (2002) 680–685.
[13] M.B. Demay, Ann. NY Acad. Sci. 1068 (2006) 204–213.
[14] A.L. Sutton, P.N. MacDonald, Mol. Endocrinol. 17 (2003) 777–791.
[15] N. Rochel, J.M. Wurtz, A. Mitschler, B. Klaholz, D. Moras, Mol. Cell 5 (2000) 173–179.
[16] N. Rochel, S. Hourai, X. Pérez-García, A. Rumbo, A. Mouriño, D. Moras, Arch. Biochem. Biophys. 460 (2007) 172–176.
[17] C. Tocchini-Valentini, N. Rochel, J.M. Wurtz, D. Moras, J. Med. Chem. 47 (2004) 1956–1961.

[18] J.L. Vanhooke, B.P. Tadi, M.M. Benning, L.A. Plum, H.F. DeLuca, Arch. Biochem. Biophys. 460 (2007) 161–165.
[19] S. Väisänen, M. Peräkylä, J.I. Kärkkäinen, A. Steinmeyer, C. Carlberg, J. Mol. Biol. 315 (2002) 229–238.
[20] A.M. Jiménez-Lara, A. Aranda, J. Biol. Chem. 274 (1999) 13503–13510.
[21] P.W. Jurutka, G.L. Murdock, Endocr. Rev. 8 (1987) 156–184.
[22] N. Swamy, W. Xu, N. Paz, J.C. Hsieh, M.R. Haussler, G.J. Maalouf, S.C. Mohr, R. Ray, Biochemistry 39 (2000) 12162–12171.
[23] R. Ray, N. Swamy, P.N. MacDonald, S. Ray, M.R. Haussler, M.F. Holick, J. Biol. Chem. 271 (1996) 2012–2017.
[24] J.K. Addo, N. Swamy, R. Ray, Steroids 64 (1999) 273–282.
[25] N. Swamy, J.K. Addo, M.R. Vskokovic, R. Ray, Arch. Biochem. Biophys. 373 (2000) 471–478.
[26] N. Swamy, S.C. Mohr, W. Xu, R. Ray, Arch. Biochem. Biophys. 363 (1999) 219–226.
[27] S. Nakajima, J.C. Hsieh, P.N. MacDonald, C.A. Haussler, M.A. Galligan, P.W. Jurutka, M.R. Haussler, Biochem. Biophys. Res. Commun. 197 (1993) 478–485.
[28] R. Ray, S. Rose, S.A. Holick, M.F. Holick, Biochem. Biophys. Res. Commun. 132 (1985) 198–203.
[29] R. Ray, M.F. Holick, Steroids 51 (1988) 623–630.
[30] R. Ray, S. Ray, S. Rose, M.F. Holick, Steroids 58 (1993) 462–465.
[31] M.L. Chen, S. Ray, N. Swamy, M.F. Holick, R. Ray, Arch. Biochem. Biophys. 370 (1999) 34–44.
[32] S. Nakajima, J.C. Hsieh, P.W. Jurutka, M.A. Galligan, C.A. Haussler, G.K. Whitfield, M.R. Haussler, J. Biol. Chem. 271 (1996) 5143–5149.
[33] N. Swamy, K.S. Persons, T.C. Chen, R. Ray, J. Cell. Biochem. 89 (2003) 909–916.
[34] N. Swamy, T.C. Chen, S. Peleg, P. Dhawan, S. Christakos, L.V. Stewart, N.L. Weigel, R.G. Mehta, M.F. Holick, R. Ray, Clin. Cancer Res. 10 (2004) 8018–8027.
[35] T.S. Lange, R.K. Singh, K.K. Kim, Y. Zou, S.S. Kalkunte, G.L. Sholler, N. Swamy, L. Brard, Chem. Biol. Drug Des. 70 (2007) 302–310.

-

Anti-growth Effect of 1,25-Dihydroxyvitamin D_3-3-bromoacetate Alone or in Combination with 5-Amino-imidazole-4-carboxamide-1-β-4-ribofuranoside in Pancreatic Cancer Cells

KELLY S. PERSONS, VIKRAM J. EDDY, SUSAN CHADID, ROSANGELA DEOLIVEIRA, ASISH K. SAHA and RAHUL RAY

Department of Medicine, Boston University School of Medicine, Boston, MA 02118, U.S.A.

Abstract. *1,25-Dihydroxyvitamin D_3-3-bromoacetate ($1,25(OH)_2D_3$-3-BE) is a vitamin D receptor-alkylating derivative of $1,25(OH)_2D_3$. The strong dose-dependent anti-proliferative and apoptotic effects of this compound in androgen-sensitive and androgen-insensitive prostate cancer cells have been reported. In this communication, it is reported that $1,25(OH)_2D_3$-3-BE strongly inhibits the growth of several pancreatic cancer cell lines. This effect is further accentuated by combination with 5-amino-imidazole-4-carboxamide-1-β-4-ribofuranoside (AICAR), an activator of AMP-activated protein kinase (AMPK)/acetyl-Co-enzyme A carboxylase (ACC) phosphorylation pathways and an inhibitor of Akt phosphorylation. It was observed that the anti-growth property of $1,25(OH)_2D_3$-3-BE, either alone or in combination with AICAR resulted in the inhibition of Akt phosphorylation in BxPC-3 cells. In conclusion, $1,25(OH)_2D_3$-3-BE displays a strong therapeutic potential, alone and in combination with AICAR, in pancreatic cancer.*

Pancreatic cancer (PAC) is the fourth most common cause of cancer related deaths in the United States, totaling approximately 32,000 fatalities per year (1). The rate of incidence of PAC is roughly the same as the rate of mortality, and five-year survival rate is less than 1%. This poor prognosis can be attributed to several factors, including propensity of the tumor to metastasize even when it is small, late detection at an advanced and often metastasized state, and intrinsic resistance to therapies with radiation and cytotoxic agents such as 5-fluorouracil, gemcitabine, either alone, or in combination (2). Certain natural products, *e.g.* genistein, have also shown limited effects in pancreatic cancer cells (3, 4).

1,25-Dihydroxyvitamin D_3 ($1,25(OH)_2D_3$), an essential nutrient for skeletal health, has strong antiproliferative effect in various cancer cells (5). However, results of several clinical studies have shown that the beneficial effect of $1,25(OH)_2D_3$ in therapeutic doses is exacerbated by its strong calcemic toxicity, leading to a search for analogs of $1,25(OH)_2D_3$ with antiproliferative activity and reduced toxicity (5, 6). In an alternative approach, combinations of $1,25(OH)_2D_3$ with standard chemotherapeutic agents have shown promise in mitigating toxicity related to $1,25(OH)_2D_3$ (7-12). Additionally, pre-treatment with $1,25(OH)_2D_3$ or one of its analogs has been shown to increase sensitivity towards radiation in certain breast and prostate cancer cells (13-15).

An alkylating derivative of $1,25(OH)_2D_3$ (1,25-dihydroxyvitamin D_3-3-bromoacetate, $1,25(OH)_2D_3$-3-BE) has been developed which covalently labels the hormone-binding pocket of nuclear vitamin D receptor (VDR) (16, 17). It has been reported previously that $1,25(OH)_2D_3$-3-BE, as well as 25-hydroxyvitamin D3-3-bromoacetate (25-OH-D_3-3-BE), a prototype of $1,25(OH)_2D_3$-3-BE without the 1-hydroxyl group, are considerably stronger antiproliferative agents than $1,25(OH)_2D_3$ in several prostate cancer cells (18-21). In this communication, it is demonstrated that $1,25(OH)_2D_3$-3-BE displays a strong antiproliferative property in PAC cells as well, and that this activity is strongly enhanced by co-dosing with 5-amino-imidazole-4-carboxamide-1-β-4-ribofuranoside (AICAR), an activator of AMP-activated protein kinase (AMPK)/acetyl-Co-enzyme A carboxylase (ACC) phosphorylation pathways (22).

Materials and Methods

Cellular assays. Standard ^{3}H-thymidine incorporation (in HS766 cells) and MTT assays (in ASPC-1 cells), and growth assays (in BxPC-3, HS766 and Mia$\overline{\text{P}}$aca cells) were employed in order to

Correspondence to: Rahul Ray, Boston University School of Medicine, Boston, MA 02118, U.S.A. Tel: +617 6388199, Fax: +617 6388194, e-mail: hapi@bu.edu

Key Words: 1,25-Dihydroxyvitamin D_3 derivative, pancreatic cancer, combination effect, 5-amino-imidazole-4-carboxamide-1-β-4-ribofuranoside, (AICAR), inhibitor of Akt-phosphorylation.

evaluate the cellular activities of $1,25(OH)_2D_3$ (a gift from Dr. Milan Uskokovic, Hoffman La-Roche, Inc., Nutley, NJ, USA), $1,25(OH)_2D_3$-3-BE (23), AICAR (Toronto Research Chemicals, Ontario, Canada) and a combination of $1,25(OH)_2D_3$-3-BE and AICAR. Cell lines were purchased from ATCC (Manassas, VA, USA) and cultured and propagated according to manufacturer's instructions.

In general, cells were incubated with various doses (as denoted in figure legends) of $1,25(OH)_2D_3$-3-BE, $1,25(OH)_2D_3$ or ethanol (vehicle) in media containing 5% fetal bovine serum for 16 h followed by ^{3}H-thymidine-incorporation or MTT assays. In the growth assay BxPC-3, HS766 and MiaPaca cells were treated with various agents $1,25(OH)_2D_3$-3-BE, $1,25(OH)_2D_3$ or AICAR, either individually or in combination on days 1, 3 and 5. On the seventh day cells were trypsinized and counted using a hemocytometer. Cells were dosed with $1,25(OH)_2D_3$ and $1,25(OH)_2D_3$-3-BE, dissolved in 0.1% v/v EtOH, or AICAR, dissolved in 0.1% v/v DMSO. For combination studies, appropriate solutions were mixed in media to maintain concentrations of EtOH and DMSO at 0.1% v/v or less. All assays were repeated six times and statistical analysis was performed by Student's *t*-test.

Western blot analysis. Lysates were made from treated cells in RIPA buffer (150 mM NaCl, 1% NP-40, 0.5% sodium deoxycholate, 0.1% SDS, 50 mM Tris, pH 7.5, 50 mM NaF, 1 mM sodium vanadate and protease inhibitors; Sigma-Aldrich, Milwaukee, WI, USA), and protein homogenates (50 μg) were run either on a 4-15% SDS polyacrylamide gel (Biorad, Hercules, CA, USA) or 4-12% MES NuPAGE gels (Invitrogen, Carlsbad, CA, USA) and transferred onto a polyvinylidene fluoride (PVDF) membrane. Analyses were carried out with primary antibodies for P-AMPK (Thr 172), AMPK, ACC and P-ACC (Ser 79) (Upstate Biotechnology, Charlottesville, VA, USA) at a dilution of 1:1000. Akt and P-Akt (Ser 473) (Cell Signaling, Danvers, MA, USA) were used at a dilution of 1:3000 and 1:2000 respectively. Dilutions for p21 (Santa Cruz, Biotechnology, Santa Cruz, CA, USA and p53 antibodies (Abcam Inc, Cambridge, MA, USA) were 1:500 and 1:1000 respectively. A secondary antibody conjugated to horseradish peroxidase (GE Healthcare, UK) was used at 1:5000 dilution. Signals were detected by chemiluminescence solution (Pierce, Rockford, IL, USA or Perkin Elmer, Boston, MA, USA) and autoradiography.

Results

$1,25(OH)_2D_3$-3-BE strongly inhibits the growth of ASPC-1, BxPC-3, HS766 and MiaPaca cells. Results of ^{3}H-thymidine and MTT assays are shown in Figures 1A and B. $1,25(OH)_2D_3$ at 10^{-8}-10^{-6}M had negligible effect in the growth of these cells, while there was approximately 60 and 20% reduction in growth with 10^{-7}M of $1,25(OH)_2D_3$-3-BE, in ASPC-1 and HS766 cells respectively. With 10^{-6}M of $1,25(OH)_2D_3$-3-BE inhibition of growth was approximately 75% and 60% in ASPC-1 and HS766 cells, respectively.

In the growth assay with BxPC-3 cells, growth inhibition by 10^{-8}-10^{-6}M of $1,25(OH)_2D_3$ were approximately 0%, 20% and 40% respectively, while the same doses of $1,25(OH)_2D_3$-3-BE caused approximately 10%, 95% and 100% growth inhibition respectively (Figure 1C). In MiaPaCa cells, 10^{-7}M, 5×10^{-7}M and 10^{-6}M of $1,25(OH)_2D_3$-3-BE caused approximately 65%, 90% and 95% growth inhibition respectively, while the same doses of $1,25(OH)_2D_3$ resulted in approximately 0%, 5% and 10% inhibition of growth respectively (Figure 1D).

A combination of $1,25(OH)_2D_3$-3-BE and AICAR strongly and synergistically inhibits the growth of BxPC-3 cells. It was observed that 10^{-5}M of AICAR had no significant effect on the growth of BxPC3 and HS766 cells, but 10^{-4}M and 10^{-3}M of AICAR strongly suppressed their growth, indicating low-efficacy of AICAR in inhibiting the growth of these cells (Figure 2A). However, when cells were co-dosed with $1,25(OH)_2D_3$-3-BE, a strong growth-inhibition of BxPC-3 cells was observed (Figure 2B). For example, 3×10^{-6}M of AICAR had no effect on cellular growth, while 3×10^{-7}M of $1,25(OH)_2D_3$-3-BE inhibited the growth by approximately 60%. When $1,25(OH)_2D_3$-3-BE and AICAR were combined (at the same doses as in individual dosing) growth inhibition increased to approximately 85%.

Evaluation of cell signaling pathways in BxPC-3 cells. AMPK and ACC-phosphorylation: As shown in Figure 3A, both phospho-AMPK and phospho-ACC are up-regulated by AICAR in a dose-dependent manner.

AMPK phosphorylation in BxPC-3 cells was also evaluated when they were treated with AICAR (10^{-4}M) and $1,25(OH)_2D_3$-3-BE (3×10^{-7}M) either individually or in combination. Results in Figure 3B demonstrate that AICAR strongly activated the level of phospho-AMPK, while $1,25(OH)_2D_3$-3-BE reduced its level significantly. The level of phospho-AMPK was partly restored by combining the two reagents.

Modulation of p21 and p53: Results of these assays are shown in Figure 4, left panel. The level of p21 was up-regulated by $1,25(OH)_2D_3$-3-BE, but not by AICAR, and combination of the two essentially reflects the level produced by $1,25(OH)_2D_3$-3-BE alone. In contrast, AICAR strongly up-regulated the level of p53, while $1,25(OH)_2D_3$-3-BE did not change the level (from control) significantly. The combination, however, showed the strongest signal.

A combination of AICAR and $1,25(OH)_2D_3$-3-BE strongly inhibited Akt-phosphorylation. Results of the Western Blot analysis are shown in Figure 4, right panel. AICAR (6×10^{-4}M) strongly inhibited Akt phosphorylation, while $1,25(OH)_2D_3$-3-BE (10^{-7}M) had a considerably weaker effect. However, when the cells were dosed with a combination of the two reagents Akt phosphorylation was almost completely eliminated.

Discussion

It has been reported that $1,25(OH)_2D_3$-3-BE and 25-OH-D_3-3-BE, alkylating derivatives of $1,25(OH)_2D_3$ and 25-OH-D_3 respectively are considerably stronger antiproliferative agents than $1,25(OH)_2D_3$ in several prostate cancer cells (18-21). The

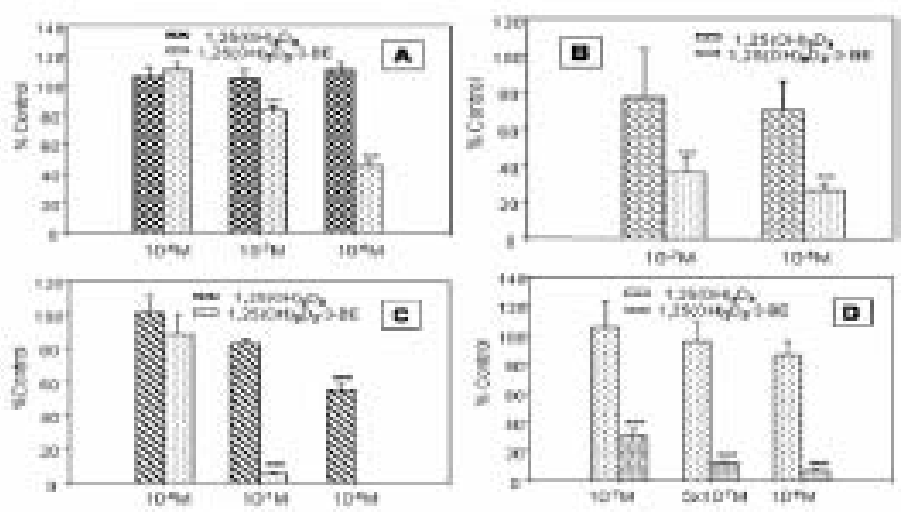

*Figure 1. A: ^{3}H-Thymidine incorporation assay of HS766 cells treated with various doses of 1,25(OH)$_2$D$_3$, 1,25(OH)$_2$D$_3$-3-BE or ethanol (control) for 16 h followed by standard ^{3}H-thymidine incorporation assay. B: MTT assay of ASPC-1 cells dosed with 1,25(OH)$_2$D$_3$, 1,25(OH)$_2$D$_3$-3-BE or ethanol (control) for 16 h. C, D: Growth assay of BxPC-3 and MiaPaca cells respectively, where cells were treated with various doses of 1,25(OH)$_2$D$_3$, 1,25(OH)$_2$D$_3$-3-BE or ethanol (control) on 1st, 3rd and 5th days. On the 7th day cells were trypsinized and counted in a hemocytometer. Results represent six replicates. Statistical analysis was carried out by Student's t-test (***p<0.001).*

present study was carried out to determine the effect of 1,25(OH)$_2$D$_3$-3-BE in PAC cells.

First, we evaluated the growth-inhibitory property of 1,25(OH)$_2$D$_3$, 1,25(OH)$_2$D$_3$-3-BE and AICAR in various PAC cells by three assays, namely ^{3}H-thymidine assay, an MTT assay and a growth assay. In the ^{3}H-thymidine assay, incorporation of radioactive thymidine in the DNA of rapidly growing cells is measured. Therefore, for this assay a short treatment period (16 h) was employed with relatively higher doses (up to 10^{-6}M) to observe a fast and maximally observable activity. Similarly, in the MTT assay cell viability was measured after a relatively quick treatment and high doses. As shown in Figure 1A and B 1,25(OH)$_2$D$_3$-3-BE strongly inhibited the growth of ASPC-1 and HS766 cells, while equivalent amounts of 1,25(OH)$_2$D$_3$ showed negligible activity towards the growth of these cells.

In the growth assay, cells were treated for a longer period (7 days) with chronic dosing of reagents on the 1st, 3rd and 5th days followed by cell counting on the 7th day. This dosing regimen mimicked the chronic dosing of a clinical situation with a relatively lower dose of the reagents to be used. In BxPC-3 and MiaPaca cells, 1,25(OH)$_2$D$_3$-3-BE strongly inhibited the growth in a dose-dependent manner, while only 10^{-6}M of 1,25(OH)$_2$D$_3$ showed significantly lower activity compared with an equivalent dose of 1,25(OH)$_2$D$_3$-3-BE (Figures 1C and D). Overall, these results showed that 1,25(OH)$_2$D$_3$-3-BE, but not 1,25(OH)$_2$D$_3$, has a strong growth-inhibitory effect in PAC cells.

The well-known resistance of pancreatic cancer cells towards chemotherapy results from evasion of apoptosis/cell cycle inhibition, which can occur via multiple pathways. Therefore, it can be hypothesized that a combination of cytotoxic agents that uses multiple pathways for inhibiting cell-growth may potentially be more effective than a single agent. AICAR is an activator of AMPK which phosphorylates and down-regulates a number of enzymes in the energy-metabolism pathway, such as ACC, fatty acid synthase, 3-hydroxy-3-methylglutaryl-CoA reductase, mammalian target of rapamycin (mTOR) *etc.* (24-32). Recently it was demonstrated by Rattan *et al.* that AICAR inhibits the growth of several cancer cell lines by activating cell cycle inhibitory proteins p21, p27, and p53 (22). It was also shown that AICAR activates AMPK and ACC phosphorylation, as well as mTOR in these cells, but inhibits Akt phosphorylation (22). These results suggested that the growth-inhibitory property of AICAR may be mediated by the inhibition of the PI3K-Akt pathway and activation of cell-cycle regulatory proteins. It was also demonstrated that AICAR is effective in a rat model of glioma (22).

It was our intention to evaluate whether combining AICAR with 1,25(OH)$_2$D$_3$-3-BE might enhance the growth-inhibitory activity of the latter in PAC cells. As shown in Figure 2A, AICAR is too low in potency to reduce the growth of BxPC-3 cells (Figure 2A). But when a low dose (3×10^{-5}M) of AICAR, with no cell-regulatory activity, was combined with 3×10^{-7}M of 1,25(OH)$_2$D$_3$-3-BE, cell-growth inhibition increased from 60% (with 1,25(OH)$_2$D$_3$-3-BE alone) to 85%. These results indicated that the growth-inhibitory property of 1,25(OH)$_2$D$_3$-3-BE is strongly accentuated by AICAR in BxPC-3 cells.

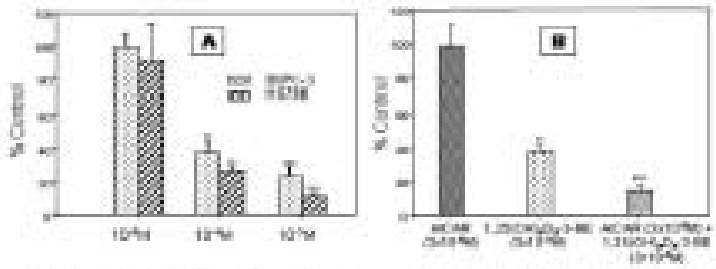

*Figure 2. A: Growth assays of BxPC-3 and HS766 cells, where cells were treated with various doses of AICAR or DMSO (control) on 1st, 3rd and 5th days. On the 7th day cells were trypsinized and counted in a hemocytometer. B: Growth assay of BxPC-3 cells treated with AICAR (3×10^{-3}M), or $1,25(OH)_2D_3$-3-BE (3×10^{-7}M) or a mixture of AICAR (3×10^{-3}M), or $1,25(OH)_2D_3$-3-BE (3×10^{-7}M) or DMSO (control) on 1st, 3rd and 5th days. On the 7th day, cells were trypsinized and counted in a hemocytometer. Results represent six replicates. Statistical analysis was carried out by Student's t-test (**p<0.01, ***p<0.001).*

AMPK is a serine/threonine protein kinase that is activated by AICAR (22). In order to determine whether its antiproliferative effect on pancreatic cancer cells is due to activation of AMPK and its down-stream target ACC, cell lysates from BxPC-3 cells, treated with AICAR were subjected to Western blot analysis. As shown in Figure 3A, both phospho-AMPK and phospho-ACC are up-regulated by AICAR in a dose-dependent manner, suggesting that growth inhibitory property of AICAR in BxPC-3 cells may be related to AMPK activation. On the other hand, when cells were treated with either AICAR (10^{-3}M) or $1,25(OH)_2D_3$-3-BE (3×10^{-7}M) individually or in combination, phospho-AMPK level was strongly up-regulated by AICAR, while the same was reduced significantly compared to the control by $1,25(OH)_2D_3$-3-BE (Figure 2B). The level of phospho-AMPK was partly restored by combining the two reagents. These results suggested that growth inhibition by AICAR and $1,25(OH)_2D_3$-3-BE may either follow different pathways, or their observed enhanced activity in combination is not manifested via AMPK activation.

Figure 3. A: Effect of AICAR (10^{-3}-10^{-6}M) on phosphorylation of AMPK and ACC in BxPC-3 cells. Cells were incubated with AICAR or DMSO control for 20 h, lysates were made and Western analysis was carried out with antibodies for phospho-AMPK and phospho-ACC. B: Effect of AICAR (10^{-3}M), $1,25(OH)_2D_3$-3-BE (3×10^{-7}M), either individually or in combination on phosphorylation of AMPK. BxPC-3 cells were treated with various reagents or vehicle control for 20 h. Then lysates were made, and Western analysis was carried out with antibody for phospho-AMPK. The blots were stripped and re-probed for total AMPK as a loading control. These results are representative of two independent experiments.

$1,25(OH)_2D_3$ is known to exert its cell-growth regulatory property via multiple direct and indirect cell-signaling pathways. In a direct effect, $1,25(OH)_2D_3$ induces expression of cyclin-dependent kinase inhibitors (p15, p19, p21, p27), and inhibits G_0-G_1 transition (33, 34). On the other hand, there is evidence to suggest that the growth-inhibitory effect of $1,25(OH)_2D_3$ and its analogs in certain cancer cells may involve up-regulation of p53 (14). In this study it was observed that p21 was up-regulated by $1,25(OH)_2D_3$-3-BE, but not by AICAR, and combination of the two essentially reflects the level produced by $1,25(OH)_2D_3$-3-BE alone (Figure 4, left panel). In contrast, the level of p53 was not different from the control when cells were treated with $1,25(OH)_2D_3$-3-BE, while AICAR strongly up-regulated it. The combination, however, showed the strongest signal, suggesting that combined synergistic effect of $1,25(OH)_2D_3$-3-BE and AICAR (observed in cellular studies) may reflect an increase in p53 regulation upon combining these reagents (Figure 4, left panel). It should be noted that in this assay, a higher concentration of $1,25(OH)_2D_3$-3-BE (10^{-6}M) was used to obtain maximal response.

Akt (protein kinase B) is a serine/threonine kinase that is involved in signal transduction by the PI3K/Akt pathway (35, 36). Akt is involved in a variety of normal cellular functions. In addition, Akt has a profound effect in tumorigenesis, cell proliferation, growth and survival. Therefore, the regulation of Akt phosphorylation by AICAR and $1,25(OH)_2D_3$-3-BE was evaluated, either alone or in combination in BxPC-3 cells. Results of the Western Blot analysis are shown in Figure 4, right panel. AICAR (6×10^{-5}M) strongly inhibited Akt phosphorylation, while $1,25(OH)_2D_3$-3-BE (10^{-7}M) had a

Figure 4. Left panel: Effect of AICAR ($1x10^{-3}$M), 1,25(OH)$_2$D$_3$-3-BE (10^{-8}M), either individually or in combination on the expression of p21 and p53 in BxPC-3 cells. Right panel: Effect of AICAR ($6x10^{-4}$M), 1,25(OH)$_2$D$_3$-3-BE (10^{-7}M), either individually or in combination on the phosphorylation of Akt in BxPC-3 cells. Cells were treated with reagents or vehicle-control for 20 h, followed by making of lysates and Western blot analysis in the usual fashion. β-Actin was used as a loading control. These results are representative of three independent experiments.

considerably weaker effect. However, when the cells were dosed with a combination of the two reagents, Akt phosphorylation was almost completely eliminated. Strong inhibition of Akt phosphorylation by AICAR suggests growth inhibition by AICAR includes the PI3K/Akt pathway as well as AMPK activation, shown earlier. In contrast, nearly complete inhibition of Akt phosphorylation suggests that this pathway may be involved in explaining the increase in growth inhibition of PAC cells when these two reagents are combined.

In summary, results from this study demonstrate that 1,25(OH)$_2$D$_3$-3-BE, wether alone or in combination with AICAR, strongly inhibits the growth of several PAC cells, possibly *via* Akt/PI3K pathway. Furthermore, these results suggest a therapeutic potential for 1,25(OH)$_2$D$_3$-3-BE, alone or in combination with AICAR in PAC.

Acknowledgements

The Authors acknowledge research support by grants from the National Cancer Institute (1R21CA123629-01A2), Department of Defense (PC 051136), and Community Technology Fund, Boston University (BR) and RO1DK19514 and PO1 H68758 (AS).

References

1 NCI, SEER Stat Fact Sheets - Cancer of the Pancreas, National Cancer Institute, 2009.

2 Xiong HQ, Rosenberg A, LoBuglio A, Schmidt W, Wolff RA, Deutsch J, Needle M and Abbruzzese JL: Cetuximab, A monoclonal antibody targeting the epidermal growth factor receptor, in combination with gemcitabine for advanced pancreatic cancer: a multicenter phase II Trial. J Clin Oncol 22: 2610-2616, 2004.

3 Li Y, Ellis KL, Ali S, El-Rayes BF, Nedeljkovic-Kurepa A, Kucuk O, Philip PA and Sarkar FH: Apoptosis-inducing effect of chemotherapeutic agents is potentiated by soy isoflavone genistein, a natural inhibitor of NF-kappaB in BxPC-3 pancreatic cancer cell line. Pancreas 28: e90-95, 2004.

4 El-Rayes BF, Ali S, Ali IF, Philip PA, Abbruzzese J and Sarkar FH: Potentiation of the effect of erlotinib by genistein in pancreatic cancer: the role of Akt and nuclear factor-kappaB. Cancer Res 66: 10553-10559, 2006.

5 Miranda S and Jones G: Promise of vitamin D analogues in the treatment of hyperproliferative conditions. Mol Cancer Ther 5: 797-808, 2006.

6 Dalhoff K, Dancey J, Astrup L, Skovsgaard T, Hamberg KJ, Lotz FI, Rosmorduc O, Eriksen S, Bach Hansen J, Steward WP, Skov T, Burcharth F and Evans TR: A phase II study of the vitamin D analogue seocalcitol in patients with inoperable hepatocellular carcinoma. Br J Cancer 89: 252-257, 2003.

7 Miranda JR, Peng Y, Potter DM, Hershberger PA, Tauch JS, Capozzoli MJ, Egorin MJ, Johnson CS and Trump DL: Pharmacokinetics of high-dose oral calcitriol: results from a phase I trial of calcitriol and paclitaxel. Clin Pharmacol Ther 72: 648-659, 2002.

8 Hershberger PA, Yu WD, Modzelewski RA, Rueger RM, Johnson CS and Trump DL: Calcitriol (1,25-dihydroxycholecalciferol) enhances paclitaxel antitumor activity *in vitro* and *in vivo* and accelerates paclitaxel-induced apoptosis. Clin Cancer Res 7: 1043-1051, 2001.

9 Miranda JR, Johnson CS, Trump DL, Christy R, Engler KL and Paleh MG: A phase I and pharmacokinetic study of intravenous calcitriol in combination with oral dexamethasone and gefitinib in patients with advanced solid tumors. Cancer Chemother Pharmacol 63: 33-40, 2009.

10 Trump DL, Potter DM, Muindi J, Brufsky A and Johnson CS: Phase II trial of high-dose, intermittent calcitriol (1,25 dihydroxyvitamin D3) and dexamethasone in androgen-independent prostate cancer. Cancer 106: 2136-2142, 2006.

11 Paleh MG, Trump DL, Muindi JR, Black ID, Bernardi RJ, Creaven PJ, Schwartz J, Brattain MG, Hutson A, French R and Johnson CS: A phase I pharmacokinetic and pharmacodynamic study of intravenous calcitriol in combination with oral gefitinib in patients with advanced solid tumors. Clin Cancer Res 13: 1216-1223, 2007.

12 Beer TM, Javle M, Lam GN, Horner WD, Wong A and Trump DL: Pharmacokinetics and tolerability of a single dose of DN-101, a new formulation of calcitriol, in patients with cancer. Clin Cancer Res 11: 7794-7799, 2005.

13 Sundaram S, Sea A, Feldman S, Strawbridge R, Hoopes PJ, Demidenko E, Binderup L and Gewirtz DA: The combination of a potent vitamin D_3 analog, EB 1089, with ionizing radiation reduces tumor growth and induces apoptosis of MCF-7 breast tumor xenografts in nude mice. Clin Cancer Res 9: 2350-2356, 2003.

14 Dotsenko G, Di X, Newsham I, Shiu R and Gewirtz DA: Potentiation of radiation sensitivity in breast tumor cells by the vitamin D3 analogue, EB 1089, through promotion of autophagy and interference with proliferative recovery. Mol Cancer Ther 5: 2286-2297, 2006.

15 Dunlap N, Schwartz GG, Eads D, Cramer SD, Shenk AN, John V and Koumenis C: 1Alpha,25-dihydroxyvitamin D(3) (calcitriol) and its analogue, 19-nor-1alpha,25(OH)(2)D(2), potentiate the effects of ionizing radiation on human prostate cancer cells. Br J Cancer 89: 746-753, 2003.

16 Ray R, Swamy N, MacDonald PN, Ray S, Hunziker MR and Hellick MF: Affinity labeling of the 1 alpha,25-dihydroxyvitamin D_3 receptor. J Biol Chem 271: 2012-2017, 1996.

17 Swamy N, Xu W, Pan N, Hsieh JC, Haussler MR, Maualouf GJ, Malik SC and Ray R: Molecular modeling, affinity labeling, and site-directed mutagenesis define the key points of interaction between the ligand-binding domain of the vitamin D nuclear receptor and 1 alpha,25-dihydroxyvitamin D_3. Biochemistry *39*: 12162-12171, 2000.

18 Chen ML, Ray S, Swamy N, Holick MF and Ray R: Mechanistic studies to evaluate the enhanced antiproliferation of human keratinocytes by 1alpha,25-dihydroxyvitamin D(3)-3-bromoacetate, a covalent modifier of vitamin D receptor, compared to 1alpha,25-dihydroxyvitamin D(3). Arch Biochem Biophys *370*: 34-44, 1999.

19 Swamy N, Peraino KS, Chen TC and Ray R: 1alpha,25-Dihydroxyvitamin D_3-3beta-(2)-bromoacetate, an affinity labeling derivative of 1alpha,25-dihydroxyvitamin D_3, displays strong antiproliferative and cytotoxic behavior in prostatic cancer cells. J Cell Biochem *89*: 909-916, 2003.

20 Swamy N, Chen TC, Peleg S, Dhawan P, Christakos S, Stewart LV, Weigel NL, Mehta RG, Holick MF and Ray R: Inhibition of proliferation and induction of apoptosis by 25-hydroxyvitamin D_3-3beta-(2)-bromoacetate, a nonsteroic and vitamin D receptor-alkylating analog of 25-hydroxyvitamin D_3 in prostatic cancer cells. Clin Cancer Res *10*: 8018-8027, 2004.

21 Lambert JR, Young CD, Peraino KS and Ray R: Mechanistic and pharmacodynamic studies of a 25-hydroxyvitamin D_3 derivative in prostatic cancer cells. Biochem Biophys Res Commun *361*: 189-195, 2007.

22 Rattan R, Giri S and Singh I: 5-Aminoimidazole-4-carboxamide-1-beta-D-ribofuranoside inhibits cancer cell proliferation *in vitro* and *in vivo* via AMP-activated protein kinase. J Biol Chem *280*: 39582-39593, 2005.

23 Ray R, Holick SA and Holick MF: Synthesis of a photoaffinity labelled analog of 1,25 dihydroxyvitamin D_3. J Chem Soc Chem Comm *11*: 702-703, 1985.

24 Corton JM, Gillespie JG, Hawley SA and Hardie DG: 5-Aminoimidazole-4-carboxamide ribonucleoside. A specific method for activating AMP-activated protein kinase in intact cells? Eur J Biochem *229*: 558-565, 1995.

25 Hawley SA, Boudeau J, Reid JL, Mustard KJ, Udd L, Makela TP, Alessi DR and Hardie DG: Complexes between the LKB1 tumor suppressor, STRAD alpha/beta and MO25 alpha/beta are upstream kinases in the AMP-activated protein kinase cascade. J Biol *2*: 28, 2003.

26 Fryer LG, Parbu-Patel A and Carling D: The Anti-diabetic drugs rosiglitazone and metformin stimulate AMP-activated protein kinase through distinct signaling pathways. J Biol Chem *277*: 25226-25232, 2002.

27 Sullivan JE, Brocklehurst KJ, Marley AE, Carey F, Carling D and Beri RK: Inhibition of lipolysis and lipogenesis in isolated rat adipocytes with AICAR, a cell-permeable activator of AMP-activated protein kinase. FEBS Lett *353*: 33-36, 1994.

28 Davies SP, Carling D and Hardie DG: Tissue distribution of the AMP-activated protein kinase, and lack of activation by cyclic-AMP-dependent protein kinase, studied using a specific and sensitive peptide assay. Eur J Biochem *186*: 123-128, 1989.

29 Kemp BE, Stapleton D, Campbell DJ, Chen ZP, Murthy S, Walter M, Gupta A, Adams JJ, Katsis F, van Denderen B, Jennings IG, Iseli T, Michell BJ and Witters LA: AMP-activated protein kinase, super metabolic regulator. Biochem Soc Trans *31*: 162-168, 2003.

30 Minokoshi Y, Kim YB, Peroni OD, Fryer LG, Muller C, Carling D and Kahn BB: Leptin stimulates fatty-acid oxidation by activating AMP-activated protein kinase. Nature *415*: 339-343, 2002.

31 Yamauchi T, Kamon J, Minokoshi Y, Ito Y, Waki H, Uchida S, Yamashita S, Noda M, Kita S, Ueki K, Eto K, Akanuma Y, Froguel P, Foufelle F, Ferre P, Carling D, Kimura S, Nagai R, Kahn BB and Kadowaki T: Adiponectin stimulates glucose utilization and fatty-acid oxidation by activating AMP-activated protein kinase. Nat Med *8*: 1288-1295, 2002.

32 Ruderman NB, Park H, Kaushik VK, Dean D, Constant S, Prentki M and Saha AK: AMPK as a metabolic switch in rat muscle, liver and adipose tissue after exercise. Acta Physiol Scand *178*: 435-442, 2003.

33 Wu W, Zhang X and Zanello LP: 1alpha,25-Dihydroxyvitamin D(3) antiproliferative actions involve vitamin D receptor-mediated activation of MAPK pathways and AP-1/p21(waf1) up-regulation in human osteosarcoma. Cancer Lett *254*: 75-86, 2007.

34 Rao A, Crum A, Welsh JE, Barclay WW, Koumenis C and Cramer SD: Vitamin D receptor and p21/WAF1 are targets of genistein and 1,25-dihydroxyvitamin D_3 in human prostate cancer cells. Cancer Res *64*: 2143-2147, 2004.

35 Gills JJ and Dennis PA: The development of phosphatidylinositol ether lipid analogues as inhibitors of the serine/threonine kinase, Akt. Expert Opin Investig Drugs *13*: 787-797, 2004.

36 Morgensztern D and McLeod HL: PI3K/Akt/mTOR pathway as a target for cancer therapy. Anticancer Drugs *16*: 797-803, 2005.

Received March 10, 2010
Revised March 24, 2010
Accepted March 26, 2010

A VITAMIN D RECEPTOR-ALKYLATING DERIVATIVE OF 1□, 25-DIHYDROXYVITAMIN D_3 INHIBITS GROWTH OF HUMAN KIDNEY CANCER CELLS AND SUPPRESSES TUMOR-GROWTH

James R. Lambert[2], Vikram J. Eddy[1], Christian D. Young[2], Kelly S. Persons[1], Sibaji Sarkar[1], Julie A. Kelly[2], Elizabeth Genova[2], M. Scott Lucia[2], Douglas V. Faller[1], and Rahul Ray[1*]

Department of Medicine[1], Boston University School of Medicine, Boston, MA; and the Department of Pathology[2], University of Colorado Denver, Aurora, CO

Running Title: An alkylating vitamin D derivative for renal cancer

Key words: vitamin D, renal cancer, anti-proliferative effect, apoptosis, anti-tumor effect

Address correspondence to: Rahul Ray, Ph.D., Department of Medicine, Boston University School of Medicine, 85 East Newton Street, Boston, MA 02118, telephone: 617-638-8199, Fax: 617-638-8194, E. mail: rayrl@bu.edu

This work was supported by National Cancer Institute grant CA 127629, Department of Defense Grant PC 051136, National Cancer Institute CA126317 (sub-contract) and Community Technology Fund, Boston University to R.R., American Cancer Society Research Scholar Grant RSG-04-170-01-CNE to J.R.L. and Department of Defense contract grant DAMD 17-03-1-0213 and National Cancer Institute CA 101992 to D.V.F.

ABSTRACT

1□,25-Dihydroxyvitamin D_3 ($1,25(OH)_2D_3$) has shown strong promise as an anti-proliferative agent in several malignancies, yet its therapeutic use has been limited by its toxicity leading to search for analogs with anti-tumor property and low toxicity. In this study we evaluated the *in vitro* and *in vivo* properties of 1,25-dihydroxyvitamin D_3-3-bromoacetate ($1,25(OH)_2D_3$-3-BE), an alkylating derivative of $1,25(OH)_2D_3$ as a potential therapeutic agent for renal cancer. Dose-response of $1,25(OH)_2D_3$-3-BE in two kidney cancer cell-lines was evaluated for its antiproliferative and apoptotic properties, and mechanisms were evaluated by Western Blot and FACS analyses. Therapeutic potential of $1,25(OH)_2D_3$-3-BE was assessed by determining its stability in human serum, and evaluating its efficacy in a mouse xenograft model of human renal tumor. We observed that $1,25(OH)_2D_3$-3-BE is significantly more potent than an equivalent concentration of $1,25(OH)_2D_3$ in inhibiting growth of A498 and Caki 1 human kidney cancer cells. $1,25(OH)_2D_3$-3-BE-mediated growth inhibition was promoted through inhibition of cell cycle progression by down-regulating cyclin A and induction of apoptosis by stimulating caspase activity. Moreover, $1,25(OH)_2D_3$-3-BE strongly inhibited Akt phosphorylation and phosphorylation of its downstream target, caspase 9. $1,25(OH)_2D_3$-3-BE appeared to be stable in human serum. In xenograft mouse model of human renal tumor, $1,25(OH)_2D_3$-3-BE was more potent at reducing tumor size compared to $1,25(OH)_2D_3$ which was accompanied by an increase in apopotosis and reduction of cyclin A staining in the tumors. These results suggest a translational potential of this compound as a therapeutic agent in renal cell carcinoma. Data from this study and extensive studies of vitamin D for the prevention of many malignancies support the potential of $1,25(OH)_2D_3$-3-BE for preventing renal cancer and the development of relevant *in-vivo* prevention models for assessing this potential, which do not exist at present.

INTRODUCTION

Kidney cancer is among the ten most common cancers in men and women and its rate has been increasing steadily over the past three decades. The American Cancer Society estimates that there were approximately 57,760 new cases of kidney cancer in the United States in the year 2009, and approximately 12,980 people died from this disease (1). Renal cell carcinoma (RCC) accounts for an estimated 90-95% of all kidney cancer and has been increasing at a rate of approximately 3% per year in the United States and Europe. Approximately 50% of localized RCC develops into a metastatic disease within a relatively short time frame (2). In addition, RCC characteristically produces no symptoms during its initial growth, making early diagnosis difficult, and is generally resistant to conventional chemo- and radiation therapies (2, 3). Current therapeutic options include radical nephrectomy for early stage disease and immunotherapy for advanced and metastatic stages. Anti-angiogenic agents and Raf-kinase-inhibiting small molecules have also shown promise in treating RCC, but are not curative (4-6). Clearly, more effective therapies and novel approaches to treatment of this disease are needed.

Numerous epidemiological studies have demonstrated the importance of vitamin D, dietary or otherwise, in preventing various cancers (7). Additionally, the therapeutic potential of 1□,25-dihydroxyvitamin D_3 ($1,25(OH)_2D_3$), the biologically active metabolite of vitamin D, and its analogs in cancer is well-documented (8). However, the inherent calcemic toxicity of this hormone, particularly in pharmaceutical doses, has prevented its general use as an anticancer agent (9-11). Thus, development of vitamin D analogs exhibiting potent antiproliferative activity but reduced systemic toxicity has become an active area of research

(8).

We have developed novel analogs of $1,25(OH)_2D_3$ and its pre-hormonal form, 25-hydroxyvitamin D_3 (25-OH-D_3), that specifically bind and label the ligand-binding pocket of the nuclear receptor for $1,25(OH)_2D_3$ (vitamin D receptor, VDR) (12, 13). Previously, we reported that 1□,25-dihydroxyvitamin D_3-3-bromoacetate ($1,25(OH)_2D_3$-3-BE) and 25-hydroxyvitamin D_3-3-bromoacetate (25-OH-D_3-3-BE), VDR-alkylating derivatives of $1,25(OH)_2D_3$ and 25-OH-D_3, respectively, are more potent than $1,25(OH)_2D_3$ in promoting antiproliferative effects on human cancer cell lines, including hormone-sensitive and hormone-insensitive prostate cancer cell lines (14-17). Lange *et al.* also reported antiproliferative and apoptotic effects of 25-OH-D_3-3-BE in high risk neuroblastoma (18).

In the present study, we compared the *in vitro* and *in vivo* growth-inhibitory properties of $1,25(OH)_2D_3$-3-BE to $1,25(OH)_2D_3$ in human renal cancer cells and examined potential molecular mechanisms underlying its activities. We observed that $1,25(OH)_2D_3$-3-BE is more potent than $1,25(OH)_2D_3$ in inhibiting the growth of A498 and Caki 1 renal cancer cells. Mechanistically, $1,25(OH)_2D_3$-3-BE-mediated growth inhibition of renal cancer cells was associated with an increase in apoptosis, arrest in the G2/M checkpoint in the cell cycle, and inhibition of Akt-phosphorylation. In nude mice $1,25(OH)_2D_3$-3-BE was more potent at reducing xenografted tumor size compared to $1,25(OH)_2D_3$ which was accompanied by an increase in apopotosis and reduction of cyclin A staining in the tumors.

MATERIALS AND METHODS

Materials: $1,25(OH)_2D_3$-3-BE was synthesized according to our published procedure (19). 1α,25-Dihydroxyvitamin D_3-3-[1-^{14}C]bromoacetate (^{14}C-$1,25(OH)_2D_3$-3-BE, specific activity 14.3 mCi/mmol) was synthesized by replacing bromoacetic acid in the synthetic scheme with [1-^{14}C]bromoacetis acid (sp. activity 14.3 mCi/mmol, DuPont, New England Nuclear, Boston, MA). Its radiochemical purity was ascertained by co-HPLC analysis with a standard sample of $1,25(OH)_2D_3$-3-BE. $1,25(OH)_2D_3$ was a generous gift from Dr. Milan Uskokovic, Hoffman La-Roche, Nutley, NJ. Concentrations of $1,25(OH)_2D_3$ and $1,25(OH)_2D_3$-3-BE were determined spectrophotometrically using an extinction coefficient of 18,400 at 265 nm. Purity of the compounds was determined by HPLC analysis (normal and reverse phases). LY294002 was from Cell Signaling Technology (Danvers, MA). A498 (HTB-44) and Caki 1 (HTB-46) cell lines were purchased from ATCC (Manassas, VA) and maintained in DMEM with 10% FBS. 3-4 weeks old athymic male mice (average weight 20 gm) were purchased from Taconic Farms (Germantown, NY) and maintained in an AALAC-approved animal care facility at Boston University School of Medicine.

Cellular Proliferation Assay: Cellular proliferation was measured using the TACS MTT Cell Proliferation kit according to the manufacturer's instructions (Trevigen, Gaithersburg, MD). Briefly, A498 and Caki 1 cells were plated in 96-well plates at 1000 cells per well. 16 hours later, cells were treated with $1,25(OH)_2D_3$-3-BE, $1,25(OH)_2D_3$ or ethanol (vehicle) control in media containing 5% FBS. The medium containing compounds was replenished every 2 days. After 7 days, MTT solution was added to each well, and the plates were incubated at 37°C for 3 hours followed by the addition of detergent reagent. The plates were incubated at 25°C for 15 h and absorbance at 570 nm measured on a microplate reader

(Spectramax 190 Plate Reader, Molecular Devices, Sunnyvale, CA).

Caspase activity assay: Caspase activity was determined using the Apo-ONE Homogeneous Caspase-3/7 assay according to the manufacturer's instructions (Promega, Madison, WI). Caspase-3/7 activity was determined following treatment of Caki 1 cells for 6 hours with $1,25(OH)_2D_3$, $1,25(OH)_2D_3$-3-BE or ethanol (vehicle) control. Fluorescence released following cleavage of the pro-fluorescent substrate, Z-DEVD-110 was measured at the emission maximum of 521 nm. The amount of fluorescent product generated is representative of the amount of active caspase-3/7 in the sample.

Cell cycle analysis and sub G0/G1 DNA content: A498 cells were plated at 5×10^5 cells in 10cm tissue culture dishes. 16 hr later the cells were treated with $1,25(OH)_2D_3$-3-BE, $1,25(OH)_2D_3$ or ethanol control for 6 hr. The cells were trypsinized, collected and centrifuged at 1500 rpm for 5 min. They were re-suspended in 1.5 ml saponin/PI solution (0.3% saponin (w/v), 2.5% PI (w/v), 0.1 mM EDTA, 10 µg/ml RNase in PBS) and incubated overnight in the dark. FACS analysis was performed using a Beckman Coulter FC500 flow cytometer. ModFit LT software (Verity Software House, Topsham, ME) was used for analysis.

Western blot analysis: A498 and Caki 1 cells were plated at 3×10^5 cells in 6 cm tissue culture dishes. 16 hr later the cells were treated with $1,25(OH)_2D_3$-3-BE, $1,25(OH)_2D_3$ or ethanol (vehicle control). At the indicated times, the cells were washed with PBS, scraped in PBS and collected by centrifugation. Total cellular extracts were prepared by re-suspending the cell pellets in RIPA buffer (150 mM NaCl, 1% NP-40, 0.5% sodium deoxycholate, 0.1% SDS, 50 mM Tris, pH 7.5) containing 50 mM NaF, 1 mM sodium vanadate (Na_3VO_4) and protease inhibitors (Protease Inhibitor Cocktail, Sigma-Aldrich, St. Louis, MO). Following 10

min incubation of the samples on ice, the extracts were cleared by micro-centrifugation for 10 min at 14,000 rpm, supernatants were transferred to new tubes and protein concentration of each extract was determined by Bradford assay. Samples were separated on 4-12% MES NuPAGE gels (Invitrogen, Carlsbad, CA) and transferred to PVDF membrane. Signals were detected by enhanced chemiluminescence (Perkin Elmer, Boston, MA) and autoradiography. The antibodies used were anti-Akt and anti-phospho Akt (Ser 473) (Cell Signaling, #9272 and #9271 respectively), anti-phospho-caspase-9 (Ser 196) (Santa Cruz, #11755), anti cyclin A (Neomarkers, Rb-1548) and anti-□ actin (Sigma, #A5441).

Serum-stability of 1,25(OH)$_2$D$_3$-3-BE: Pooled human serum (1 ml) was spiked with ^{14}C-1,25(OH)$_2$D$_3$-3-BE (100,000 cpm) for one hr at 37^{0}C followed by extraction with 5 x 1 ml of ethyl acetate. Combined organic extract was dried under argon and the residue was re-dissolved in a small volume of 5% H$_2$O-MeOH, and analyzed in an Agilent 1100 Series HPLC system (Thermo-Fisher, Waltham, MA), connected to a Packard Flow Scintillation Analyzer (Model no. 150TR, Meriden, CT), using 5% H$_2$O-MeOH as mobile phase, flow rate1.5 ml/min, detection 265 nm (for non-radioactive materials), Agilent C18 analytical column (Thermo-Fisher, Waltham, MA). Prior to the analysis of the radioactive sample a mixture of standard samples of 1,25(OH)$_2$D$_3$ and 1,25(OH)$_2$D$_3$-3-BE was analyzed under same conditions of HPLC-analysis.

Xenograft tumor growth in athymic mice: Caki 1 cells were grown, trypsinized and re-suspended in PBS to obtain a concentration of 5x10^6 cells/100 µL. Cell suspensions (100 µL aliquots) were injected subcutaneously in the flanks of athymic mice. When tumors grew to approximately 100 mm^3 the animals were separated into 6 animals per group, and were

treated with 1,25$(OH)_2D_3$-3-8E, 1,25$(OH)_2D_3$ (dissolved in 5% dimethylacetmide in sesame oil, 0.75 µg/kg body weight/100 µl), or vehicle by intraperiteneal injection every third day. Tumor size and body weights were measured on days of injection. Treatments stopped once the control group tumors reached an average volume of 1.5 cm^3 when animals were killed. Tumors were excised and stored in 10% neutral buffered formalin, and blood samples were collected by cardiac puncture. Statistical analysis of tumor size was carried out by Students t-test. Serum-calcium of the treated animals was measured according to manufacturer's instructions (Quantichrom Calcium Assay Kit, #DICA-500, BioAssay Systems, Hayward, CA)..

Histochemistry: Mouse tumors were fixed in 10% neutral buffered formalin for 48 hours before tissue processing into paraffin wax. Five micron sections were cut and mounted onto positively charged slides. Hematoxylin and eosin (H & E) staining was performed using standard methods. Briefly, sections were deparaffinized with xylene, rinsed through graded alcohols and hydrated to water. The nuclei were stained for 5 minutes in Harris hematoxylin (Anatech, Battle Creek, MI), differentiated in acid alcohol (1% HCl in 70% alcohol by volume) and 1% ammonium hydroxide. The non nuclear elements were stained with alcoholic eosin (Anatech, Battle Creek, MI) for 3 dips and dehydrated through graded alcohols to xylene. The sections were covered with cover slips using Cytoseal 60 synthetic resin (Richard Allan via Thermo Fisher, Waltham, MA).

Immunohistochemistry: Antibodies for cyclin A (LabVision via Thermo, Waltham, MA) were optimized for immunohistochemistry on the Ventana NexES autostainer (Ventana Medical Systems, Tucson, AZ) at an operating temperature of 37°C. 5 µm fresh cut paraffin sections were deparaffinized in xylene, rinsed in graded alcohols and hydrated to water. Antigen retrieval was performed in a Decloaker chamber for 5 minutes at 125°C (22 psi). The retrieval

solution was pH 9.5 BORG. Primary antibody for cyclin A was used at 1:100 and incubated for 30 minutes. A Ventana I-VIEW detection kit was modified to only detect rabbit antibodies by substituting a biotinylated goat anti-rabbit secondary (Jackson ImmunoResearch, West Grove, PA) diluted 1:50 in PBS pH 7.6. Sections were counterstained in Mayer's hematoxylin for 2 minutes, dehydrated in alcohols, cleared in xylene and coverglass mounted as for histochemistry.

Pathological analysis: H & E stained and anti-cyclin A stained tissue sections of subcutaneous tumors were examined by a single pathologist (M.S.L.) blinded as to the treatment group. On H & E sections, the number of apoptotic bodies in the tumors per 10 random high power (400x) fields was recorded for each animal. For cyclin A analysis, the percent of brown cyclin A positive tumor nuclei was assessed for each tumor, counting 500 nuclei in multiple random fields.

RESULTS

$1,25(OH)_2D_3$-3-BE is more potent than $1,25(OH)_2D_3$ in inhibiting the growth of renal carcinoma cells. In this study, we examined the effect of $1,25(OH)_2D_3$-3-BE on the growth of the human renal cancer cell lines A498 and Caki 1. Cells were treated with $1,25(OH)_2D_3$-3-BE or $1,25(OH)_2D_3$ and cellular proliferation was quantitated by MTT assay. In both A498 and Caki-1 cells, treatment with 10^{-8}M $1,25(OH)_2D_3$-3-BE almost completely inhibited cellular proliferation, while an equivalent amount of $1,25(OH)_2D_3$ inhibited growth by approximately 10 percent (Fig. 1). Caki 1 cells were more sensitive to $1,25(OH)_2D_3$-3-BE than were A498 cells. Approximately 90% growth-inhibition was observed with 10^{-7}M of $1,25(OH)_2D_3$-3-BE in Caki 1 cells, while approximately 30% growth inhibition was observed in A498 cells (Fig. 1). These results demonstrate that $1,25(OH)_2D_3$-3-BE elicits stronger antiproliferative effects in A498 and Caki 1 cells compared $1,25(OH)_2D_3$ on an equimolar basis.

Under microscopic visualization, we noted distinct morphological changes in the appearance of both A498 and Caki 1 cells in response to $1,25(OH)_2D_3$-3-BE treatment. As shown in Figure 1B, after 6 hr of treatment with $1,25(OH)_2D_3$-3-BE, both A498 and Caki 1 cells displayed cell rounding and began detaching from the plates. Interestingly, cells treated with $1,25(OH)_2D_3$ did not display these characteristics and exhibited morphological features similar to vehicle treated control cells.

$1,25(OH)_2D_3$-3-BE promotes G2/M arrest of A498 cells. The cellular mechanism(s) leading to growth inhibition by $1,25(OH)_2D_3$ are complex. In prostate cancer cells, $1,25(OH)_2D_3$ causes cells to arrest in the G_0/G_1 phase of the cell cycle (20). This effect is thought to be mediated by increased expression of the cyclin-dependent kinase (CDK) inhibitors p21 and

p27, and other cell-cycle regulators (21, 22). To examine the effect of $1,25(OH)_2D_3$-3-BE on cell cycle progression in A498 cells, we measured cell cycle distribution by flow cytometry of propidium iodide stained cells following 6 hours of exposure to $1,25(OH)_2D_3$-3-BE, $1,25(OH)_2D_3$, or ethanol (vehicle control). As shown in Fig. 2A, the cell cycle distributions were similar in control and in $1,25(OH)_2D_3$-treated cells. However, cells, treated with $1,25(OH)_2D_3$-3-BE showed an approximately 2-fold increase in the relative proportion of cells in G2/M compared to control and $1,25(OH)_2D_3$ treated cells. In addition, a population of cells with a sub-diploid DNA content appeared suggesting that $1,25(OH)_2D_3$-3-BE may activate a G2/M checkpoint arrest in renal cancer cells, preventing progression through the cell cycle.

$1,25(OH)_2D_3$-3-BE reduces the level of cyclin A in A498 and Caki 1 cells. Cyclins control progression through the cell cycle via their association with cyclin-dependent kinases. Cyclin A controls the transition from G2 to mitosis and its expression has been shown to have predictive value in the clinical stages of renal cancer (23, 24) Due to our observation that $1,25(OH)_2D_3$-3-BE arrests cells in the G2/M checkpoint, and the importance of cyclin A in renal cancer, we investigated cyclin A expression in A498 and Caki 1 cells treated with either $1,25(OH)_2D_3$ or $1,25(OH)_2D_3$-3-BE We observed that 6 hour treatment of Caki 1 and A498 cells with 10^{-9}M $1,25(OH)_2D_3$-3-BE strongly reduced cyclin A, while the same concentration of $1,25(OH)_2D_3$ failed to do so (Fig. 2B) indicating that $1,25(OH)_2D_3$-3-BE may cause arrest at the G2/M checkpoint in these cells through down-regulation of cyclin A.

$1,25(OH)_2D_3$-3-BE treatment induces apoptosis in Caki 1 cells. Cellular growth inhibition mediated by $1,25(OH)_2D_3$ correlates with increased apoptosis in some studies. For example, it is reported that $1,25(OH)_2D_3$ induces apoptosis in LNCaP prostate cancer and MCF-7 breast cancer cells (25, 26), but this result is not universal (20). Previously, we reported that

1,25$(OH)_2D_3$-3-BE induces apoptosis in PC-3 prostate cancer cells (15, 16). Thus, we investigated the role of apoptosis in 1,25$(OH)_2D_3$-3-BE-mediated growth inhibition of renal cancer cells.

We observed rounding and sloughing of cells treated with 1,25$(OH)_2D_3$-3-BE, but not with 1,25$(OH)_2D_3$ or vehicle control in both Caki 1 and A498 cell lines (Fig. 1B). To determine if the striking morphological changes in kidney cancer cells in response to 1,25$(OH)_2D_3$-3-BE-treatment are related to induction of apoptosis, we performed flow cytometric analysis of nuclear DNA content following exposure to 1,25$(OH)_2D_3$-3-BE or 1,25$(OH)_2D_3$ in Caki 1 cells. As shown in Fig. 3A, the sub-G0/G1 (hypo-diploid) fraction, indicative of apoptotic cells, was equivalent between control and 1,25$(OH)_2D_3$-treated cells (8-11%). However, the 1,25$(OH)_2D_3$-3-BE-treated cells showed a large increase in this sub-G0/G1 population (74%).

Caspases are a family of proteases which play an essential role in apoptotic cell death, and caspase-activation is considered a hallmark of apoptosis. To examine the role of 1,25$(OH)_2D_3$-3-BE in caspase activation, we performed a caspase activity assay on Caki 1 cells following treatment with 1,25$(OH)_2D_3$ and 1,25$(OH)_2D_3$-3-BE. This assay detects activation of caspases 3 and 7 through cleavage of a fluorescent substrate specific for caspases 3 and 7. As seen in Table 1, no caspase activity was observed in cells treated with ethanol control or 1,25$(OH)_2D_3$. However, strong activation of caspase 3 and 7 activity was observed in cells treated with 1,25$(OH)_2D_3$-3-BE. Taken together, the results of sub G0/G1 DNA analysis and the caspase activation assay demonstrate the ability of 1,25$(OH)_2D_3$-3-BE to stimulate apoptosis in renal cancer cells.

1,25$(OH)_2D_3$-3-BE inhibits Akt phosphorylation in A498 cells. To investigate the molecular

mechanism of $1,25(OH)_2D_3$-3-BE-induced apoptosis in renal cancer cells cells, we examined the activation status of the pro-survival kinase, Akt in A498 cells. Akt is activated by its phosphorylation at threonine 308 and serine 473, events which promote cell survival and proliferation (27). Therefore, we analyzed the activation status of Akt by immunoblot analysis with an antibody specifically recognizing phosphorylated Akt (ser 473) following treatment of A498 and Caki 1 cells with $1,25(OH)_2D_3$ or $1,25(OH)_2D_3$-3-BE. Results of this analysis are shown in Figure 3B. $1,25(OH)_2D_3$-3-BE strongly reduced the level of phosphorylated Akt in both cell lines. An equimolar concentration of $1,25(OH)_2D_3$ also reduced Akt phosphorylation, but to a much lower extent than did $1,25(OH)_2D_3$-3-BE. These results suggest that the apoptotic function of $1,25(OH)_2D_3$-3-BE in renal cancer cells may be mediated, at least partially, by inhibition of signaling through the Akt pathway.

Caspase-9 is a downstream target of Akt. Activated (phosphorylated) Akt phosphorylates caspase-9 on serine 196 and inhibits its protease activity leading to cell survival. Thus, a potential molecular mechanism whereby $1,25(OH)_2D_3$-3-BE promotes apoptosis centers on the ability of $1,25(OH)_2D_3$-3-BE to inhibit Akt activation resulting in increased caspase-9 activity. To address this hypothesis, we examined caspase-9 phosphorylation in Caki 1 cells following treatment with $1,25(OH)_2D_3$-3-BE and $1,25(OH)_2D_3$. As shown in Fig. 3C, $1,25(OH)_2D_3$-3-BE, but not $1,25(OH)_2D_3$, inhibited phosphorylation of caspase-9. As a control, we used the PI3K/Akt inhibitor LY294002 to confirm that inhibition of Akt activity leads to decreased phosphorylation of caspase-9. These results further implicate Akt and its downstream target, caspase-9, as targets for the molecular mechanism whereby $1,25(OH)_2D_3$-3-BE promotes apoptosis in renal cancer cells.

$1,25(OH)_2D_3$-3-BE is stable in human serum. HPLC-profile of ^{14}C-$1,25(OH)_2D_3$-3-BE,

1

incubated in human serum for 60 min at 37°C shows a single peak (Fig. 4B) that matches with the peak for a standard sample of ^{14}C-1,25(OH)$_2$D$_3$-3-BE (Fig. 4A), indicating that ^{14}C-1,25(OH)$_2$D$_3$-3-BE is stable in human serum at 37°C for at least one hr.

1,25(OH)$_2$D$_3$-3-BE inhibits tumor-growth in a mouse xenograft model.

The effect of 1,25(OH)$_2$D$_3$-3-BE on the growth of renal cell tumors was evaluated in xenografts in nude mice. Caki 1 cells were injected subcutaneously in athymic nude mice and allowed to grow until the tumors reached approximately 100 mm^3 in size at which time 1,25(OH)$_2$D$_3$-3-BE, 1,25(OH)$_2$D$_3$ or vehicle control were administered. In comparison to 1,25(OH)$_2$D$_3$-3-BE and 1,25(OH)$_2$D$_3$ treatment, the vehicle-treated control animals generated tumors which grew rapidly throughout the time course. In contrast, the tumors in the 1,25(OH)$_2$D$_3$-3-BE-treated group showed a significant reduction in size compared to control animals tumors and 1,25(OH)$_2$D$_3$-3-BE was more effective than 1,25(OH)$_2$D$_3$ in inhibiting tumor growth (Fig. 5A). To examine potential toxic effects of 1,25(OH)$_2$D$_3$-3-BE treatment, the body weights of the mice were determined each time compounds were administered. As shown in Figure 5B, we did not observe a difference in body weights between any of the treatment groups. Importantly, serum calcium values of the 1,25(OH)$_2$D$_3$ and 1,25(OH)$_2$D$_3$-3-BE-treated animals were not significantly different from the vehicle-control (Fig. 5C) denoting lack of toxicity. Collectively, these results demonstrate that 1,25(OH)$_2$D$_3$-3-BE is an effective agent at reducing renal cancer xenografts an appears to be well tolerated at this dose and time course.

1,25(OH)$_2$D$_3$-3-BE reduces cyclin A levels and increases apoptosis in tumor samples.

We observed significant inhibition of cyclin A levels in our cell culture models of 1,25(OH)$_2$D$_3$-3-BE action. Therefore, we examined cyclin A staining in tumors from mice treated with

1,25$(OH)_2D_3$-3-BE, 1,25$(OH)_2D_3$ and vehicle (control). Immunohistochemical analysis of cyclin A in the xenografts demonstrated significant reduction in the percentage of cells having nuclear cyclin A staining with both 1,25$(OH)_2D_3$ and 1,25$(OH)_2D_3$-3-BE (Fig. 6A). Importantly, the reduction in cyclin A was more pronounced in tumors derived from 1,25$(OH)_2D_3$-3-BE treated animals (Fig. 6C).

Because we observed potent stimulation of apoptosis by 1,25$(OH)_2D_3$-3-BE *in vitro*, we examined the presence of apoptotic bodies, as an indication of apoptosis, in the xenografts. The number of apoptotic bodies per high power field was increased in tumors from the 1,25$(OH)_2D_3$-3-BE treated animals suggesting that 1,25$(OH)_2D_3$-3-BE stimulated apoptosis in vivo (Figs. 6B and 6C). However, 1,25$(OH)_2D_3$ did not significantly increase apoptosis in the xenografts. These findings are in concordance with our observations that, compared to 1,25$(OH)_2D_3$, 1,25$(OH)_2D_3$-3-BE is a more potent inducer of apoptosis in renal cancer cells in vitro.

1

DISCUSSION

There is a paucity of information about the effect of $1,25(OH)_2D_3$ and its analogs in renal cancer. Nagakura *et al.* demonstrated that $1,25(OH)_2D_3$ and some of its metabolites inhibited the growth of renal cancer cell line KU-2 (28). In addition, Fuzioka *et al.* demonstrated that $1,25(OH)_2D_3$ inhibited the growth of murine Renca renal cancer cell line-induced tumor in a mouse model (29). These results suggest potential utility of $1,25(OH)_2D_3$ and its analogs in treating renal cancer.

We observed that $1,25(OH)_2D_3$-3-BE is a significantly stronger antiproliferative agent compared with equimolar amounts of $1,25(OH)_2D_3$ both *in vitro* (Fig. 1) and in a mouse xenograft tumor model (Fig. 5). Greater efficacy of $1,25(OH)_2D_3$-3-BE compared to $1,25(OH)_2D_3$ can potentially be explained by its proposed ability to titrate and engage all VDR molecules, due to the kinetic nature of the alkylation process. This is an important consideration in cases where VDR level is low. For example, Trydal *et al.* determined VDR level in 23 primary renal cell carcinomas and compared these levels with autologous normal kidney tissue. They reported that VDR levels for the renal cell carcinomas were approximately three times lower than autologous normal kidney tissue (30). We evaluated VDR levels in Caki 1 and A-498 cells, treated with $1,25(OH)_2D_3$, $1,25(OH)_2D_3$-3-BE or vehicle, and observed comparable levels of VDR by immunoblot analysis suggesting that changes in VDR levels do not reflect response to $1,25(OH)_2D_3$-3-BE (data not shown).

In Caki 1 cells, we observed $1,25(OH)_2D_3$-3-BE induces apoptosis, in addition to cell-cycle arrest, as evidenced by sub G0/G1 DNA analysis and arrest at the G2/M checkpoint (Figs. 2 and 3). $1,25(OH)_2D_3$-3-BE also strongly stimulated caspase 3/7 activity, a hallmark of apoptosis (Table 1). The induction of apoptosis by $1,25(OH)_2D_3$ has been shown to involve

up-regulation of pro-apoptotic Bax and Bcl-XL, Bcl-2 family proteins that regulate the intrinsic pathway for apoptotic induction (25, 26). However, in A498 cells 1,25$(OH)_2D_3$-3-BE (as well as 1,25$(OH)_2D_3$) failed to activate these proteins (data not shown), suggesting that activation of caspases (by 1,25$(OH)_2D_3$-3-BE) in kidney cancer cells may follow a different pathway.

Akt is a serine/threonine kinase which is activated by many signals in a phophatidylinositol-3'-kinase (PI3K)-dependent manner (31, 32). Akt is involved in a variety of normal and tumorigenic functions such as cell proliferation, growth and survival. Hara *et al.* screened 45 tumor samples from renal cell carcinoma patients and reported that phosphorylated Akt expression increased significantly in comparison to associated normal kidney tissue and that an Akt inhibitor induced apoptosis in KU19-20 and Caki-2 cells which have high Akt activity (33). We observed that 1,25$(OH)_2D_3$-3-BE strongly inhibited Akt-phosphorylation in A498 and Caki 1 cells (Fig. 3B), indicating that the ability of 1,25$(OH)_2D_3$-3-BE to inhibit Akt activation may be critical in the molecular mechanism of its action.

Caspase 9 is a downstream effector of Akt-activity. As presented in Figure 3B, we observed complete inhibition of caspase-9 phosphorylation following 1,25$(OH)_2D_3$-3-BE treatment of Caki 1 cells. Interestingly, 1,25$(OH)_2D_3$ did not inhibit caspase-9 phosphorylation, potentially revealing a key mechanism explaining the observed differences in the ability of 1,25$(OH)_2D_3$-3-BE and 1,25$(OH)_2D_3$ to promote apoptosis in renal cancer cells.

The stability of a drug in serum is a key pharmacokinetic property. Serum stability is particularly important for 1,25$(OH)_2D_3$-3-BE, because it contains an ester bond which may be prone to hydrolysis by esterases. Therefore, we determined the stability of 1,25$(OH)_2D_3$-3-BE in human serum. HPLC-profile of an organic extract of a serum sample, spiked with ^{14}C-

$1,25(OH)_2D_3$-3-BE showed the intact peak of ^{14}C-$1,25(OH)_2D_3$-3-BE after one hr incubation at 37^0C (Fig. 4). This result attests to the stability of $1,25(OH)_2D_3$-3-BE in serum, and enhances its potential as a therapeutic agent.

In order to evaluate the potential of $1,25(OH)_2D_3$-3-BE in renal cancer, we carried out an *in vivo* study with an athymic mouse model of human renal cancer. In this study we observed that tumors in vehicle-treated, control, animals grew rapidly throughout the time course. Significantly, $1,25(OH)_2D_3$-3-BE, but not $1,25(OH)_2D_3$ inhibited tumor-growth (Fig. 5A), reflecting the *in vitro* growth-inhibitory property of $1,25(OH)_2D_3$-3-BE in kidney cancer cells. In addition, higher efficacy of $1,25(OH)_2D_3$-3-BE in inhibiting tumor growth compared to $1,25(OH)_2D_3$ was reflected by decreased cyclin A nuclear staining and increased apoptosis in the tumors (Figs. 6A-C). It is noteworthy that the molecular weights of $1,25(OH)_2D_3$-3-BE and $1,25(OH)_2D_3$ are 537.80 kD and 416.65 kD respectively. Therefore, if we consider equimolar concentrations of these compounds, $1,25(OH)_2D_3$-3-BE is actually approximately 1.3–fold more active than $1,25(OH)_2D_3$.

$1,25(OH)_2D_3$-3-BE did not show significant toxicity as reflected in the gross body weights of the animals throughout the study (Fig. 5B). As indicated in Fig. 5B $1,25(OH)_2D_3$ apparently caused some weight-gain. But, upon statistical analysis body-weights of $1,25(OH)_2D_3$ - treated animals were not significantly different from other groups (vehicle-control and $1,25(OH)_2D_3$-3-BE). Furthermore, serum calcium values were not significantly different among the groups (Fig. 5C).

We have demonstrated that $1,25(OH)_2D_3$-3-BE covalently attaches to the ligand-binding pocket of VDR (13), thus possibly making it less prone to catabolic degradation and higher

activation of VDR. It can be argued that such a process may lead to 'apparent higher dose of $1,25(OH)_2D_3$' and enhance toxicity. But, increasing the effective dose of $1,25(OH)_2D_3$ by covalent labeling also means that we will require less of $1,25(OH)_2D_3$-3-BE to bring about significant effect. We chose a dose of 0.75 µg/kg for both $1,25(OH)_2D_3$ and $1,25(OH)_2D_3$-3-BE at which level none of them showed any toxicity (Fig. 5B and 5C).

In summary, the results presented herein demonstrate that $1,25(OH)_2D_3$-3-BE strongly suppresses growth of kidney cancer cells *in vitro* and tumor growth *in vivo*. These studies suggest further pre-clinical investigations, and continued mechanistic investigations of $1,25(OH)_2D_3$-3-BE in inhibiting renal cancer tumorigenesis are warranted to evaluate its translational potential as a therapeutic agent in renal cell carcinoma. Considered together with extensive data on vitamin D in various cancer-prevention settings, these results also have important implications for renal-cell–cancer prevention. There are, however, no preclinical *in-vivo* models, for example genetically engineered models, for prevention research in this setting, and so such models should be developed for studying the vitamin D analog reported here as well as for studying other potentially effective preventive agents. Such prevention study would be especially relevant for people at a high risk of renal cell cancer (34–36).

FIGURE LEGENDS

Fig. 1. $1,25(OH)_2D_3$-3-BE is more potent than $1,25(OH)_2D_3$ in inhibiting the growth of renal carcinoma cells. (A) A498 cells (left panel) and Caki 1 cells (right panel) were treated with various doses of $1,25(OH)_2D_3$-3-BE or $1,25(OH)_2D_3$ or ethanol (vehicle). After seven days, MTT solution was added to each well and absorbance read on a microplate reader. Absorbances from treated cells are plotted as percent of vehicle. Eight replicates for each treatment was performed. Error bars represent standard error of the mean (SEM). **"**, $p<0.01$; **"**,$p<0.001$. (B) Morphologic appearance of Caki 1 and A498 cells following treatment with $1,25(OH)_2D_3$-3-BE. Cells were treated for 4 hr (Caki 1) and 6 hr (A498) with 10^{-8}M $1,25(OH)_2D_3$, $1,25(OH)_2D_3$-3-BE or ethanol control and phase contrast photomicrographs were obtained at 200x original magnification. The experiment was repeated three times and representative fields are shown.

Fig. 2. (A) $1,25(OH)_2D_3$-3-BE arrests A498 cells in G2/M. FACS analysis was performed on PI-saponin-stained A498 cells treated for 6 hr with 10^{-8}M $1,25(OH)_2D_3$, $1,25(OH)_2D_3$-3-BE or ethanol (vehicle) control. The percent of cells in G0/G1, S and G2/M phases of the cell cycle were calculated using Modfit software. (B) $1,25(OH)_2D_3$-3-BE reduces cyclin A levels in Caki 1 and A498 cells. A498 and Caki 1 cells were treated with 10^{-8}M $1,25(OH)_2D_3$ (D), $1,25(OH)_2D_3$-3-BE (BE) or ethanol control (E) for 6 hr. Whole cell extracts were prepared and Western blot analysis performed for detection of levels of cyclin A. □-Actin was used as a loading control. The results are representative of two independent experiments.

Fig. 3. $1,25(OH)_2D_3$-3-BE promotes apoptosis of Caki 1 cells. (A) Sub G0/G1 DNA FACS

analysis of Caki 1 cells treated with $1,25(OH)_2D_3$ or $1,25(OH)_2D_3$-3-BE. Caki 1 cells were grown to 60-70% confluence, and then were incubated with 10^{-8}M of either $1,25(OH)_2D_3$ or $1,25(OH)_2D_3$-3-BE for 6 hours. The cells were harvested and stained with propidium Iodide. Fluorescence was measured in a FACS analyzer (B) $1,25(OH)_2D_3$-3-BE inhibits phosphorylation of Akt in A498 and Caki 1 cells. A498 and Caki 1 cells were incubated with 5×10^{-7}M of $1,25(OH)_2D_3$ and $1,25(OH)_2D_3$-3-BE or ethanol control for 24 hours and Western analysis used to asses the levels of phosphorylated Akt (p-Akt). The blot was stripped and re-probed for total Akt as a loading control. The results are representative of two independent experiments. (C) $1,25(OH)_2D_3$-3-BE inhibits Akt-mediated phosphorylation of caspase-9. Caki 1 cells were incubated with 5×10^{-7}M of $1,25(OH)_2D_3$, $1,25(OH)_2D_3$-3-BE, the PI3K/Akt inhibitor LY294002 (10 □M) or ethanol control for 6 hours and Western analysis used to asses the levels of phosphorylated caspase-9 (p-Caspase 9). The blot was stripped and re-probed for □-actin as a loading control. The results are representative of three independent experiments.

Fig. 4. HPLC profiles of (A) a standard sample of ^{14}C-$1,25(OH)_2D_3$-3-BE, and (B) organic extract of a sample of human serum, spiked with ^{14}C-$1,25(OH)_2D_3$-3-BE. Conditions: C18 column, 5% H_2O-MeOH: mobile phase, on-line radioactivity-detection. The experiment was repeated three times and representative data shown.

Fig. 5. $1,25(OH)_2D_3$-3-BE inhibits tumor growth in a mouse xenograft growth in a mouse xenograft model. (A) Caki 1 xenografted tumor growth in response to administration of $1,25(OH)_2D_3$ and $1,25(OH)_2D_3$-3-BE (0.75 μg/kg body weight each). Tumor size was measured at the indicated days after injection of tumor cells. Inset: Graphical representation

of tumor volumes at the completion of the experiment. *=p<0.01 by Students T test. (B) $1,25(OH)_2D_3$ and $1,25(OH)_2D_3$-3-BE do not induce toxicity in mice. At each time where tumor size was measured the mice were weighed as a measure of toxic effects of $1,25(OH)_2D_3$ and $1,25(OH)_2D_3$-3-BE. (C) Serum-calcium values of treated animals were determined by a calcium-assay kit using manufacturer's procedure (BioAssay System). Statistical analysis was done by Students T test.

Fig. 6. $1,25(OH)_2D_3$-3-BE stimulates apoptosis and reduces cyclin A levels in renal cancer xenografts. (A) Immunohistochemical analysis of cyclin A levels in xenografts. The tumors derived from control, $1,25(OH)_2D_3$ and $1,25(OH)_2D_3$-3-BE treated mice were examined for cyclin A levels. Arrows indicate positive nuclear staining for cyclin A. (B) Apoptotic bodies are increased in tumors from $1,25(OH)_2D_3$-3-BE treated mice. Circles indicate representative apoptotic bodies. (C) Quantification of cyclin A staining (left panel) and apoptotic bodies (right panel). Positive nuclear staining for cyclin A and the number of apoptotic bodies in control tumors (Con), tumors derived from $1,25(OH)_2D_3$ treated mice (D) and tumors derived from $1,25(OH)_2D_3$-3-BE treated mice were counted as described in Materials and Methods. For cyclin A statistical analysis (students T test), *=P<0.005 and **=P<0.0005. For the number of apoptotic bodies *=P<0.02.

Table 1

$1,25(OH)_2D_3$-3-BE stimulates caspase-3/7 activity activity in Caki 1 cells

Caspase-3/7 activity was determined following treatment of Caki 1 cells for 6 hours with $1,25(OH)_2D_3$, $1,25(OH)_2D_3$-3-BE or ethanol (vehicle) control. Fluorescence released following cleavage of the pro-fluorescent substrate, Z-DEVD-110 was measured at the emission maximum of 521 nm. The amount of fluorescent product generated is representative of the amount of active caspase-3/7 in the sample. SE= standard error

Treatment	Fluorescence Units	+/- SE
EtOH	0	0
$1,25(OH)_2D_3$	0	0
$1,25(OH)_2D_3$-3-BE	17841	821

Reference List

1. Jemal A, Siegel R, Ward E, Hao Y, Xu J, Murray T, Thun MJ. Cancer statistics, 2008; CA Cancer J Clin 2008; 58:71-96.

2. van Spronsen DJ, Mulders PF, de Mulder PH. Novel treatments for metastatic renal cell carcinoma. Crit Rev Oncol Hematol 2005; 55:177-91.

3. Lam JS, Leppert JT, Figlin RA, Belldegrun AS. Role of molecular markers in the diagnosis and therapy of renal cell carcinoma. Urology 2005; 66:1-9.

4. Mancuso A, Sternberg CN. New treatments for metastatic kidney cancer. Can J Urol 2005; 12 (Suppl 1):66-70.

5. Ko YJ, Atkins MB. Chemotherapies and immunotherapies for metastatic kidney cancer. Curr Urol Rep 2005; 6:35-42.

6. Rini BI, Small EJ. Biology and clinical development of vascular endothelial growth factor-targeted therapy in renal cell carcinoma. J Clin Oncol 2005; 23:1028-43.

7. Giovannucci E. The epidemiology of vitamin D and cancer incidence and mortality: a review (United States). Cancer Causes Control 2005; 16:83-95.

8. Matsuda S, Jones G. Promise of vitamin D analogues in the treatment of hyperproliferative conditions. Mol Cancer Ther 2006; 5:797-808.

9. Muindi JR, Johnson CS, Trump DL, Christy R, Engler KL, Fakih MG. A phase I and pharmacokinetics study of intravenous calcitriol in combination with oral dexamethasone and gefitinib in patients with advanced solid tumors. Cancer Chemother Pharmacol 2009; 65:33-40.

10. Fakih MG, Trump DL, Muindi JR, Black JD, Bernardi RJ, Creaven PJ, Schwartz J, Brattain MG, Hutson A, French R, Johnson CS. A phase I pharmacokinetic and pharmacodynamic study of intravenous calcitriol in combination with oral gefitinib in patients with advanced solid tumors. Clin Cancer Res 2007;13:1216-23.

11. Trump DL, Potter DM, Muindi J, Brufsky A, Johnson CS. Phase II trial of high-dose, intermittent calcitriol (1,25 dihydroxyvitamin D3) and dexamethasone in androgen-independent prostate cancer. Cancer 2006; 106:2136-42.

12. Ray R, Swamy N, MacDonald PN, Ray S, Haussler MR, Holick MF. Affinity labeling of the 1 alpha,25-dihydroxyvitamin D_3 receptor. J Biol Chem 1996;271:2012-17.

13. Swamy N, Xu W, Paz N, Hsieh JC, Haussler MR, Maalouf GJ, Mohr SC, Ray R. Molecular modeling, affinity labeling, and site-directed mutagenesis define the key points of interaction between the ligand-binding domain of the vitamin D nuclear receptor and 1α,25-dihydroxyvitamin D_3. Biochemistry 2000; 39:12162-71.

14. Chen ML, Ray S, Swamy N, Holick MF, Ray R. Mechanistic studies to evaluate the enhanced antiproliferation of human keratinocytes by 1α,25-dihydroxyvitamin D_3-3-bromoacetate, a covalent modifier of vitamin D receptor, compared to 1α,25-dihydroxyvitamin D_3. Arch Biochem Biophys 1999; 370:34-44.

15. Swamy N, Persons KS, Chen TC, Ray R. 1α,25-Dihydroxyvitamin D_3-3beta-(2)-bromoacetate, an affinity labeling derivative of 1α,25-dihydroxyvitamin D_3 displays strong antiproliferative and cytotoxic behavior in prostate cancer cells, J Cell Biochem 2003; 89:909-16.

16. Swamy N, Chen TC, Peleg S, Dhawan P, Christakos S, Stewart LV, Weigel NL, Mehta RG, Holick MF, Ray R. Inhibition of proliferation and induction of apoptosis by 25-hydroxyvitamin D_3-3β-(2)-Bromoacetate, a nontoxic and vitamin D receptor-alkylating analog of 25-hydroxyvitamin D_3 in prostate cancer cells. Clin Cancer Res 2004;10:8018-27.

17. Lambert JR, Young CD, Persons KS, Ray R. Mechanistic and pharmacodynamic studies of a 25-hydroxyvitamin D3 derivative in prostate cancer cells. Biochem Biophys Res Commun 2007;361:189-95.

18. Lange TS, Singh RK, Kim KK, Zou Y, Kalkunte SS, Sholler GL, Swamy N, Brard L. Anti-proliferative and pro-apoptotic properties of 3-bromoacetoxy calcidiol in high-risk neuroblastoma. Chem Biol Drug Des 2007; 70:302-10.

19. Ray R, Ray S, Holick MF. 1α,25-Dihydroxyvitamin D_3-3 -bromoacetate, an affinity labeling analog of 1α,25-dihydroxyvitamin D_3 receptor. Bioorg Chem 1994; 22:276-83.

20. Zhuang SH, Burnstein KL. Antiproliferative effect of 1alpha,25-dihydroxyvitamin D3 in human prostate cancer cell line LNCaP involves reduction of cyclin-dependent kinase 2 activity and persistent G1 accumulation. Endocrinology 1998; 139:1197-1207.

21. Yang ES, Burnstein KL. Vitamin D inhibits G1 to S progression in LNCaP prostate cancer cells through p27Kip1 stabilization and Cdk2 mislocalization to the cytoplasm, J Biol Chem 2003; 278:46862-868.

22. Moffatt KA, Johannes WU, Hedlund TE, Miller GJ. Growth inhibitory effects of 1alpha, 25-dihydroxyvitamin D(3) are mediated by increased levels of p21 in the prostatic carcinoma cell line ALVA-31. Cancer Res 2001; 61:7122-29.

23. Pagano M, Pepperkok R, Verde F, Ansorge W, Draetta G. Cyclin A is required at two points in the human cell cycle. EMBO J 1992; 11:961-71.

24. Aaltomaa S, Lipponen P, Ia-Opas M, Eskelinen M, Syrjanen K, Kosma VM. Expression of cyclins A and D and p21(waf1/cip1) proteins in renal cell cancer and their relation to clinicopathological variables and patient survival. Br J Cancer 1999; 80:2001-7.

25. Blutt SE, McDonnell TJ, Polek TC, Weigel NL. Calcitriol-induced apoptosis in LNCaP cells is blocked by overexpression of Bcl-2. Endocrinology 2000; 141:10-7.

26. Simoli-Campbell M, Narvaez CJ, Tenniswood M, Welsh J. 1,25-Dihydroxyvitamin D3 induces morphological and biochemical markers of apoptosis in MCF-7 breast cancer cells. J Steroid Biochem Mol Biol 1996; 58:367-76.

27. Alessi DR, Andjelkovic M, Caudwell B, Cron P, Morrice N, Cohen P, Hemmings BA. Mechanism of activation of protein kinase B by insulin and IGF-1. EMBO J 1996; 15:6541-51.

28. Nagakura K, Abe E, Suda T, Hayakawa M, Nakamura H, Tazaki H. Inhibitory effect of 1 –alpha,25-dihydroxyvitamin D3 on the growth of the renal carcinoma cell line. Kidney Intl 1986; 29:834-40.

29. Fuzioka T, Hasegawa M, Ishikura K, Matsuhita Y, Sato M, Tanji S. Inhibition of tumor growth and angiogenesis by vitamin D3 agents in murine renal cell carcinoma. J Urol 1988; 160:247-51.

30. Trydal T, Bakke A, Aksnes L, Aarskog D. 1,25-Dihydroxyvitamin D3 receptor measurement in primary renal cell carcinomas and autologous normal kidney tissue. Cancer Res 1988; 48:2458-61.

31. Morgensztern D, McLeod HL. PI3K/Akt/mTOR pathway as a target for cancer therapy. Anticancer Drugs 2005; 16:797-803.

32. Gills JJ, Dennis PA. The development of phosphatidylinositol ether lipid analogues as inhibitors of the serine/threonine kinase. Akt, Expert Opin Investig Drugs 2004; 13:787-97.

33. Hara S, Oya M, Mizuno R, Horiguchi A, Marumo K, Murai M. Akt activation in renal cell carcinoma: contribution of a decreased PTEN expression and the induction of apoptosis by an Akt inhibitor. Ann Oncol 2005; 16:928-33.

34. Lonser RR, Glenn GM, Walther M, et al. von Hippel-Lindau disease. Lancet 2003;361:2059–67.

35. Purdue MP, Johansson M, Zelenika D, et al. Genome-wide association study of renal cell carcinoma identifies two susceptibility loci on 2p21 and 11q13.3. Nat Genet (in press).

36. Chow W-H, Dong LM, Devesa SS. Epidemiology and risk factors for kidney cancer. Nat Rev Urol 2010;7:245–57.

Fig. 1

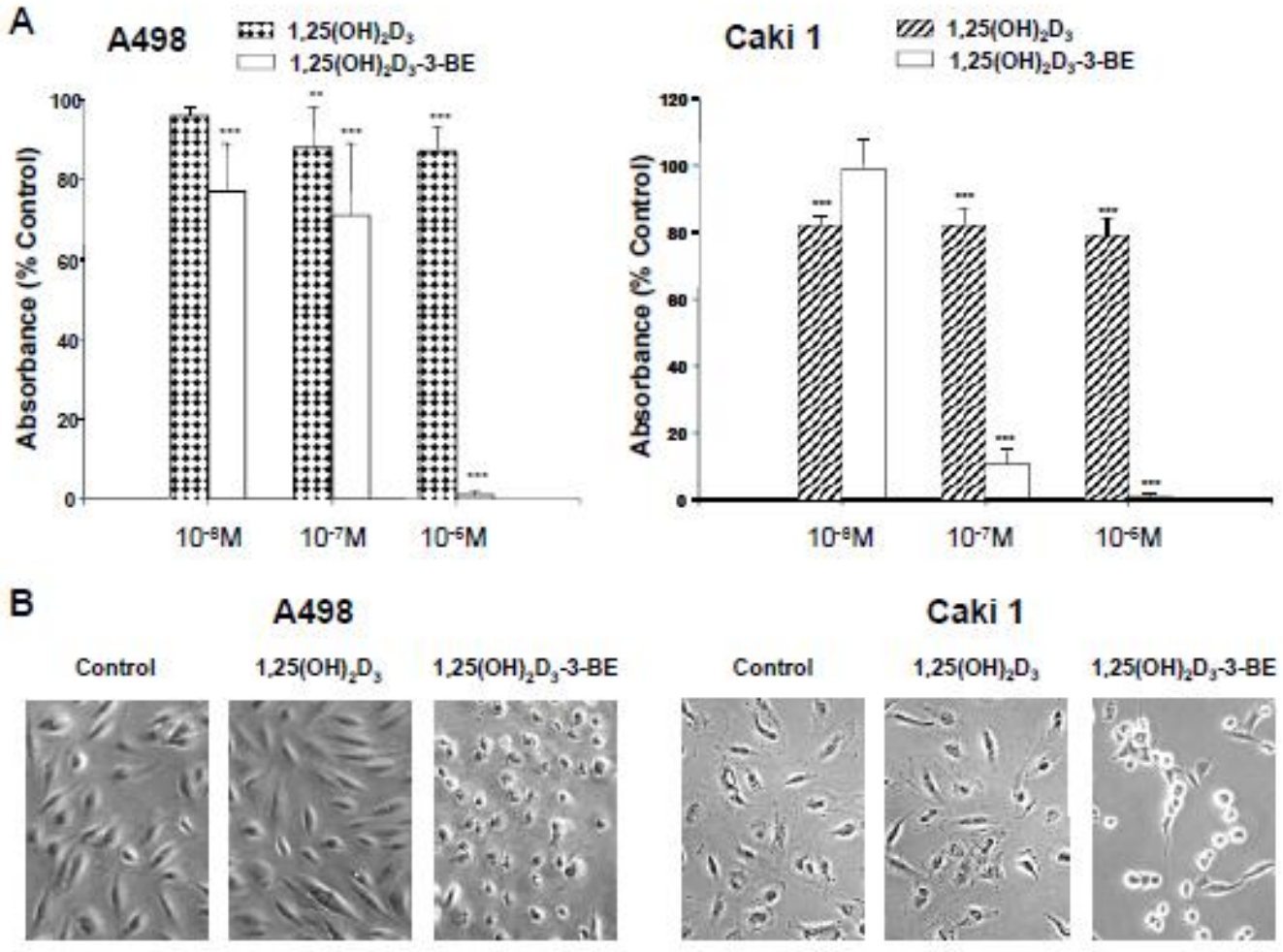
A
A498
1,25(OH)2D3
1,25(OH)2D3-3-BE
Absorbance (% Control)
100
80
60
40
20
0
10-8M
10-7M
10-6M
Caki 1
1,25(OH)2D3
1,25(OH)2D3-3-BE
120
100
80
60
40
20
0
10-8M
10-7M
10-6M
B
A498
Control
1,25(OH)2D3
1,25(OH)2D3-3-BE
Caki 1
Control
1,25(OH)2D3
1,25(OH)2D3-3-BE

Fig. 2

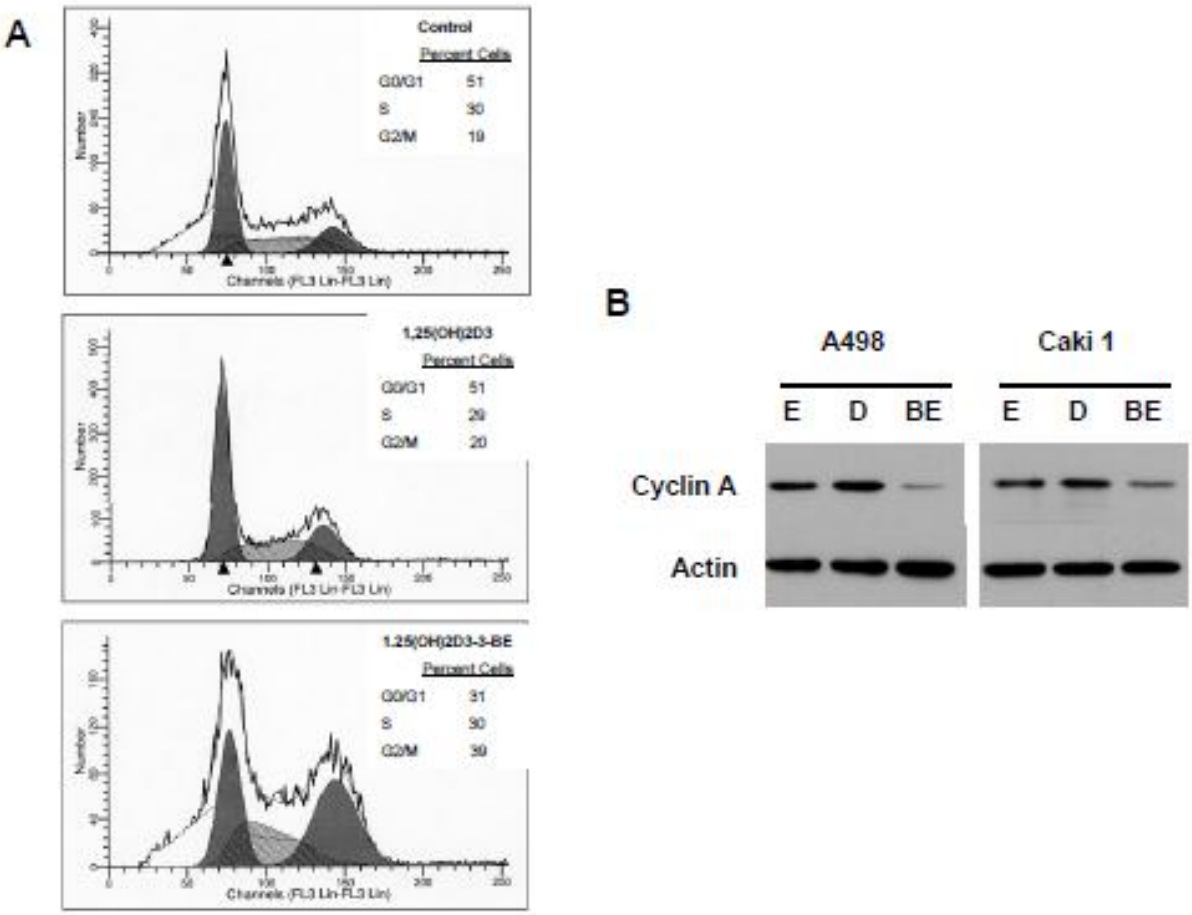
A
Control
Percent Cells
G0/G1 51
S 30
G2/M 19
Number
Channels (FL3 Lin-FL3 Lin)
1,25(OH)2D3
Percent Cells
G0/G1 51
S 29
G2/M 20
Number
Channels (FL3 Lin-FL3 Lin)
1,25(OH)2D3-3-BE
Percent Cells
G0/G1 31
S 50
G2/M 39
Number
Channels (FL3 Lin-FL3 Lin)
B
A498
Caki 1
E D BE E D BE
Cyclin A
Actin

Fig. 3

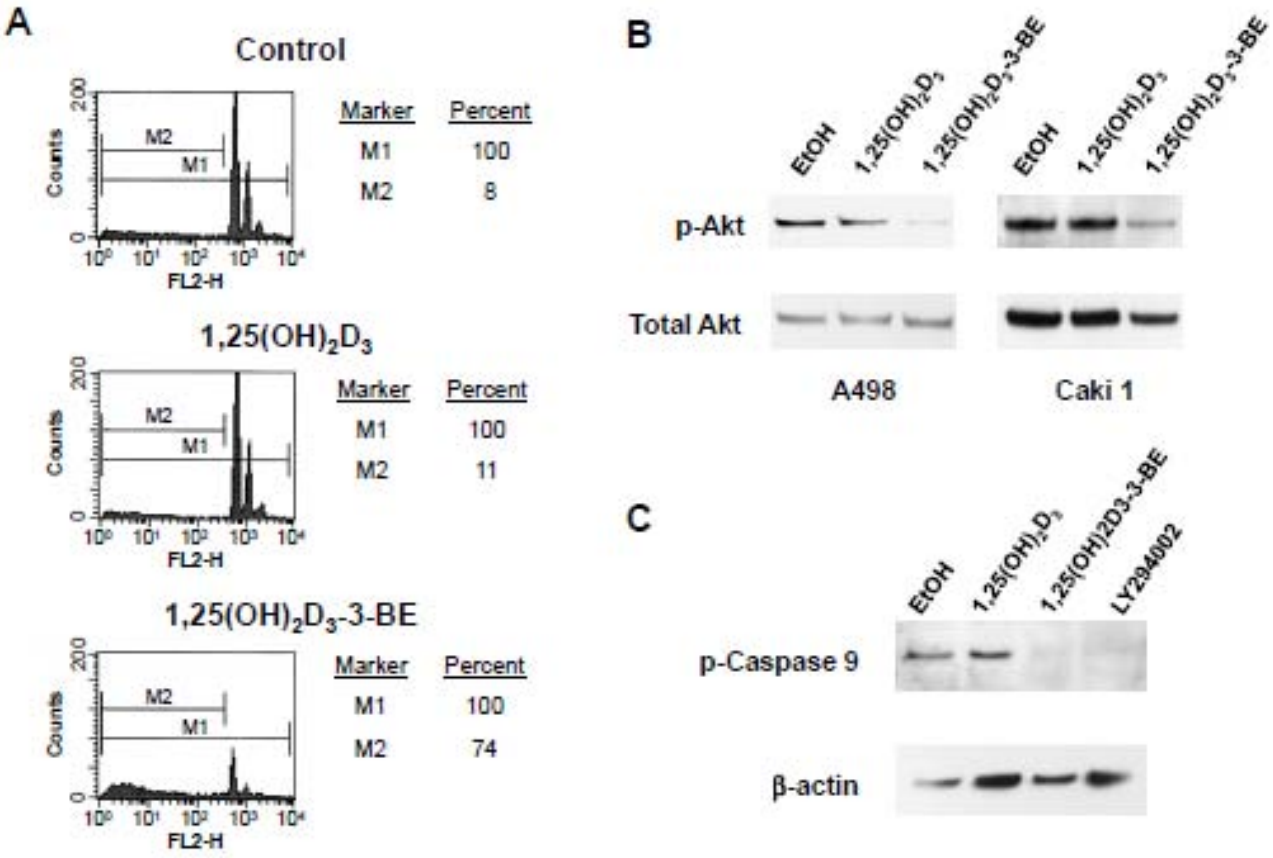
A
Control
Counts
M2
M1
FL2-H
Marker Percent
M1 100
M2 8
1,25(OH)2D3
Marker Percent
M1 100
M2 11
1,25(OH)2D3-3-BE
Marker Percent
M1 100
M2 74
B
EtOH
1,25(OH)2D3
1,25(OH)2D3-3-BE
p-Akt
Total Akt
A498
Caki 1
C
EtOH
1,25(OH)2D3
1,25(OH)2D3-3-BE
LY294002
p-Caspase 9
β-actin

Fig. 4

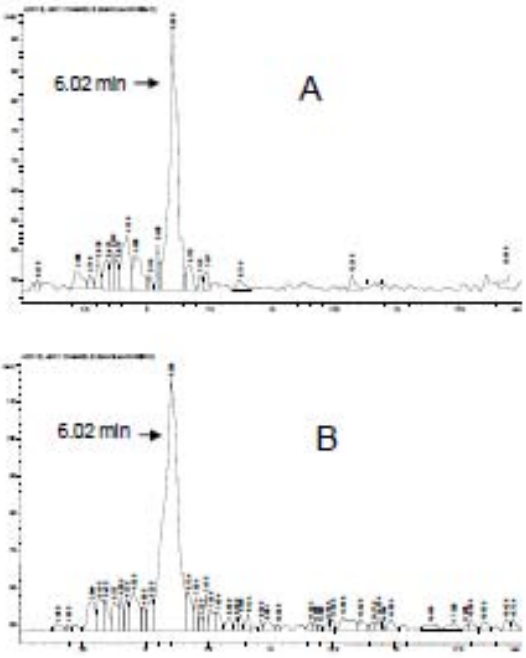

Fig. 5

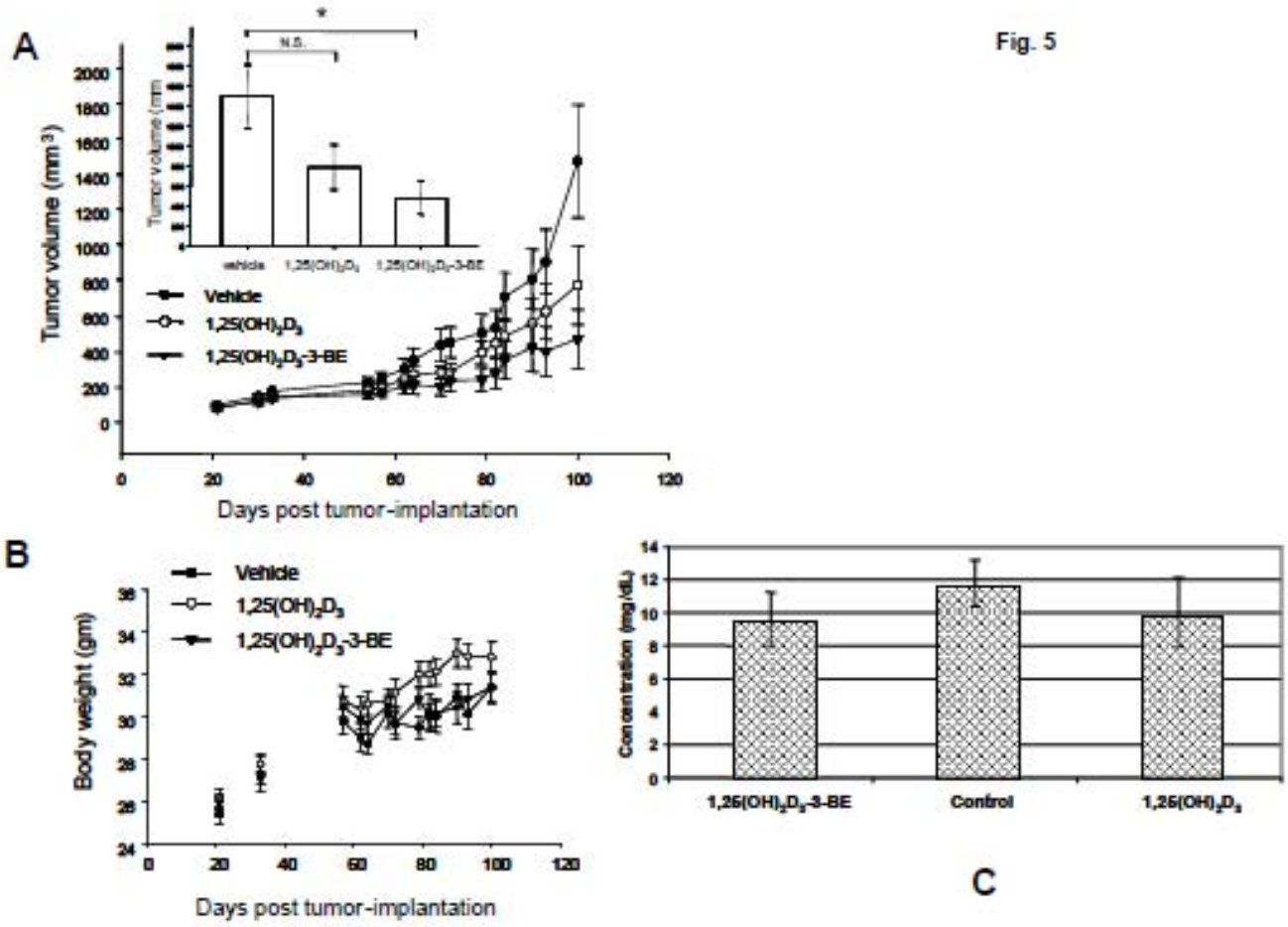
A
Tumor volume (mm3)
Days post tumor-implantation
Vehicle
1,25(OH)2D3
1,25(OH)2D3-3-BE
N.S.
*
B
Body weight (gm)
Days post tumor-implantation
C
Concentration (mg/dL)
1,25(OH)2D3-3-BE
Control
1,25(OH)2D3

Fig. 6

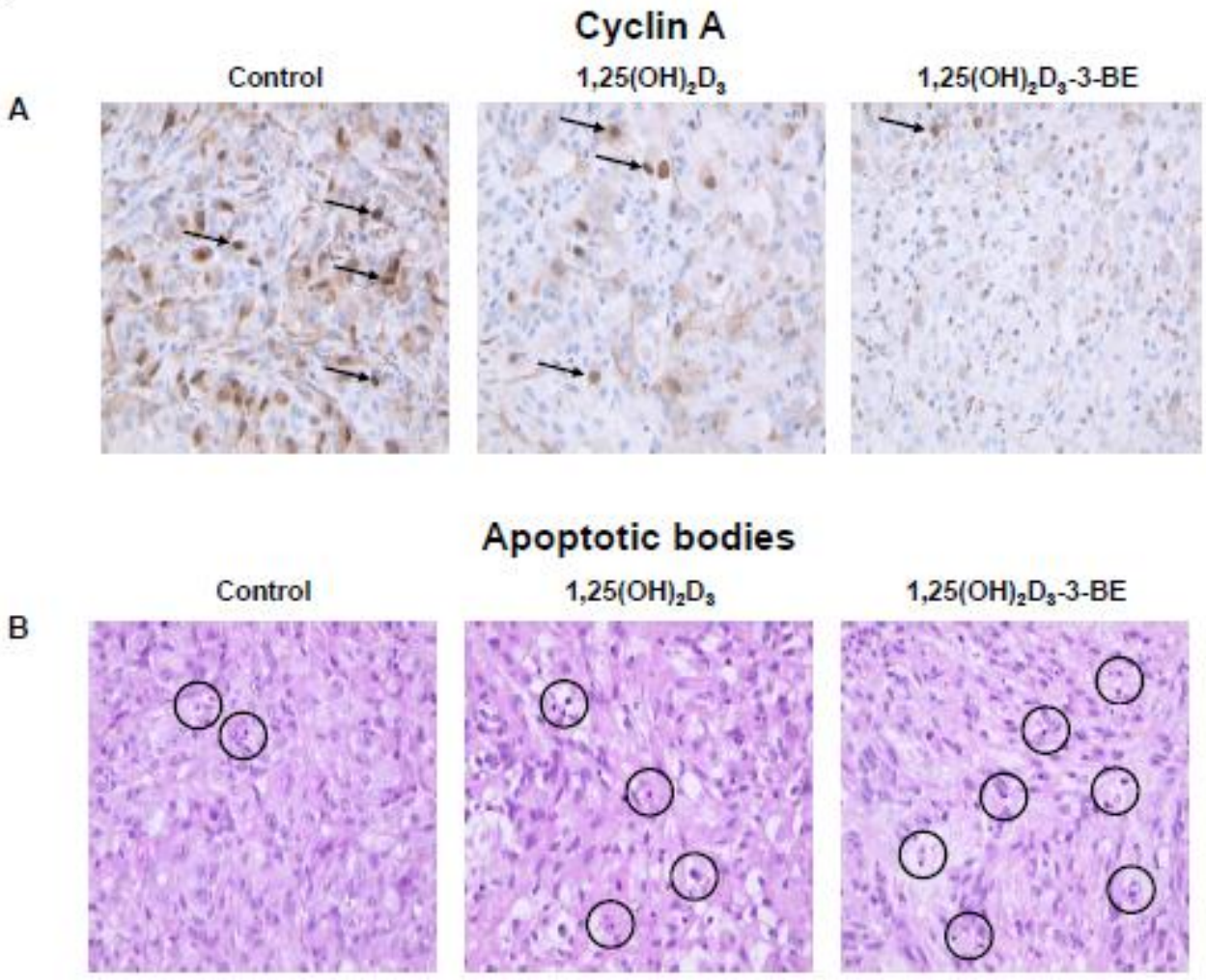
Cyclin A
A
Control
1,25(OH)2D3
1,25(OH)2D3-3-BE
Apoptotic bodies
B
Control
1,25(OH)2D3
1,25(OH)2D3-3-BE

Fig. 6

C

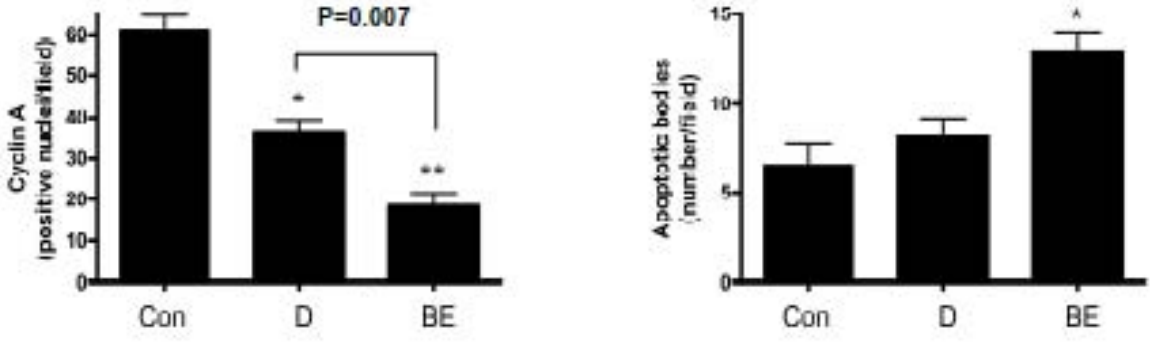
P=0.007
Cyclin A
(positive nuclei/field)
60
50
40
30
20
10
0
*
**
Con
D
BE
Apoptotic bodies
(number/field)
15
10
5
0
*
Con
D
BE

Editorial Manager(tm) for Pharmaceutical Sciences
Manuscript Draft

Manuscript Number: PHARMA-10-20R1

Title: Liposomal 1,25-dihydroxyvitamin D3-3β-bromoacetate is a stronger growth-inhibiting agent than its un-encapsulated counterpart in prostate cancer cells

Short Title: Liposomal 1,25-dihydroxyvitamin D3-3β-bromoacetate and prostate cancer

Article Type: Research Article

Section/Category: Journal of Steroids & Hormonal Science

Keywords: Liposomal 1,25-dihydroxyvitamin D3-3β-bromoacetate, vitamin D receptor alkylating agent, prostate cancer

Corresponding Author: Rahul Ray

Corresponding Author's Institution:

First Author: Rahul Ray

Order of Authors: Rahul Ray

Manuscript Region of Origin: USA

Abstract: Cytotoxic drugs in liposomal vehicles target tumors and protect the drugs from premature degradation. 1,25-Dihydroxyvitamin D3-3β-bromoacetate (1,25(OH)2D3-3-BE), a vitamin D receptor-alkylating agent inhibits the growth of prostate cancer cells. Aim of the study was to evaluate the efficacy of a liposomal preparation of 1,25(OH)2D3-3-BE versus 1,25(OH)2D3-3-BE in modulating the growth of prostate cancer cells. Results demonstrate that liposomal 1,25(OH)2D3-3-BE is significantly better than 1,25(OH)2D3-3-BE in inhibiting the growth. In addition, liposomal 1,25(OH)2D3-3-BE was found to be stable in human serum. Taken together, results of the studies delineated here suggest a therapeutic potential of liposomal 1,25(OH)2D3-3-BE in prostate cancer.

Suggested Reviewers:

Opposed Reviewers:

Response to Reviewers: Rebuttal:

On behalf of the authors I would like thank the reviewers for a careful review of our manuscript. We have made changes/additions/deletions according to the suggestions of the reviewer/s. We hope that it will be sufficient for the manuscript to be accepted for publication.

Changes are highlighted with yellow in the revised manuscript.

1. In the Running Title: "Experimental Study (July 21, 2010)" is removed

2. In the Abstract (as suggested by the reviewer):

Added: "Cytotoxic drugs in liposomal vehicles target tumors and protect the drugs from premature degradation" has been replaced by (according to the suggestion of the reviewer):

Deleted: "Encapsulating cytotoxic drugs in liposomal vehicles allows for the targeting of tumors while protecting the drugs from premature degradation."
Typographical errors: We apologize for this oversight. They are corrected and highlighted with yellow (deletions are 'crossed out').

3. Figure Legends: Completely revamped according to the suggestion of the reviewer.

4. Figures: All axes have been made uniform.

Thank you very much for your consideration.

Rahul Ray

To whom it may concern:

On behalf of the authors I would like to submit the manuscript entitled 'Liposomal 1α,25-dihydroxyvitamin D_3-3β-bromoacetate is a stronger growth-inhibiting agent than its naked counterpart in prostate cancer cells' to be considered for publication in **Journal of Steroids and Hormonal Science**.

This manuscript includes a critical study to develop a liposomal formulation of the title compound, a novel derivative of vitamin D, and evaluate its therapeutic/translational potential in prostate cancer, in line with the stated goals of this journal.

Thank you for your attention.

Rahul Ray

Figure

Click here to download Figure: Figs for paper Final.ppt

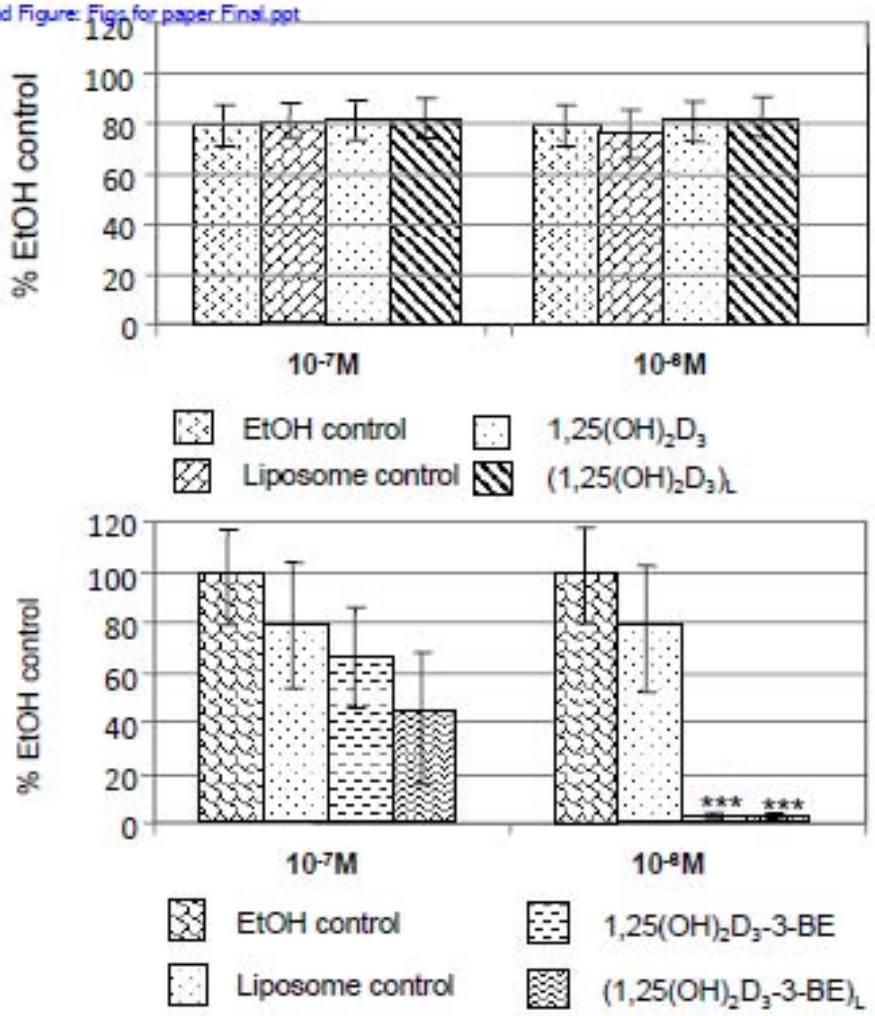

Figure 1

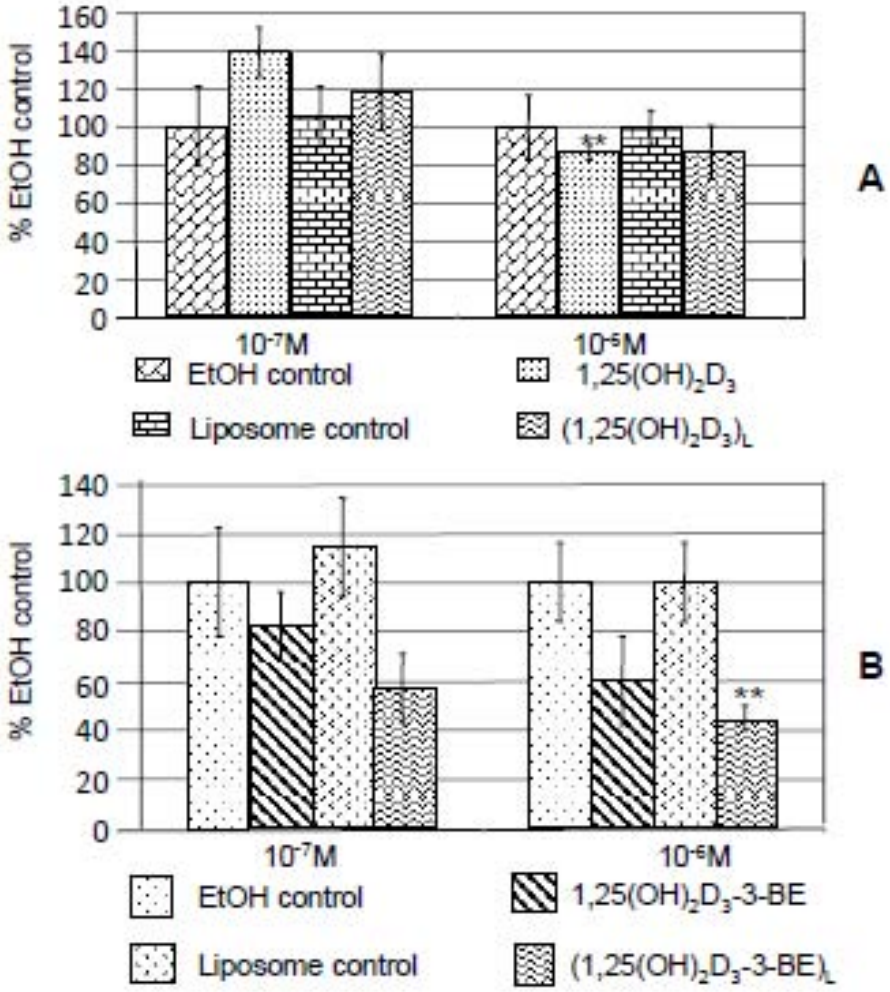
% EtOH control
160
140
120
100
80
60
40
20
0
**
A
10-7M
10-6M
EtOH control
1,25(OH)2D3
Liposome control
(1,25(OH)2D3)L
% EtOH control
140
120
100
80
60
40
20
0
**
B
10-7M
10-6M
EtOH control
1,25(OH)2D3-3-BE
Liposome control
(1,25(OH)2D3-3-BE)L

Figure 2

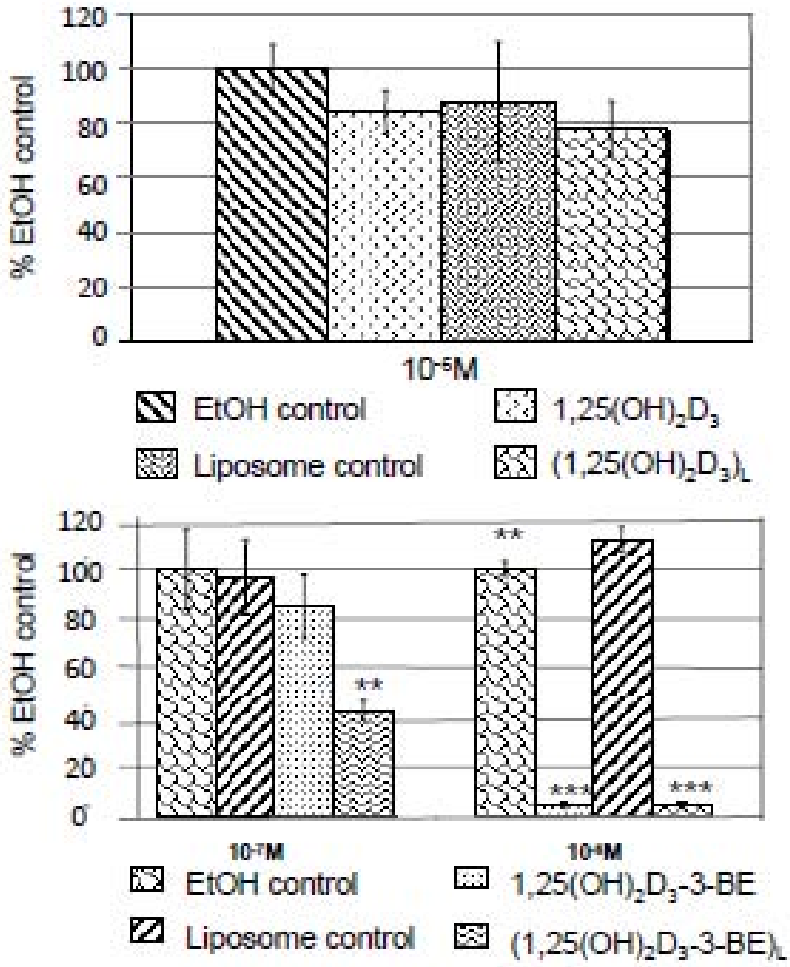
120
100
80
60
40
20
0
% EtOH control
10⁻⁵M
EtOH control
1,25(OH)2D3
Liposome control
(1,25(OH)2D3)L
A
120
100
80
60
40
20
0
% EtOH control
**
**
***
10⁻⁷M
10⁻⁸M
EtOH control
1,25(OH)2D3-3-BE
Liposome control
(1,25(OH)2D3-3-BE)L
B

Figure 3

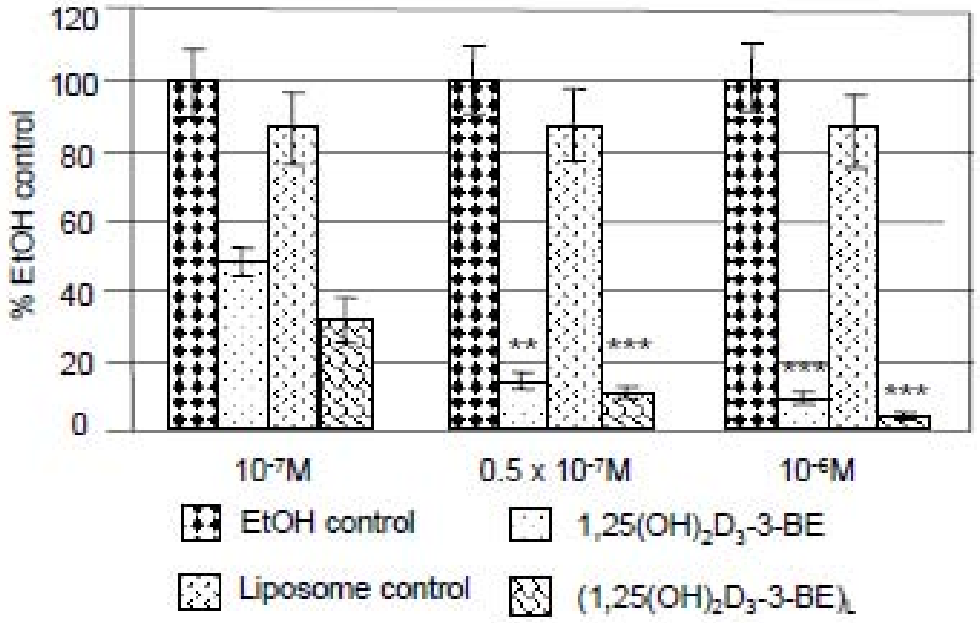
120
100
80
60
40
20
0
% EtOH control
**
***
***
***
10-7M
0.5 x 10-7M
10-6M
EtOH control
1,25(OH)2D3-3-BE
Liposome control
(1,25(OH)2D3-3-BE)L

Figure 4

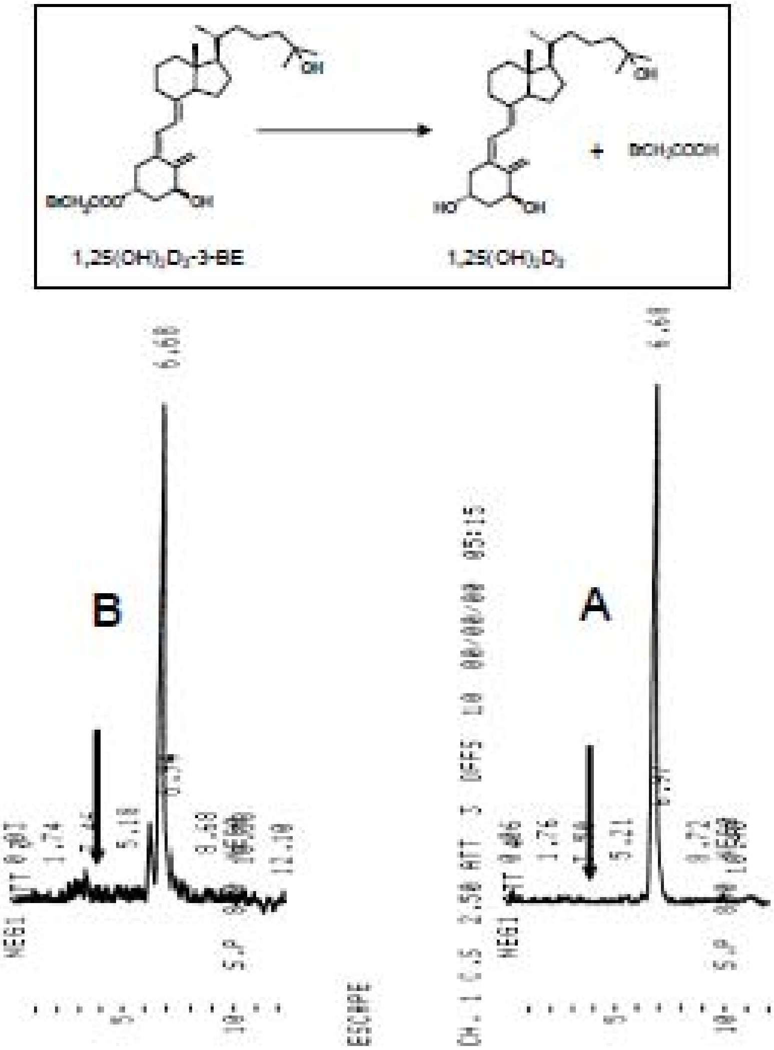

Figure 5

Liposomal 1,25-dihydroxyvitamin D_3-3β-bromoacetate is a stronger growth-inhibiting agent than its un-encapsulated counterpart in prostate cancer cells

Kelly S. Persons, ShwethaHareesh, Vikram J. Eddy, and Rahul Ray*

Boston University School of Medicine, 85 East Newton Street, Boston, MA 02118, U.S.A.

*Corresponding author, Boston University School of Medicine, Boston, MA, U.S.A., Tel: +617-638-8199, Fax: +617-638-8194, e. mail: bapi@bu.edu

Running Title: Liposomal 1,25-dihydroxyvitamin D_3-3β-bromoacetate and prostate cancer ~~(Experimental study, July 21, 2010)~~

Abstract: Encapsulating cytotoxic drugs in liposomal vehicles allows for the targeting of tumors while protecting the drugs from premature degradation. ~~Cytotoxic drugs in liposomal vehicles target tumors and protect the drugs from premature degradation.~~ 1,25-Dihydroxyvitamin D_3-3β-bromoacetate ($1,25(OH)_2D_3$-3-BE), a vitamin D receptor-alkylating agent inhibits the growth of prostate cancer cells. The aim of the study was to evaluate the efficacy of a liposomal preparation of $1,25(OH)_2D_3$-3-BE versus $1,25(OH)_2D_3$-3-BE in modulating the growth of prostate cancer cells. Results demonstrate that liposomal $1,25(OH)_2D_3$-3-BE is significantly better than $1,25(OH)_2D_3$-3-BE in inhibiting the growth. In addition, liposomal $1,25(OH)_2D_3$-3-BE was found to be stable in human serum. Taken together, results of the studies delineated here suggest a therapeutic potential of liposomal $1,25(OH)_2D_3$-3-BE in prostate cancer.

Key words: Liposomal 1,25-dihydroxyvitamin D_3-3β-bromoacetate, vitamin D receptor alkylating agent, prostate cancer

1. Introduction:

Liposomes are recognized as important vehicles for cytotoxic drugs because they can protect the drugs from degradation in circulation, thereby protecting healthy cells and tissues from exposure to lethal drug doses. Additionally, liposomes can extravasate through leaky tumor vasculature selectively over normal tissues and release drugs into the tumor [1-4].

1,25-Dihydroxyvitamin D_3 ($1,25(OH)_2D_3$) is an antiproliferative and anti-cancer agent [5]. But its clinical applicability has been limited by hyper-calcemia and related toxicity, brought in by high therapeutic doses [6-8]. Paradoxically high doses are required to counter its rapid catabolic degradation. 1α,25-dihydroxyvitamin D_3-3β-bromoacetate ($1,25(OH)_2D_3$-3-BE) was developed in our laboratory to counter this problem by covalently attaching $1,25(OH)_2D_3$ deep inside the ligand-binding pocket of vitamin D receptor (VDR), the transcriptional factor that regulates the biological activities of $1,25(OH)_2D_3$ [9-14]. In recent publications it was ~~has been~~ demonstrated that $1,25(OH)_2D_3$-3-BE and 25-hydroxyvitamin D_3-3-bromoacetate, the counterpart of $1,25(OH)_2D_3$-3-BE without the 1-hydroxyl group, are considerably stronger antiproliferative agents than $1,25(OH)_2D_3$ in prostate and pancreatic cancer cells [12-15], as well as high-risk neuroblastoma cells [16].

In the present communication we report that a liposomal preparation of $1,25(OH)_2D_3$-3-BE has a better growth-inhibitory property in three prostate cancer cell lines than the un-encapsulated ~~naked~~ compound ($1,25(OH)_2D_3$-3-BE) and the parent hormone, $1,25(OH)_2D_3$ (un-encapsulated ~~naked~~ and liposomal). We also report that liposomal $1,25(OH)_2D_3$-3-BE is stable in human serum, thereby attesting therapeutic potential of liposomal $1,25(OH)_2D_3$-3-BE in prostate cancer.

2. **Materials and Methods**: All chemicals were obtained from Sigma-Aldrich, Milwaukee, WI, unless mentioned otherwise. Cell-lines were obtained from ATCC (Manasas, VA).

Preparation of liposomes: A solution of cholesterol (1 µg), dimethylphosphotidyl choline (DMPC) (20 µg) and $1,25(OH)_2D_3$ (1 µg, a kind gift from Dr. Milan Uskokovic, Hoffman La-Roche, Nutley, NJ) or $1,25(OH)_2D_3$-3-BE (1 µg, synthesized in our laboratory, reference [17]) in chloroform was dried in a stream of argon. Phosphated saline (PBS, 2.5 ml) was added to the solid residue followed by mixing by brief vortexing and the mixture was sonicated for 15 min. The milky solution was incubated at 50°C for 50 min and frozen at -77°C for 20 min. This heating and freezing cycle was repeated once, and the preparation was stored at 4°C for use in assays. Prior to each assay the liposomal preparation was sonicated and vortexed briefly for proper mixing.

In a separate experiment a chloroform solution of cholesterol, DMPC and $1,25(OH)_2D_3$ was spiked with ^{3}H-$1,25(OH)_2D_3$ (100,000 cpm, sp. activity 120 Ci/mM, Amersham, GE Healthcare), followed by mixing (in PBS) and sonication etc. The preparation was centrifuged at 4°C in an ultracentrifuge (Beckman Ultracentrifuge L7-65) using a Beckman 50.2 Ti rotor at 35,000 rpm for 60 min. The supernatant and pellet (dispersed in one ml of PBS) were mixed with scintillation fluid and counted. We routinely obtained >90% incorporation of radioactivity in the pellet.

Antiproliferation assays: We tested antiproliferative activity of $1,25(OH)_2D_3$, liposomal $1,25(OH)_2D_3$ $(1,25(OH)_2D_3)_L$, $1,25(OH)_2D_3$-3-BE and liposomal $1,25(OH)_2D_3$-3-BE $(1,25(OH)_2D_3$-3-BE$)_L$ in LNCaP, PC-3 and DU-145 prostate cancer cells by MTT assay (according to manufacturer's procedure (Trevigen, Gaithersburg, MD) or ^{3}H-thymidine incorporation assay (see below) .

^{3}H-thymidine-incorporation assay: In a typical assay cells were grown to 50-60% confluence in 24-well plates in DMEM media containing 10% FBS, serum-starved for 20 hours, followed by treatment with various concentrations of $1,25(OH)_2D_3$ or $1,25(OH)_2D_3$-3-BE (as 0.1% ethanolic solution) or ethanol (vehicle) or $(1,25(OH)_2D_3)_L$ or $(1,25(OH)_2D_3$-3-BE$)_L$ or blank liposome in serum-containing medium for 16 hr. After the treatment, media was removed from the wells and replaced with media containing ^{3}H-thymidine (0.1µCi, Sigma-Aldrich, Milwaukee, WI) per well. Plates were incubated for 3 hr at 37°C followed by the following sequence of steps. Liquid was removed by aspiration, cells washed thoroughly (3X0.5 ml) with PBS, ice-cold 5% perchloric acid solution (0.5 ml/well) added, incubated on ice for 20 min, perchloric acid removed by aspiration, replaced with 0.5 ml of fresh perchloric acid, incubated at 70°C for 20 minutes. Finally, solution from each well was mixed with scintillation fluid and counted in a liquid scintillation counter. There were six (6) wells per sample, and statistics was carried out by Student's t test.

Growth assay: DU-145 cells were treated with various doses (as indicated in **Figure 4**) of $1,25(OH)_2D_3$-3-BE,$(1,25(OH)_2D_3$-3-BE$)_L$, ethanolor blank liposomeon 1st, 3rd and 5th days, followed by harvesting of the cells (by trypsinization) on 7th day and counting the cells in a hemocytometer. There were three (3) wells per sample, and statistics was carried out by Student's t test.

Serum-stability study of $(1,25(OH)_2D_3$-3-BE$)_L$: One ml of pooled human serum was incubated at 37°C for 60 minutes with a sample of $(1,25(OH)_2D_3$-3-BE$)_L$ (10 µg) followed by extraction with 5x0.5ml of ethyl acetate. The organic layer was dried in a stream of nitrogen and the residue was analyzed by HPLC (Agilent 1100 series, Thermo-Scientific, Waltham, MA, 5% H_2O-MeOH mobile phase, 1.5 ml/min, 265 nm detection, Agilent C18 column). A standard sample of $1,25(OH)_2D_3$-3-BEwas also analyzed by HPLC under same conditions.

3. **Results**:

3.1: *$(1,25(OH)_2D_3$-3-BE$)_L$ has the strongest growth-inhibitory property in comaprison with$1,25(OH)_2D_3$-3-BE, $1,25(OH)_2D_3$, and $(1,25(OH)_2D_3)_L$ in prostate cancer cells.*

In growth-inhibition studies with androgen-sensitive LNCaP and androgen-insensitive PC-3 and DU-145 prostate cancer cells, 10^{-7-8}M of $1,25(OH)_2D_3$ or $(1,25(OH)_2D_3)_L$ failed to show any significant effect (**Figures 1A, 2A and 3A** respectively). But, in all these cell-lines 10^{-7}M of $1,25(OH)_2D_3$-3-BE and $(1,25(OH)_2D_3$-3-BE$)_L$ displayed considerable antiproliferative effect (**Figures 1B-3B**). Importantly, in each case $(1,25(OH)_2D_3$-3-BE$)_L$ showed a stronger antiproliferative effect than naked $1,25(OH)_2D_3$-3-BE. For example, in LNCaP, PC-3 and DU-145 cells, 10^{-7}M of $1,25(OH)_2D_3$-3-BE inhibited growth by approximately 35%, 20% and 15% respectively, while an equivalent dose of $(1,25(OH)_2D_3$-3-BE$)_L$ inhibited growth by approximately 55%, 45% and 55% respectively (**Figures 1B-3B**). Growth of LNCaP and DU-145 cells was particularly sensitive to 10^{-6}M of $1,25(OH)_2D_3$-3-BE and $(1,25(OH)_2D_3$-3-BE$)_L$, and their growth was almost completely inhibited (**Figures 1B and 3B**) In comparison, PC-3 cells were less sensitive to these treatments (**Figure 2B**). A 10^{-6}M dose may be considered supra-physiological, but we employed this dose ~~level~~ simply to compare the effects between $1,25(OH)_2D_3$ and $1,25(OH)_2D_3$-3-BE and their liposomal formulations. Collectively these results showed that $1,25(OH)_2D_3$-3-BE, particularly in liposomal formulation has strong growth-inhibitory effect in prostate cancer cells.

3.2: *$(1,25(OH)_2D_3$-3-BE$)_L$ has stronger anti-growth effect than $1,25(OH)_2D_3$-3-BE in a chronic and long-term growth assay in DU-145 cells.*

In the next study DU-145 cells ~~cells~~ were treated three times in a week-long growth assay to mimic chronic administration of drugs in *in vivo* studies. Results of this assay, shown in **Figure 4**, demonstrate that $(1,25(OH)_2D_3$-3-BE$)_L$ has a stronger anti-growth effect than $1,25(OH)_2D_3$-3-BE in a dose-dependent manner.

3.3: *$(1,25(OH)_2D_3$-3-BE$)_L$ is stable in human serum.*

Serum-stability assay of $(1,25(OH)_2D_3$-3-BE$)_L$ by HPLC produced a sharp peak with a retention time of 6.68 min and a small shoulder at approximately 6 min (**Figure 5B, Bottom Panel**). Most importantly, $1,25(OH)_2D_3$-3-BE did not produce a peak for $1,25(OH)_2D_3$ (indicated by arrow). These results strongly suggested that $1,25(OH)_2D_3$-3-BE is stable in human serum for at least up to 60 min at 37^0C.

4. Discussion: $1,25(OH)_2D_3$ inhibits growth of many cancer cells, suggesting its potential as a cancer therapeutic agent. However, its clinical use has been limited by its toxicity in pharmacological doses [8]. Requirement of high clinical dose is related to its rapid catabolic degradation (warranting higher doses) and lack of selectivity for tumor cells over normal cells. As discussed earlier, these problems can potentially be alleviated by encapsulating $1,25(OH)_2D_3$ in liposomes/nanosomes. It would be even better if an analog of $1,25(OH)_2D_3$ with a better therapeutic index (than $1,25(OH)_2D_3$) is subjected to the same process. In previous publications we have demonstrated that $1,25(OH)_2D_3$-3-BE possesses considerably stronger antiproliferative activity than $1,25(OH)_2D_3$ in prostate and pancreatic cancer cells [12, 15], underscoring therapeutic potential of $1,25(OH)_2D_3$-3-BE. However, evaluationevalaution of such a translational potential requires development of an effective formulation of the compound.

Liposomes have been touted as tumor-specific and effective carriers of cytotoxic drugs [1]. However, they are not devoid of significant problems including premature destruction to causetoxicity to healthy tissues~~healthy tissue toxicity~~or in the other extreme, undesirably long stability to prevent effective delivery to thetumor cells [1]. These problems have been addressed to some extent by preparing sterically~~y~~hindered pegylated liposomes [18,19] and incorporation of spore-proteins [20-23].

As a prelude to more elaborate studies we have developed a simple yet highly efficient method to encapsulate $1,25(OH)_2D_3$ and $1,25(OH)_2D_3$-3-BE in liposomes and evaluated anti-growth properties of these~~these~~formulations~~formulations~~ in prostate cancer cells.

Results of our *in vitro* studies show that $(1,25(OH)_2D_3$-3-BE$)_L$ has stronger growth-inhibitory

property than $1,25(OH)_2D_3$-3-BE, $1,25(OH)_2D_3$ and $(1,25(OH)_2D_3)_L$ (**Figures 1-3**) in all three prostate cancer cells. In addition, $(1,25(OH)_2D_3$-3-BE$)_L$ is significantly more efficacious as an antiproliferative agent than $1,25(OH)_2D_3$-3-BE in a chronic growth assay with DU-145 cells (**Figure 4**).

$1,25(OH)_2D_3$-3-BE is an ester of $1,25(OH)_2D_3$, and its hydrolysis *in vivo* would produce equivalent amounts $1,25(OH)_2D_3$ and bromoacetic acid, thereby reducing its efficacy (**Figure 5, Inset**). HPLC-analysis indicates that $(1,25(OH)_2D_3$-3-BE$)_L$ is stable in human serum for at least up to one hourhr as denoted by the absence of $1,25(OH)_2D_3$ peak in the HPLC of the organic-extract of $(1,25(OH)_2D_3$-3-BE$)_L$ (**Figure 5**).

In summary, results, delineated in this study demonstrate that $(1,25(OH)_2D_3$-3-BE$)_L$ has a stronger growth-inhibitory effect than $1,25(OH)_2D_3$-3-BE in prostate cancer cells. This information, coupled with its serum-stability ~~of~~strongly suggests a therapeutic potential of $(1,25(OH)_2D_3$-3-BE$)_L$ in androgen-sensitive and androgen-insensitive prostate cancer.

Acknowledgement: Authors acknowledge research-support by grants from National Cancer Institute (1R21CA127629-01A2, 1R43CA12617-01A1) and Department of Defense (PC 051136).

Figure Legends:

Figure 1:Cytotoxicity of $1,25(OH)_2D_3$, $(1,25(OH)_2D_3)_L$,$1,25(OH)_2D_3$-3-BEor $(1,25(OH)_2D_3$-3-BE$)_L$ in LNCaP cells. Cells were treated with ethanol (control), blank liposome (control), various doses of $1,25(OH)_2D_3$, $(1,25(OH)_2D_3)_L$,$1,25(OH)_2D_3$-3-BEor $(1,25(OH)_2D_3$-3-BE$)_L$ for 16 hr. Metabolic activity in reagent-treated cells relative to controls was quantitated using a tetrazolium-based (MTT) chromogenic assay. OD was measured spectrophotometrically at 450 nm. There were six replicates for each sample. Statistics was done by student's t test. ***p<0.001, **p<0.01.

Figure 2:Cytotoxicity of $1,25(OH)_2D_3$, $(1,25(OH)_2D_3)_L$,$1,25(OH)_2D_3$-3-BEor $(1,25(OH)_2D_3$-3-BE$)_L$ in PC cells. Cells were treated with ethanol (control), blank liposome (control), various doses of $1,25(OH)_2D_3$, $(1,25(OH)_2D_3)_L$,$1,25(OH)_2D_3$-3-BEor $(1,25(OH)_2D_3$-3-BE$)_L$ for 16 hr followed by ^{3}H-Thymidine incorporation assay by a procedure described in Materials and Methods section. There were six replicates for each sample. Statistics was done by student's t test: ***p<0.001, **p<0.01.

Figure 3::Cytotoxicity of $1,25(OH)_2D_3$, $(1,25(OH)_2D_3)_L$,$1,25(OH)_2D_3$-3-BEor $(1,25(OH)_2D_3$-3-BE$)_L$ in DU-145 cells. Cells were treated with ethanol (control), blank liposome (control), various doses of $1,25(OH)_2D_3$, $(1,25(OH)_2D_3)_L$,$1,25(OH)_2D_3$-3-BEor $(1,25(OH)_2D_3$-3-BE$)_L$ for 16 hr followed by ^{3}H-Thymidine incorporation assay by a procedure described in Materials and Methods section. There were six replicates for each sample. Statistics was done by student's t test: ***p<0.001, **p<0.01.

Figure 4:Growth assay of DU-145 cells, as they were treated with$1,25(OH)_2D_3$-3-BEor $(1,25(OH)_2D_3$-3-BE$)$L. Cells were with ethanol (control), blank liposome (control), various doses of $1,25(OH)_2D_3$-3-BEor $(1,25(OH)_2D_3$-3-BE$)_L$on 1st, 3rd and 5th days, harvested on 7th day and counted in a hemocytometer. There were three replicates for each sample. Statistics was done by student's t test: ***p<0.001, **p<0.01.

Figure 5:Evaluation of the serum-stability of $(1,25(OH)_2D_3$-3-BE$)_L$. One ml of human serum was incubated at 37°C for 60 minutes with a sample of $(1,25(OH)_2D_3$-3-BE$)_L$ (10 µg) followed by extraction with ethyl acetate and HPLC-analysis of the organic-extract. A standard sample of $1,25(OH)_2D_3$-3-BE was also analyzed by HPLC under same conditions. Inset: Graphic depiction of hydrolytic production of equimolar amount of $1,25(OH)_2D_3$ and bromoacetic acid from $1,25(OH)_2D_3$-

3-BE.

References:

[1] V. Torchilin, Multifunctional Nanocarriers. Adv. Drug Deliv. Rev. 58 (2006) 1532-1555.
[2] L. Brannon-Peppas, J. Blanchette, Nanoparticle and targeted systems for cancer therapy. Adv. Drug Deliv.Rev. 56 (2004) 1649-1658.
[3] D.C. Drummond, O. Meyer, K. Hong, D.B. Kirpotin, D. Papahadjopoulos, Optimizing liposomes for delivery of chemotherapeutic agents to solid tumors. Pharmacol. Rev. 51 (1999) 691-743.
[4] R. Jain, R. Delivery of molecular medicine to solid tumors. Science 271 (1996) 1079–1080.
[5] S. Matsuda, G. Jones, Promise of vitamin D analogues in the treatment of hyperproliferative conditions. Mol. Cancer Thera. 5 (2006) 797-808.
[6] M.G. Fakih, D.L. Trump, J.R. Muindi, J.D. Black, R.J. Bernardi, P.J. Creaven, J. Schwartz, M.G. Brattain, A. Hutson, R. French, C.S. Johnson, A phase I pharmacokinetic and pharmacodynamic study of intravenous calcitriol in combination with oral gefitinib in patients with advanced solid tumors. Clin. Cancer Res. 13 (2007) 1216-1223.
[7] D.L. Trump, D.M. Potter, J. Muindi, A. Brufsky, C.S. Johnson, Phase II trial of high-dose, intermittent calcitriol (1,25 dihydroxyvitamin D3) and dexamethasone in androgen-independent prostate cancer. Cancer 106 (2006) 2136-2142.
[8] T.M.Beer, M.N. Javle, C.W. Ryan, M. Garzotto, G.N. Lam, A. Wong, W.D. Henner, C.S. Johnson, D.L. Trump, Phase I study of weekly DN-101, a new formulation of calcitriol, in patients with cancer. Cancer Chemother Pharmacol. 59 (2007) 581-587.
[9] R. Ray, N. Swamy, P.N. MacDonald, S. Ray, M.R. Haussler, M.F. Holick, Affinity labeling of 1α,25-dihydroxyvitamin D_3 receptor. J. Biol. Chem. 271 (1996) 2012-2017.
[10] M.L. Chen, S. Ray, N. Swamy, M.F. Holick, R. Ray, Anti-proliferation of human keratinocytes with 1α, 25-dihydroxyvitamin D_3-3-bromoacetate, an affinity labeling analog of 1,25-dihydroxyvitamin D_3: mechanistic studies. Arch. Biochem. Biophys. 370 (1999) 34-44.
[11] N. Swamy, W. Xu, N. Paz, J-C. Hsieh, M.R. Haussler, G.F. Maalouf, S.C. Mohr, R. Ray, Molecular modeling, affinity labeling and site-directed mutagenesis define the key points of interaction between the ligand-binding domain of the vitamin D nuclear receptor and 1,25-dihydroxyvitamin D_3. Biochem. 39 (2000) 12162-12171.
[12] N. Swamy, K.S. Persons, T.C. Chen, R. Ray, 1α,25-Dihydroxyvitamin D_3-3β-(2)-bromoacetate, an affinity labeling derivative of 1,25-dihydroxyvitamin D_3 displays strong antiproliferative and cytotoxic behavior in prostate cancer cells. J. Cell. Biochem. 89 (2003) 909-916.
[13] N. Swamy, T.C. Chen, S. Peleg, P. Dhawan, S. Christakos, L.V. Stewart, N.L. Weigel, R.G. Mehta, M.F. Holick, R. Ray, Inhibition of proliferation and induction of apoptosis by 25-hydroxyvitamin D_3-3-bromoacetate in prostate cancer cells. Clin. Cancer Res. 10 (2004) 8018-8027.
[14] J.L. Lambert, C.D. Young, K.S. Persons, R. Ray, Mechanistic and pharmacodynamic studies of a 25-hydroxyvitamin D_3 derivative in prostate cancer cells. Biochem.Biophys. Res. Comm. 361 (2007) 189-195.
[15] K.S. Persons, V.J. Eddy, S. Chadid, R. Deoliviera, A.K. Saha, R. Ray, Anti-growth effect of 1,25-Dihydroxyvitamin D_3-3-bromoacetate alone or in cmbination with 5-amino-imidazole-4-carboxamide-1-{beta}-4-ribofuranoside in pancreatic cancer cells. Anticancer Res. 30 (2010) 1875-1880.
[16] T.S. Lange, R.K. Singh, K.K. Kim, Y. Zou, S.S. Kalkunte, G.L. Sholler, N. Swamy, L. Brard, Antiproliferative and pro-apoptotic properties of 3-bromoacetoxycalcidiol in high risk neuroblastoma. Chem. Biol. Drug Des. 70 (2007) 302-310.
[17] R. Ray, S. Ray, M.F. Holick, 1α,25-Dihydroxyvitamin D_3-3β-(2)-bromoacetate, an affinity-

labeling analog of 1□ ,25-Dihydroxyvitamin D_3. Bioorg.Chem 22 (1994) 276-283.
[18] F. Yuan F, M. Leunig, S.K. Huang, D.A. Berk, D. Papahadjopoulos, R.K. Jain RK, Microvascular permeability and interstitial penetration of sterically stabilized (stealth) liposomes in a human tumor xenograft. Cancer Res. 54 (1994) 3352-3356.
[19] D. Papahadjopoulos, T.M. Allen, A. Gabizon, E. Mayhew, K. Matthay, S.K. Huang, K.D. Lee, M.C. Woodle, D.D. Lasic, C. Redemann, F.J. Martin, Sterically stabilized liposomes: improvements in pharmacokinetics and antitumor therapeutic efficacy. Proc. Natl. Acad. Sci. USA 88 (1991) 11460-11464.
[20] I. Cheong, X. Huang, K. Thornton, L.A. Diaz Jr, S. Zhou, Targeting cancer with bugs and liposomes: ready, aim, fire. Cancer Res. 67 (2007) 9605-9608.
[21] L.A. Diaz Jr, I. Cheong, C.a. Foss, X. Zhang, B.A. Peters, N. Agrawal, C. Bettegowda, B. Karim, G. Liu G, K. Khan, X. Huang, M. Kohli, L.H. Dang, P. Hwang, A. Vogelstein, E. Garrett-Mayer, B. Kobrin, M. Pomper, S. Zhou, K.W. Kinzler, B. Vogelstein, D.L. Huso, Pharmacologic and toxicologic evaluation of C. novyi-NT spores. Toxicol. Sci. 88 (2005) 562-575.
[22] N. Agrawal, C. Bettegowda, I. Cheong, J.F. Geschwind, C.G. Drake, E.L. Hipkiss, M. Tatsumi, L.H. Dang, L.A. Diaz Jr, M. Pomper, M. Abusedera, R.L. Wahl, K.W. Kinzler, S. Zhou, D.L. Huso, B. Vogelstein, Bacteriolytic therapy can generate a potent immune response against experimental tumors. Proc. Natl. Acad. Sci. USA. 101 (2004) 15172-15177..
[23] I. Cheong, X. Huang, C. Bettegowda, L.A. Diaz Jr, K.W. Kinzler, S. Zhou, B. Vogelstein, A bacterial protein enhances the release and efficacy of liposomal cancer drugs. Science 314 (2006) 1308-1311.